CENTRALE LILLE

THESE

Présentée en vue
d'obtenir le grade de

DOCTEUR

En

Spécialité :
Chimie théorique, physique, analytique

Par
Adrien FUSINA

DOCTORAT délivré conjointement par CENTRALE LILLE et Universität Regensburg

Titre de la thèse :

Hydrotropic Concepts Applied to the Water-solubilization of Polyphenols : Example of Meglumine, Modeling, Physicochemical Study and Applications

Concepts Hydrotropiques Appliqués à la Solubilisation Aqueuse des Polyphénols : Exemple de la Méglumine, Modélisation, Étude Physico-chimique et Applications

Soutenue le 28 novembre 2023 devant le jury d'examen :

Présidente	Mme Claire BORDES	Maître de Conférences	Université Claude Bernard Lyon 1
Rapporteur	M. Michael, GRADZIELSKI	Professeur	Technische Universität Berlin
Rapportrice	Mme Amélie BOCHOT	Professeur	Université Paris-Saclay
Examinateur	M. Dominik HORINEK	Professeur	Universität Regensburg
Invitée	Mme Anne-Laure FAMEAU	Chargée de Recherche	INRAE
Directrice	Mme Véronique NARDELLO-RATAJ	Professeur	Centrale Lille Institut
Co-directeur	M. Werner KUNZ	Professeur	Universität Regensburg

Thèse préparée dans le Laboratoire UCCS
Ecole Doctorale SMRE 104

Centrale Lille
Cité Scientifique – CS20048 – 59651 Villeneuve d'Ascq Cedex – France
Tél. + 33 (0)3 20 33 53 53 – https://centralelille.fr

Hydrotropic Concepts Applied to the Water-solubilization of Polyphenols : Example of Meglumine, Modeling, Physicochemical Study and Applications

Dissertation

zur Erlangung des Doktorgrades der Naturwissenschaften (Dr. rer. nat.)
der Fakultät Chemie und Pharmazie
der Universität Regensburg

vorgelegt von
Adrien Fusina
aus Marseille
2023

Acknowledgements

The work presented in this thesis results from a collaboration between Centrale Lille Institute and the University of Regensburg. The first half was carried out in the Colloids Catalysis and Oxidation (CISCO) team of the UCCS (Unité de Catalyse et de Chimie du Solide) laboratory at the Université de Lille, and the second half at the Chair of Physical Chemistry II at the Institute of Physical and Theoretical Chemistry at the University of Regensburg. This cooperative project involved a lot of people who made it possible and I would like to thank them here.

First of all, I would like to address my sincere gratitude to Professor Véronique NARDELLO-RATAJ and Professor Werner KUNZ for making this project possible and supervising me during these 3 years. I would like to thank both of them for giving me the opportunity to undertake this international cooperation, and of course for their invaluable scientific guidance throughout the project.

I am also very grateful to Dr Didier TOURAUD for his continuous interest, his innovative ideas, and his support, especially during my time at the University of Regensburg.

I would like to acknowledge Prof. Antje BAEUMNER, Ferdinand HOLZHAUSEN, and Michael LÖSSL for their major contribution to the work on liposomes. Their knowledge and expertise in the field of liposomes as well as their guidance for the experimental work were highly valuable.

My sincere thanks go to Prof. Michael GRADZIELSKI, Prof. Amélie BOCHOT, Prof. Dominik HORINEK, and Prof. Claire BORDES, for accepting to assess my work, based on their various expertise, and to Dr. Anne-Laure FAMEAU for attending my defense and for the helpful scientific discussions we had.

I would also like to warmly thank the members of the CISCO team who were always available to help. I thank Jean-François DECHEZELLES for his kindness and support. Thank you Jeff for your useful advices on all kind of subjects and of course for your wonderful sense of humor. I also thank Jesús Fermin ONTIVEROS for his help and availability. It was really pleasant working with you even before the thesis. Thank you also to Christel PIERLOT, your kindness and enthusiasm are an example for every student, and your tennis skills are an example for every player. I thank Raphaël LEBEUF for his valuable help in the lab (a big thank for the HPLC) and everywhere else. Your availability and commitment were always very welcome. Thank you also to Mike ORTEGA who is essential to the lab and seemingly knows everyone in Lille. We had some really good times. Finally, I would also like to thank Loïc LECLERCQ and Prof. Jean-Marie AUBRY, for their scientific and enjoyable discussions.

My gratitude also goes to all the members of the Chair of Physical Chemistry II who welcomed me in Regensburg and helped me in every way. I sincerely thank Rainer MÜLLER for his help with the practical work of the students at the University, and for accepting me into the 11 a.m. lunchtime group. Thank you also to Eva MÜLLER, for your help and your availability. I would also like to thank my office colleague Jelena TSURKO for her kindness, I wish you all the best. My sincere thanks go also to the secretariat staff

Rosemarie ROEHRL, Bianca HEILGTAG, and Steffi MEINEL for their assistance and patience and for helping me through the administrative process of a university I was not familiar with. Many thanks also to all other members of the chair for their help and kindness.

I would like to thank the interns who helped me with the experiments. Thank you to Estelle DIAZ for your work on meglumine soaps and Eduard WOLF for your work on metformin. It was really pleasant working with you two and I am sure we all learned from each other.

Finally, I would like to address my deepest gratitude to all the Ph.D. students, master students, and all the others I had the chance of meeting and spending time with during my time in Lille and in Regensburg, this project would not have been the same without them.

Jordan (Jojo), my trusty partner from the practical work at Chimie Lille and the HT-SMART-FORMU platform up to the Ph.D., we have really seen it all, and I surely will miss singing Renaud and Francis Cabrel with you. Grégory, my Greg, one of the most ancient staff member of the university and loyal lab partner, your cheerfulness and (loud) laughter always set the mood in the office, the lab, the gym and everywhere. Also, a big thank for teaching me to play darts, and enduring my sense of humor all this time (chafouin!). Lucie, lulu the lab princess, I have to admit you really were the best of us (but not at “Can’t Stop!”). Also, I will never forget that COVID “anecdote” in Bordeaux, thanks a lot for that! Valentin, my Bardou, the second princess of the lab, your (noticeable) presence played a big part in the office mood in Lille, and I am very grateful for that, even if I know you always preferred Greg. Tristan, thanks for the best desk location in the office, and for all the memorable moments we spent in Lille. Don’t worry Tristi, we will never forget your legendary run at “Can’t Stop!”. Alexandre, I feel you belong to the rest of us even if you were officially from UMET, and you made me laugh like no other. Also, I think you have picked up Greg’s bad habits of yelling and filming way too much at inappropriate times. A great thank also to the former Ph.D. students and colleagues, Agathe (Gagouthe), Guillaume, Charles, and Yaoyao. Finally, a big thank to Juliette and Juliette (Jul and Roulietta), and all the others who worked with us at CISCO, you gave us a truly memorable summer. I would also like to kindly thank our successors on the HT-SMART-FORMU platform, Adeline (Hellooo), Leila, Valentin, and Manon.

Next I would like to express my sincere thanks to all students of the University of Regensburg I had the chance to meet. Nadja and Michi, my office colleagues, who helped me in all the possible ways at the university, and for the scientific discussions as well. Basti, Jonas, Moritz, and Eva, I really enjoyed the lunch breaks and the cooking sessions with you (even the bad fish), and in general all moments at the university and elsewhere. Patrick, I am so sorry I missed the Chemcup, I guess football is really not for me. I hope to see you all at the boulder gym real often, Lena and Vanessa too. Florian, I hope everything will be fine for you, it was a pleasure working with you, your enthusiasm and positivity are really inspiring. Many thanks also to Verena, Selina, Julia, and all the others.

My deepest thanks go to my friends of Lille, Nice, Paris and elsewhere. We do not see each other as often as we used to, but each time is memorable. You supported (and endured me) all this time, and for that you have my greatest gratitude. A special thank to Vince, Pich, Flo, Mathou and Elvire.

I would also like to address a very special thank to a very special person. Lea, I am so glad I met you. You not only made every day better at the University, you also made every other day brighter and will surely continue to do so in the future. Your support was unparalleled during the good and the bad moments, and I hope I will be able to support you as well for the rest of your Ph.D. and after that. I am grateful for everything you did.

Finally, I would like to thank my family for their support and their love. For my parents, who are always there for me even if I give far too little news, for my sister Alice and my brother-in-law Pierrick who got married during this thesis, and for my grand-parents who are always thinking about me, from the bottom of my heart, thank you.

Résumé

Cette thèse s’inscrit dans le cadre d’une cotutelle entre Centrale Lille et l’Université de Regensburg. Les différentes problématiques soulevées dans ce travail portent sur la compréhension et l’utilisation de phénomènes de solubilisation en phase aqueuse, en particulier relevant de concepts d’hydrotropie, avec le double objectif de rationnaliser à la fois la recherche de nouveaux agents hydrotropiques et les comportements de solubilisation de composés polyphénoliques, notamment en vue d’applications en pharmaceutique, agroalimentaire ou encore en cosmétique. En effet, de nombreux composés naturels restent encore limités dans leur utilisation, ou bien leur exploitation de par leur faible solubilité aqueuse. Dans le domaine pharmaceutique, cette problématique conduit à employer un panel de technologies de vectorisation d’actif (« drug delivery »), non sans contraintes. Il en va de même pour l’industrie agro-alimentaire ou cosmétique. L’augmentation de la faible solubilité aqueuse de molécules naturelles est de plus particulièrement pertinente dans le contexte de la chimie verte et de la réduction de l’emploi de solvants organiques et de procédés énergivores. Celle-ci peut ainsi trouver des applications très concrètes également dans le domaine de l’extraction de composés naturels.

Un système spécifique a d’abord été étudié en profondeur, il s’agit de la solubilisation de la quercétine en phase aqueuse par l’aminocarbohydrate méglumine en fonction du pH. En effet la quercétine est un polyphénol célèbre pour ses propriétés antioxydantes puissantes ainsi que de nombreuses activités biologiques avérées, comme son rôle dans la réduction de risque de maladies cardiovasculaires (*coronary heart diseases*, CHD), ou suspectées, e.g. sa possible action anticancéreuse. On retrouve ce composé ainsi que de nombreux polyphénols dans le régime alimentaire humain au travers de la consommation de fruits, légumes et autres produits issus de végétaux tels que le thé, le vin ou la bière. La quercétine en particulier est présente en grande quantité dans l’oignon rouge. Cependant, sa métabolisation par l’organisme est grandement limitée par sa très faible solubilité aqueuse, due à un fort π-stacking (phénomène de cohésion intermoléculaire des systèmes π de composés aromatiques) et à la formation de nombreuses liaisons hydrogène (HB) intermoléculaires qui confèrent une grande stabilité à la forme crystalline de la quercétine, et donc une dissolution limitée. A l’instar des autres composés polyphénoliques, l’augmentation du pH provoque la déprotonation successive de ses groupes hydroxyles, ce qui charge négativement la quercétine et accroît son affinité pour les solvants polaires comme l’eau, augmentant ainsi sa solubilité. Cependant, la quercétine étant un antioxydant puissant, elle est particulièrement sensible à l’oxydation, qui est accentuée par la déprotonation de ses groupes hydroxyles, ce qui mène à la dégradation de la structure de la quercétine par ouverture de son cycle central, et in fine à la formation de produits d’oxydation plus petits. De plus, même si ces composés présentent aussi pour la plupart des propriétés antioxydantes, il est intéressant de conserver la quercétine dans son état natif jusqu’au moment où son activité biologique est requise, ou pour concevoir des méthodes d’extraction.

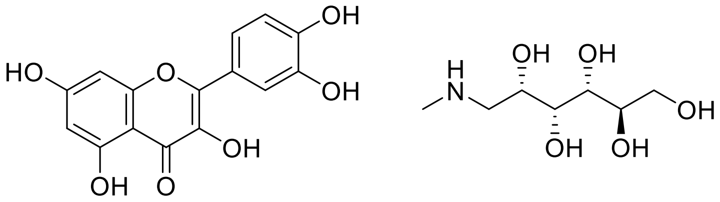

Figure 0.1. Structures chimiques de la quercétine (gauche) et de la méglumine (droite).

Dans cette optique, le premier chapitre de cette thèse s’intéresse au pouvoir solubilisant de la *N*-méthyl-D-glucamine, connue sous le nom de méglumine, une osamine dérivée du sorbitol, traditionnellement utilisée pour le traitement de la Leishmaniose ou sous forme de complexe d’antimoine servant d’agent de contraste pour l’imagerie médicale. Son utilisation sous forme d’additif pour augmenter la solubilité aqueuse de composés pharmaceutiques a nouvellement été reporté pour quelques composés, sans toutefois faire ressortir un mécanisme de solubilisation clair.

Dans ce chapitre, l’influence de la concentration de méglumine sur la solubilité dans l’eau de la quercétine sur une large gamme de pH est mesurée par spectroscopie UV-Visible. L’effet solubilisant de la méglumine apparaît nettement à partir de pH 8 et va croissant avec l’augmentation du pH. Une étude par RMN ^{1}H est menée pour mieux comprendre le mécanisme de solubilisation. Le shift des différents signaux de la méglumine en fonction du ratio méglumine-quercétine est suivi pour identifier quelles fonctions de la molécule interagissent avec le polyphénol. Il s’avère que la méglumine interagit électrostatiquement avec la forme déprotonée de la quercétine pour former un sel, probablement de ratio molaire (1:1) ou (2:1). Les nombreux groupes hydroxyles de la méglumine aident de plus à la solvatation du complexe par liaisons hydrogènes avec les molécules d’eau. Cet apport de méglumine hydratée proche de la quercétine provoque probablement un affaiblissement du π-stacking de cette dernière. De plus, la géométrie plane de la forme native de la quercétine, qui est aussi une des raisons expliquant sa grande propension au π-stacking, est modifiée par sa déprotonation, ce qui amoindrit encore la cohésion du π-stacking. Ce phénomène est vraisemblablement dû à l’équilibre céto-énolique de la quercétine qui est déplacé dans le sens de la cétone non-plane lors de la déprotonation.

L’objectif de cette solubilisation étant de conserver, au moins pour un temps, la quercétine dans son état natif, le degré d’oxydation de cette dernière en fonction des différents paramètres a été quantifié par HPLC, RMN et titration de H_2O_2. Il en ressort qu’autour de pH 8, la quercétine est déjà 6 à 7 fois plus soluble en présence de 250 mM de méglumine par rapport à l’eau pure au même pH, et ne se dégrade que d’environ 30 % en 2 heures. Ce compromis est intéressant car il laisse suffisamment de temps pour concevoir des protocoles où la solubilisation de la quercétine est nécessaire sur une courte période, comme par exemple une extraction en phase aqueuse.

Enfin, comme précédemment énoncé, l’effet solubilisant dû à la présence de la méglumine ne s’observe réellement qu’à partir de pH 8, ce qui laisse penser que la première (ou les deux premières) déprotonation de la quercétine ne survient qu’aux alentours de cette valeur de pH. Toutefois, il est extrêmement compliqué d’obtenir expérimentalement des valeurs précises pour les cinq potentielles constantes de déprotonation (pK_as) de la quercétine en raison de sa propension à se dégrader à cause de l’oxydation. Il n’existe donc pas de consensus actuel dans la littérature scientifique, ni sur les valeurs de ces pK_as, ni même sur l’ordre dans lequel les groupes hydroxyles de la quercétine se déprotonent avec l’augmentation du pH. Pour confirmer l’hypothèse de la nécessité d’au moins une déprotonation pour déclencher l’effet solubilisant de la méglumine, et pour parer à l’oxydation, une méthode computationnelle a été développée grâce au logiciel de modélisation COSMO-RS. Ce logiciel est capable de prédire une valeur de pK_a pour un couple acide-base donné. La détermination de l’ordre de déprotonation des groupes hydroxyles de la quercétine a donc consisté à modéliser toutes les formes ioniques théoriques de la quercétine et à calculer les pK_as pour chaque paire de formes déprotonée N et N+1 fois, et à sélectionner pour chaque niveau les pK_as les plus faibles, donc les déprotonations les plus énergétiquement favorisées. L’ordre de déprotonation ainsi obtenue est en accord avec plusieurs études de la littérature, et apporte des précisions quant au mécanisme de solubilisation par la méglumine à pH 8. Ainsi, le calcul des pK_as associés à ces déprotonations par le logiciel COSMO-RS, bien que peu précis, tend à confirmer l’hypothèse de la double déprotonation de la quercétine (donc doublement négativement chargée) à pH 8. Enfin, les deux premiers groupes hydroxyles à se déprotoner sont situés de chaque côté de la quercétine, ce qui permet à deux molécules de méglumine d’interagir avec une molécule de quercetin sans gêne stérique. Ces travaux ont fait l’objet d’une publication dans *Journal of Molecular Liquids* en 2022 (voir l’annexe A.8).

Le deuxième chapitre rapporte une application concrète de la capacité de la méglumine à solubiliser raisonnablement la quercétine en milieu modérément basique. En effet, il présente l’encapsulation de la quercétine dans des liposomes directement depuis une solution aqueuse de méglumine à pH environ 9. Les liposomes sont des auto-assemblages sphériques de composés lipidiques amphiphiles, formant une double couche, hydrophile à l’extérieur et hydrophobe en son sein. Les liposomes sont donc capables d’encapsuler autant des composés hydrophiles dans leur cœur, que des composés hydrophobes à l’intérieur de leur double couche.

Pour encapsuler la quercétine, une méthode classique dite de « film mince » (*Thin-Film Method*) est ici adaptée en s’inspirant d’un autre procédé d’encapsulation liposomale dite de « saut de pH » (*pH-jump* ou *pH-driven Method*) qui consiste à augmenter la solubilité dans l’eau de composés phénoliques en augmentant le pH, puis à les forcer à migrer dans la double couche hydrophobe des liposomes formés simultanément, en abaissant de nouveau le pH. Cette méthode présente l’immense avantage de n’utiliser aucun solvant organique au cours de l’encapsulation des composés hydrophobes, ce qui est particulièrement pertinent au regard des problématiques actuelles de chimie verte. Toutefois, de nombreuses molécules naturelles, comme la quercétine, ne supportent pas l’augmentation du pH à des valeurs allant jusqu’à 12, et se dégradent bien trop vite pour être effectivement encapsulées dans les liposomes. La méthode de « film mince » est un procédé standard de synthèse de liposomes qui consiste à dissoudre les composés lipidiques dans un mélange de solvants organiques puis de faire évaporer progressivement celui-ci par évaporateur rotatif, ce qui a pour conséquence de former un mince film de lipides sur la paroi du ballon par effet hydrophobe. Enfin, l’ajout de la solution d’encapsulation (classiquement aussi en phase organique, ici en solution aqueuse) permet de redissoudre la double couche lipidique qui forme spontanément des assemblages sphériques. Cette méthode a été choisie car même si elle requiert un minimum de solvants organiques pour la formation du film initial, elle est peu énergivore et permet l'utilisation de lipides classiques pour les synthèses de liposomes, ce qui est pratique pour déterminer l'influence de nouveaux paramètres. De plus, la méthode de saut de pH permet d'augmenter la solubilité aqueuse de composés phénoliques à encapsuler, mais l'augmentation de pH n'a pas d'influence significative sur la solubilité des lipides classiquement employés, d'où la nécessité d'utiliser des composés plus hydrophiles, comme des caséinates de sodium ou des saponines. Quelques précautions expérimentales, notamment l'utilisation de flacons en verre brun et le dégazage des solutions avec de l'azote, ont en outre été prises pour minimiser l'oxydation de la quercétine pendant le procédé.

La couleur jaune pâle des liposomes est visible à l'œil nue à la fin de la synthèse, ce qui donne un premier indice sur la présence de quercétine encapsulée. Pour la détection et la quantification de celle-ci, plusieurs méthodes sont utilisées. De plus, les échantillons sont préalablement lysés, c'est-à-dire que les liposomes sont détruits par ultrasons ou bien par dilution dans un solvant organique, pour permettre de déterminer la présence et la quantité de quercétine à l'intérieur. La spectroscopie UV-Visible directe s'avère ne pas être suffisante pour détecter sans ambiguïté la quercétine dans les échantillons de liposomes. L'encapsulation de la quercétine dans les liposomes est donc confirmée par une méthode électrochimique (Voltampérométrie Différentielle à Impulsions, DPV) qui repose sur l'oxydation contrôlée de la quercétine. Cependant, la structure chimique très proche de certains produits d'oxydation de la quercétine, tel que l'acide protocatéchuique, ne permet probablement pas à cette méthode de détecter de façon discriminante la quercétine native. Pour confirmer la présence de quercétine native, une méthode de mesure quantitative par Chromatographie Liquide à Haute Performance (HPLC) est utilisée. Une courbe de calibration de la concentration de quercétine dans le méthanol pur en fonction de l'absorbance est réalisée par HPLC. Les liposomes sont ensuite lysés par dilution dans le méthanol et par un bref passage dans un bain à ultrasons et la quantité de quercétine non-oxydée peut alors être estimée. En outre, la caractérisation des propriétés des liposomes obtenues, telles que le diamètre moyen, la distribution en taille, la teneur moyenne en lipides ou encore la charge de surface (potentiel ζ) révèlent que la présence de méglumine n'a pas d'influence significative sur la méthode de synthèse choisie, ce qui montre que des procédés classiques peuvent être facilement adaptés pour exploiter l'effet solubilisant de la méglumine.

Ce chapitre montre ainsi, comme preuve de concept, la possibilité de l'utilisation de la méglumine pour l'encapsulation de la quercétine dans des liposomes depuis une solution aqueuse, à pH modérément basique.

Dans le chapitre III, l'étude de la solubilité des composés polyphénoliques a été élargie à un set de six composés, comprenant deux flavonols structurellement proches, la quercétine et le morin, la flavanone naringénine, ainsi que le stilbène *trans*-resvératrol et les chalconoïdes phlorétine et xanthohumol. L'objectif de ce chapitre est double : d'une part, mieux cerner les différentes causes de la faible solubilité aqueuse des polyphénols en relation avec leur structure chimique, et d'autre part rationnaliser l'effet solubilisant d'agents hydrotropiques sur des polyphénols précis en fonction de leur structure, pour donner également un nouvel axe de recherche de composés hydrotropiques.

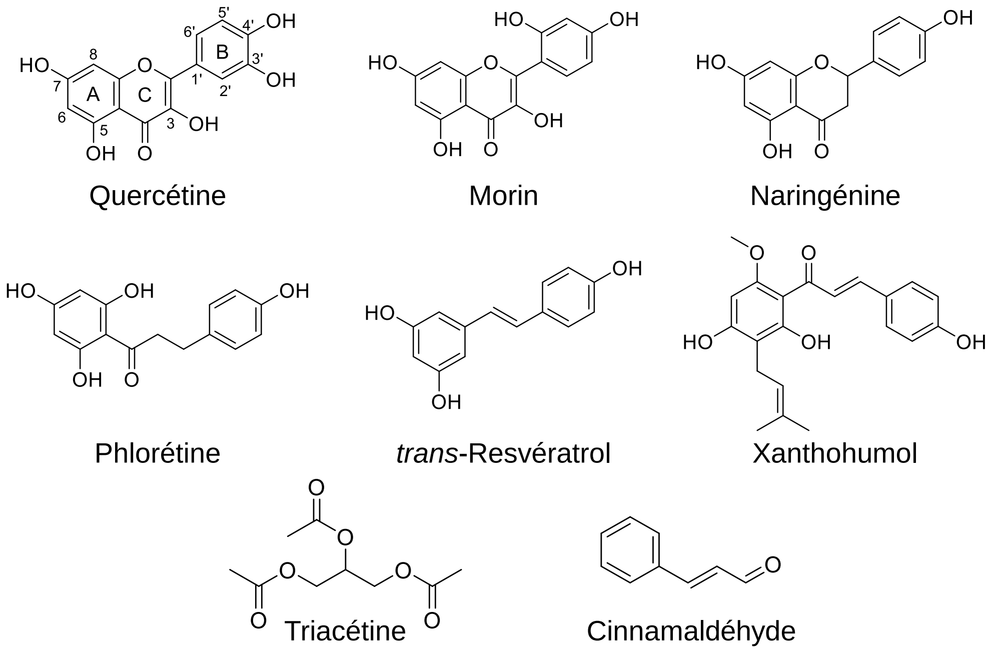

Figure 0.2. Structures chimiques des polyphénols et des solvants étudiés.

Pour ce faire, la solubilité des polyphénols sélectionnés est d'abord évaluée dans des mélanges binaires éthanol/triacétine et éthanol/cinnamaldéhyde, par spectroscopie UV-Visible. Ensuite, le logiciel de modélisation COSMO-RS est de nouveau utilisé, cette fois pour calculer les potentiels chimiques de solvatation μ_{solv} des différents polyphénols dans les mélanges de solvants, afin de prédire les solubilités relatives de ceux-ci, les éventuelles synergies de solubilisation entre les solvants en fonction des composés, et pour mieux comprendre les différents phénomènes de solubilisation observés. La répartition de la densité de charge de surface calculée par COSMO-RS (σ-profiles et σ-surfaces) est aussi utilisée pour expliquer les résultats obtenus par spectroscopie UV-Visible en fonction de la concentration en un solvant donné.

Par la suite, des composés hydrotropiques conventionnels et potentiels tirés de la littérature pharmaceutique sont comparés en fonction de leur capacité à agir en tant qu'hydrotropes pour les flavonoïdes étudiés, en particulier la quercétine, c'est-à-dire à présenter un effet solubilisant exponentiel en fonction de la concentration jusqu'à une valeur plateau. Les additifs testés sont soit des hydrotropes reconnus comme le salicylate de sodium, le nicotinamide, la *N*,*N*-diméthylbenzamide (DMBA), la *N*,*N*-diéthylnicotinamide (DENA) et le pyrogallol, ou bien des composés dont des propriétés hydrotropiques ou solubilisantes ont été reportées dans la littérature, sans qu'ils ne soient reconnus sans ambigüité comme hydrotropes au regard des définitions actuelles. Ces composés sont par exemple l'acide pyroglutamique (PCA), la thymine, le tryptophane ou encore le phloroglucinol.

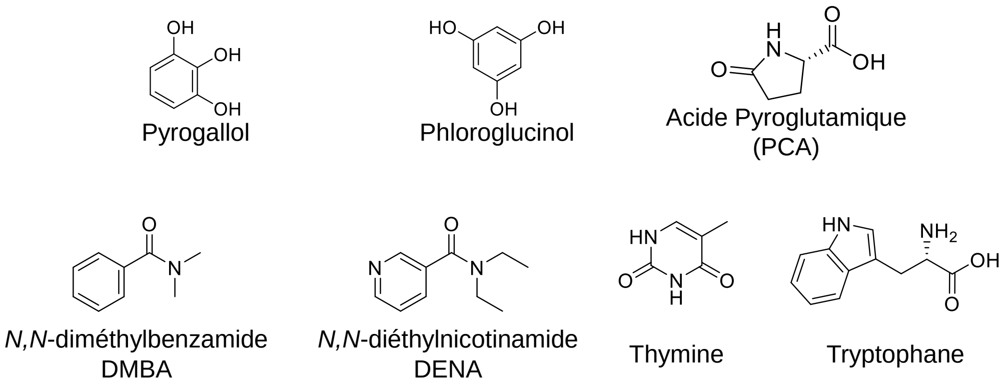
Pyrogallol
Phloroglucinol
Acide Pyroglutamique (PCA)
N,N-diméthylbenzamide DMBA
N,N-diéthylnicotinamide DENA
Thymine
Tryptophane

Figure 0.3. Structures chimiques des hydrotropes et potentiels agents hydrotropiques étudiés.

En particulier, le cas du phloroglucinol et du pyrogallol, deux trihydroxybenzènes qui diffèrent par la position de leurs trois groupes hydroxyles est étudié pour la solubilisation de la quercétine, du morin et de la naringénine. Les groupes hydroxyles du pyrogallol sont tous adjacents, ce qui le rend très soluble dans l'eau, et il est reconnu comme hydrotrope dans la littérature. Le phloroglucinol au contraire ne possède aucun groupe hydroxyle adjacent à un autre, ce qui rend sa structure symétrique dans le plan du cycle aromatique et limite fortement sa solubilité aqueuse. Cependant, même à faible concentration le phloroglucinol semble capable d'augmenter la solubilité des flavonoïdes étudiés, en particulier le morin. De plus, dans la gamme de concentration où il est comparable au pyrogallol, c'est-à-dire quand les deux sont solubles, le phloroglucinol semble même légèrement plus efficace pour solubiliser la quercétine. L'effet solubilisant des deux trihydroxybenzènes provient vraisemblablement de leur capacité à affaiblir le π-stacking des polyphénols, ou plus exactement à promouvoir un π-stacking préférentiel entre les polyphénols et eux plutôt que simplement entre polyphénols. La nature moins encombrée de ces complexes par rapport aux empilements de quercétine ou de morin explique leur plus grande solubilité aqueuse. De plus, la géométrie du morin, qui à l'inverse de la quercétine n'est pas parfaitement plane en raison d'une possible liaison hydrogène intramoléculaire, explique vraisemblablement le π-stacking moins intense et donc sa meilleure solubilité en présence de phloroglucinol. Cependant les meilleurs résultats du phloroglucinol par rapport au pyrogallol dans le cas de la solubilisation de la quercétine sont plus difficiles à expliquer. L'hypothèse avancée est la meilleure « compatibilité » entre la quercétine et le phloroglucinol en raison de la structure symétrique de celui-ci, qui pourrait promouvoir plus efficacement un π-stacking préférentiel que dans le cas du très solvaté pyrogallol.

Enfin, pour évaluer l'effet solubilisant potentiel du phloroglucinol à plus grande concentration, sa solubilité aqueuse a été boostée en s'inspirant de la méthode d'hydrotropie facilitée, c'est-à-dire en ajoutant au système soit un cosolvant (dans ce cas l'éthanol), soit un deuxième hydrotrope. En effet, le système offrant la plus grande solubilité de la quercétine est la combinaison du phloroglucinol et du pyrogallol, jusqu'à une concentration d'environ 20 % en pyrogallol. Le cas du phloroglucinol est de plus intéressant car c'est un des produits d'oxydation principaux de nombreux polyphénols, en particulier la quercétine. L'augmentation de la solubilité de cette dernière au cours de sa dégradation oxydative pourrait ainsi en partie être due à l'interaction de la quercétine native avec ses propres produits d'oxydation à l'instar de ce qui est observé avec le phloroglucinol.

Ce chapitre tente ainsi de rationnaliser d'une part la solubilisation des polyphénols en fonction de leur structure chimique en identifiant dans quelle mesure celle-ci est influencée par exemple par l'hydrophobie d'un solvant ou sa capacité à être donneur de liaisons hydrogène, ou si elle nécessite l'emploi d'un agent anti-stacking. D'autre part, cette étude tente de rationnaliser la recherche de composés présentant des propriétés hydrotropiques mais n'étant pas considérés comme des hydrotropes à cause de leur trop faible solubilité aqueuse. Ceux-ci peuvent ainsi s'avérer intéressants si leur solubilité est dopée par des techniques d'hydrotropie facilitée.

Le dernier chapitre de ce travail de thèse s'intéresse à la possibilité d'utiliser la méglumine ainsi que certains dérivés de la guanidine, dont la metformine (1,1-diméthylbiguanide) en association avec des acides gras linéaires. Le cation guanidinium, qui forme la base de la structure des guanides et guanidines, est un cation très particulier du fait de sa géométrie et de la répartition de sa charge, et il joue un rôle prépondérant dans la faculté des polypeptides d'arginine (un acide aminé possédant une fonction guanidine) à pénétrer les membranes cellulaires, malgré une répulsion électrostatique en apparence forte. Ce phénomène est d'ailleurs nommé « *arginine magic* » et n'a été que récemment élucidé. La metformine est quant à elle l'agent antidiabétique (pour le diabète de type 2) non basé sur la sécrétion d'insuline le plus prescrit dans le monde. Cependant, la metformine est très hydrophile, et contrairement à l'arginine, est peu perméable au niveau des différentes barrières biologiques, ce qui la rend faiblement biodisponible et requiert l'utilisation de fortes doses. D'autres part, les acides gras, en plus de rentrer dans la composition de la membrane cellulaire, trouvent de nombreuses applications en détergence et en cosmétique où leur intérêt est récemment renouvelé, malgré une faible solubilité aqueuse pour les longues chaînes carbonées.

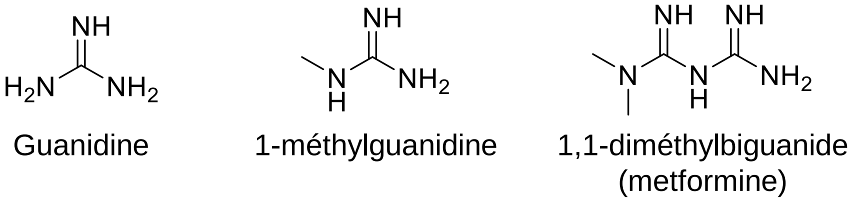
Guanidine
1-méthylguanidine
1,1-diméthylbiguanide
(metformine)

Figure 0.4. Structures chimiques des dérivés de guanidine utilisés.

L'objectif de ce chapitre est de montrer la possibilité d'associer les acides gras linéaires à des composés aminés hydrophiles pour augmenter la solubilité aqueuse des premiers ainsi que le caractère amphiphile des seconds. Pour ce faire, deux protocoles sont utilisés pour synthétiser ces « savons », l'un *in situ* directement en phase aqueuse et l'autre *ex situ* en les faisant précipiter depuis un mélange de solvants organiques. Les amphiphiles ainsi obtenus sont caractérisés par des méthodes classiques du domaine des tensioactifs, à savoir la tension de surface et la concentration micellaire critique (CMC), la température (ou point) de Krafft, c'est-à-dire la température à laquelle le savon devient soluble en phase aqueuse, la solubilisation micellaire de composés d'intérêt, telle que la curcumine ou encore une fois la quercétine, ou encore la formation et la stabilisation d'émulsions.

La réduction du point de Krafft en particulier est un aspect majeur de la recherche de nouveaux contre-ions pour les acides gras. En effet, les savons dits « classiques », c'est-à-dire de sodium et de potassium, ont des points Krafft très élevés, déjà de 45 et 30°C, respectivement, pour des chaînes de 14 carbones, ce qui ne permet pas leur utilisation à température ambiante. Les quatre dérivés principaux testés, à savoir la méglumine, la metformine, la guanidine et la méthylguanidine, présentent tous des points de Krafft entre 0 et 7°C en C_{12}, et la méglumine possède une température de Krafft inférieur à 20°C en C_{14}.

De plus, l'utilisation de la méglumine et de la metformine en association avec l'acide laurique (C_{12}) s'avère prometteuse dans la solubilisation micellaire de quercétine et de curcumine. Enfin, la caractérisation précise d'émulsions obtenues par deux protocoles avec des savons de méglumine de différentes longueurs de chaînes et différentes phases apolaires tend à montrer la bonne association entre les acides gras et la méglumine. Une étude plus approfondie des comportements de phases de ces composés, notamment par microscopie et calorimétrie différentielle à balayage (DSC), ainsi que l'étude de l'influence précise du ratio molaire du contre-ion par rapport à l'acide gras, serait particulièrement pertinente pour compléter cette étude.

Abstract

This thesis is part of a joint PhD project between Centrale Lille and the University of Regensburg. The various issues raised in this work concern the understanding and use of solubilization phenomena in aqueous phase, in particular those relating to hydrotropy concepts, with the dual aim of rationalizing both the search for new hydrotropic agents and the solubilization behavior of polyphenolic compounds, particularly with a view to applications in pharmaceuticals, agri-food or cosmetics. Indeed, many natural compounds are still limited in their use or exploitation by their low aqueous solubility. In the pharmaceutical field, this issue has led to the use of a range of drug delivery technologies, not without constraints. The same applies to the food and cosmetics industries. Increasing the low aqueous solubility of natural molecules is particularly relevant in the context of green chemistry and the reduction in the use of organic solvents and energy-intensive processes. It also has very practical applications in the extraction of natural compounds.

Firstly, a specific system was studied in depth: the pH-dependent solubilization of quercetin in the aqueous phase by the aminocarbohydrate meglumine. Indeed, quercetin is a polyphenol renowned for its powerful antioxidant properties, as well as numerous biological activities, either recognized, such as its role in reducing the risk of coronary heart disease (CHD), or suspected, e.g. its possible anticancer action. This compound, along with many other polyphenols, is found in the human diet through the consumption of fruit, vegetables and other plant-based products such as tea, wine and beer. Quercetin in particular is found in large quantities in red onions. However, its metabolism by the body is greatly limited by its very low aqueous solubility, due to strong π-stacking (the phenomenon of intermolecular cohesion of the π systems of aromatic compounds) and the formation of numerous intermolecular hydrogen bonds (HB), which confer great stability on the crystalline form of quercetin, and therefore limited dissolution. As with other polyphenolic compounds, increasing pH causes successive deprotonation of its hydroxyl groups, negatively charging quercetin and increasing its affinity for polar solvents such as water, thus increasing its solubility. However, as quercetin is a powerful antioxidant, it is particularly sensitive to oxidation, which is accentuated by deprotonation of its hydroxyl groups, leading to degradation of the quercetin structure by cleavage of its central ring, and ultimately to the formation of smaller oxidation products. Moreover, even though most of these compounds also have antioxidant properties, it is interesting to preserve quercetin in its native state until its biological activity is required, or to design extraction methods.

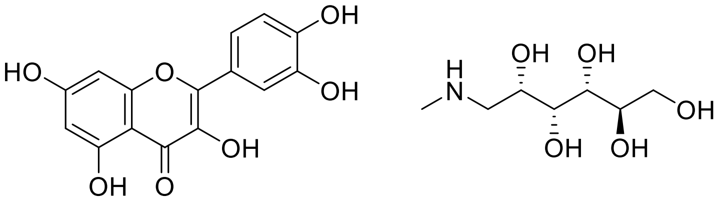

Figure 0'.1. Chemical structures of quercetin (left) and meglumine (right).

To this end, the first chapter of this thesis focuses on the solubilizing power of *N*-methyl-D-glucamine, known as meglumine, an amino sugar derived from sorbitol, traditionally

used for the treatment of Leishmaniasis or as an antimony complex serving as a contrast agent for medical imagery. Its use as an additive to increase the aqueous solubility of pharmaceutical compounds has recently been reported for a few compounds, without however highlighting a clear solubilization mechanism.

In this chapter, the influence of meglumine concentration on the water solubility of quercetin over a wide pH range is measured by UV-Visible spectroscopy. The solubilizing effect of meglumine appears clearly from pH 8 and grows with increasing pH. A ^{1}H NMR study is carried out to better understand the solubilization mechanism. The shift of the different meglumine signals as a function of the meglumine-quercetin ratio is monitored to identify which functions of the molecule interact with the polyphenol. It turns out that meglumine interacts electrostatically with the deprotonated form of quercetin to form a salt, probably with a molar ratio of (1:1) or (2:1). Meglumine's numerous hydroxyl groups also help solvating the complex via hydrogen bonds with water molecules. This addition of hydrated meglumine close to quercetin probably weakens the latter's π-stacking. In addition, the flat geometry of quercetin's native form, which is also one of the reasons for its high tendency to π-stacking, is modified by its deprotonation, further weakening π-stacking cohesion. This phenomenon is probably due to the keto-enolic equilibrium of quercetin, which is shifted in the direction of the non-planar ketone upon deprotonation.

The aim of this solubilization being to preserve quercetin in its native state, at least for a time, the degree of oxidation of the latter as a function of the various parameters was quantified by HPLC, NMR and H_2O_2 titration. At around pH 8, quercetin is already 6 to 7 times more soluble in the presence of 250 mM meglumine than in pure water at the same pH, and degrades by only around 30 % in 2 hours. This is an interesting compromise, as it leaves sufficient time to design protocols where quercetin solubilization is required over a short period, such as aqueous phase extraction.

Finally, as previously stated, the solubilizing effect due to the presence of meglumine is only really observed from pH 8 onwards, suggesting that the first (or first two) deprotonation of quercetin only occurs around this pH value. However, it is extremely complicated to experimentally obtain precise values for the five potential deprotonation constants (pK_as) of quercetin due to its inclination to degrade through oxidation. There is therefore no current consensus in the scientific literature, either on the values of these pK_as, or even on the order in which quercetin's hydroxyl groups deprotonate with increasing pH. To confirm the hypothesis of the need for at least one deprotonation to trigger the solubilizing effect of meglumine, and to overcome oxidation, a computational method was developed using the COSMO-RS modeling software. This software is capable of predicting a pK_a value for a given acid-base couple. Determining the order of deprotonation of quercetin hydroxyl groups therefore involved modeling all the theoretical ionic forms of quercetin and calculating the pK_as for each pair of forms deprotonated N and N+1 time, and selecting for each level the lowest pK_as, hence the most energetically favored deprotonations. The order of deprotonation thus obtained is in agreement with several studies in the literature, and provides clarification of the mechanism of solubilization by meglumine at pH 8. Thus, the calculation of the pK_as associated with these deprotonations by the COSMO-RS software, although not very precise, tends to confirm the hypothesis of the double deprotonation of quercetin (thus twice negatively charged) at pH 8. Finally, the first two hydroxyl groups to deprotonate are located on each side of quercetin, enabling two meglumine molecules to interact with one quercetin molecule without steric hindrance. This work was published in the *Journal of Molecular Liquids* in 2022 (see Appendix A.8).

The second chapter reports on a concrete application of meglumine's ability to reasonably solubilize quercetin in a mildly alkaline environment. Indeed, it presents the encapsulation of quercetin in liposomes directly from an aqueous meglumine solution at pH around 9. Liposomes are spherical self-assemblies of amphiphilic lipid compounds, forming a double layer, hydrophilic on the outside and hydrophobic within. Liposomes are therefore able to encapsulate both hydrophilic compounds in their core, and hydrophobic compounds within their double layer.

To encapsulate quercetin, a classic "thin-film method" is adapted here, taking inspiration from another liposomal encapsulation process known as the "pH-jump" or "pH-driven method", which involves increasing the water-solubility of phenolic compounds by raising the pH, then forcing them to migrate into the hydrophobic double layer of liposomes simultaneously formed by lowering the pH again. This method has the major advantage of using no organic solvents during encapsulation of the hydrophobic compounds, which is particularly relevant to current green chemistry issues. However, many natural molecules, such as quercetin, do not tolerate pH increases up to 12, and degrade far too quickly to be effectively encapsulated in liposomes. The "thin film" method is a standard procedure for liposome synthesis, in which lipid compounds are dissolved in a mixture of organic solvents and then progressively evaporated by rotary evaporator, resulting in the formation of a thin lipid film on the flask wall due to the hydrophobic effect. Finally, the addition of the encapsulation solution (usually also in organic phase, here in aqueous solution) dissolves again the lipid double layer, which spontaneously forms spherical assemblies. This method was chosen because although it requires a minimum of organic solvents for initial film formation, it is energy-efficient and allows the use of conventional lipids for liposome synthesis, which is convenient for assessing the influence of new parameters. In addition, the pH-jump method can be used to increase the aqueous solubility of phenolic compounds to be encapsulated, but the pH increase has no significant influence on the solubility of the lipids conventionally used, hence the need to use more hydrophilic compounds, such as sodium caseinates or saponins. A number of experimental precautions, including the use of brown glass flasks and flushing of solutions with nitrogen, were also taken to minimize oxidation of quercetin during the process.

The pale-yellow color of liposomes is visible to the naked eye at the end of synthesis, giving an initial indication of the presence of encapsulated quercetin. Several methods are then used to detect and quantify quercetin. In addition, samples are first lysed, i.e. the liposomes are destroyed by ultrasound or by dilution in an organic solvent, to enable the presence and quantity of quercetin inside the liposomes to be determined. Direct UV-Visible spectroscopy has proved insufficient to unambiguously detect quercetin in liposome samples. The encapsulation of quercetin is therefore confirmed by an electrochemical method (Differential Pulse Voltammetry, DPV) based on the controlled oxidation of quercetin. However, the very close chemical structure of certain quercetin oxidation products, such as protocatechuic acid, means that this method is unlikely to detect native quercetin in a discriminating manner. To confirm the presence of native quercetin, a quantitative measurement method using High-Performance Liquid Chromatography (HPLC) is used. A calibration curve of quercetin concentration in pure methanol versus absorbance is performed by HPLC. The liposomes are then lysed by dilution in methanol and a brief passage through an ultrasonic bath, and the amount of non-oxidized quercetin can then be estimated. Characterization of liposome properties such as mean diameter, size distribution, mean lipid content and surface charge (ζ-potential) reveals that the presence of meglumine has no significant influence on the chosen synthesis method, showing that conventional processes can be easily adapted to exploit the solubilizing effect of meglumine.

As a proof of concept, this chapter shows how meglumine can be used to encapsulate quercetin in liposomes from an aqueous solution at moderately alkaline pH.

In chapter III, the study of the solubility of polyphenolic compounds was extended to a set of six compounds, including two structurally related flavonols, quercetin and morin, the flavanone naringenin, as well as the stilbene trans-resveratrol and the chalconoids phloretin and xanthohumol. The aim of this chapter is dual: on the one hand, to better identify the various causes of the low aqueous solubility of polyphenols in relation to their chemical structure, and on the other, to rationalize the solubilizing effect of hydrotropic agents on specific polyphenols in relation to their structure, to also provide a new line of research into hydrotropic compounds.

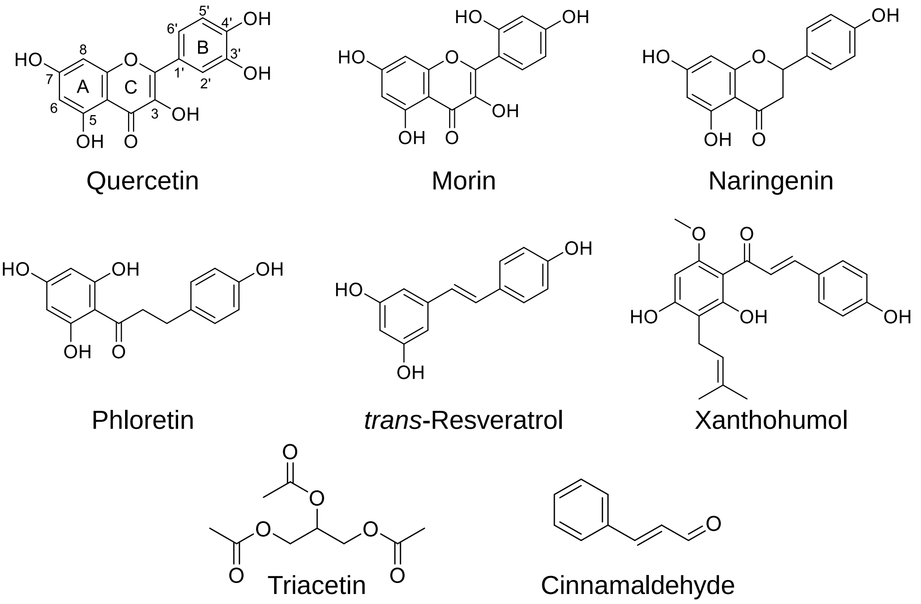

Figure 0'.2. Chemical structures of the polyphenols and solvents studied.

To achieve this, the solubility of selected polyphenols is first assessed in binary ethanol/triacetin and ethanol/cinnamaldehyde mixtures, using UV-Visible spectroscopy. Next, the COSMO-RS modeling software is again used, this time to calculate the chemical solvation potentials µsolv of the different polyphenols in the solvent mixtures, in order to predict their relative solubilities, possible solubilization synergies between solvents depending on the compounds, and to better understand the different solubilization phenomena observed. The surface charge density distribution calculated by COSMO-RS (σ-profiles and σ-surfaces) is also used to explain the results obtained by UV-Visible spectroscopy as a function of the concentration of a given solvent.

Subsequently, conventional and potential hydrotropic compounds from the pharmaceutical literature are compared in terms of their ability to act as hydrotropes for the flavonoids studied, in particular quercetin, i.e. to exhibit an exponential solubilizing effect as a function of concentration up to a plateau value. The additives tested are either recognized hydrotropes such as sodium salicylate, nicotinamide, *N*,*N*-dimethylbenzamide (DMBA), *N*,*N*-diethylnicotinamide (DENA) and pyrogallol, or compounds whose hydrotropic or solubilizing properties have been reported in the literature, without them being unambiguously recognized as hydrotropes under current definitions. Examples include pyroglutamic acid (PCA), thymine, tryptophan and phloroglucinol.

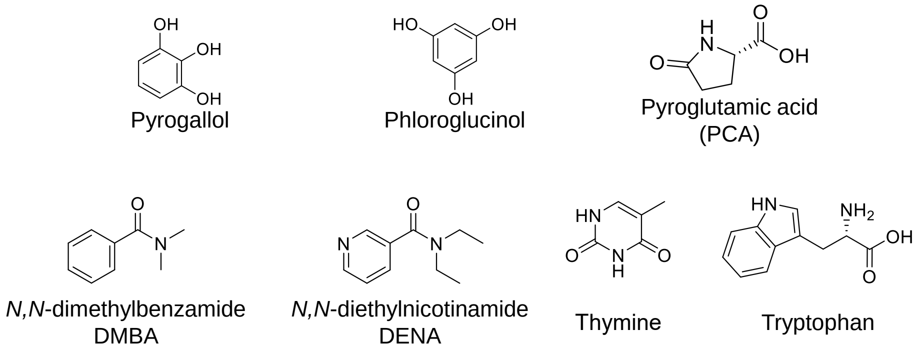

Figure 0'.3. Chemical structures of hydrotropes and potential hydrotropic agents studied.

In particular, the case of phloroglucinol and pyrogallol, two trihydroxybenzenes that differ in the position of their three hydroxyl groups, is studied for the solubilization of quercetin, morin and naringenin. Pyrogallol's hydroxyl groups are all adjacent, making it highly soluble in water, and it is recognized as a hydrotrope in the literature. Phloroglucinol, on the other hand, has no adjacent hydroxyl groups, making its structure symmetrical in the plane of the aromatic ring and severely limiting its aqueous solubility. However, even at low concentrations, phloroglucinol seems capable of increasing the solubility of the flavonoids studied, particularly morin. Moreover, in the concentration range where it is comparable to pyrogallol, i.e. when both are soluble, phloroglucinol seems even slightly more effective at solubilizing quercetin. The solubilizing effect of the two trihydroxybenzenes probably arises from their ability to weaken the π-stacking of polyphenols, or more accurately to promote preferential π-stacking between polyphenols and themselves rather than simply between polyphenols. The less crowded nature of these complexes compared with quercetin or morin stacks explains their greater aqueous solubility. Furthermore, the geometry of morin, which unlike quercetin is not perfectly planar due to possible intramolecular hydrogen bonding, probably explains the less intense π-stacking and hence its better solubility in the presence of phloroglucinol. However, the better results of phloroglucinol compared with pyrogallol in the case of quercetin solubilization are more difficult to explain. The hypothesis put forward is the better "compatibility" between quercetin and phloroglucinol due to the latter's symmetrical structure, which could more effectively promote preferential π-stacking than in the case of the highly solvated pyrogallol.

Finally, to assess the potential solubilizing effect of phloroglucinol at higher concentrations, its aqueous solubility was boosted following the facilitated hydrotropy approach, i.e. by adding to the system either a cosolvent (in this case ethanol) or a second hydrotrope. Indeed, the system exhibiting the greatest solubility of quercetin is the combination of phloroglucinol and pyrogallol, up to a concentration of around 20 % pyrogallol. The case of phloroglucinol is also interesting, as it is one of the main oxidation products of many polyphenols, in particular quercetin. The increase in quercetin solubility during oxidative degradation could therefore be partly due to the interaction of native quercetin with its own oxidation products, as observed with phloroglucinol.

On the one hand, this chapter attempts to rationalize the solubilization of polyphenols according to their chemical structure, by identifying to what extent this is influenced, for example, by the hydrophobicity of a solvent or its capacity to be a hydrogen bond donor, or whether it requires the use of an anti-stacking agent. On the other hand, this study attempts to rationalize the search for compounds with hydrotropic properties but which are not considered hydrotropes due to their insufficient aqueous solubility. Such compounds may prove interesting if their solubility is enhanced by hydrotropic techniques.

The final chapter of this thesis explores the possibility of using meglumine and certain guanidine derivatives, including metformin (1,1-dimethylbiguanide), in association with linear fatty acids. The guanidinium cation, which forms the basis of the structure of guanides and guanidines, is a very special cation in terms of its geometry and charge distribution, and plays a key role in the ability of arginine (an amino acid with a guanidine function) polypeptides to penetrate cell membranes, despite an apparently strong electrostatic repulsion. This phenomenon is known as "arginine magic" and has only recently been elucidated. Metformin is the most widely prescribed anti-diabetic agent (for type 2 diabetes) not based on insulin secretion. However, metformin is highly hydrophilic, and unlike arginine, is not very permeable across the various biological barriers, making it poorly bioavailable and thus requiring the use of high dosage levels. On the other hand, fatty acids, in addition to their role in cell membrane composition, have numerous applications in detergents and cosmetics, where their interest has recently been renewed, despite the low aqueous solubility of long carbon chains.

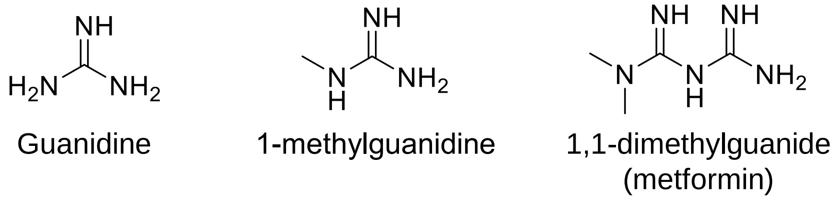

Guanidine

1-methylguanidine

1,1-dimethylguanide (metformin)

Figure 0'.4. Chemical structures of the guanidine derivatives used.

The aim of this chapter is to demonstrate the possibility of combining linear fatty acids with hydrophilic amino compounds to increase the aqueous solubility of the former and the amphiphilic character of the latter. To this end, two protocols are used to synthesize these "soaps", one in situ directly in the aqueous phase and the other ex situ by precipitating them from a mixture of organic solvents. The amphiphiles thus obtained are characterized by classic surfactant methods, namely surface tension and critical micellar concentration (CMC), Krafft temperature (or point), i.e. the temperature at which the soap becomes soluble in aqueous phase, micellar solubilization of compounds of interest, such as curcumin or once again quercetin, and emulsion formation and stabilization.

Krafft point reduction in particular is a major aspect of the search for new counterions for fatty acids. Indeed, the so-called "classic" soaps, i.e. sodium and potassium, have very high Krafft points, already 45 and 30°C, respectively, for 14-carbon chains, which makes them unsuitable for use at room temperature. The four main derivatives tested, namely meglumine, metformin, guanidine and methylguanidine soaps, all have Krafft points between 0 and 7°C at C_{12}, and the meglumine soap has a Krafft temperature below 20°C for C_{14}.

Furthermore, the use of meglumine and metformin in combination with lauric acid (C_{12}) shows promising results in the micellar solubilization of quercetin and curcumin. Finally, the precise characterization of emulsions obtained by two protocols with meglumine soaps of different chain lengths and different apolar phases tends to show the effective association between fatty acids and meglumine. Further study of the phase behavior of these compounds, notably by microscopy and Differential Scanning Calorimetry (DSC), as well as the precise influence of the molar ratio of counterion to fatty acid, would be particularly relevant to complete this study.

Table of contents

Résumé vi

Abstract xiv

General introduction 1

Chapter I — Enhancement of water-solubilization of quercetin by meglumine: mechanism investigation and quercetin deprotonation modeling 3

I.1. Introduction 5

I.2. Bibliographic background 5

- I.2.1. Concepts of solubilization 5
  - I.2.1.1. Solvation, solubility and solubilization 5
  - I.2.1.2. pH influence on solubility 8
  - I.2.1.3. π-stacking 8
- I.2.2. Drug delivery 10
- I.2.3. Polyphenols 11
  - I.2.3.1. Classification 11
  - I.2.3.2. Natural sources and dietary polyphenols 12
  - I.2.3.3. Properties 13
    - I.2.3.3.1. Alleged biological activities 13
    - I.2.3.3.2. Autoxidation and antioxidant activity 15
    - I.2.3.3.3. Solubility, bioavailability, and pharmacokinetics of quercetin 18
  - I.2.3.4. Specific structural properties of quercetin 20
    - I.2.3.4.1. Dissociation constants and deprotonation order 20
    - I.2.3.4.2. Influence of geometry on intermolecular interactions of quercetin . 23
- I.2.4. Meglumine 24
  - I.2.4.1. History and uses 24
  - I.2.4.2. Properties 25

I.3. Experimental part 25

- I.3.1. Materials 25
- I.3.2. Methods 25
  - I.3.2.1. Solubilization measurements 25
  - I.3.2.2. UV-Visible spectroscopy 26
  - I.3.2.3. ^{1}H NMR spectroscopy 26
  - I.3.2.4. Quercetin oxidation stability assessment 26
    - I.3.2.4.1. Oxidation precaution measures 26
    - I.3.2.4.2. Oxidation products detection with ^{1}H NMR 26
    - I.3.2.4.3. Quercetin oxidation state quantification with HPLC 27
    - I.3.2.4.4. Ferrous Oxidation-Xylenol Orange (FOX) method 27
- I.3.3. Deprotonation modeling with COSMO-RS software 28
  - I.3.3.1. Theoretical background and working principle of COSMO-RS calculations: polarization surfaces 28

I.3.3.2. Deprotonation order prediction via minimum dissociation constants calculations 29

I.4. Quercetin solubilization in aqueous solution with meglumine 30

I.4.1. Solubility of quercetin in water as a function of pH 30
I.4.2. Meglumine concentration influence on quercetin water-solubility 31
I.4.3. Deprotonation order simulation with COSMO-RS.....................................32
I.4.4. Mechanism of quercetin solubilization with meglumine.............................33

I.5. Impact of meglumine on quercetin oxidation stability...35

I.5.1. Determination of the presence of native quercetin and/or oxidation products in solution 36
I.5.2. Oxidation quantification with HPLC...37
I.5.3. Oxidation quantification with the Ferrous Oxidation Xylenol orange (FOX) method 38

I.6. Extension of the scope to other polyphenols...40

I.6.1. Xanthohumol solubilization with meglumine...40
I.6.2. Comparison of the polyphenol solubilization efficacy of meglumine.........41

I.7. Conclusions 43

Chapter II ─ Application of quercetin solubilization with meglumine: liposome encapsulation at moderate pH using modified pH-driven method 47

II.1. Introduction 49

II.2. Bibliographic background...49

II.2.1. Liposomes technology 49
II.2.2. pH-driven methods...51

II.3. Experimental part 52

II.3.1. Materials 52
II.3.2. Liposomes preparation...52
II.3.3. Liposomes characterization and quercetin concentration assessment 53

II.4. Quercetin-loaded liposomes formulation..54

II.4.1. Liposomes characterization 54
II.4.2. Liposomal quercetin detection...55
II.4.3. Liposomal quercetin quantification and oxidation state assessment 56

II.5. Conclusions..57

Chapter III ─ Solubilization of polyphenols with biocompatible hydrotropes: on the role of π-stacking in hydrotropy phenomena 59

III.1. Introduction...61

III.2. Bibliographic background..62

III.2.1. Definitions and concepts of hydrotropy 62
III.2.2. Classical hydrotropes 66

III.2.3. Pharmaceutical and biochemical literature research strategy 67

III.3. Experimental part 68

III.3.1. Materials 68
III.3.2. Methods 68
III.3.2.1. Solubilization measurements 68
III.3.2.2. Solubilization behavior modeling with COSMO-RS 69

III.4. Solubilization in binary solvents mixtures: study of polyphenols structure-low solubility relation 69

III.4.1. Solubilization trials of polyphenols in triacetin/ethanol and cinnamaldehyde/ethanol systems 69
III.4.2. Solubilization modeling and synergetic effects predictions with COSMO-RS 73

III.5. Quercetin hydrotropic solubilization investigation 78

III.5.1. Solubilization trials with classical hydrotropes 78
III.5.2. Extension to potential hydrotropic agents 79

III.6. Small phenol and π-stacking aggregation influence on quercetin solubility: phloroglucinol and pyrogallol 82

III.6.1. Solubilization enhancement comparison between phloroglucinol and pyrogallol 82
III.6.2. Facilitated hydrotropy inspired enhancement of phloroglucinol water-solubility 84

III.7. Conclusions: outlook for the search of hydrotropic compounds 87

Chapter IV ─ Meglumine and metformin as new counterion for fatty acids: brief characterization and perspectives 91

IV.1. Introduction 93

IV.2. Bibliographic background 93

IV.2.1. Surfactants: definition and applications 93
IV.2.2. Surface tension, micellization, and other phase behaviors 94
IV.2.3. Krafft point 96
IV.2.4. Emulsions 97
IV.2.5. Soaps: carboxylic acid salts 98
IV.2.6. Counterion influence and Hofmeister series 99
IV.2.7. Guanidines and metformin 101

IV.3. Materials and methods 104

IV.3.1. Materials 104
IV.3.2. Methods 105
IV.3.2.1. Samples preparation 105
IV.3.2.2. Soap synthesis assessment via ^{1}H NMR 105
IV.3.2.3. Krafft point measurement 106
IV.3.2.4. Surface tension and CMC measurement 106

IV.3.2.5. Micellar solubilization 106
IV.3.2.6. Emulsification process 106
IV.3.2.7. Emulsion properties assessment 107
IV.3.2.7.1. Emulsion morphology analysis 107
IV.3.2.7.2. Stability measurement 108

IV.4. Synthesis and characterization of amino-carboxylate with meglumine or guanidine derivatives as counterion 108

IV.4.1. Krafft points determination 111
IV.4.2. Critical Micelle Concentrations 114
IV.4.3. Micellar solubilization of quercetin and curcumin 115

IV.5. Characterization of meglumine-carboxylates emulsification capacity 116

IV.5.1. Emulsions characterization 117
IV.5.2. Stability measurement: Multiple Light Scattering 120

IV.6. Conclusions 121

General conclusion 125

References 131

Appendix 153

A.1. List of Abbreviations 153

A.2. pK_a calculations for quercetin deprotonation order determination 157

A.3. HPLC calibration method for quercetin quantification 160

A.4. COSMO-RS calculations for the polyphenols set 161

A.5. Experimental pK_a determination of pyroglutamic acid 162

A.6. Micrograph of phase behavior of guanidine soaps 162

A.7. Turbiscan profiles of $MegC_n$ emulsions 163

A.8. Publication ─ Enhancement of water solubilization of quercetin by meglumine and application of the solubilization concept to a similar system 165

General introduction

Water is often considered as the universal solvent, not only because of its physical and chemical properties which enable it to dissolve more compounds than any other solvent, but also because it is non-toxic, readily available, very inexpensive in industrial processes and easy to handle. The rise and recognition in recent years of green chemistry as a major objective of scientific research has also led to a reduction in the use of organic solvents.

Aqueous solubility however, is a major issue for many compounds, particularly in the food and pharmaceutical industries. Indeed, it is estimated that between 70 and 90 % of new candidate active pharmaceutical ingredients (APIs) are poorly, if at all, soluble in water[1], which rules out facilitated oral administration, and compels the use of higher drug doses (with increased side-effect risks) or drug delivery technologies, each with its own advantages and limitations, but all having in common the addition of extra process steps.

The emergence of dietary supplements as a popular trend, coupled with a drive to reduce drug doses, is prompting more and more individuals to seek out "nutraceuticals", products that straddle the boundary between food and medicine. In this category, polyphenols are particularly well known by the general public for their antioxidant properties, but in recent years they have increasingly attracted the attention of researchers for their wide range of potential biological activities. Indeed, polyphenols represent one of the largest family of chemical compounds, with several thousand members discovered to date. The major obstacle to the widespread use of these compounds is their very low aqueous solubility. However, few studies have focused on the reasons for the low aqueous solubility of polyphenols in relation to their structure. In fact, unlike for example alkanes, for which the causes of low aqueous solubility are easily linked to their apolarity, polyphenols have hydroxyl groups that can form hydrogen bonds with a polar solvent such as water.

In this context, there is a resurgence in the interest in “simple” phenomena such as hydrotropy to increase the aqueous solubility of compounds of interest. Hydrotropy is a concept introduced over a century ago by Neuberg to describe the solubilizing potential of certain aromatic salts that occurs without structuring. It is now better understood and encompasses a diversity of structurally very different compounds and more or less independent phenomena. However, the very definition of a hydrotrope remains a matter debate, as it is not based on a well-defined chemical structure, as is the case for surfactants, for example. Furthermore, the search for an effective solubilizing agent must be considered in relation to the structure of the solute. The capacity of a solubilizing agent, such as conventional hydrotropes (sodium xylene sulfonate, short amphiphiles, etc.), is generally based on one particular solubilization mechanism, and is therefore unlikely to work effectively on a multitude of solutes with different structures.

Through the study of a selection of polyphenolic solutes, the work presented in this thesis aims to identify relations between the hydrotropic action of certain compounds and the structures of both themselves and the solutes. In addition, the extent to which a solubilizing agent can be recognized as a hydrotrope, or hydrotropic agent, was investigated by examining solubilizers from the pharmaceutical literature which were used without interest regarding the solubilization mechanism. In this perspective, chapter I will focus on a specific example of the solubilization enhancement of the polyphenol quercetin by the hydrophilic solubilizer meglumine. Quercetin is a polyphenol renowned for its antioxidant activity, its role in limiting cardiovascular disease, and its many alleged beneficial biological activities such as anticancer. Meglumine is an amino derivative of glucose, and its presence has been shown to increase the aqueous solubility of a number of drugs, without however possessing amphiphilic properties due to a lack of hydrophobicity. Its influence on the water solubility of quercetin over a wide pH range, the extent of their interactions such as ionic ones, the formation of hydrogen bonds or its impact on the π-stacking of quercetin have been studied in depth in chapter I. In addition, its impact on quercetin oxidation was investigated.

Chapter II logically follows this effective solubilization by presenting a concrete example of application; the proof of concept of the feasibility of a modified protocol for the encapsulation of quercetin in liposomes at mildly basic pH using a minimum of organic solvent.

Chapter III covers a set of polyphenols representative of compounds frequently found in the human diet. The relation between the structure of these phenolic compounds and their low aqueous solubility was investigated, as well as their behavior in the presence of hydrotropes and compounds exhibiting hydrotropic properties, depending on their mode of action. To this end, the modeling software COSMO-RS was used to gain further insights into their solubilization behavior in regards to two binary solvents systems, ethanol/triacetin and ethanol/cinnamaldehyde, as well as to predict potential synergies of solubilization. Lastly, the combination of two small trihydroxybenzenes, the hydrotrope pyrogallol and one of quercetin major oxidation product, phloroglucinol, was studied as a potential solubility enhancement system for quercetin and other flavonoids, similarly to facilitated hydrotropy. The preferential π-stacking between these small phenols and quercetin was investigated as the main solubilisation mechanism.

In chapter IV, we examine the possibility of using meglumine, as well as metformin and other related compounds, as counterions to linear fatty acids. Indeed, another aspect of the poor bioavailability of certain substances is their low permeability, i.e. their ability to penetrate certain biological membranes. This capacity is affected by parameters such as the polarity, hydrophobicity, size or charge of the compounds, and can therefore, as with APIs solubility, be enhanced to improve drug action. In this perspective, fatty acids could help highly hydrophilic molecules become more available. These prospects will be briefly explored in terms of the possibility of associating these fatty acids with amino counterions to form soaps, and will be evaluated accordingly using conventional surfactant criteria such as CMC, Krafft temperature, solubilizing capacity and emulsifying capacity. This served as a proof of concept and could be a starting point for further development in this direction.

Chapter I

—

Enhancement of water-solubilization of quercetin by meglumine: mechanism investigation and quercetin deprotonation modeling

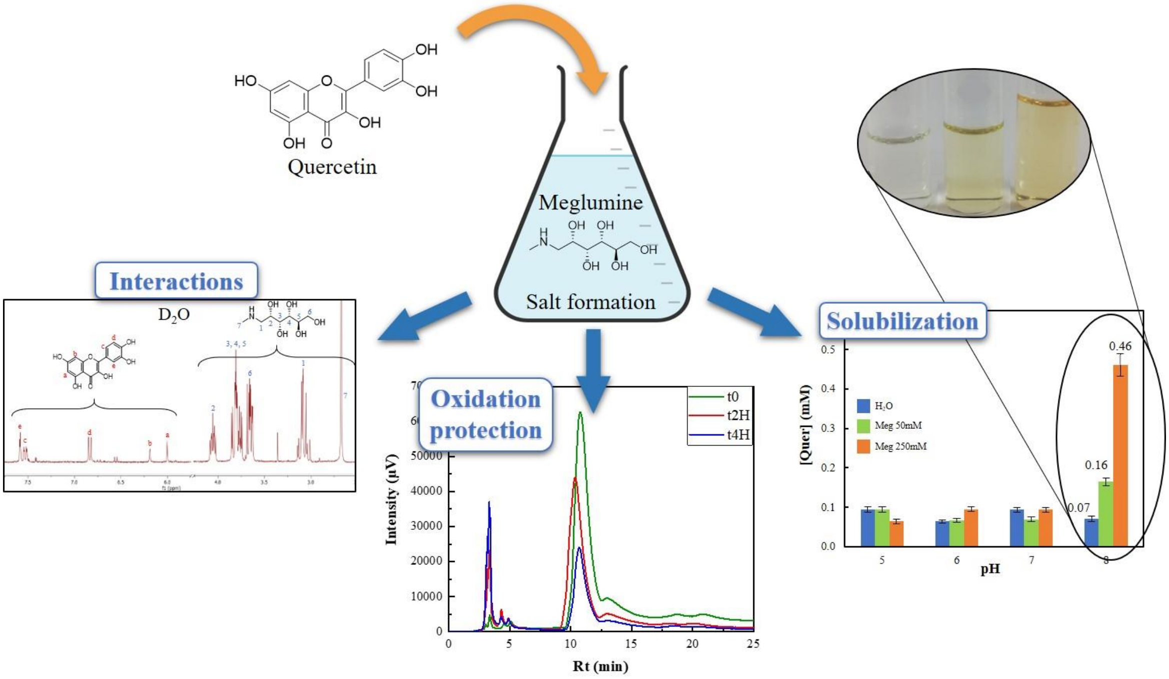
Quercetin
Meglumine
Salt formation
Interactions
D$_2$O
Oxidation protection
t0
t2H
t4H
Intensity (µV)
Rt (min)
Solubilization
[Quer] (mM)
pH
H$_2$O
Meg 50mM
Meg 250mM
0.46
0.16
0.07

I.1. Introduction

In solution chemistry, solubility is a key parameter. The solvation of organic compounds opens up a wide range of applications, from catalysis to biology. Water is often considered the universal solvent, due to its versatile physicochemical properties (high polarity, which translates into a high dielectric constant, great potential for hydrogen-bonding, easily adjustable pH value, possibility of using salts for the salting-in or salting-out effect[2], etc.), its ubiquity in biology and therefore its importance in pharmaceuticals, and its suitability for industrial applications, due to its safety, cost, availability and ease of use. Although water also has major disadvantages for industrial applications, namely its temperature-limited range in liquid state and its large heat capacity that makes distillation process highly energy consuming, solubilization of hydrophobic compounds in water still represents a great achievement for many fields, such as pharmaceutics. This enables for example the formulation of orally delivered drugs, or the reduction of drugs concentration which can in term reduce hazardous side effects.

Among the numerous hydrophobic substances that would benefit from being solubilized in water, polyphenols often come to mind. This vast family of compounds is still very much researched, as polyphenols lie on the borderline between potential Active Pharmaceutical Ingredients (APIs) and dietary supplements. Indeed, many of them are investigated for their biological activity and potential therapeutic effects.

However, many of these aromatic compounds are very little water-soluble, which restricts their use. To overcome this issue, numerous techniques have been developed to increase the aqueous solubility of highly hydrophobic compounds, all of which holding their own advantages and drawbacks. Meglumine, a very hydrophilic aminocarbohydrate, has been reported to enhance the water solubility of several drug molecules, with little to no data as how this solubilization is achieved. This constituted the initial framework for this part of our study. This chapter focuses mainly on the solubilization of quercetin in aqueous solution, among others. A number of key concepts will therefore first be presented, as well as other methods enabling the incorporation of hydrophobic compounds into aqueous media, in order to highlight the distinctive features of the mechanisms involved in our study.

I.2. Bibliographic background

I.2.1. Concepts of solubilization

I.2.1.1. Solvation, solubility and solubilization

Solvation

Solvation is the mechanism involved in the dissolution of a solute into a solvent, and the dispersion of the solute molecules in the solvent, which become solvated, i.e. they are surrounded by solvent molecules. It occurs spontaneously (within intrinsic solubility limits) when the Gibbs energy of the solution is decreased compared to the sum of Gibbs energies of the solvent and the solute, separately, i.e. when the formation of solvent-solute interactions represents a gain in energy compared to the solute-solute and solvent-solvent ones. Solvation is in this sense a stabilization of the solute in solution. All these interactions involve electrostatic and van der Waals forces, hydrogen bonding and others. Relevant parameters for solvation include solvent polarity, temperature, hydrophobic interactions or hydrogen bonding ability among others[3].

Solvation is described by enthalpy and entropy through the Gibbs energy of solvation ΔG_{solv}, as the process of solvation involves the creation of a cavity in the solvent, a separation of a solute molecule from the bulk, the filling of the solvent cavity by the solute and the dispersion in the solvent (see Figure I.1). The creation of solute-solvent interaction is enthalpically favorable and the dispersion of the solute in the solvent is an entropically favorable process.

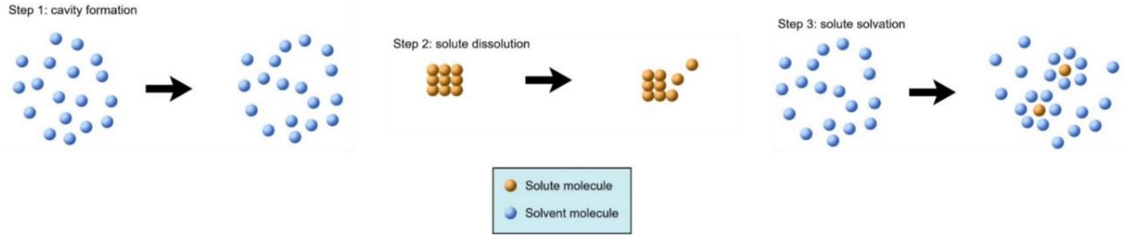

Figure I.1. Schematic representation of the different steps in the solvation process.

It should also be noted that it is possible that a solute may only be partially solvated depending on its structure. Finally, in the case of water as the solvent, solvation is called hydration.

Solubility and solubilization

Solubility (also referred to as maximal solubility, or intrinsic solubility mostly to describe the solubility of a non-ionized species) is a chemical parameter that reflects a substance's inclination towards a given solvent or solvent system, by describing the maximum amount of solute able to be dissolved and solvated in this solvent system. It refers to the analytical composition of a saturated solution, and is as such a quantitative term, although derivatives of the term *soluble* are frequently used qualitatively in biology and pharmaceutics and are based on arbitrary thresholds (see Table I.1). It is generally expressed as a concentration, often given in g/L (generally µg/mL in biology, biochemistry, and pharmaceutics), mol/L, or in weight or mole fraction. By definition, however, it is possible to describe a compound as *soluble* in a solvent at a given concentration lower than its maximum solubility.

Table I.1. Solubility criteria according to the United States Pharmacopeia (USP)[4].

Terminology	**Part of solvent for 1 part of solute**
Very soluble	< 1
Freely soluble	1 – 10
Soluble	10 – 30
Sparingly soluble	30 – 100

Slightly soluble	100 – 1000
Very slightly soluble	1000 – 10,000
Practically insoluble	≥ 10,000

Solubility is a thermodynamic property and is as such fundamentally affected by factors like temperature, pressure, ionization (thus pH), among others (or partial pressure for solvated gases for example)[5]. Solubilization is defined by the IUPAC recommendations as a "process which an agent increases the solubility or the rate of dissolution of a solid or liquid solute"[6] and will be in the rest of this work used accordingly as the effective solvation of a greater amount of a substance into a solvent compared to the solubility of this substance in the same experimental conditions (temperature, pH, etc.).

Finally, mention should be made of the supersaturation phenomenon, which refers to a metastable state in which the concentration of a solvated solute exceeds the intrinsic solubility of the solute. It is achieved by diverse means such as temperature changes, solvent evaporation, or mixing of saturated and near-saturated solutions. Supersaturation can also be seen as a transition state between the solvated state in a saturated solution and crystallization[7]. This phenomenon has practical applications in pharmaceutics as it is often use to formulate oral delivered drugs of low water-solubility active ingredient (SDDS, for Supersaturation Drug Delivery Systems), and where the precipitation is delayed by additives (precipitation inhibitors). Supersaturation is then achieved in the body, typically the stomach or the small intestine[8]. Furthermore, the fundamental differences between the thermodynamically stable solubilization phenomenon and the metastable supersaturation induce differences in biological-relevant parameters, such as free drug concentration, which in turn influence properties such as permeability and absorption of active ingredient molecules[9].

Hydrophily and hydrophobicity

Hydrophily refers to the attraction of a compound or part of a compound towards water. On the contrary, hydrophobicity of a substance refers to being repelled from water molecules through intermolecular forces. The hydrophily (or hydrophoby) is generally quantified by the octane-water partition coefficient P (sometimes noted K_{ow}) or distribution coefficient D (see eq. $\mathrm{I.1}$ and $\mathrm{I.2}$), which represent the ratio of concentrations of a substance in a mixture of two immiscible solvents at equilibrium, octanol and water, i.e. comparing the solubilities of the compound in both solvents. Distribution coefficient accounts for both nonionized and ionized compounds, while the partition coefficient is generally defined as the ratio of the nonionized concentrations only.

$$\log P_{\frac{o}{w}} = \log\left(\frac{[solute]_{octanol}^{nonionized}}{[solute]_{water}^{nonionized}}\right) \qquad (\mathrm{I.1})$$

$$\log D_{\frac{o}{w}} = \log\left(\frac{[solute]_{octanol}^{ionized} + [solute]_{octanol}^{nonionized}}{[solute]_{water}^{ionized} + [solute]_{water}^{nonionized}}\right) \qquad (\mathrm{I.}\,2)$$

These parameters are often simulated and can be useful to assess comparatively the water-solubility of compounds in absence of experimental solubility data for example.

Another particularly important and interesting concept in the field of solubilization are the phenomena associated with the general term *hydrotropy*. These concepts will not be presented here, as they will be extensively described in the third chapter of this thesis.

I.2.1.2. pH influence on solubility

Many organic compounds are weak acids or bases as they bear ionizable groups. Upon pH change, the polarization of these groups is responsible for a modification of the overall solubility of these substances. Charged molecules are more soluble than neutral ones, therefore is pH a key parameter in the study of the solubility of polarizable compounds, as the ratio between their neutral and ionized form(s) is governed by the pH of the solution relative to their pK_a(s). The pH dependence of the solubility of ionizable compounds is described by the Henderson–Hasselbalch (HH) equations (see eq. I. 3 and I. 4):

$$for\ acidic\ compounds:\ \log S_{tot} = \log S_0 + \log(1 + 10^{pH-pKa}) \qquad (\mathrm{I.}\,3)$$

$$for\ basic\ compounds: \log S_{tot} = \log S_0 + \log(1 + 10^{pKa-pH}) \qquad (\mathrm{I.}\,4)$$

with S_{tot} the total solubility, and S_0 the intrinsic solubility, i.e. the solubility of nonionized species. The pH dependence of a specie can be predicted using the HH equations as long as the intrinsic solubility and the pK_a of that specie are known[10]. In pharmaceutics, the knowledge of pH dependence of drugs solubility is essential, as medium pH in the different parts of the body is a fixed parameter which influences greatly the drug absorption[5].

I.2.1.3. π-stacking

Among the many intermolecular interactions influencing solubility, π-stacking (or π-π-stacking), is of the utmost importance when studying aromatic compounds such as polyphenols. It has long been recognized that aromatic compounds interact specifically with each other, and that this attractive interaction is particularly important in solution chemistry and biology, as it is partly responsible for crystal and protein stability[11]. To explain this counter-intuitive attractive interaction between π systems, two main models have emerged since the 90s; the Hunter-Sanders model and the Wheeler-Houk model.

Hunter-Sanders

The Hunter-Sanders picture make two major assessments. Firstly, the geometries of the π-π-interaction are governed by electrostatic interactions, i.e. rather than a repulsive direct π-π-interaction in a face-to-face geometry (π-stack), it is the π-σ-attraction resulting from other types of geometries (offset π-stack or edge-on) which leads to a favorable interaction. Secondly, this model also states that the major energetic contribution, rather than coming from this electrostatic attraction, arises from van der Waals interactions, which are proportional to the area of π-overlap and vary with the solvent[12].

Furthermore, Hunter and Sanders investigated the influence of the presence of a polarizable group such as a heteroatom on the aromatic ring, as it affects the density of the π-system.[12] According to this model, in a π-stack geometry, as the π-π-interaction is predominant, a π-deficient atom will stabilize the stacking by decreasing the π-electron repulsion. Reciprocally, a π-rich group will destabilize the stacking interaction.

Wheeler-Houk

On the other hand, Wheeler and Houk stated that in the case of an interaction between a substituted and a non-substituted benzene in π-stack (also called sandwich configuration), the substituents directly interact with the π-system of the other aromatic compound through electrostatic interactions rather than indirectly by affecting the density of their own compound π-system[13]. These considerations also arise from the work of Ranger *et al.* who found that binding energies linearly increase with the number of substituents (no matter on which compound) in a π-stack conformation, in contradiction with the polarization-oriented model of Hunter and Sanders in this geometry[14].

Beyond

It is now generally accepted that the substituents of an aromatic system interact with the π-system of others mainly through direct electrostatic interactions as stated by Wheeler and Houk. However, other major contributions to these interactions come from induction, dispersion (predominant in the case of methyl for example[15]), and exchange-repulsion interactions[16–19]. In conclusion, both Hunter-Sanders and Wheeler-Houk models contribute together to understanding the π-π-stacking phenomenon, but the Wheeler-Houk picture is generally dominant[16].

Moreover, studies exploring this topic are relatively recent, and further research is needed to allow for a complete generalization of these concepts to be practically used for exemple in solubility prediction. The main limitation to this generalization is that substituents effects calculations are generally performed based on the interaction between a substituted and a non-substituted benzene, for simplicity reasons of prediction models. As a result, there is a lack of theoretical data on the aggregation of multi-stacked systems (apart for from some well-studied systems like carbon nanotubes) and between several substituted aromatic systems.

Finally, the influence of π-stacking itself on solubility of aromatic systems is not trivial. Indeed, even though it appears to inhibit solubilization by acting as a cohesive force for crystalline structures, it also can be used to as a driving force for solubilization by creating a preferential interaction with another component with better solvation properties (see section III.6).

I.2.2. Drug delivery

Solubilization finds a major application field in pharmaceutics for drug delivery purposes, as the vast majority of new Active Pharmaceutical Ingredients (APIs) are poorly water-soluble (90 % of drug molecules in the discovery process and 40 % of marketed drug compounds[20]), thereby hindering their bioavailability and hence their therapeutic value. The distinction and comparison between the methods studied in this work and other solubilization systems currently used in drug delivery is therefore very relevant. Also, the use of surfactants for micellar solubilization and emulsions will be discussed in the last part of this work.

Inclusion complex

One of the most widespread drug delivery methods is based on inclusion complexes and other cage-like molecules like the famous β- and γ-cyclodextrins. The structure of these excipient is composed of a hydrophobic cavity and a hydrophilic exterior. In the case of cyclodextrins, this is due to the cyclic arrangement of the pyranose units which compose it, forming a cone-shape structure[20]. Hydrophobic APIs are entrapped inside the cavity and the complex retains the aqueous solubility of cyclodextrins thanks to its hydrophilic exterior surface. This technique is praised for its simplicity and also allows for a degree of controlled release, but can be tricky in presence of different APIs in terms of competitivity[21].

Solid dispersions: Liposomes and other lipid nanocarriers

Another set of well-established techniques for carrying hydrophobic compounds in the body are solid dispersions. These mainly include Solid Lipid Nanoparticles (SLNs), Nanostructure Lipid Carriers (NLCs), and other vesicles. The most prominent example of NLCs are liposomes. They are self-assembled spherical structures composed of a bilayer (or multiple layers) of lipidic amphiphilic compounds such as phospholipids. This allows for the entrapment of hydrophobic APIs inside the lipidic bilayer of liposomes as well as the encapsulation of hydrophilic drugs in the interior cavity. Liposomes offer many advantages over other drug delivery technologies, such as greater bioavailability (skin or membrane penetration), possible targeted delivery with surface functionalization, time- or stimulus-dependent release of drugs, reduction of drug concentration, and better stability.[20,21]

Cocrystals

Cocrystals are the result of crystallization of an API with another, therapeutically inactive molecule (called coformer) with specific stoichiometric compositions, where cohesion of the crystal is mainly due to hydrogen bonding. The influence of cocrystal formation on a drug solubility arises from its impact on lattice energy, i.e. the energy required to break the solid structure, and on solvent affinity[22]. This makes the potential increase of solubility dependent on the activities or concentrations of the cocrystal components in the solution. The major risk arises then from recrystallization and subsequent loss of solubility which can occur with a slight excess of coformer[22]. Finally, it is worth mentioning that there is an increasing debate on the classification of cocrystals, as many of them are difficult to distinguish from salts[23].

I.2.3. Polyphenols

Polyphenols are phenolic compounds with multiple phenol rings*. The terms phenols and polyphenols cover around 8000 known natural compounds[24]. In plants, their roles are very diverse and often part of complex mechanisms. Generally, polyphenols are involved in ultraviolet (UV) radiation protection, attraction of pollinators, or protection against microbial invasion to mention but the most common[25]. The diversity of their structures explains the wide variety of functions they assume.

I.2.3.1. Classification

Phenolic compounds are categorized in multiple classes and subclasses according to their structure. Figure I.2 shows a simplified representation of this classification and provides a few examples for each of the subclasses[*].

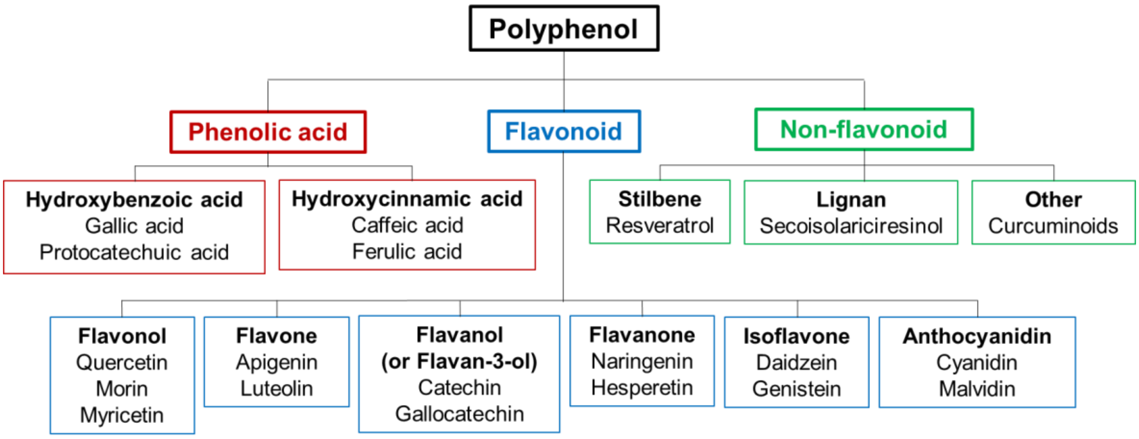
Polyphenol
Phenolic acid
Flavonoid
Non-flavonoid
Hydroxybenzoic acid
Gallic acid
Protocatechuic acid
Hydroxycinnamic acid
Caffeic acid
Ferulic acid
Stilbene
Resveratrol
Lignan
Secoisolariciresinol
Other
Curcuminoids
Flavonol
Quercetin
Morin
Myricetin
Flavone
Apigenin
Luteolin
Flavanol
(or Flavan-3-ol)
Catechin
Gallocatechin
Flavanone
Naringenin
Hesperetin
Isoflavone
Daidzein
Genistein
Anthocyanidin
Cyanidin
Malvidin

Figure I.2. Polyphenols classification.

Flavonoids represent more than 4000 different polyphenols. Their structure is based on a flavane (2-phenyl-benzo-c-pyrane) skeleton with the 3 rings being labelled A, B, and C (see Figure I.3). The substitution of the pyranyl C ring (double bond, carbonyl or hydroxyl group) determines the subclass the polyphenols belong to and the substitution of groups A and B differentiates compounds within these subclasses (Figure I.3). Chalcones (phloretin, xanthohumol,…) are sometimes also considered as flavonoids, because their structure represents an “open” version of the flavonoid skeleton.

---

[*] It is commonly accepted for phenolic compounds with several hydroxyl groups but only one ring to be considered as polyphenols. This will also be the case in this work.

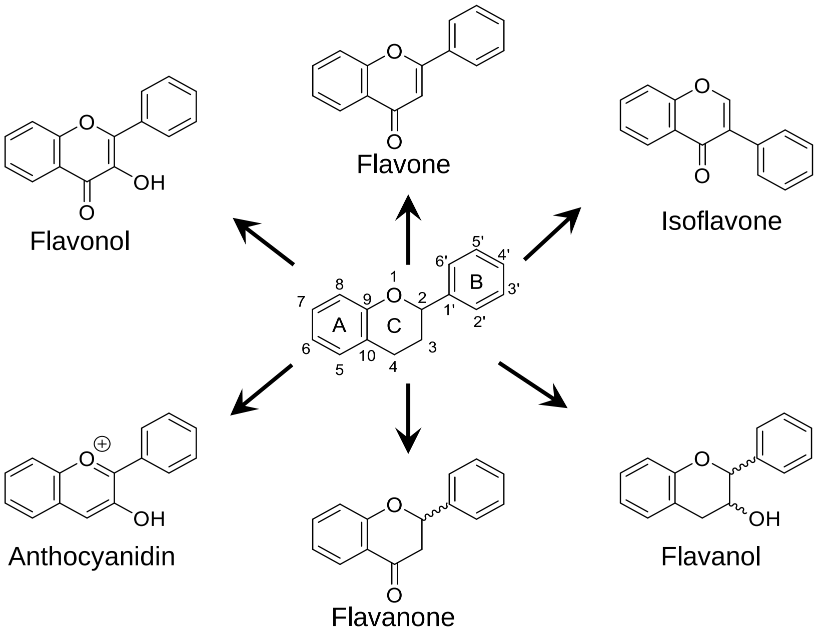

Figure I.3. General chemical structure of flavonoids subclasses. Inspired from reference [26].

Among flavonoids, flavonols and flavanones will receive in this work particular attention, namely with quercetin and morin belonging to the former and naringenin to the latter. Flavonols are characterized by the presence of a double bond between the C2 and C3 carbons and an oxygen atom in position C3. They can exist as aglycone if the latter is a hydroxyl group, or as heteroside with one or more sugar units linked to it, the principals being D-glucose and L-rhamnose. One of the most famous representatives of this sub-class is quercetin (Figure I.4).

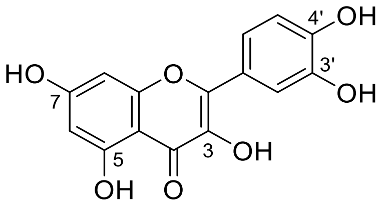

Figure I.4. Chemical structure of quercetin.

I.2.3.2. Natural sources and dietary polyphenols

Phenolic compounds are secondary metabolites mostly found in plants. Many of them are responsible for the coloration of the flowers, leaves, vegetables, and fruits[27], but they are also present in other parts of plants (roots, stems, etc.). Flavonols for example are present in at least 80 % of higher plants, mostly in flowers and leaves[28]. As these compounds are present in high concentrations in fruit and vegetables, they are an intrinsic part of both animal and human diets. Flavonoids and phenolic acids make up 60 % and 30 % of dietary polyphenols, respectively.[29] Beverages like coffee, tea, fruit juices, cacao products, wine, beer, and even vinegar are important flavonoid sources accounting for at least 25-30 % of the total flavonoid intake, where fruits and vegetables represent around 50 %. Average intake of all flavonoids is estimated to be 1 g/day[28] with quercetin being one of the most abundant dietary flavonoids[30]. Figure I.5 shows the average quantities of quercetin found in food sources according the database Phenol-Explorer.

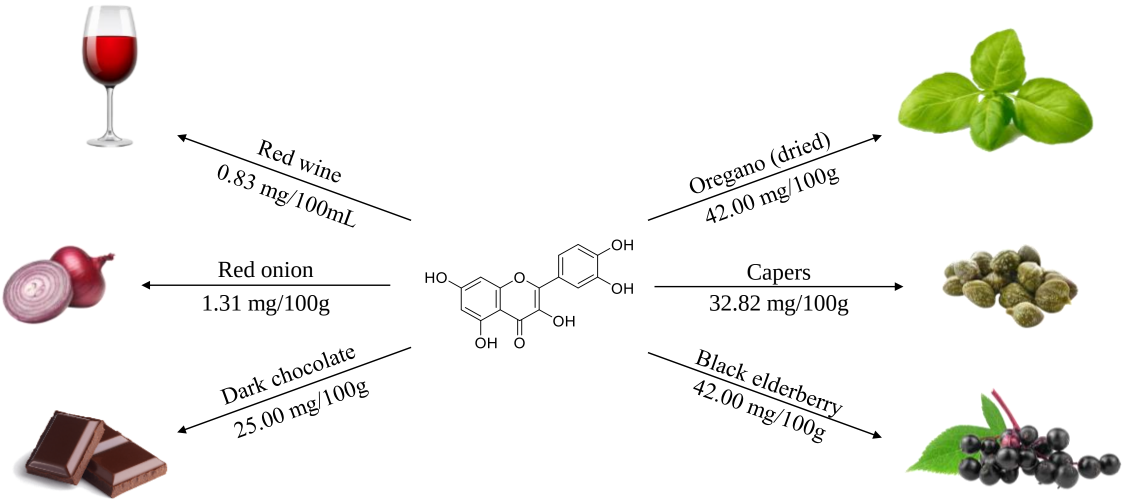

Figure I.5. Examples of abundant sources of dietary quercetin (data from Phenol-Explorer (http://phenol-explorer.eu/).

All in all, most food sources contain complex and often poorly characterized mixtures of polyphenols, with for example different monomer and oligomer distribution or several glycosides derivatives for a single polyphenol[31] .

I.2.3.3. Properties

Polyphenols have gained extreme popularity in the past four decades and have been since then widely studied for their chemical and biological properties. Numerous studies reported potential health benefits with the intake of a polyphenols-rich diet and have been focused on understanding the individual effects of these compounds, as well as possible synergies and antagonisms[32,33]. Nevertheless, this attention came somewhat late for such a large group of phytochemicals. This can be explained by the shear diversity and the complexity of the chemical structures and therefore properties of these compounds.

I.2.3.3.1. Alleged biological activities

The most notable recognized biological properties of polyphenols are their antioxidant, anti-inflammatory and anti-cancer activities. Some phenolic compounds exhibit rarer activities such as antiarthritic or antiplasmodic properties for example in the case of morin[34,35] while naringenin is known to exhibit antiulcer and anti-bacterial activities in addition to its anti-inflammatory property[36,37]. It is also recognized that polyphenols help reduce the risk of cardiovascular diseases[21]. Indeed, it has been shown that a polyphenols-rich diet could be efficient in reducing cancer risk and coronary heart diseases (CHD) occurrence, a phenomenon known as the "French paradox", describing the seemingly unintuitive relation between the fat-rich diet and tobacco consumption and the relatively low occurrence of these pathologies among the French population (then extended to other Mediterranean populations[38]) in comparison with other European countries. Research had since been focusing on discriminating the polyphenols responsible for this pattern. For instance, the stilbene *trans*-resveratrol, mostly found in red wine in the human diet, has been identified as one possible candidate. The dihydrochalcone phloretin is another example, widely found in apples[39–41]. Finally, xanthohumol, a compound primarily found in hop (*Humulus lupulus L.*), and therefore included in the human diet through beer consumption, has gained popularity in the past decade in the scientific community for its alleged neuroprotective properties[42]. The principal alleged beneficial biological activities of known polyphenols are summarized in Figure I.6.

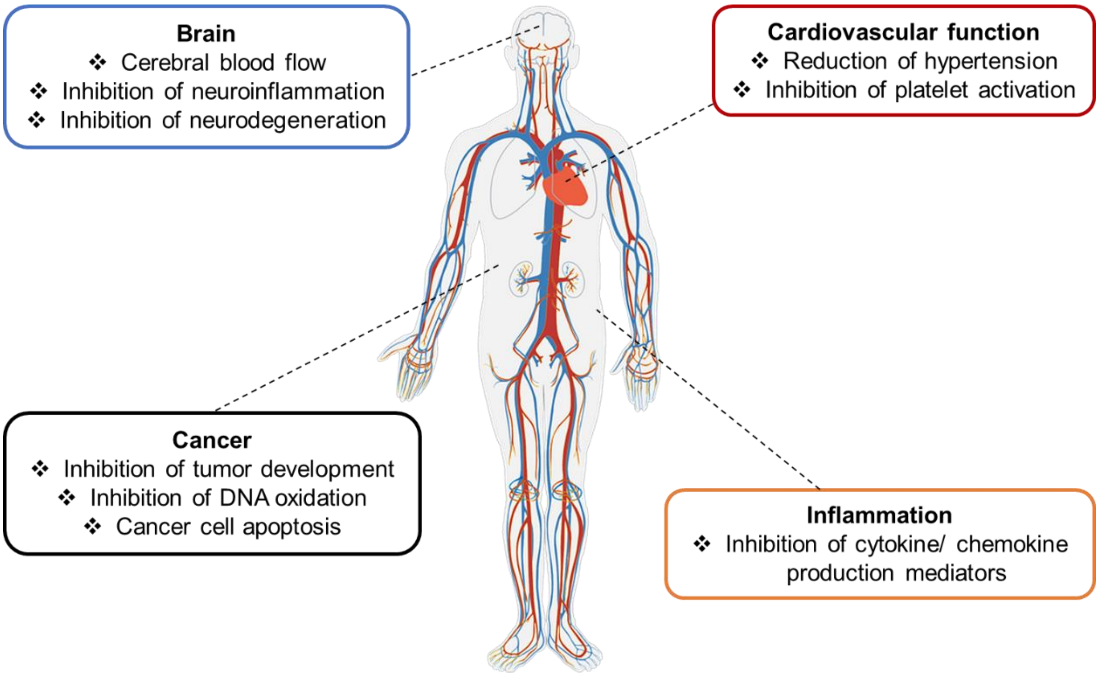
Brain
❖ Cerebral blood flow
❖ Inhibition of neuroinflammation
❖ Inhibition of neurodegeneration
Cardiovascular function
❖ Reduction of hypertension
❖ Inhibition of platelet activation
Cancer
❖ Inhibition of tumor development
❖ Inhibition of DNA oxidation
❖ Cancer cell apoptosis
Inflammation
❖ Inhibition of cytokine/ chemokine production mediators

Figure I.6. Overview of the potential beneficial effects of polyphenols on human health. Inspired from reference [26].

Quercetin meanwhile, is well known for its therapeutic properties, in particular antioxidative and anti-inflammatory, but could also exhibit very promising anticancer activities[21] and is one of the most researched flavonoids for the explanation of the “French paradox”[43]**.** More specifically, quercetin has been shown to inhibit platelet aggregation and secretion *in vitro*[44]. This effect has been shown to be specific to quercetin's structure, indeed saturation of the C2-C3 double bond, and/or a lack of carbonyl on C4 or glycosylation (in C3) reduces the inhibitory effect by a factor of 10. Interestingly enough, uptake of supplementary quercetin in the form of capsule of anhydrous quercetin in healthy individuals led to higher quercetin concentrations in plasma but did not alter cardiovascular or thrombogenic risk factors compared to dietary intakes associated with lower CHD mortality[45]. Finally, quercetin has been investigated for its neuroprotective activity. It has indeed been demonstrated that quercetin significantly attenuated manganese-induced neurotoxicity in rat[46].

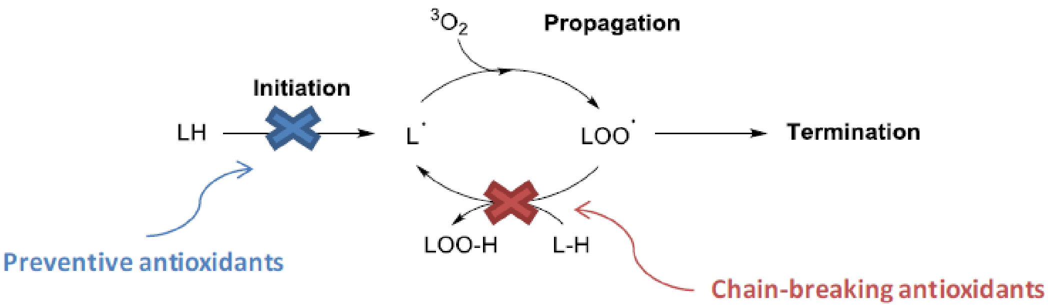

Figure I.7. Mechanisms of inhibition of oil oxidation by primary and secondary antioxidants. Reproduced with permission from reference [47].

It should also be emphasized that quercetin metabolites formed after absorption by the body may express distinct biological activities or at a different level than native quercetin[26]. The ability of certain quercetin metabolites to retain antioxidant potency for instance has been established (in rat[48]), when some studies argue that some metabolites have lower antioxidant effect (for reduction of ferric ion Fe^{3+} in FRAP assay[49]). Another study showed the ability of certain quercetin glucuronides metabolites to inhibit xanthine oxidase and lipoxygenase as well as the unconjugated quercetin, and therefore to act as potent anti-inflammatory agents, where other were less efficient[50]. Conservation of anti-inflammatory effectiveness in the metabolites was found to depend on the conjugation position. In any case, discrepancies observed between *in vitro* and *in vivo* results call for the utmost caution when claiming any therapeutic activity for polyphenols[49].

I.2.3.3.2. Autoxidation and antioxidant activity

In nature, free radicals' production, responsible for oxidation, may be the result of stress or other external factors. Oxidation damage caused by free radicals to biomolecules like lipids, proteins or nucleic acids can be harmful to cells and lead to hepatic and infectious diseases or neurological, gastrointestinal, immunological disorders among many others[51]. Moreover, the presence of metals can lead to conversion into even more toxic species[51]. An antioxidant is a compound that undergoes oxidation instead of the compound of interest it is intended to protect.

Many phenolic compounds are potent antioxidants able to scavenge free radicals and reacting oxygen species (ROS) through three main mechanisms: single electron transfer (SET), proton exchange (hydrogen atom transfer, HAT) and transition metal chelation (TMC), described in Figure I.8[52,53].

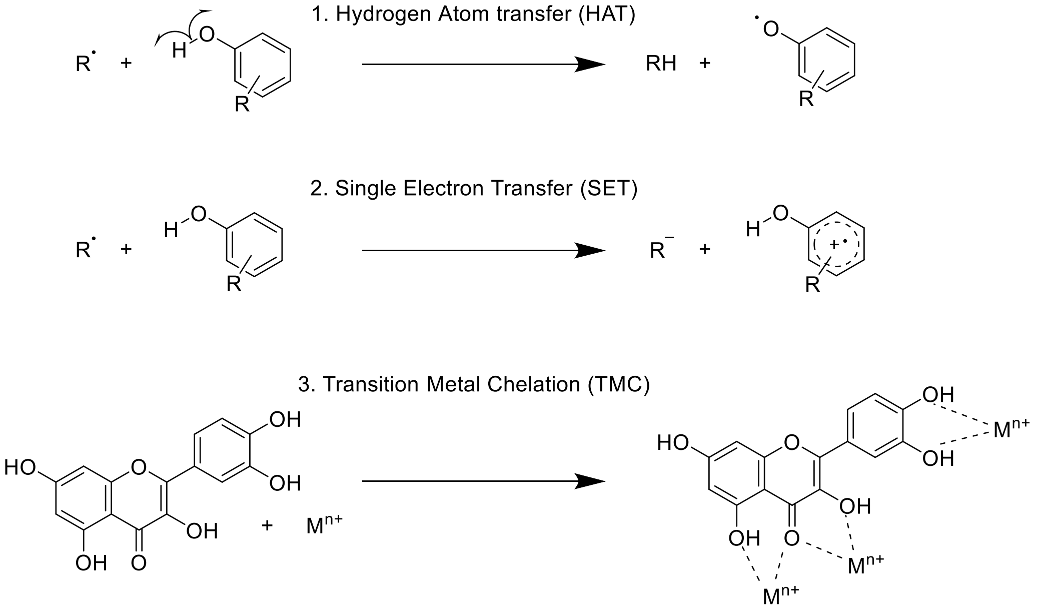
1. Hydrogen Atom transfer (HAT)
R•
+
H
O
R
RH
+
O
R
2. Single Electron Transfer (SET)
R•
+
H
O
R
R−
+
H
O
+•
R
3. Transition Metal Chelation (TMC)
HO
O
OH
OH
OH
OH
O
+
Mn+
HO
O
OH
OH
OH
OH
O
Mn+
Mn+
Mn+

Figure I.8. Mechanisms of phenolic antioxidative activity (example of quercetin for TMC). Inspired from reference [53].

In apolar solvents, polyphenols express their antioxidant activity through lipid radical inhibition following the HAT mechanism. In polar solvents however, polyphenols have been found to react according to another mechanism, the Sequential Proton Loss Electron Transfer (SPLET), which involves the equilibrium between phenol and phenolate forms[54,55]. Rapidly, this corresponds to the transfer of an electron from the phenolate form to the radical, which then receives a labile proton[47] (see Figure I.9).

$$ArO{-}H + R^{\bullet} + S \rightarrow ArO^{-} + R^{\bullet} + SH^{+}$$

$$ArO^{-} + R^{\bullet} + SH^{+} \rightarrow ArO^{\bullet} + R^{-} + SH^{+} \rightarrow ArO^{\bullet} + R{-}H + S$$

Figure I.9. Reactions of phenolic oxidation in polar solvent (S) according to the SPLET mechanism.

As the SPLET mechanism is mostly dependent on the polarity of the solvents and the acidity of the phenols, pK_a is thus a key parameter for polyphenols oxidation. Furthermore, as the oxidation mechanism relies on hydrogen and/or electron transfer, polyphenols with a greater stoichiometry will generally have a greater capacity to scavenge radicals. The Bond Dissociation Enthalpy (BDE), which is the energy required to perform a homolytic break on a phenolic bond ($ArO{-}H$)[56], as well as the kinetic constants k for proton transfer from phenols to alkoxyl $RO^{\bullet}$ and peroxyl $ROO^{\bullet}$ radicals (see Figure I.8, 1.) are also relevant means to quantify the reactivity of phenolic compounds towards oxidation. These parameters are however mostly relevant in the case of HAT mechanism, and will therefore not be extensively considered in the experimental part of this study in contrast to pK_a, as most of it is carried out in aqueous solution, i.e. in polar solvent.

Other experimental methods for the determination of antioxidant activity include ABTS assay, diphenylpicrylhydrazyl (DPPH) test and the Trolox Equivalent Antioxidant Capacity

(TEAC) assay, which measure the antioxidant capacity in comparison to a standard, Trolox[57].

Specificity of C3-OH on flavonoid oxidation

Not all polyphenols or even flavonoids have the same behavior towards oxidation phenomena. Several predominant criteria have been identified[58,59]:

- the presence of a C2-C3 conjugated double bond
- the presence of a hydroxyl group carried by carbon C3
- to a lesser extent the orthodiphenolic structure of the B ring (3',4'dihydroxy substituted)

There also seems to be a synergy between the presences of the C2-C3 double bond and the C3-OH group[59], i.e. there seems to be a clear distinction in oxidation resistance between flavonols (quercetin, myricetin, fisetin, kaempferol, etc.) on the one hand, and flavones and flavanones on the other. The importance of the C3-OH in the oxidation reactivity has also been highlighted by Wang and coworkers who identified similarities between quercetin and fisetin behaviors regarding oxidative degradation and factors affecting it (alkaline pH and high temperature enhances degradation rates)[60] but discrepancies with luteolin (same structure as quercetin without the C3-OH).

Quercetin autoxidation mechanism

Quercetin in particular, which combines all three criteria mentioned above, is believed to be even more reactive towards oxidation than the other flavonols. The Trolox Equivalent Antioxidant Capacity (TEAC) value reported for quercetin is 4.72 ± 0.10, compared to 1.34 ± 0.08, 2.55 ± 0.02, and 3.12 ± 0.28 for kaempferol, morin, and myricetin, respectively.

It has been reported that in the presence of air, quercetin undergoes quick degradation, which is catalyzed by temperature and pH.[61] However, the precise mechanisms of quercetin oxidation pathways are still debated. These pathways firstly depend strongly on the medium and can therefore vary[62]. It is widely accepted that the process includes the cleavage of the γ-pyrone fragment (ring C) with formation of a depside under the form of 4,6-dihydroxy-2-(3,4-dihydroxybenzoyloxy)benzoic acid[63]. The most frequently invoked mechanism involves then a nucleophile attack on the C4 carbonyl group of the depside, i.e. a decarbonylation, releasing carbon monoxide CO[64]. Zenkevich *et al*. showed however through direct head-space analysis that the concentration of released CO in moderately-basic medium (pH ~ 8-10) in aqueous solution was not in total agreement with this mechanism, and proposed instead a pathway involving a decarboxylation with formation of carbon dioxide CO_2 [63]. Furthermore, their hypothesis would give a preponderant role to the keto-enol tautomerization of quercetin in the oxidation mechanism (see section I.2.3.4.2).

Finally, the behavior of quercetin in the presence of metallic cations has been extensively studied in the literature[65], but will not be investigated in this study. In any case, one of the most important aspects of quercetin oxidation for this study is not the mechanism(s) at work but the various oxidation by-products that may result from this cleavage.

Oxidation sub-products of quercetin

In this section, the first intermediaries formed directly upon cleavage of the γ-pyrone fragment are not considered as oxidation products, because their lifespan under oxidation favorable conditions is significantly short compared to the so-called “final” oxidation sub-products of quercetin. There are three main oxidation products of quercetin, namely protocatechuic (3,4-dihydroxy-benzoic acid) and phloroglucinic (2,4,6-trihydroxybenzoic acid) acids and phloroglucinol (1,3,5-trihydroxybenzene)[63,64] (see Figure I.10). Phloroglucinol itself would result from the oxidative decarboxylation of the phloroglucinic acid. The structure of these products makes them more soluble in water than native quercetin, but has also repercussion on other phenomena, such as π-stacking (see section III.6.2).

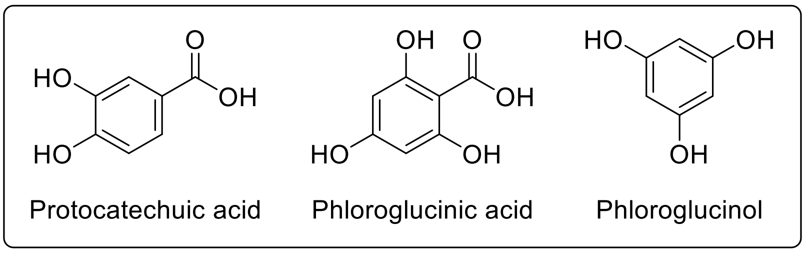

Figure I.10. Chemical structure of the main oxidation products of quercetin: protocatechuic acid, phloroglucinic acid, and phloroglucinol.

I.2.3.3.3. Solubility, bioavailability, and pharmacokinetics of quercetin

Due to their wide range of biological activities and relative abundance in natural sources, polyphenols have been recognized as very promising therapeutic agents. However, the efficacy of these compounds as active ingredients is closely linked to their bioavailability. Bioavailability is a pharmacological concept that describes the ability of an active ingredient absorbed by the body to reach the blood circulatory system. For orally delivered compounds such as dietary supplement, bioavailability often simply refers to the absorbed fraction of the ingested drug. Bioavailability involves a number of parameters, such as the aqueous solubility of compounds, intestinal absorption, distribution at tissues level, excretion among the most important[31]. These parameters obviously depend on the chemical structure of the active ingredients. For instance, numerous polyphenols are not highly hydrophilic or hydrophobic, and therefore are expected to be active at water-lipid interfaces[31]. It is also essential to note that due to the great diversity of polyphenols, their bioavailability differ significantly from one another, and the most abundant polyphenols in human diet are not necessarily the most bioavailable[31].

Furthermore, the enzymatic reactions (e.g. hydrolysis of glycosides derivatives by the gut microflora) and the conjugation of polyphenols after absorption have a strong influence on bioavailability. Indeed, through methylation, sulfation and glucuronidation, the 3 main types of conjugation mechanisms[31], metabolites can exhibit a strongly different bioavailability relative to native polyphenols. For example, pharmacokinetic analysis of quercetin metabolites in plasma after intake of 270 g fried onions revealed significant concentrations of quercetin-3'-O-sulfate and quercetin-3-O-glucuronide and to a lesser extent presence of isorhamnetin-3-O-glucuronide, quercetin-3-O-diglucuronide and quercetin-3-O-glucuronide-O-sulfate[26], and the diversity of these structure naturally affects the various solubility and permeability factors. In addition, the many interactions that can occur between polyphenols and other dietary compounds, such as binding with proteins or polysaccharides, can impact absorption[31]. Finally, the human diet can also affect physiological parameters such as gut pH, intestinal fermentation, transit time, excretion, etc., and indirectly influence polyphenols absorption[31].

Despite the difficulty of grasping all these factors, it is nevertheless possible to better characterize a given drug according to its bioavailability. In order to do so, a classification has been introduced by Amidon and coworkers in 1995[66]. This Biopharmaceutic Drug Classification, later renamed Biopharmaceutics Classification System (BCS), sorts substances into four groups or classes according to two parameters considered as central for bioavailability: aqueous solubility and intestinal permeability (see Figure I.11).

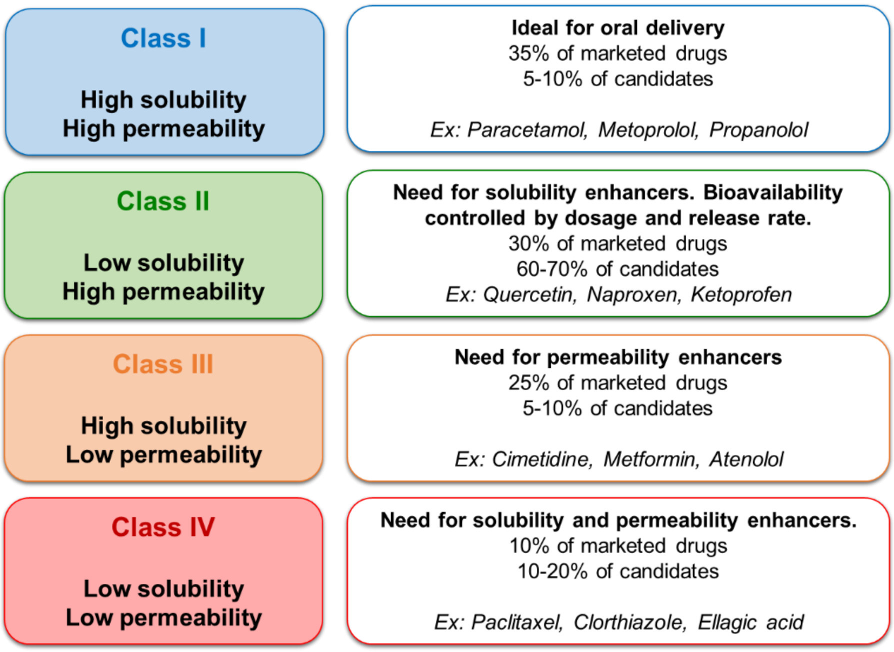

Class I **High solubility** **High permeability**	**Ideal for oral delivery** 35% of marketed drugs 5-10% of candidates *Ex: Paracetamol, Metoprolol, Propanolol*
Class II **Low solubility** **High permeability**	**Need for solubility enhancers. Bioavailability controlled by dosage and release rate.** 30% of marketed drugs 60-70% of candidates *Ex: Quercetin, Naproxen, Ketoprofen*
Class III **High solubility** **Low permeability**	**Need for permeability enhancers** 25% of marketed drugs 5-10% of candidates *Ex: Cimetidine, Metformin, Atenolol*
Class IV **Low solubility** **Low permeability**	**Need for solubility and permeability enhancers.** 10% of marketed drugs 10-20% of candidates *Ex: Paclitaxel, Clorthiazole, Ellagic acid*

Figure I.11. Schematic representation of the Biopharmaceutics Classification System as first conceptualized by Amidon *et al.* Adapted with permission from reference [1].

Although simplistic, this approach allows to quickly understand on which parameters one can play to optimize the bioavailability of a product whose characteristics are sufficiently well known to be classified in a category. In order to do so, several protocols for solubility and permeability measurements *in vitro* and *in vivo* have been standardized[67]. It should be noted that sub-categories have since been added to refine this concept, for example with the division of BCS class II and IV in 3 sub-classes for acid, base and neutral specifications, based on pK_a of the drugs[68], and that dissolution kinetics of the drug are also considered. In addition, this methodology has been recommended by the FDA (Food and Drug Administration) in the USA as a powerful tool to be used as guideline for the industry[69].

Given these considerations, it appears that the compounds over which one has the most leverage to optimize bioavailability are those of BCS Class II. Quercetin belongs to this category. As such, it is well-known that the major hindrance to the development of quercetin as an orally delivered active ingredient is its virtual insolubility at physiological pH (< 0.05 mM[70]). It is thought that around 1 % of ingested quercetin is actually absorbed by the body[71], even if it could not be fully representative of the absorption and metabolism mechanisms of dietary flavonoids because of their wide diversity and distribution and therefore their potential interactions[30]. Indeed, pharmacokinetics of quercetin and its metabolites are complex have been the subject of dedicated studies[61,72,73]. The very poor aqueous solubility of quercetin probably directly results from the stability of its crystalline form, which can be explained by a dense network of hydrogen bonds and π-stacking[74]. Furthermore, quercetin is known to aggregate with other compounds, like proteins[75] and pigments such as anthocyanidins, where the interaction with quercetin induce a color change through modification of the overall π-system[76].

I.2.3.4. Specific structural properties of quercetin

I.2.3.4.1. Dissociation constants and deprotonation order

***pK$_a$* values**

As phenolic compounds bear hydroxyl groups, there are prone to become negatively charged through deprotonation. The state of charge as well as the distribution and equilibria between the different forms of polyphenols, described by the acidic constant pK$_a$, are particularly important for several reasons. Firstly, the aqueous solubility of polyphenols is closely linked to their charge state, as charged compounds are significantly more soluble than neutral ones (in polar solvents). Moreover, as described in the section I.2.3.3.2, in polar matrixes, therefore in aqueous solutions, polyphenols undergo an oxidative mechanism involving an equilibrium between phenols and phenolates. Thus, the antioxidant activity is closely linked to the pH of the medium and therefore also to the pK$_a$ of the polyphenols.

For most polyphenols, pK$_a$ values have been experimentally determined (generally by spectrophotometry or potentiometry) and are available from numerous studies. However, a number of oxidation-sensitive polyphenols, notably flavonols, degrade too rapidly in alkaline media (see section I.2.3.3.2) to precisely quantify all pK$_a$ values, despite these being expected to be lower than those of flavanols, for example, due to the conjugation of the A and C rings, which facilitates deprotonation by charge delocalization[77]. One of the most striking examples of this is once again quercetin. It is well known that in even mildly alkaline medium (pH > 8), quercetin oxidizes very rapidly to form numerous by-products (see section I.2.3.3.2). The consequence is that no values for pK$_a$ 3, 4 and 5 of quercetin can be easily obtained by standard experimental methods. Another difficulty is the very low aqueous solubility of quercetin at physiological pH, resulting in disparities even for the values of the first two pK$_a$s, which should yet be experimentally more easily obtainable.

Other protocols have been used to overcome these obstacles with more or less success, while many authors rely on simulation values. Enhancing the solubility of quercetin in aqueous solvent by mixing water with a fraction of organic solvent such as ethanol or methanol is for example a common practice but introduces a slight deviation in pH measurement, and ultimately in pK_a values. Temperature or ionic strength are other two other factors influencing deprotonation, thereby making comparison of literature data even more hazardous. Table I.2 summarizes a few examples of quercetin pK_as values found in the literature.

Table I.2. Some pKa values of quercetin reported in the literature. Number in brackets represent the hydroxyl group being deprotonated.

Methods	Conditions	pK_a1	pK_a2	pK_a3	pK_a4	pK_a5	Reference
Spec[†]	H_2O/ EtOH	7.03 (3’or 4’)	9.15 (7)	/	/	/	78
Spec	H_2O, $I = 0.10$ ($NaNO_3$)	5.7	7.1	8.0	9.9	11.0	79
Spec	H_2O /MeOH (1:1)	8.45	9.31	11.12	/	/	80
SPARC[†]	$I = 0$	7.04 (7)	8.55 (4’)	11.26 (5)	13.06 (3)	/	77
CE[†]	$I = 0.05$	7.19 (7)	9.36 (4’)	11.56 (5)	/	/	77
Pot[†]	H_2O, $I = 0$	7.59	9.33	11.56	/	/	81
Pot	H_2O, $I = 0$, T = 28°C	3.52	9.36	/	/	/	82
Pot	H_2O, $I = 0.0024$ (NaNO3), T = 28 °C	3.47	9.24	/	/	/	82
Pot	H_2O, $I = 0.034$ (NaNO3), T = 28 °C	3.36	8.99	/	/	/	82
Pot	H_2O, $I = 0.062$ (NaNO3), T = 28 °C	3.29	8.78	/	/	/	82

It is clear that the precision of the determined values seems paradoxical given the wide disparities between values that are associated with the same deprotonation.

Hydroxyl groups deprotonation order

Another major challenge, particularly important for understanding quercetin solubilization and oxidation mechanisms, is assigning an acidity constant value to a specific hydroxyl group. A number of studies have attempted to determine the order of deprotonation of quercetin's 5 hydroxyl groups (albeit theoretically to some extent, as it has been established that the last 2 or even 3 deprotonations are not commonly experimentally observed). The most common experimental methods for that determination are spectrophotometric titration, capillary electrophoresis, as well as ^1H NMR and ^{13}C NMR chemical shifts monitoring of the hydroxyl groups.

Although there is no strong agreement in the literature, the deprotonation order 4’-OH < 7-OH (alternatively 7-OH < 4’-OH) < 3’-OH < 3-OH < 5-OH[83] seems to be generally recognized as the most probable one. Most studies agree that the 5-OH group is always associated to the highest pK_a value, as its deprotonation should be hindered by intramolecular hydrogen bonding with the adjacent carbonyl group. Group 3-OH is also generally seen as less readily deprotonable than the groups present on rings A and B. Álvarez-Diduk and coworkers agree for instance with this deprotonation order, which they obtained using a computational method in order to compare the Gibbs Free Energies upon deprotonation on each site, where the site of minimum energy for each deprotonation being the most likely to be deprotonated[84]. One exception is the work of Milane *et al.* who reported the first deprotonation to concern the 3-OH, by comparing the ^{1}H NMR chemical shifts assigned to the 5 hydroxyl groups upon deprotonation[85].

[†] Spec = spectrophotometry, Pot = potentiometry, CE = capillary electrophoresis, I = ionic strength. Note that the pK_a number is not assigned to a particular hydroxyl group but just reflects the number of pK_a effectively determined by each method.

I.2.3.4.2. Influence of geometry on intermolecular interactions of quercetin

Keto-enol tautomerization

Quercetin can undergo a keto-enolic equilibrium (Figure I.12). This equilibrium appears to play an important role in its solubilization and stability. Indeed, in its enol form, quercetin is an almost completely planar molecule in its preferential conformations[86], but its geometry is strongly modified in its ketone form, and this process is accompanied by a modification of its dipole moment and by breakage or formation of intramolecular specific interactions like hydrogen-bonds and attractive van der Waals interactions[87].

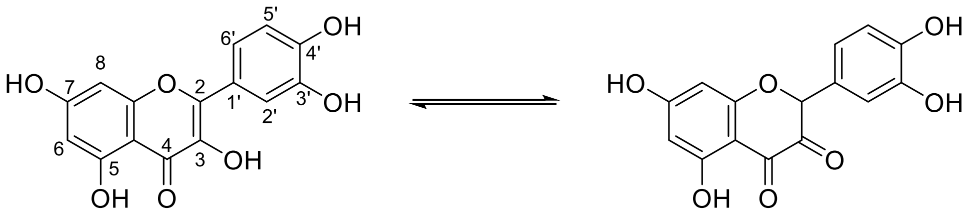

Figure I.12. Keto-enol tautomerization of quercetin.

Computational study from Brovarets' *et al.* showed that the tautomerization of quercetin through intramolecular proton transfer can occur according to different pathways, the most probable one being a single proton transfer from the 3-OH group to the C2' carbon atom of the B ring (see Figure I.12) assisted by the strong (~28.5 kcal.mol^{-1}) intramolecular 3-HO··· HC2' hydrogen-bond[87].

Furthermore, it was reported that tautomerization occurs preferentially between the monoanionic forms of quercetin[88]. Thus, the tautomerization which very probably induces a solubility enhancement of quercetin by breaking the π-stacking could be triggered by a pH increase, which also increases quercetin water-solubilization through the formation of (poly)phenates.

Hydrogen bonds network and π-stacking

Quercetin possesses 5 hydroxyl groups, and in total 5 potential hydrogen bond (HB) donors (the hydrogen atom of the hydroxyl groups) and 14 potential hydrogen bond acceptors (lone pairs of electrons of the oxygen atoms of the keto and the carbonyl groups, and the one of the hydroxyl groups), enabling the potential formation of a significant number of both intra- and intermolecular hydrogen bonds. The 5-OH group is very likely to form an intramolecular hydrogen bond with the adjacent carbonyl group (see Figure I.4 and Figure I.17. Graphical representation of surface polarization as calculated by COSMO-RS software, here with the example of quercetin in its native form. The dotted line in the quercetin structure represents hydrogen bond predicted by COSMO-RS.), thus greatly hampering its deprotonation. This is however not the only effect that hydrogen bonds can have on quercetin's properties. The great amount of potential intermolecular hydrogen bonds of quercetin from all sides is also responsible for its extreme stability in crystal form, alongside π-stacking, and plays an important role in quercetin interaction with water molecules, whether in solution or in solid form[74].

Moreover, the planarity of the enol form could explain its stability in water compared to the ketone through the attractive interactions resulting from van der Waals, hydrogen-bonding and preferential π-stacking. This could also explain why quercetin is stable in non-protic solvents such as DMSO, where the tautomerization is unfavored.

I.2.4. Meglumine

I.2.4.1. History and uses

N-Methyl-D-glucamine, commonly known as meglumine (see structure in Figure I.13), is an aminocarbohydrate derived from glucose used mainly in pharmacy and cosmetics. It has been historically first used as contrast agent for medical imagery[89], and as treatment for Leishmaniosis disease (as antimonial complex)[90].

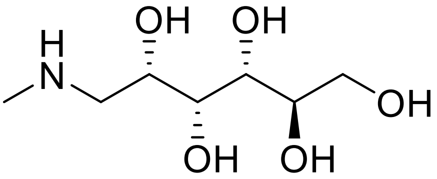

Figure I.13. Chemical structure of meglumine.

It has also been discovered in the last century that it could act as a solubilizer for the poorly water-soluble rutin[91] and it was later confirmed that meglumine could interact with the weakly acidic carboxylic or carbamic groups of nonsteroidal anti-inflammatory and analgesic drugs (NSAID) by salt formation[92]. Surprisingly, it's only much more recently that meglumine has been widely employed as a solubilizer for poorly water-soluble active ingredients such as triclosan[93], celecoxib[94], sulfamerazine[95,96], indomethacin[97], or honokiol[98]. However, meglumine is nowadays mostly known as a complex of flunixin, a NSAID widely used for cattle and horses. Meglumine is also used as part as larger solubilization systems, often in association with β-cyclodextrin[95,99,100]. Meglumine has also been recently designated as a hydrotrope by Li *et al.* to describe its role in the solubilization of glimepiride[101]. Degot *et al.* identified it as a solubilizer of curcumin[102]. The main goal of all these studies is to enhance the bioavailability of an active ingredient by tuning its water-solubility or to help encapsulate it in a given delivery system. Another recent field of application worth mentioning is catalysis. Meglumine has been marketed as green catalyst for a wide range of reactions[103–105].

I.2.4.2. Properties

Meglumine has many advantageous features. It is highly water-soluble, very inexpensive and edible[106], which allows it to be easily processed in a wide range of formulations. With a pK_a of 9.6[102], meglumine is a potent base and an aqueous solution of a few percent commonly exhibit a pH between 10.7 and 11.3. Its solubilization properties come most likely through proton exchange of its amino group to form a salt with the weakly acidic drugs[91,92]. The interaction between meglumine and carboxylic acids will be discussed in more details in Chapter IV.

I.3. Experimental part

I.3.1. Materials

Meglumine (> 99 %) was purchased from TCI Chemicals and quercetin (HPLC grade) from Merck, as for xylenol orange tetrasodium salt. Curcumin (≥ 97 %), Naringenin (≥ 93 %), and *trans*-resveratrol (≥ 98 %) were also purchased from TCI Chemicals, gallic acid (≥ 95 %) from Acros, and phloretin (≥ 90 %) from Symrise. NaOH, HCl, MeOH, and acetone, were used for pH adjustments and UV-vis measurements. Deionized water from Milli-Q Millipore equipment was used to prepare all solutions (18.20 MΩ resistivity).

I.3.2. Methods

I.3.2.1. Solubilization measurements

Solubilization experiments of quercetin and other polyphenols were carried out by UV-vis spectroscopy. Aqueous stock solutions of 50 and 250 mM meglumine (roughly corresponding to 1 and 5 wt%, respectively) were prepared by dissolving meglumine in ultrapure water. 3 mL samples were prepared at 20 °C and pH was adjusted by addition of an appropriate amount of aqueous HCl or NaOH. Quercetin was added stepwise until visible precipitation occurred, indicating complete saturation. The samples were shaken manually for about 30 s for homogenization. Unsolubilized quercetin was removed either by centrifugation (5000 rpm, 5 min, 20 °C) and the supernatant recovered, or by filtration (PTFE, 0.45 µm). No difference on quercetin solubilization was observed between these two variations of the protocol. Dilutions with methanol (1:100 to 1:500) were carried out prior to UV-vis spectroscopy measurements. A Beer-Lambert calibration curve of native quercetin in methanol was constructed to calculate the amount of solubilized quercetin. All the measurements were carried out within 10 min after the addition of quercetin to minimize the oxidation process. Every sample was prepared in triplicate to ensure reproducibility and statistical reliability. The same protocol was applied with the other phenols tested, namely curcumin, gallic acid, naringenin, phloretin, and trans-resveratrol.

I.3.2.2. UV-Visible spectroscopy

UV–vis spectra were recorded on an Agilent Technologies Cary 60 UV–vis spectrometer in 1 cm path length quartz cells. Native quercetin was measured at $\lambda = 370$ nm.

I.3.2.3. ^{1}H NMR spectroscopy

NMR spectra were recorded on an Avance III 3 (Bruker, US) at 300 MHz for ^{1}H. Spectra of meglumine and solubilized quercetin in aqueous phase were recorded in D_2O, and DMSO-d_6 was used for pure quercetin analysis. TMSP-d_4 was added for calibration.

I.3.2.4. Quercetin oxidation stability assessment

I.3.2.4.1. Oxidation precaution measures

Since quercetin has been shown to be particularly sensitive to oxidation, a number of experimental preventive measures were taken. Presence of oxygen, direct light and temperature are indeed factors to be controlled in order to slow down quercetin degradation, which is inevitable at working pH values (pH > 8). Samples were protected from light with aluminum foil and the solubilization experiments were carried out over a short period of time (about 20 min). Temperature was set at 20 °C. After filtration or centrifugation, samples were diluted in methanol and immediately measured by UV-vis spectroscopy. HPLC was used to quantify the degradation rate of native quercetin at different pH values in order to estimate the incidence of oxidation on the precision of the solubilization measurements (see section I.5.2).

I.3.2.4.2. Oxidation products detection with ^{1}H NMR

The presence of quercetin degradation products upon degradation was characterized by ^{1}H NMR. Temporal monitoring of quercetin degradation was carried out to identify the appearance of peaks corresponding to the various oxidation products and simultaneously highlight the decrease until complete disappearance of the parent quercetin peaks. Quercetin reference spectrum was performed in DMSO-d_6 as quercetin is too little soluble to produce signals in D_2O. A first monitoring was realized without meglumine, with a ratio of NaOH to quercetin of 5:1 in D_2O over 1 h, and others were conducted in aqueous solution and in the presence of meglumine (ratio meglumine to quercetin 1:1 and 5:1 with pH 9,0 and 10,0, respectively). Shortly, approximately 15 mg of quercetin was precisely weighed in a 5 mL volumetric flask with the appropriate mass of meglumine to obtain (1:1) and (5:1) meglumine to quercetin molar ratio and dissolved in ultrapure water. The samples were then diluted in D_2O (1:2). After 5 min of stirring in a water bath at 25 °C, the solutions were filtrated (PTFE, 0.2 µm) and analyzed several times at regular intervals by NMR. For interactions analysis with meglumine, the evolution of the chemical shifts of meglumine signals was monitored as a function of meglumine-to-quercetin ratio, varying from 1:1 to 10:1.

I.3.2.4.3. Quercetin oxidation state quantification with HPLC

Monitoring of the oxidation process was carried out by High-Performance Liquid Chromatography on a Shimadzu instrument equipped with a Uptisphere RP C18 (250 × 4.6 mm, 2.5 µm) protected by a guard column (LC_{18}). The column temperature was maintained at 30 °C. The mobile phase consisted of methanol–water (50:50, v/v), and the elution was carried out isocratically at a flow rate of 1 mL/min and monitored with a UV-vis detector simultaneously at 210 and 370 nm. A calibration curve of peak area versus concentration of non-oxidized quercetin was built in methanol in order to determine the concentration of native quercetin over time (see Figure A.1 and Figure A.2 in Appendix A.3). Furthermore, the retention time (R_t) of quercetin solubilized in aqueous solution with meglumine does not significantly differ from that of quercetin in methanol (13.5 and 13.1 min, respectively), where the R_t of small oxidation products range from 3 to 5 min, so the presence of meglumine does not interfere with signal identification. Finally, the area under the curve produced by the signal from quercetin in aqueous solution solubilized by meglumine is very similar to that for the same concentration of quercetin in methanol (2.38 mmol/L calculated for quercetin in meglumine aqueous solution for 2.5 mmol/L prepared), thereby confirming the validity of the calibration curve for quercetin in methanol.

I.3.2.4.4. Ferrous Oxidation-Xylenol Orange (FOX) method

It has been seen in section I.2.3.3.2 that one hypothesis regarding the autoxidation mechanism of quercetin in the presence of oxygen involves the production of hydrogen peroxide (H_2O_2) in stoichiometric quantities upon its degradation. Thus, titration of released hydrogen peroxide can be used to monitor quercetin oxidation kinetics. H_2O_2 formation rate was determined with the Ferrous Oxidation-Xylenol Orange (FOX) assay[107]. This method is based on the reaction of ferrous ion with peroxide (Figure I.14) which here applies to hydrogen peroxide.

$$Fe^{2+} + ROOH \rightarrow Fe^{3+} + R^{\bullet} + OH^{-}$$

Figure I.14. Reaction of ferrous ion with peroxide to form ferric ion.

The amount of ferric ion Fe^{3+} formed is then determined by adding the compound xylenol orange (added as tetrasodium salt, noted XO, see structure in Figure I.15) which forms stoichiometrically a complex (see Figure I.16). This orange-brown complex absorbs sharply at λ = 560 nm, which makes it easy to quantify precisely.

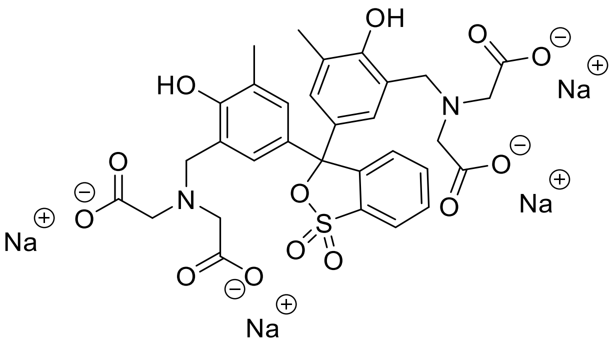

Figure I.15. Chemical structure of xylenol orange tetrasodium salt.

$$Fe^{3+} + XO \rightarrow [Fe^{3+}\text{-}XO]$$

Figure I.16. Complexation of ferric ion with xylenol orange.

Ferrous ion Fe^{2+} and XO are introduced stoichiometrically by preparing the “FOX reagent”: 2.5 mM XO and 2.5 mM Mohr salt (ferrous ammonium sulfate, $(NH_4)_2Fe(SO_4)_2•6H_2O$) are dissolved in 1.1 M perchloric acid $HClO_4$. A calibration curve of [Fe^{3+}-XO] complex concentration against absorbance at $\lambda = 560$ nm was constructed by adding the FOX reagent to aqueous solution of known H_2O_2 concentrations and letting the complexation occur for 30 min (RT, dark). The same protocol was then applied to samples containing quercetin and meglumine to determine the influence of meglumine on the oxidation rate of quercetin at a given pH value. Meglumine aqueous solutions were prepared at chosen concentrations by precisely weighting meglumine and dissolving it in ultrapure water. pH was set using 5 M and 1 M HCl solutions at chosen values, and then these meglumine stock solutions were used to dilute a quercetin DSMO solution to reach selected ratios.

I.3.3. Deprotonation modeling with COSMO-RS software

I.3.3.1. Theoretical background and working principle of COSMO-RS calculations: polarization surfaces

COSMO-RS (Conductor-like Screening Model, Realistic Solvation) is a software based on quantum chemistry and statistical thermodynamics used for molecular modeling[108]. It calculates the chemical potential μ of a solute in a pure liquid phase at infinite dilution, which can then be converted into physicochemical parameters. Quercetin was drawn in all possible states of charge and the COSMOconf script.19 was used for conformational analysis. COSMOtherm (C30_1301 version, COSMOlogic, Leverkusen, Germany) was then used to calculate the pK_a values of quercetin. Figure I.17 shows the σ-profile and the σ-surface of quercetin, i.e. a two-dimensional representation of the polarizability of quercetin.

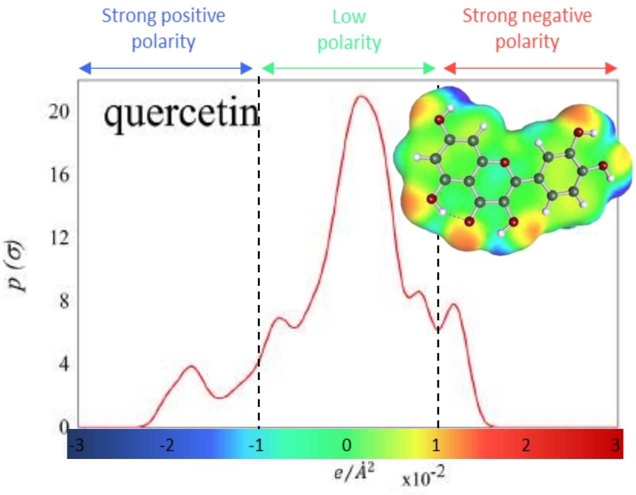

Figure I.17. Graphical representation of surface polarization as calculated by COSMO-RS software, here with the example of quercetin in its native form. The dotted line in the quercetin structure represents hydrogen bond predicted by COSMO-RS.

I.3.3.2. Deprotonation order prediction via minimum dissociation constants calculations

As seen in section I.2.3.4.1., there is no real common agreement in the literature on the deprotonation order of the five hydroxyl groups of quercetin upon pH increase, although the order established by Lemańska *et al.* (4'-OH < 7-OH < 3'-OH < 3-OH < 5-OH[83]) can be fairly trusted. The importance of knowing the first deprotonation sites (particularly the first two) of quercetin being paramount in elucidating solubilization and autoxidation mechanisms, it was decided to attempt to establish it by simulation and compare our finding with the available literature data. This was achieved using COSMO-RS software.

COSMOtherm, a COSMO-RS software package, is already recognized to be able to predict accurately pK_a values of acids and phenols[109,110] in aqueous solution, at infinite dilution. The calculation of pK_a values by COSMOtherm is based on the equation (I. 5) and therefore also partially on experimental data (94 acids and 75 bases) used for constants A and B calculation.

$$pK_a = A\left(\frac{\Delta G^j_{neutral} - \Delta G^j_{ion}}{RT \ln 10}\right) + B \qquad (I.5)$$

With $\Delta G^j_{neutral}$ the free Gibbs energy of the neutral form (or n-ionic form) and ΔG^j_{ion} the free Gibbs energy of the deprotonated form (n+1-ionic form) and A and B experimental constants[109].

For the pK_a calculations, each hydroxyl group was considered a potential site for each deprotonation. Thus, every possible anionic form of quercetin was manually drawn in the software for surface polarization optimization and then each combination of an anionic form (or neutral for the first deprotonation) and all the possible anionic forms of the next deprotonation was calculated (see Figure I.18). For each deprotonation level, the deprotonated form yielding the lowest pK_a value is considered the most likely to occur, because requiring the lowest energy. The results are presented in section I.4.3.

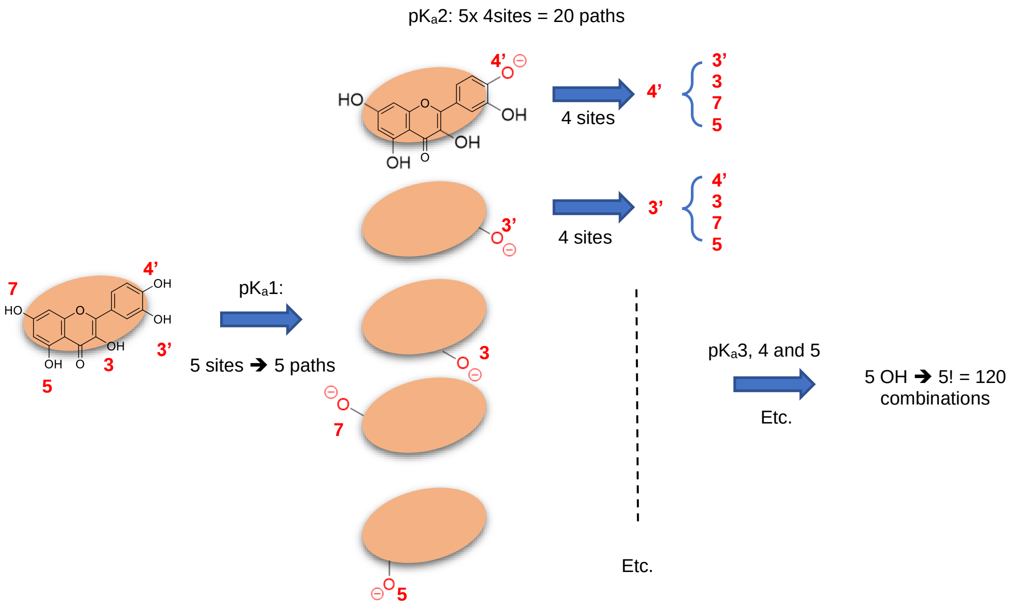

Figure I.18. Graphical representation of the number of possible deprotonation combination of quercetin.

I.4. Quercetin solubilization in aqueous solution with meglumine

I.4.1. Solubility of quercetin in water as a function of pH

Quercetin in its neutral form is virtually insoluble in water with reported solubility values not exceeding a few tens of micromoles per liter (between 0.17–7.7 µg/mL corresponding to 5.62 x10^{-4}–2.55 x10^{-2} mM[111] or < 0.05 mM[70]). By raising the pH, quercetin becomes increasingly negatively charged upon deprotonation, which consequently enhances its water-solubility. The solubility of quercetin in pure water at different pH values was tested by tuning the pH with NaOH and HCl additions. Table I.3 showed photographs of ultrapure water samples on a pH range varying from 5 to 11 saturated with quercetin and then filtrated (PTFE, 0.2 µm). Up until pH 9, the maximum solubility of quercetin does not exceed 0.1 mM, and ranges from 0.6 to roughly 1.6 mM for pH values 10 and 11.

Table I.3. Photographs of water samples at different pH saturated with quercetun and filtered.

pH	5	6	7	8	9	10	11
Sample						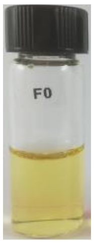	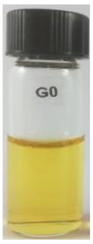

It should be noted that, as seen in section I.2.3.3.2, quercetin undergoes an autoxidation phenomenon alongside its deprotonation, i.e. with the increase of pH. As a result, at alkaline pH values, native quercetin is partially degraded and rapidly there is a coexistence between quercetin with several oxidation products of lower molar mass and greater water solubility. Some of these oxidation products have a structure close to that of native quercetin, and therefore absorb at the same wavelength, 370 nm. As a consequence, the two phenomena, i.e. the solubilization of quercetin by deprotonation and the overall increase in solubility due to the growing concentration of more soluble oxidation by-products overlap and are challenging to measure distinctly. To differentiate between these two sources and to confirm the solubilization results obtained with UV-vis spectroscopy, the same tests were carried out and analyzed with HPLC, where different retention time allow to distinguish between native quercetin and oxidation by-products (see section I.5.2).

I.4.2. Meglumine concentration influence on quercetin water-solubility

In order to discriminate between the increase of solubility due to deprotonation itself and due to the presence of meglumine, the solubilization of quercetin was conducted with two different meglumine concentration and compared to control samples without meglumine at the same pH values on a wide pH range. Figure I.19 presents the solubilization results of quercetin in presence of meglumine as a function of pH. It should be noted that the pH of meglumine dissolved in water is naturally around 11.

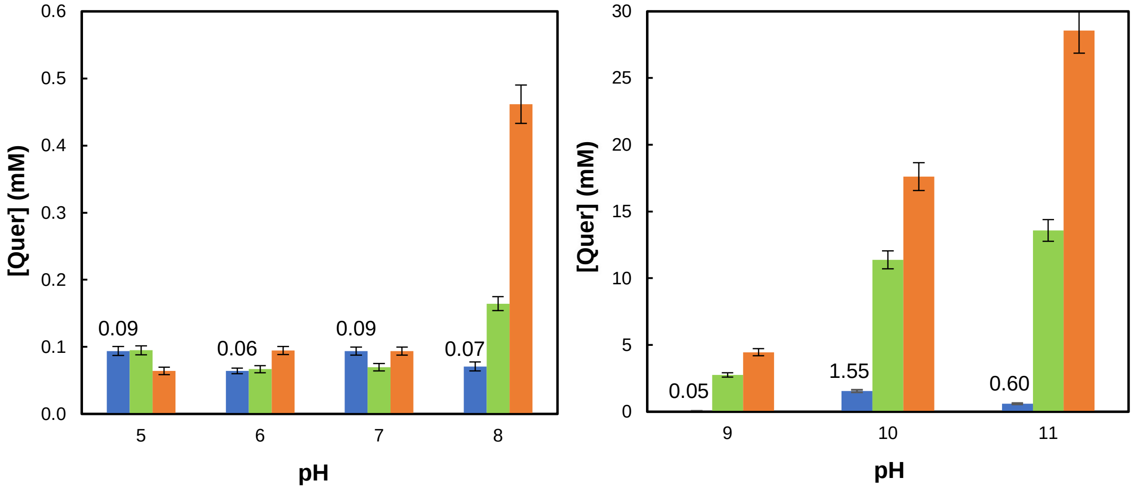

Figure I.19. Maximum solubility of quercetin in water as a function of pH and meglumine concentration. Blue: Ultrapure water (no meglumine). Green: 50 mM meglumine in ultrapure water. Orange: 250 mM in ultrapure water. Displayed data are the average values of two measurements. The results are shown in two different graphs to adapt the scale of the quercetin concentration axis.

It can be seen from Figure I.19 that the solubility of quercetin is closely correlated to meglumine concentration from pH 8 and above. At lower pH values, there is no noticeable effect compared with control samples. At pH 8, the maximum solubility of quercetin in water is increased by a factor 5 with 250 mM of meglumine. This increase is even more pronounced at pH 9 and higher, however as autoxidation phenomenon can happen, the solubility values achieved at high pH offer less interest for practical applications. Furthermore, the effective aqueous solubilization of quercetin by meglumine is confirmed by the presence of characteristic quercetin peaks alongside the signals of meglumine in D_2O (see Figure I.23).

I.4.3. Deprotonation order simulation with COSMO-RS

Every possible state of charge of quercetin was drawn and optimized by COSMOconf to determine the most energetically stable conformers. Then for each state of charge, the deprotonation of one additional hydroxyl group was calculated. Figure I.20 presents the exemple of the first deprotonation, i.e. between the neutral and monoanionic forms of quercetin. For this deprotonation, the hydroxyl groups 4’ and 7 gave the lowest pK$_a$ values, however the hydroxyl groups 3’ and 3 do not yield much higher pK$_a$s. As a result, it can be hypothesized that their deprotonation is slightly less favorable than that of groups 4' and 7, but can still be considered. This means that at pH values around these pK$_a$s, all four monoanionic forms (An 4’, 7, 3’ and 3) can coexist. On the other hand, deprotonation of group 5 first seems highly unlikely. This is consistent with this group being able to form an intramolecular hydrogen bond with the adjacent carbonyl group (see Figure I.17).

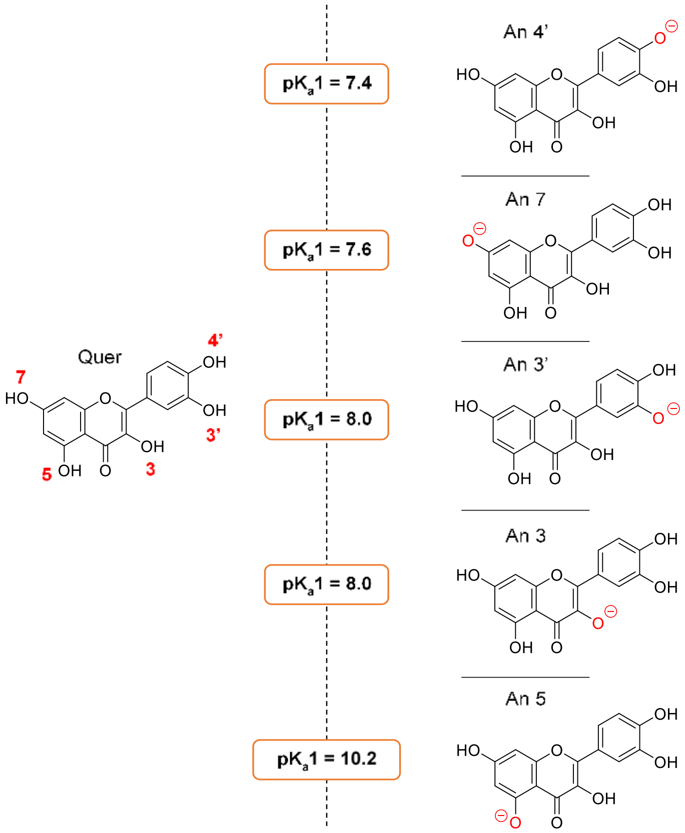

Figure I.20. pKa calculations of the first deprotonation of quercetin using COSMO-RS software. NB: “An” stands for “Anion”.

The pK$_a$ calculations for almost every possible calculation (a few very improbable deprotonations have been left out) have been listed in Table A.1 toTable A.5 in appendix A.2 for each deprotonation. Thus, according to this approach, i.e. considering for each deprotonation that the one(s) with the lowest pK$_a$ value is the most likely to occur, the following order of deprotonation is obtained: 4’-OH < 7-OH < 3-OH < 3’-OH < 5-OH, represented in Figure I.21.

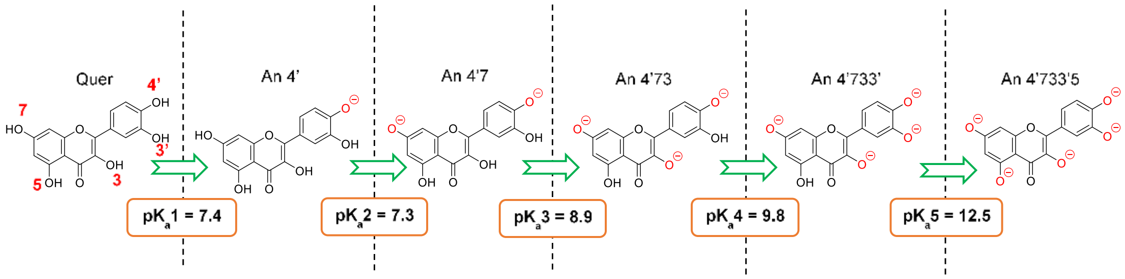

Figure I.21. pK_a calculations for the most probable deprotonation order of quercetin according to the COSMO-RS method. NB: “An” stands for “Anion”.

This finding is in good agreement with the work of Álvarez-Diduk *et al.*[84], and only differs from the one establisher by Lemańska *et al.* [83] with respect to the third (and thus the fourth) deprotonation, i.e. between groups 3-OH and 3’-OH. Indeed, assuming that the 4’-OH group is already deprotonated, the deprotonation of group 3’-OH should be electronically disadvantaged compared to 3-OH, which is consistent with the results obtained with COSMO-RS, as the pK_a of deprotonation of anion 4’7 to 4’73’ is more than one pK_a unit above that of deprotonation of anion 4’7 to 4’73 (see Table A.2 in Appendix A.2).

I.4.4. Mechanism of quercetin solubilization with meglumine

The interactions between meglumine and quercetin were more deeply studied. Meglumine itself can exhibit a range of different interactions with solutes, depending highly on the solvent. Like for quercetin, the hydroxyl groups of meglumine can act simultaneously as hydrogen bonds acceptors and donors. For example, meglumine can form stable crystals with flunixin through complexation in organic solvent, where the cohesion arises from $O-H\cdots O$ and $N-H\cdots O$ hydrogen bonds[112]. Meglumine has been shown to associate with carboxylic acids via its amino group, and to form hydrogen bonds via its hydroxyl groups only with water molecules from the solvent[113–115].

Acid-base interaction and salt formation

The structure of meglumine suggests that it could interact with quercetin in different ways, for instance through proton exchange between the amine group of meglumine and the hydroxyl groups of quercetin. The aromatic rings of quercetin could also act as hydrogen bond acceptors toward hydrogen bonds donors such as the amine group or the oxygen atoms of the hydroxyl groups of meglumine.

For identification purpose of the signals of native quercetin which is virtually insoluble in water, a reference spectrum was carried out in DMSO-d_6 (see Figure I.22). As mentioned before, 1H NMR carried out immediately after solubilization with meglumine confirmed the presence of quercetin in its native form in aqueous solution (see Figure I.23).

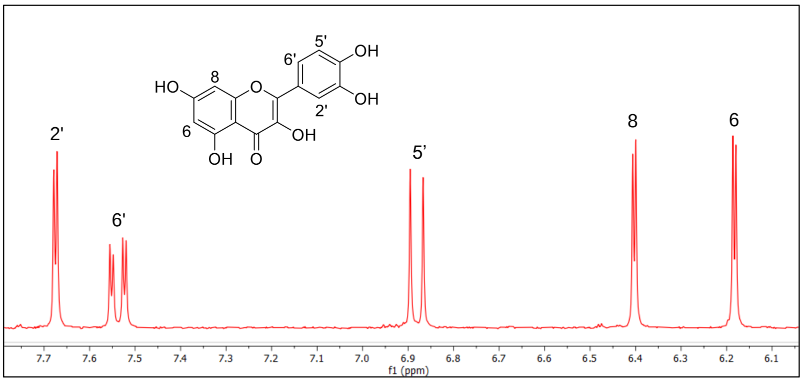

Figure I.22. ^{1}H NMR spectrum of pure quercetin in DMSO-d_6.

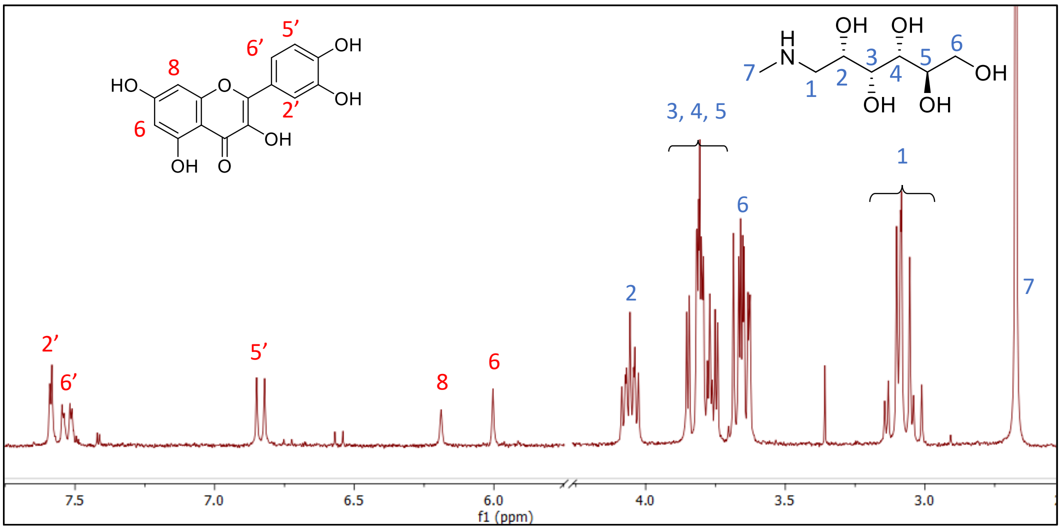

Figure I.23. ^{1}H NMR spectrum of quercetin in D_2O in the presence of meglumine (pH ≈ 11).

In order to gain more insights on the mechanism of solubilization, the interactions between quercetin and meglumine were investigated using ^{1}H NMR spectroscopy. Figure I.24 shows the evolution of the meglumine signals at different meglumine to quercetin ratios in D_2O.

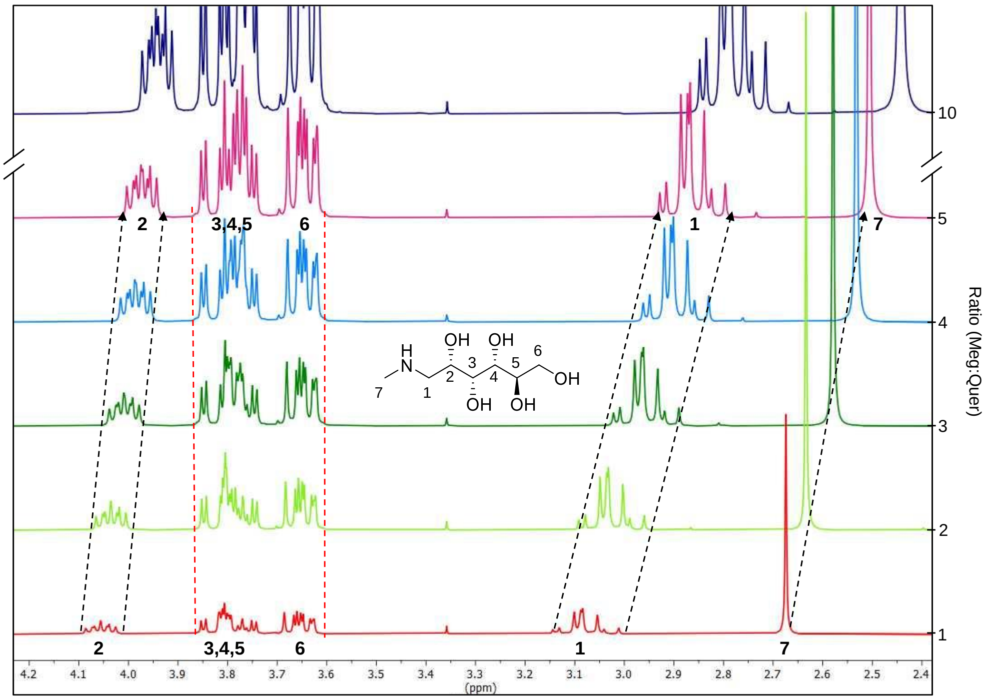

Figure I.24. ^{1}H NMR spectra of meglumine (Meg) in the presence of quercetin (Quer) in D_2O at increasing meglumine to quercetin molar ratios from bottom (1:1) to top (10:1). Dotted lines serve as visual guides for the evolution of the chemical shifts.

The most striking feature of this test is the strong de-shielding of the protons 1, 7 and 2 to a lesser extent, even with a slight change in the ratio between meglumine and quercetin. This de-shielding of the protons adjacent to the amine function of meglumine suggests a salt formation with quercetin. In comparison, the signals of protons 3 to 6 stay practically identical no matter the ratio in the range of the study, indicating that the hydroxyl groups of meglumine do not strongly interact with quercetin.

Lastly, the hypothesis of salt formation between meglumine and quercetin is consistent with the almost instantaneous solubilization of quercetin in aqueous meglumine solutions. The hydroxyl groups of meglumine would in this case further help hydration by bringing water molecules through hydrogen bonds with the sugar moiety of meglumine. Furthermore, meglumine is positively charged at pH below 9.6. The ionic interactions should also be enhanced with deprotonation of the hydroxyl functions of quercetin above pH 7. In fact, although the often cited ΔpK_a rule, that states that the pK_a difference between the opposite charged molecules must be at least one unit for salt formation to occur[116], is respected for the first, second and probably third deprotonation of quercetin, it has already been established that meglumine could form salts with solutes even if the pK_a difference between the two is less than 1[98]. This is consistent with the further significant increase in quercetin solubility in the presence of meglumine at high pH (see Figure I.19).

I.5. Impact of meglumine on quercetin oxidation stability

As it has been seen in section I.2.3.3.2, quercetin is very sensitive to oxidation and is quickly and completely transformed in presence of oxygen, a phenomenon intensified by light and temperature. Furthermore, as mentioned above (section I.4.1), quercetin oxidation products are more water-soluble, so accurate quantification of the oxidative state of quercetin during solubilization processes is crucial. To this end, oxidation was monitored by an ^{1}H NMR and an HPLC follow-up.

I.5.1. Determination of the presence of native quercetin and/or oxidation products in solution

NMR monitoring consisted in tracking the disappearance of peaks characteristic of native quercetin, while at the same time detecting the appearance of peaks due to oxidation products. Figure I.25 represents ^{1}H NMR spectra of aqueous solutions (D_2O) at different ratios of meglumine to quercetin were temporally monitored and compared to the effect of NaOH equivalent in the same ratio.

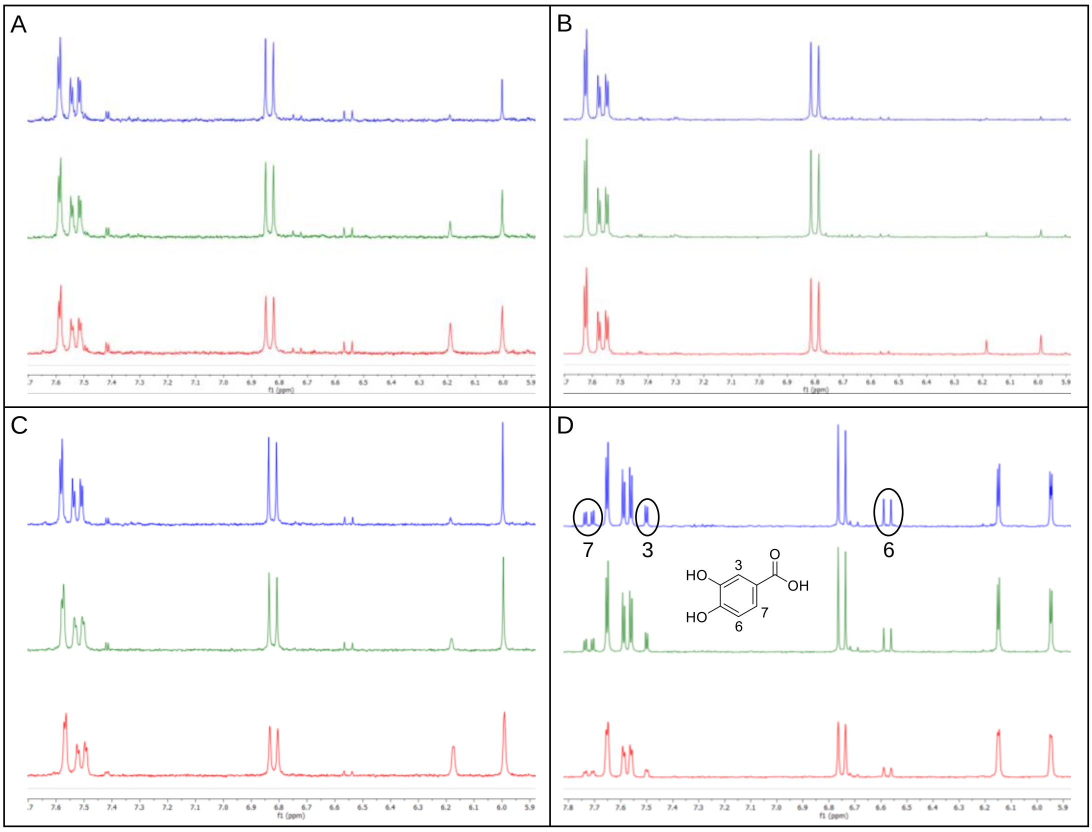

Figure I.25. 1H NMR spectra of quercetin in aqueous solutions in D2O over time. A. Meglumine to quercetin molar ratio of (1:1) (pH = 9.0). B. Meglumine to quercetin molar ratio of (5:1) (pH = 10.0). C. NaOH to quercetin molar ratio of (1:1). D. NaOH to quercetin moar ratio of (5:1). Red: t_0. Green: t_0 + 30 min. Blue: t_0 + 1 h. The structure of protocatechuic acid is also given in D.

The main obstacle in characterizing quercetin oxidation by NMR lies in the fact that its oxidation products yield signals that may overlap with those of native quercetin. Furthermore, as it is not experimentally feasible to obtain a spectrum of pure quercetin in water, the study of the shifts of quercetin signals upon oxidation is limited. One of the main oxidation derivatives of quercetin is protocatechuic acid. With a molar ratio of (5:1) of NaOH to quercetin, the peaks corresponding to its protons appear unequivocally (see Figure I.25, D).

On the other hand, phloroglucinic acid and phloroglucinol, two other major oxidation products of quercetin[63], generate one single peak in the form of a singlet around 6 ppm in water. This peak is probably responsible for the asymmetric decrease of signals corresponding to protons noted 6 and 8 on Figure I.22, located in D_2O at around 6 and 6.2 ppm, respectively (Figure I.25, A. and D.), as it overlaps with the first one. Thus, the decrease of the peak at 6.2 ppm, namely the signal of proton 8, should alone clearly indicate the chemical modification of quercetin structure upon oxidation. This decrease is fairly evident with NaOH as well as with meglumine in equimolar ratio (Figure I.25, A. and D.), but surprisingly is far less obvious with a (5:1) meglumine to quercetin ratio (Figure I.25, B.), as both signals 6 and 8 appear to decrease rather simultaneously. The reason for that is not clear but it appears that meglumine has an influence on quercetin oxidation mechanism, for it differs from the one induced only by deprotonation upon pH increase.

I.5.2. Oxidation quantification with HPLC

In order to achieve a precise quantification of the temporal degradation of quercetin and the formation of its oxidation sub-products, HPLC analyses were carried out. Figure I.26 shows the chromatograms of the follow-up of quercetin degradation over a period of 2 or 4 h.

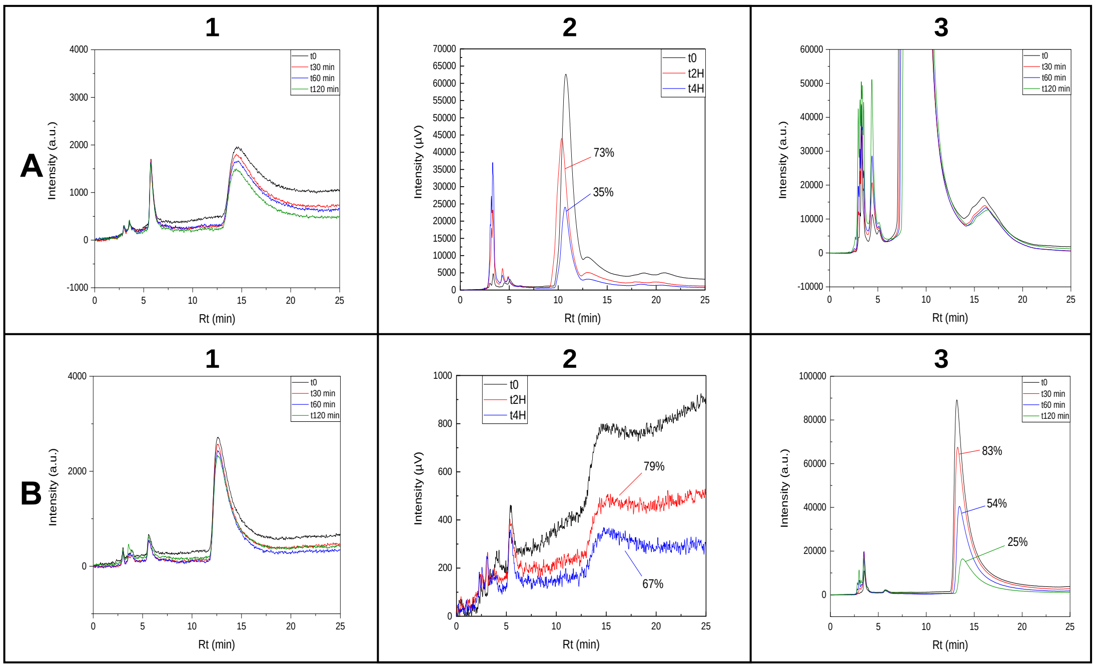

Figure I.26. Chromatograms for the temporal monitoring of quercetin oxidative degradation. **A**. In the presence of meglumine. **B**. With NaOH. **1**. At pH 7.35. **2**. At pH 8.4. **3**. At pH 11. All spectra were recorded at λ = 370 nm. Percentages expressed represent the amount of unaltered quercetin.

Whether in the presence of meglumine or not, at physiological pH (around pH 7.4), quercetin solubility is particularly low. In both cases, nevertheless, quercetin degradation over a two-hour period remains limited. Around pH 8 with just NaOH equivalents (see Figure I.26, B, 2), although the low solubility of quercetin decreases the precision of quantification, around 70 % of unaltered quercetin remains after 4 h. At the same pH value, in the presence of meglumine, 25-29 % degradation is observed after 2 h, and 65 % after

4 h, which means that even with a probable predominance of mono- and dianionic forms of quercetin, a non-negligible percentage of native quercetin remains after a few hours. From an application point of view, this result remains interesting as it may enable the development of quick solubilization or extraction techniques which do not require long-term stability. In any case, it would seem that quercetin is slower oxidized without meglumine. However, it is delicate to compare the samples, as the concentration of quercetin solubilized with meglumine at that pH is significantly higher than without it, probably resulting in a facilitated oxidation. Furthermore, at pH 11, it is clear that the degradation of quercetin in the presence of sodium hydroxide is particularly swift (see Figure I.26, B, 3), yielding only about 24 to 25 % of intact quercetin after 2 h, although the chromatogram with meglumine is somewhat partially unclear.

Another important point to note is the validation by HPLC of solubilization results obtained by UV-vis spectroscopy. Indeed, at pH 8 in meglumine aqueous solution (t_0), the concentration of quercetin obtained from the peak area method is 0.454 mM, versus 0.462 mM obtained with UV-vis spectroscopy.

I.5.3. Oxidation quantification with the Ferrous Oxidation Xylenol orange (FOX) method

An additional method was also investigated to try to better understand the oxidative degradation kinetics of quercetin more specifically, the so-called Ferrous Oxidation-Xylenol orange (FOX) method. The reactions on which this method is based are detailed in section I.3.2.4.4. The principle of the experiment is to measure the UV-vis absorbance of the [Fe^{3+}-XO] complex formed in the presence of H_2O_2 released by quercetin upon oxidation to determine the rate of peroxide formation and therefore the rate of oxidation. Furthermore, this method could potentially overcome the solubility challenges encountered for quercetin at moderate alkaline pH without meglumine, as it not based on a direct measurement of quercetin. The formation of hydrogen peroxide being equimolar upon oxidative breaking of quercetin, the rate of H_2O_2 directly represents the number of quercetin molecules breaking each minute. Figure I.27 shows the comparison of quercetin samples in aqueous solution on the presence or not of meglumine at physiological and slight alkaline pH.

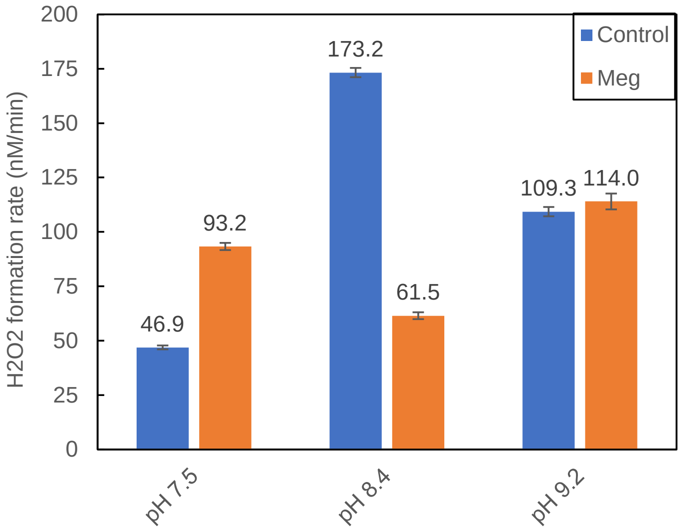

Figure I.27. H_2O_2 formation rate of quercetin samples in aqueous solution with (orange) and without (blue) meglumine at different pH values.

Several observations can be made. Firstly, at pH 7.5, the oxidation rate of quercetin with meglumine is 2 times higher than the one with meglumine, but is almost 3 times higher at pH 8.4, which seems in contradiction with previous results (see Figure I.26). However, it is also important to bear in mind that because of experimental requirements, these H_2O_2 rates are measured 30 min after the beginning of the oxidation process, to ensure the steady formation of the complex, and represent a rate calculated from the total amount of H_2O_2 formed after 30 min. The temporal evolutions of these rates are compared in Figure I.28.

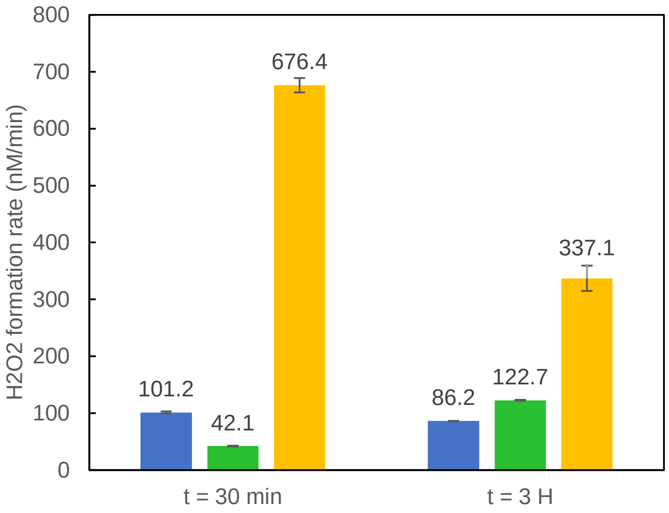

Figure I.28. Temporal evolution of H_2O_2 formation rate of 0.1 mM quercetin samples in aqueous solution at pH 8. Blue: quercetin alone. Green: (100:1) meglumine-to-quercetin. Yellow: (1000:1) meglumine-to-quercetin.

It seems clear from Figure I.28 that the oxidation rate of quercetin is dependent on the meglumine-to-quercetin ratio. In the absence of meglumine, the slight reduction of the oxidation rate with time seems logical with the reduction of quercetin concentration upon oxidation degradation. This behavior is also found with a large excess of meglumine (ratio 1000:1) but way stronger, with a reduction of the H_2O_2 formation rate of more than 50 %

between 30 min and 3 h, although the absolute values of these rates are significantly higher than in the absence of quercetin. Surprisingly, at a 100:1 ratio between meglumine and quercetin, not only is the H_2O_2 formation rate after 30 min more than two times smaller than for the control sample, but it also increases between 30 min and 3 h contrary to the other ratios, suggesting that meglumine could have a slight protective effect on quercetin oxidation, but this effect reverses with time, maybe as the quercetin concentration diminishes and the meglumine-to-quercetin ratio increases. As this ratio becomes too great, the excess meglumine molecules supposedly act primarily as base, increasing the oxidation of quercetin.

I.6. Extension of the scope to other polyphenols

The enhanced solubility of quercetin obtained with meglumine prompts the question of the generalization of this mechanism to other polyphenols. To this end, selected compounds were tested at pH 8, where solubilization with meglumine was found to be the most interesting for quercetin, as a compromise between satisfactory solubility enhancement and reasonable oxidation. The idea was to confirm the criteria on pK_a and on the accessibility of the hydroxyl groups to ensure the solubilization, i.e. that the target compound should be at least one or two times deprotonated and easily approachable at working pH to interact efficiently with meglumine. One particular compound, xanthohumol, meets these criteria well, and is strongly resistant to oxidation, so it was investigated on a larger pH range.

I.6.1. Xanthohumol solubilization with meglumine

Xanthohumol (see structure in Figure I.29) is a major component of hop. Although the biological properties of xanthohumol have recently been extensively investigated[117], very few studies have focused on the determination of its dissociation constants. Arczewska *et al.* reported the following values: $pK_a1 = 7.4 \pm 0.3$, $pK_a2 = 8.6 \pm 0.3$, and $pK_a3 = 8.9 \pm 0.3$, attributed to hydroxyl groups 2, 4, and 4’, respectively (see Figure I.29)[118].

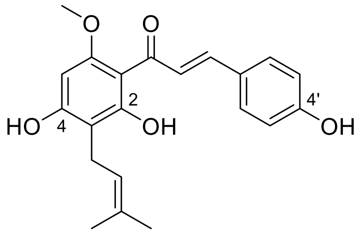

Figure I.29. Chemical structure of xanthohumol.

Figure I.30 shows the maximum solubility of xanthohumol between pH 6 and 11 at different meglumine concentrations.

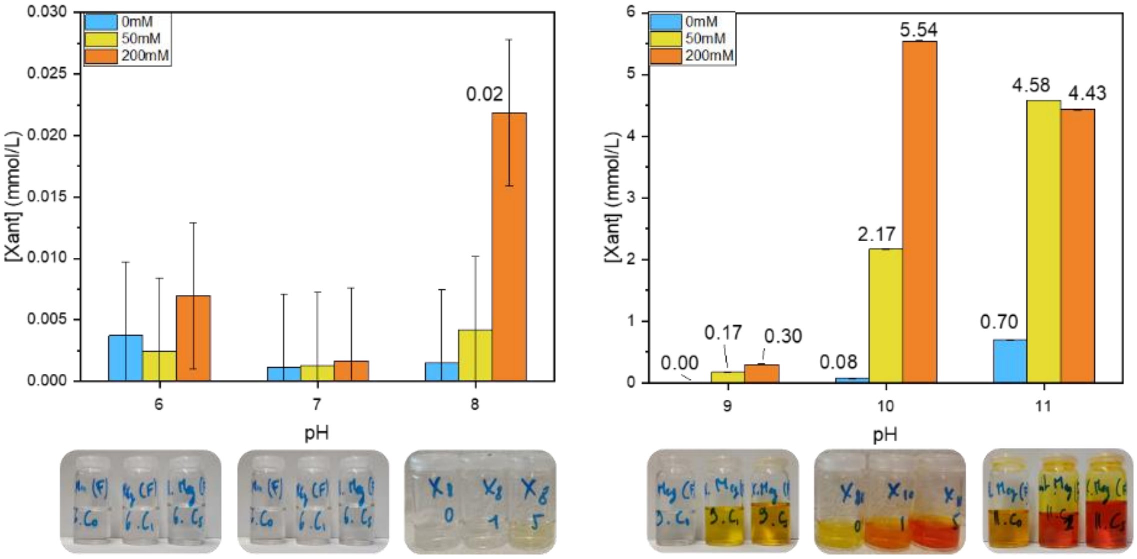

Figure I.30. Maximum solubility of xanthohumol as a function of pH and meglumine concentration. Blue: ultrapure water (no meglumine). Yellow: 50 mM meglumine in ultrapure water. Orange: 200 mM meglumine in ultrapure water. The results are shown in two different graphs to adapt the scale of the xanthohumol concentration axis.

As seen with quercetin (see section I.4.2) it can be already observed at pH 8 that the highest concentration of meglumine (200mM) has a significant effect on the aqueous solubilization of xanthohumol (almost 10-fold). Then, at pH 9 and above, the solubility enhancement effect of meglumine at fixed pH is indisputable. Indeed, at pH 10, xanthohumol's solubility increases by more than 27 times with 50 mM meglumine, and around 70 times with 200 mM. Xanthohumol appears then as a suitable candidate to be solubilize with meglumine, as its resistance towards oxidation is much higher.

I.6.2. Comparison of the polyphenol solubilization efficacy of meglumine

Phenolic compounds were chosen as representative of different families of polyphenols, such as flavanones (naringenin), dihydrochalcones (phloretin), stilbenoids (resveratrol), or simple phenolic acids (gallic acid). The effect of meglumine on their water-solubility was investigated around pH 8 with roughly 50 and 200 mM meglumine in ultrapure water. Table I.4 presents the results of these tests, together with the values of the different dissociation constants available in the literature, or from this work in the case of quercetin.

Table I.4. Water-solubility of tested polyphenols with different meglumine concentrations at pH 8.1 ± 0.1 (same protocol as for quercetin solubility tests).

Phenols tested	Structure	pK_a	Meglumine concentration (mmol/L)		
			0	48	201
			Solubilized polyphenol concentration (mmol/L)		
Quercetin	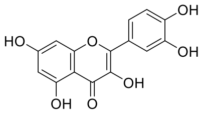	$pK_a1 = 7.4$‡ $pK_a2 = 7.3$‡ $pK_a3 = 8.9$‡ $pK_a4 = 9.8$‡ $pK_a5 = 12.5$‡	0.07	0.16	0.46
Gallic acid	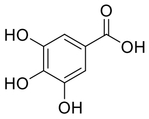	pK_a1 (acid) = 4.0[119] pK_a2 = 8.7[119] pK_a3 =11.4[119] pK_a4 > 13[119]	207	283	319
Curcumin	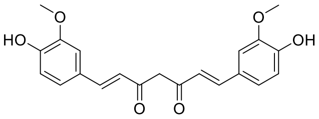	pK_a1 = 8.4[120], 7.7-8.5[121] pK_a2 = 9.9[120], 8.5-10.4[121] pK_a3 = 10.5[120], 9.5-10.7[121]	< 0.005	< 0.005	< 0.005
Naringenin	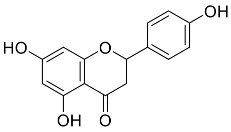	pK_a1 = 7.5[80], 7.1[36] pK_a2 = 8.4[80], 8.8[36] pK_a3 = 9.8[80]	1.5	1.7	2.0
Phloretin	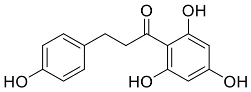	pK_a1 =7.3[122], 7.6[123]	1.1	4.8	9.1
Resveratrol	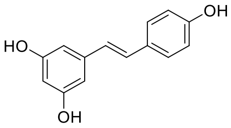	pK_a1 = 8.8[124], 9.1[125] pK_a2 = 9.8[124], 9.7[125] pK_a3 = 11.4[124], 10.5[125]	2.1	2.1	2.6

---

‡ Calculated with COSMO-RS (see section I.4.3).

Apart from gallic acid, which interacts strongly whit meglumine very probably because of its carboxylic acid group, a few polyphenols seem able to interact with meglumine in the same fashion as quercetin and xanthohumol. Indeed, meglumine seems to be able to interact efficiently with phloretin and to a lesser extent with naringenin and resveratrol, and seems to have minimal to none effect on curcumin at this pH. Degot *et al.* showed that meglumine was able to facilitate the extraction of curcumin by enhancing its solubility in a triacetin/ethanol/water system, and also in pure aqueous solution[126]. However, without either buffer or medium acidification, an aqueous meglumine solution exhibits a pH well above 8, and this basicity is probably responsible for the increased extraction yield. The first pK_a of curcumin is too high to yield lot of charged molecules at pH 8. This is presumably the same case with resveratrol. Phloretin on the other hand is thought to have its first pK_a around 7.3-7.6, which makes it an ideal compound for interaction with meglumine. Finally, and more surprisingly, naringenin is also believed to be one time deprotonated around pH 8, as its first pK_a is between 7.1 and 7.5. One hypothesis is that naringenin and phloretin are not poorly water-soluble for the same reasons. This will be explored in greater detail in Chapter III.

I.7. Conclusions

In this chapter, it was demonstrated that meglumine can effectively increase the solubility of quercetin as well as other phenolic compounds in aqueous media, notably xanthohumol and phloretin, even at an only very slightly alkaline pH. In order to understand the solubilization mechanism of quercetin, its state of charge as a function of the pH has to be assessed. However, neither the pK_a values nor the deprotonation order of its 5 hydroxyl groups could be obtained with confidence from literature data, so no predominance diagram could be formulated. Therefore, pK_a values of quercetin were calculated using COSMO-RS software, and the deprotonation order was assessed with a new method developed for this purpose using the calculation from this software, resulting in the order of facility of deprotonation as follow: 4'-OH < 7-OH < 3-OH < 3'-OH < 5-OH.

Together with the charge state of quercetin and shifts in meglumine ^1H NMR signals, it has been shown that the solubilization mechanism is based on proton exchange between the amine function of meglumine and the first hydroxyl groups of quercetin susceptible to being deprotonated. Cohesive forces like van der Waals interactions, hydrogen bonding between quercetin molecules and π-stacking are thought to be decreased by the presence of meglumine, possibly also due to a geometry modification of quercetin structure from planar to non-planar through keto-enol tautomerization. The high solubility of the complex could then be the result of the many possible hydrogen bonds between the hydroxyl groups of meglumine and water molecules, enabling good solvation.

Based on these results, it is possible to form general prediction rules for solubilization with meglumine. The first relates to the pK_a(s) of the phenolic compound to be solubilized in relation with the medium pH. As the solute must be at minima one time deprotonated, the pH should be set at least one unit higher than its (first) pK_a, or if the pH is not an adjustable parameter, the solubilization will be effective only with compound having a low enough

pK_a. Secondly, the hydroxyl group(s) to be deprotonated has to be accessible enough to interact efficiently with meglumine. Parameters such as hydrogen-bonding or π-stacking should be considered.

When working at medium or strong alkaline pH, oxidation of polyphenols must be accounted for. ^{1}H NMR and HPLC are both relevant methods to quantify oxidation degradation. In the case of quercetin, a reasonable compromise was found between acceptable degradation (25–30 % degradation after 2 h) and fairly increased water-solubility (around 0.45 mmol/L) around pH 8 with meglumine.

Moreover, it should be noted that the behavior of meglumine is remarkable in that it resembles that of a hydrotrope (meaning solubilizing). This is particularly surprising when considering the absence of a real hydrophobic part in its structure. The means that hydrotropy in its global sense of a water-solubility enhancement should therefore be enlarged beyond “simple” amphiphilicity (cf. the work of Mehringer[127,128]).

Finally, in view of the structure of quercetin or the other phenolic compounds tested for the generalization of solubilization with meglumine (section I.6.2), it appears that it is not necessarily trivial to establish a direct relationship between the structure of polyphenols and their aqueous solubility. The their chapter of this thesis will focus on other solubilization techniques for polyphenolic structures, among which binary solvent systems and π-stacking, in order to better understand the structural factors behind low aqueous solubility.

Chapter II

–

Application of quercetin solubilization with meglumine: liposome encapsulation at moderate pH using modified pH-driven method

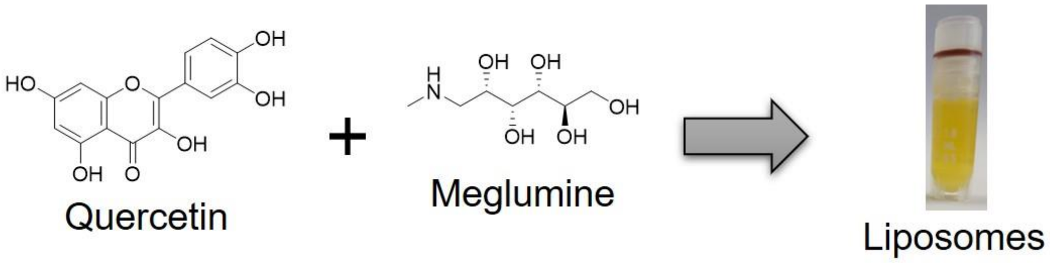
HO
O
OH
OH
OH
OH
O
Quercetin
+
H
N
OH
OH
OH
OH
OH
Meglumine
Liposomes

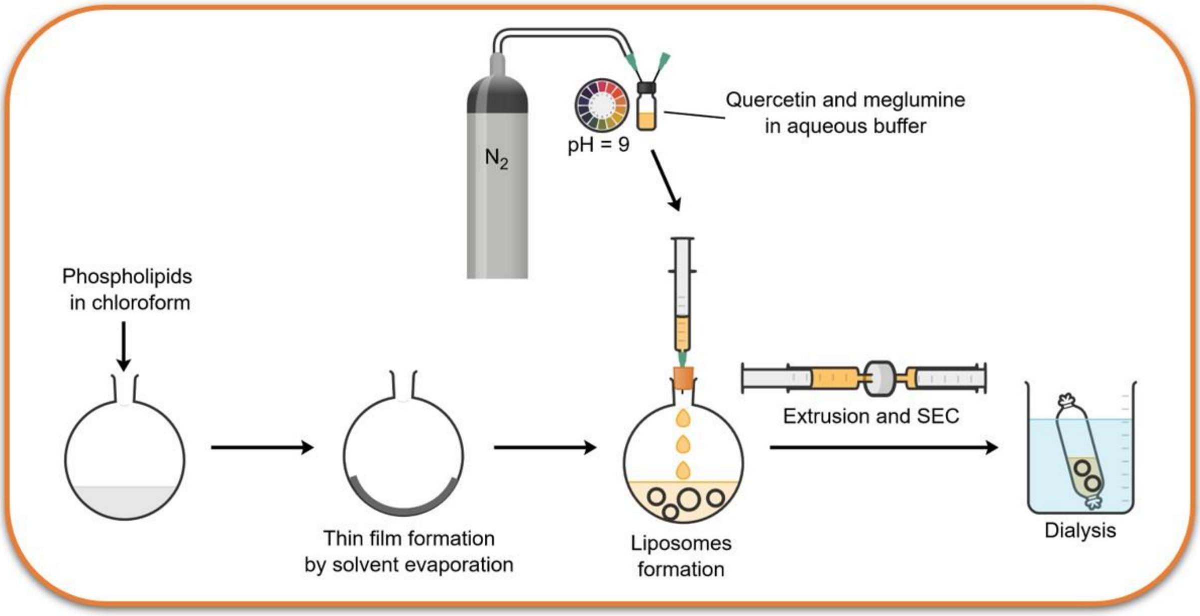
N$_2$
pH = 9
Quercetin and meglumine
in aqueous buffer
Phospholipids
in chloroform
Thin film formation
by solvent evaporation
Liposomes
formation
Extrusion and SEC
Dialysis

II.1. Introduction

As mentioned in the first part of this work, drug delivery of quercetin is an area of great interest. One solution to overcome the poor water-solubility of quercetin is the use of lipid carriers, including nanostructured lipid carriers (NLCs) and liposomes[21]. However, in order to form the liposomes and to load the lipophilic polyphenols into the liposome’s bilayers, they are often solubilized in organic solvents or solvents mixtures (methanol, acetone, chloroform, etc.) during the process. One solvent-free method has been developed recently and is based on the increase of solubility of numerous biological compounds (such as polyphenols) with increasing pH. Pan and coworkers showed the possibility of entrapping curcumin into caseinate structure directly in aqueous phase[129] and Peng *et al.* adapted this concept to develop a protocol for curcumin encapsulation into liposomes[130], now known as the “pH-driven” or “pH-jump” method. One major obstacle to the transposition of this method to quercetin is the fragility of the latter towards oxidation, even in mildly alkaline media. Indeed, although these oxidation products also exhibit interesting biological properties, mainly antioxidant activity (see section I.2.3.3), it is interesting to preserve quercetin in its native state until successful delivery of the drug, to maximize these properties and avoid early oxidation chain reactions.

Using this idea as a starting point, we propose to use meglumine in order to solubilize quercetin in water at moderate pH before loading it into standard liposomes. It must be noted that, since here the pH is set to only slightly alkaline values, the liposomes that would spontaneously form with the pH-driven would not have optimal properties (size, size distribution, etc.) due to the lack of phospholipid solubility at these pH values. The protocol used here is, therefore, an adaptation of the thin-film method (TFM) where the amount of organic solvents is minimized to solubilize the phospholipids and allow the formation of a film upon evaporation. In this study, liposomes were loaded with quercetin using a meglumine-rich aqueous solution at pH 9 with minimum use of organic solvents. The properties of the synthetized liposomes were assessed, and the amount of native and oxidized quercetin was determined.

II.2. Bibliographic background

II.2.1. Liposomes technology

Liposomes are self-assembling vesicles structured with a lipid bilayer (see Figure II.1), commonly composed of phospholipids, which are amphiphilic compounds and can be neutral, or positively or negatively charged. This allows liposomes to entrap hydrophobic compounds (in the bilayer) as well as hydrophilic ones (in the aqueous core). Liposomes structure is also very similar to cellular membrane, which makes them efficient drug carriers. In addition, the sensitivity of the liposomes structure to stimuli such as pH, temperature, or others enables a targeted and controlled drug release. Finally, liposomes often allow for a reduction of drug concentration, and a better stability (for example for storage purposes). For these reasons, they have become one of the most successful drug delivery system to date[131].

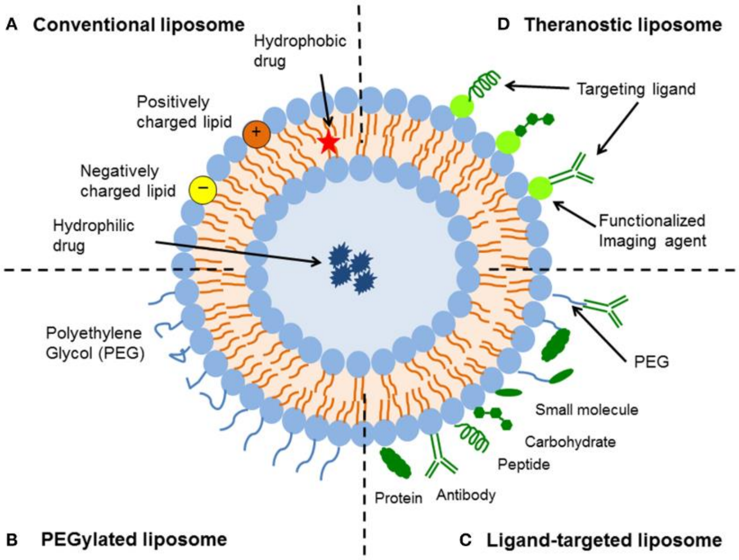
A Conventional liposome
Hydrophobic drug
Positively charged lipid
Negatively charged lipid
Hydrophilic drug
D Theranostic liposome
Targeting ligand
Functionalized Imaging agent
Polyethylene Glycol (PEG)
PEG
Small molecule
Carbohydrate
Peptide
Protein
Antibody
B PEGylated liposome
C Ligand-targeted liposome

Figure II.1. Representation of the structure of a liposome. Reproduced with permission from reference [132].

Liposomes are classified according to their size and lamellarity: small unilamellar vesicles (SUV), large unilamellar vesicles (LUV), multilamellar vesicle (MLV), and multivesicular vesicles (MVV)[133], or based on their preparation method, of which the two main categories are reverse-phase evaporation or vesicle extrusion techniques[131]. The thin-film hydration method is one of the most common process for liposomes synthesis and belongs to the category of reverse-phase evaporation (see Figure II.2). In short, it consists in dissolving the phospholipids in organic solvent, then the evaporation of the solvent phase to create a thin film of lipids, and finally the dispersion of this film in aqueous phase where it self-assembles into liposomes due to the non-affinity of its apolar lipidic chain towards water.

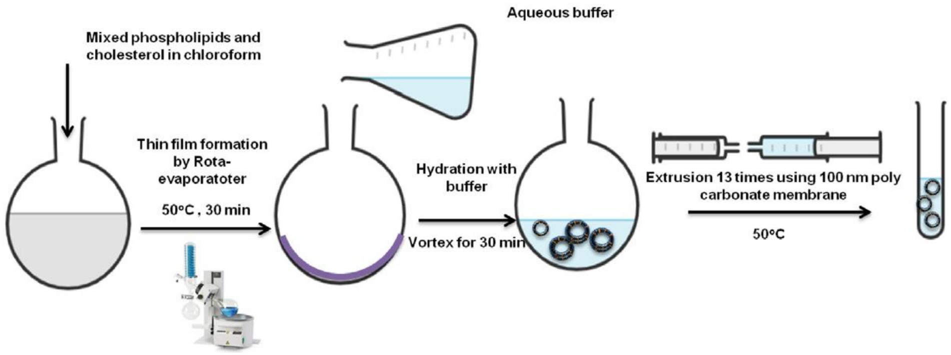
Mixed phospholipids and cholesterol in chloroform
Thin film formation by Rota-evaporatoter
50°C , 30 min
Aqueous buffer
Hydration with buffer
Vortex for 30 min
Extrusion 13 times using 100 nm poly carbonate membrane
50°C

Figure II.2. Thin-film extrusion method. Reproduced with permission from reference [133].

The structure of the phospholipids used influences greatly liposomes characteristics such as size, stability, electric charge, etc[133]. Moreover, liposome surface functionalization is a common approach to improve or to confer additional properties to liposomes. PEG, as well as peptide, protein, carbohydrate or antibody can thus be fixed at the membrane surface of the liposome, generally for specific targeting. Cholesterol is also often added to decrease the permeability of the lipid bilayer in order to prevent or decrease the release of hydrophilic encapsulated drug in the core through diffusion across the bilayer.

Quercetin-loaded liposomes

As many polyphenols, and quercetin in particular, are biologically promising, but poorly water-soluble compounds, their delivery with liposomes and other NLCs has been extensively studied. Indeed, liposomes have be proven to be well-suited not only for drug delivery[134,135] but also for polyphenols[136,137] and quercetin encapsulation[138–140]. Liposomal encapsulation of quercetin has been proven to be efficient for reduction of oxidative liver damage *in vivo* (in rats)[138] and liposomal quercetin seems to be able to exhibit its anti-inflammatory properties successfully[139].

II.2.2. pH-driven methods

As green chemistry challenges are becoming increasingly relevant, reducing the use of organic solvents in favor of water has become a major issue for formulators. To avoid using these solvents and to simplify the process of liposomes formation, Pan et al. introduced in 2014 a pH-driven method (PDM) for loading curcumin into casein micelles[129] (see Figure II.3), and Peng and coworkers tested it on resveratrol and quercetin[130]. They exploited the fact that (poly)phenates formed upon deprotonation in alkaline conditions are more water-soluble than polyphenols. The drugs can be therefore loaded from an aqueous phase (alkaline medium) into the lipophilic part of liposomes through pH reduction (drop in solubility with re-protonation). In short, lipids and hydrophobic compound are put in solution together at neutral pH, and large multilamellar vesicle (MLVs) are formed by mechanical agitation. A great increase in pH then induces simultaneously the breaking of the MLVs into small unilamellar vesicles (SUVs) or smaller multilamellar vesicles and solubilization of the hydrophobic compound into the aqueous phase. A final drop in the pH causes the hydrophobic compound to migrate into the bilayer of the liposomes and the subsequent non-encapsulated fraction to precipitate.

The major drawback of this technique is the rapid degradation of numerous polyphenols in alkaline conditions through autoxidation. It is particularly true with quercetin, which undergoes a quick oxidation mechanism at even slightly alkaline pH, resulting in the breaking of the molecule into a multitude of sub-products (see section I.2.3.3.2). Peng and coworkers thus reported that after 1 h at pH 9, only 40 % of quercetin remained, and this amount dropped to 20 % at pH 10 and virtually 0 % at pH 11 after 1 h[130]. This method is therefore highly dependent on the compound to be encapsulated, and is not easily applicable to oxidation-sensitive products.

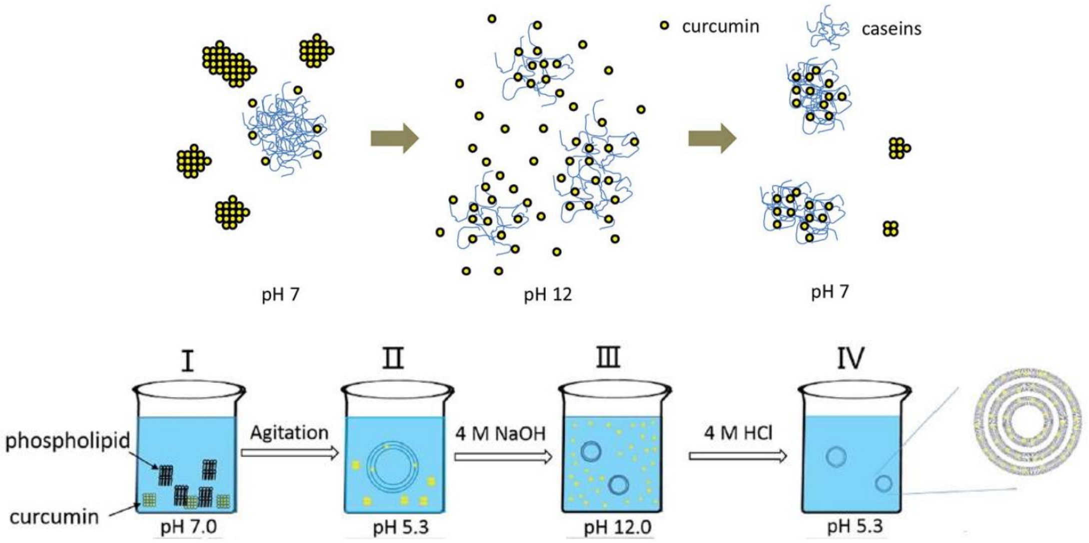

Figure II.3. Top: principle of the first pH-driven method for encapsulating curcumin into caseinate structures. Reproduced with permission from reference [129]. Bottom: application of the pH-driven method for encapsulation of curcumin into liposomes. Reproduced with persmission from reference [141].

II.3. Experimental part

II.3.1. Materials

Meglumine (> 99 %) was purchased from TCI Chemicals, quercetin monohydrate (HPLC grade) from Merck, and methanol (HPLC grade) from VWR international. HSS buffer (10 mM HEPES, 200 mM NaCl, 200 mM Sucrose, 0.01 % NaN_3, pH 7.5), and HMS buffer (10 mM HEPES, 250 mM Meglumine, 70 mM NaCl, 0.01 % NaN_3, pH 7.0) were home-made.

II.3.2. Liposomes preparation

Anionic liposomes were prepared following a modified version of established protocol[142,143] by the thin-film method and inspired by the pH-driven method[129,141,144]. Two different buffers were used for dialysis, a classical sucrose buffer (HSS), and a meglumine one (HMS). Liposomes samples were named after these buffer solutions.

Encapsulant preparation

Encapsulant was prepared by dissolving DPPC (33.12 mg, 44.12 µmol), DPPG (9.04 mg, 12.14 µmol), DMPE-PEG2000-biotin (3.40 mg, 1.17 µmol), and cholesterol (1.22 mg, 3.16 µmol) in 3 mL chloroform and 0.5 mL methanol in a round glass flask. The solvents were then removed slowly with a rotary evaporator until a thin film formed on the glass. Concurrently, 7.50 mg of quercetin (5 mM), 219.6 mg of meglumine (250 mM), and 13.15 mg NaCl (50 mM) were precisely weighted in 450 µL HEPES buffer (200 mM, pH 7.5) and 3.15 mL double distilled H_2O. 900 µL HCl (1.0 M) was added to adjust the pH to 9. Then 2 mL of the quercetin solution was added to the glass flask via syringe and septum, and the flask was vortexed and sonicated until complete dissolution of the film. This operation was repeated with another 2 mL of the quercetin solution.

Extrusion

Liposomes were extruded 21 times successively through 1.0 µm and 0.4 µm polycarbonate membrane (Whatman, Florham Park, NJ, USA) using a mini extruder (Avanti Polar Lipids, Inc.). The extrusion temperature was set to 35°C.

Size Exclusion Chromatography

Size Exclusion Chromatography was carried out with a Sephadex G-50 (Sigma-Aldrich) column (20 × 1.7 cm) with HMS or HSS buffer as eluent.

Dialysis

Liposomes were dialyzed over two days (buffer exchanged twice) at room temperature with a dialysis membrane from Spectra/Por® (exclusion size 12–14 kDa) in HMS (pH 7.0) and HSS buffer (pH 7.5), respectively.

Precaution for quercetin oxidation

In order to minimize quercetin autoxidation as much as possible, the first steps of the liposome’s synthesis were carried out under nitrogen gas atmosphere and in brown glass containers until the pH was dropped to physiological value and quercetin concurrently encapsulated. The temperature on the method was also reduced from typical 60°C to 35°C as a high temperature is a catalyst to the autoxidation reaction of quercetin. It was found out that this reduction of the temperature had no effect on the properties of the obtained liposomes.

II.3.3. Liposomes characterization and quercetin concentration assessment

Total Lipid concentration

Liposomes’ total lipid concentration was assessed using Inductively Coupled Plasma-Optical Emission Spectrometry (ICP-OES) using a SPECTROBLUE TI/EOP (SPECTRO Analytical Instruments GmbH, Kleve, Germany). Size, polydispersity and ζ-potential were determined with Dynamic Light Scattering (DLS) measurements using a Malvern Zetasizer Nano-ZS (Malvern Panalytical, Germany).

Detection of quercetin

The successful encapsulation of quercetin was assessed using a Differential Pulse Voltammetry (DPV) method adapted from Arvand *et al.*[145]. This method is based on the controlled redox reaction of quercetin by imposing precise voltage steps. In short, a home-made laser-induced graphene (LIG) electrode was used to conduct DPV measurements with minor adjustments from Arvand *et al.*: range 0.2-0.5 V, E_{step} 0.01 V, E_{pulse} 0.025 V, and t_{pulse} 0.05 s. Liposomes samples were each diluted 1:2 or 1:4 in HMS buffer with 0.1 M glycine. DPV measurements were conducted once before and once after lysis of the liposomes via treatment by sonication for 5 min. Each liposome concentration was prepared in triplicates. It should be noted that this method was not able to discriminate between native quercetin and several oxidation products of quercetin bearing adjacent hydroxyl groups (see section I.2.3.3.2) and was therefore only used as a detection method rather than for quantification.

Quantification of quercetin and oxidation

To complete and validate the results obtained with the electrochemical method, High-Performance Liquid Chromatography quantification was carried out. HPLC was performed on a Waters system equipped with a RP-18 ACE Equivalent column (250 × 4.6 mm, 2.5 µm) with a Waters 2487 Dual λ Absorbance Detector set at 210 and 370 nm. The mobile phase consisted in two solvents, Millipore water with 0.1 % TFA (A) and methanol (B). An isocratic 50:50 mixture was applied for the total duration of the sample analysis (25 min). The mobile phase flow rate was 1.0 mL/min and the injection volume was 10 µL. Liposomes samples were each diluted 1:10 or 1:5 in pure methanol and treated by sonication for 3 min to ensure lysis before the injection. Each sample was analyzed 3 times. A calibration curve of quercetin in methanol was previously prepared based on peaks area. A sample of quercetin in highly basic aqueous solution (pH > 11 obtained with 0.1 M NaOH) was also prepared and analyzed repeatedly to identify the retention times of quercetin oxidation products. In addition, certain known oxidation products of quercetin (phloroglucinol and phloroglucinic acid) were analyzed in their pure state in aqueous solution using the same method, to further validate the ability of the established method to effectively separate native quercetin from degraded derivatives, and thus to obtain a quantification accounting for the oxidative state of quercetin.

II.4. Quercetin-loaded liposomes formulation

II.4.1. Liposomes characterization

Liposomes samples were analyzed by DLS and ICP-OES to ensure that the adapted protocol and the presence of meglumine did not significantly influence the properties of the liposomes (size, surface charge, and total lipid concentration). In the following, liposomes samples are referred to as HSS (prepared in sucrose buffer) or HMS (prepared in meglumine buffer) (see section II.3.2). Furthermore, two fractions of each sample were collected after Size Exclusion Chromatography (SEC), a medium-concentrated fraction (M) and a high-concentrated one (H). If not otherwise mentioned, results are shown for the high-concentrated liposome fraction. Both HMS and HSS samples yielded total lipid (tL) concentrations around 5 mM (4.54 ± 0.06 mM for HMS and 5.53 ± 0.02 mM for HSS). Average diameters were measured 206.4 ± 1.5 nm for HMS sample and 173.4 ± 1.3 nm for HSS and a polydispersity index (PI) of 0.27 ± 0.01 and 0.23 ± 0.01 was determined for HMS and HSS, respectively. Liposomes size is generally comprised between 30 nm and a few micrometers depending on the synthesis process, mostly the extrusion step. Here they were extruded through a 0.2 µm membrane (i.e. 200 nm), so their size and distribution are fairly suitable. Finally, as negatively charged liposomes should be formed with this particular synthesis, ζ-potential was measured. Both HMS and HSS were indeed negatively charged as expected, with -10.6 ± 1.3 mV for HMS and -9.0 ± 0.9 mV for HSS. Overall, it can be stated that the adapted Thin-film protocol modified with pH adjustment and presence of meglumine successfully yielded liposomes in line with what might be expected given the proportions of lipids used.

II.4.2. Liposomal quercetin detection

After the SEC step in the synthesis, it could already be visually assessed that some quercetin had been entrapped inside the liposomes, as both samples were yellow colored (see Figure II.4). However, HSS liposomes were excluded after a few tens of minutes to allow the column to be cleaned of the quercetin left by the HMS passage, and HSS sample color turned slightly darker, suggesting the probable oxidation of part of the quercetin.

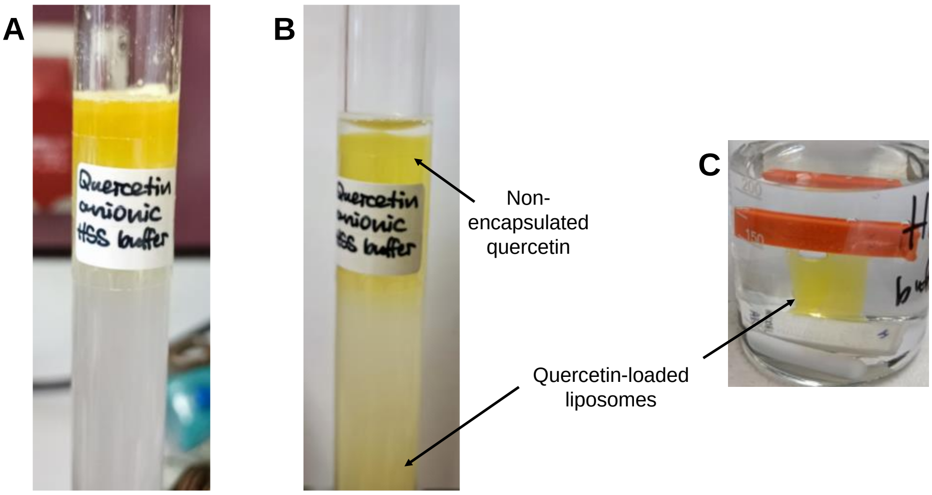

Figure II.4. SEC and dialysis steps from the HMS liposomes synthesis. A. SEC at t_0. B. SEC after a few minutes, the separation between non-encapsulated quercetin and liposomes is clearly visible in the middle of the column. C. Dialysis at t_0 after the SEC.

However, conventional quercetin detection techniques such as UV-vis spectroscopy proved unsuitable, probably due to the low concentration of quercetin inside the liposomes. An electrochemical process based on Differential Pulse Voltammetry (DPV) measurement adapted from Arvand *et al.* was then carried out[145] with a home-made electrode (see section II.3.3 for experimental details). The detection method was first tested on oxidized and fresh quercetin solutions between 0.01 and 50 µM in HMS buffer. The oxidized solutions were made by direct addition of NaOH before neutralizing again with HCl. The results of the DPV measurements on both HSS and HMS liposomes solutions are displayed in Figure II.5.

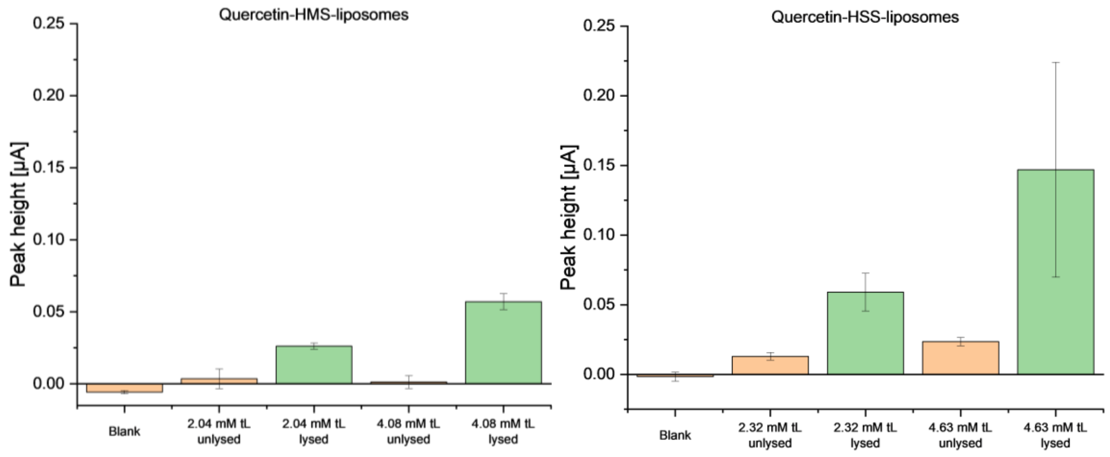

Figure II.5. DPV measurements signals of lysed (green) and unlysed (orange) HMS liposomes (left) and HSS liposomes (right) as a function of the total lipid concentration.

It is clear from Figure II.5 that for both liposomes samples, quercetin is detected with a higher intensity after the destruction of the liposomes (lysed), thereby demonstrating that quercetin was indeed encapsulated inside. However, as mentioned in section II.3.3, this method is not able to differentiate between native quercetin or oxidation products such as phloroglucinic acid, phloroglucinol, or protocatechuic acid which could also undergo the same redox reaction and be mistakenly detected as quercetin. Furthermore, it is not known if these oxidation products yield the same intensity, so that the total concentration of native and oxidized quercetin is hardly quantifiable using this method. Interestingly, HSS unlysed sample also exhibited a signal, although much weaker that lysed liposomes. This could mean that a portion of quercetin or more probably one or several oxidation products of quercetin leaked through the bilayer of the liposomes. From this method, it can be assumed that concentrations or quercetin and its oxidation products are within the range of 0.25-2.5 µM per mM tL of the respective liposomes, however a more precise quantification is needed. Moreover, even though HMS liposomes exhibited a visibly stronger yellow color, HSS liposomes yielded higher signals in the electrochemical measurements. It could thus be hypothesized that HMS liposomes contain more unoxidized quercetin compared to HSS ones, as oxidized quercetin could yield larger signals.

II.4.3. Liposomal quercetin quantification and oxidation state assessment

The detection and the precise quantification of native quercetin encapsulated in liposomes is a significant challenge for two main reasons: the very low solubility of quercetin in solution at neutral pH, and the superposition of signals of native and oxidized quercetin in the most common measurement methods. Indeed, classical protocols for Entrapment Efficacy (EE) measurement in liposomes consists in measuring the concentration of non-encapsulated product at the end of the process and thus determining the amount of encapsulated product by subtraction with the initial concentration. However, after the pH drop to physiological value during the entrapment step, the solubility of free quercetin in the solution drops as well, and it partially precipitates, making it very difficult to measure with classical spectroscopic measurement methods. Furthermore, the tested electrochemical method proved to be to be only semi-quantitative with respect to native quercetin. The samples were thus analyzed via HPLC after the liposomes had been lysed by dilution in MeOH and brief sonication. Figure II.6 shows one chromatogram for the high fraction of HMS and one for HSS.

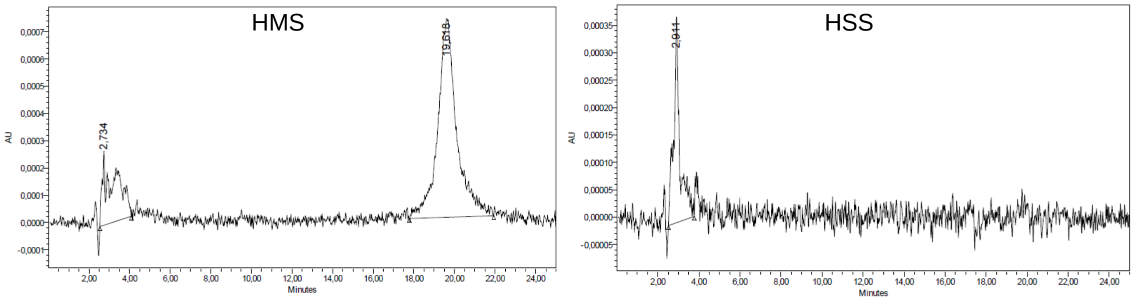

Figure II.6. Chromatograms of lysed HMS liposomes (left) diluted 1:5 in MeOH, and lysed HSS liposomes (right) diluted 1:10 in MeOH.

With the selected HPLC eluents and parameters, it was assessed that the retention time R_t of quercetin was around 20 min, where phloroglucinol, phloroglucinic acid, and protocatechuic acid exhibited signals around 2-5 min. As it is evident in Figure II.6, both HMS and HSS liposomes samples exhibited oxidation of quercetin, but while it accounts for approximately 20 % of the peaks area for HMS, it is the only signal visible with HSS, confirming the assumption that quercetin was oxidized in this sample. Finally, the concentration of native (non-oxidized) quercetin in HMS liposomes was determined around 17.9 µM, corresponding to 4.0 µM/mM tL, higher than expected with DPV measurements alone.

II.5. Conclusions

In this section, the feasibility of encapsulating the water-insoluble flavonoid quercetin in liposomal formulations was investigated following the good solubilization results obtained with meglumine. An alternative protocol was experimented in the framework of green chemistry, using meglumine ability to solubilize quercetin in aqueous solution at reasonable pH. It was confirmed that a swift synthesis with simple precautions against oxidation was enough to form standard liposomes with a fair amount of quercetin entrapped. Indeed around 17.9 µM of native quercetin could be encapsulated inside HMS liposomes. This protocol could be optimized by screening different pH values and the initial amount of quercetin in solution. For the synthesis of functionalized liposomes, it would also be necessary to test the feasibility of this method and the influence of meglumine on their properties. This study serves as a proof of concept of the potential use of meglumine in practical formulations, particularly in the field of drug delivery or dietary supplement. It should be noted that no claims regarding the drug delivery properties or the biological activities both *in vivo* or *in vitro* of these formulations are made in this work.

Chapter III

–

Solubilization of polyphenols with biocompatible hydrotropes: on the role of π-stacking in hydrotropy phenomena

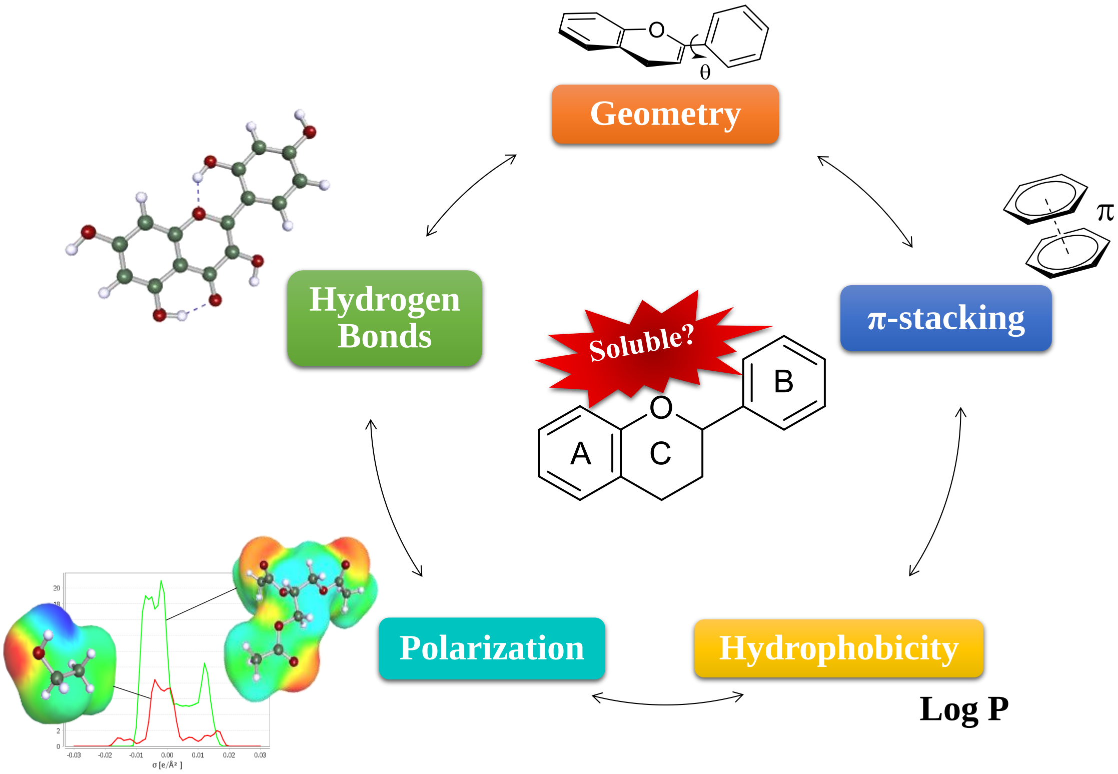
θ
O
Geometry
Hydrogen Bonds
π
π-stacking
Soluble?
O
A
B
C
Polarization
Hydrophobicity
Log P
20
18
2
0
-0.03
-0.02
-0.01
0.00
0.01
0.02
0.03
σ [e/Å²]

III.1. Introduction

One of the challenges in addressing the issue of low water-solubility of polyphenolic compounds is that many of them are not poorly soluble for the same reasons. In this chapter, six polyphenols were selected as a representative set of test compounds to try to unfold their “main hydrophobicity factor”. The structural differences between these compounds seem to exclude the possibility to find or design a versatile solubilizing agent that could be used under similar conditions with all of them. Furthermore, an understanding of the solubilization mechanisms for these polyphenols could help extraction processes or even support the design of simpler drugs for oral absorption or nutraceutics. And since one goal could be to improve pharmaceutical and possibly edible formulations, the use of biocompatible solvents or even direct solubilization in water is preferred. Binary mixtures of solvents and co-solvents that independently should be effective on a specific part of the target molecule, as well as hydrotropes, have been tested to provide information on the poor solubility of these compounds. In this perspective, the solubilization of studied polyphenols was investigated in mixtures of triacetin or cinnamaldehyde and ethanol. All these solvents are approved for food applications and cinnamaldehyde, an aromatic derivative mainly found in cinnamon bark[146] is reported to have moderate antioxidant properties but also to reduce cholesterol[146,147]. Furthermore, the use of a therapeutic agent in combination with a solvent exhibiting a biological activity may be additive, but also synergistic[33,148]. Besides, Degot *et al.* successfully used binary mixtures of triacetin and ethanol to solubilize the notorious polyphenol curcumin.[126] The influence of structure geometry, hydrogen bonding, and polarization was assessed to complete this view on this enlarged set of polyphenols. Additionally, theoretical calculations could help predict solubility test and potential synergetic effects, and to that end COSMO-RS software was used to gain further insights in the solubilization mechanisms at play.

It is well known that the solubility of polyphenols increases not only with pH, i.e. through deprotonation but also with oxidation. The main reason provided is the greater aqueous solubility of oxidation products compared to native molecules. Another hypothesis that might be complementary is the hydrotropic action of certain oxidation products on the initial structures. For example, simpler phenols could penetrate the flavonoid layers and thus weaken the overall π-stacking. Indeed, π-stacking is a phenomenon that plays a major role in many biological activities because of its implication in protein aggregation and polyphenol solubilization. However, the stacking of several phenolic compounds with one another as an obstacle to solubilization is far less investigated. It is therefore vital to understand at least qualitatively the influence of the compound structure on π-stacking intensity. Furthermore, the major importance of this phenomenon in the solubilization mechanisms of natural molecules drives the search for efficient anti-stacking agents. Phloroglucinol (benzene-1,3,5-triol) is one of the oxidation by-products of many flavonoids (they are sometimes referred to as “phloroglucinol compounds”, see section I.2.3.3.2). It results from the degradation of phloroglucinic acid. In this perspective, phloroglucinol was investigated as a potential hydrotrope for native flavonoids, particularly those that exhibit a strong stacking, i.e. quercetin and morin. It was compared to pyrogallol, another benzene-triol, which is already recognized as a hydrotrope in the literature.

III.2. Bibliographic background

III.2.1. Definitions and concepts of hydrotropy

What is a hydrotrope?

The concept of hydrotropy was introduced by Neuberg in 1916 as a new terminology to describe the striking and powerful solubilizing effect of several water-soluble aromatic salt (anionic) compounds on a variety of hydrophobic molecules.[149,150] Hydrotropes were defined as short amphiphiles for which the hydrophobic part is too small to induce the formation of highly aggregated structures, like micelles with surfactants. Hydrotropes were initially mostly aromatic compounds substituted with a hydrophile group such as sulfonate, for instance with sodium xylene sulfonate (NaXS or SXS), sulfate, or carboxylate. Since Neuberg's visionary first publication, the definition of hydrotropy has evolved to encompass a multitude of other compounds and attempt to account for the various effects responsible for this effect. In addition, a deeper understanding of distinct solubilization phenomena is now available, notably through the work of Hofmeister, Winsor, Bancroft, or McBain (this will be discussed in detail in section IV.2). However, Neuberg already pointed out the differences between hydrotropy and salting-in effect of ions such as thiocyanate in solubilizing aliphatic/ hydrophobic compounds, although the difference was more unclear regarding protein solubilization.[149]

Furthermore, and setting aside the well-studied surfactants, there are now a multitude of different names given to molecules capable of increasing the solubility of hydrophobic compounds in water, like solubilizers, solubilizing agents, or co-solvents. Ethanol for example is often referred to as a hydrotrope, but the denomination co-solvent is also well-suited as its structuring in water is not really enhanced by the presence of a hydrophobic compound (except close to the phase separation boundary, as in the case with the water-ethanol-*n*-octanol system[151] and so does not fulfill the property A mentioned below[152]. Short hydrotropic amphiphiles like C_iE_j, C_iP_j, C_iGly_j (see section III.2.2) are also sometimes named “solvo-surfactant”[153] to highlight their volatility as opposed to ionic hydrotropes such as sodium xylene sulfonate (NaSX or SXS). It should be pointed out that although hydrotropes are not easily defined, they are clearly different from surfactants in that they do not exhibit a well-structured self-assembly such as micellization, and the amount of hydrotrope to reach in order for the solubilization effect to effectively occur is in general much higher (≈ 1 M) than for surfactants (CMC ≈ $10^{-2} – 10^{-3}$ M). Finally, some studies now prefer the term “hydrotropic agent” rather than hydrotrope to establish the fact that the solubilizing agent exhibits similarities in its properties with hydrotropes without necessarily entering the debate of the mechanism-linked definition for example with aggregation.

Nowadays, the definition commonly found describes a hydrotrope as a compound that does not self-aggregate in aqueous solution, but increases the solubility of hydrophobic compounds in water by clustering around them and thus compensating for the hydrophobic effect.[152] However, the diversity of chemical and physical effects involved in hydrotropy, and the diversity of structures recognized as hydrotropes (see section III.2.2), greatly complicate the establishment of a unified and coherent concept to describe hydrotropy.[149] In an attempt to clear the ambiguity of the hydrotrope definition, and inspired from other works on hydrotropic solubilization[154–156], and to account for the specificity of hydrotropic effect in water compared to organic solvent, Kunz *et al.* proposed in 2016 a two-point definition[152];

- *"A hydrotrope is a substance whose structuring in water is enforced by the presence of a third, water-immiscible compound (property A)"*
- *"Hydrotrope is then a substance, whose structuring in the organic solvent is enforced by the presence of water (property B)"*

This definition is deliberately vague about the nature of hydrotrope-hydrotrope and hydrotrope-solute structuring so as not to favor one hypothesis regarding the driving force of hydrotropy, and to account for the lack of clear structuring, as with surfactants. The different mechanisms thought to be responsible for the hydrotropy effect are explained in greater detail the next subsection.

Mechanism of hydrotropic solubilization

There is still much debate in the scientific community on the main driving forces of the hydrotropic solubilization effect. Over time, several non-mutually exclusive hypotheses have been put forward in an attempt to explain this phenomenon. These hypotheses are commonly classified as self-aggregation of hydrotropes (i.e. a non-cooperative aggregation), preferential hydrotrope-solute interaction (i.e. a cooperative association), and water structure alteration (see Figure III.1).

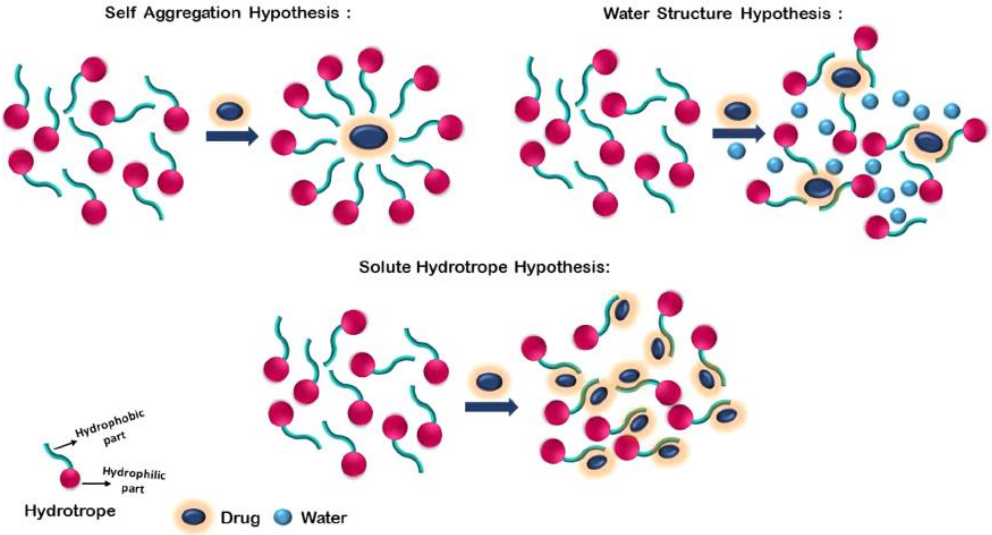
Self Aggregation Hypothesis :
Water Structure Hypothesis :
Solute Hydrotrope Hypothesis:
Hydrophobic part
Hydrophilic part
Hydrotrope
Drug
Water

Figure III.1. Schematic representation of the mechanisms of hydrotropic drug solubilization according to the three main hypotheses. Reproduced with permission from reference [157].

The hypothesis of non-cooperative aggregation of hydrotropic molecules as a driving force for solubilization has been put forward by part of the scientific community based on molecular dynamics simulations[158] and osmometry studies.[159] This view considers self-aggregation of hydrotropes as a prerequisite for hydrotropic solubilization. Indeed, the Critical Aggregation Concentration (CAC), defined as the CMC counterpart for hydrotropes, i.e. the concentration where structuring occurs spontaneously, has been reported to be slightly lower than another concentration, the Minimum Hydrotropic Concentration (MHC) already suspected by Saleh *et al.*[160], which is defined as the concentration above which the hydrotropic solubilization takes place, suggesting that aggregation of hydrotropes drives the solubilization effect[161]. The MHC is also considered to be only dependent on the hydrotrope, and therefore not influenced by the hydrophobic compound.[161]

On the other hand, this was shown mainly for conventional anionic aromatic hydrotropes such as sodium salicylate (NaSal), nicotinamide, or sodium xylene sulfonate. Other compounds which are not prone to self-aggregation, such as ethanol, urea, or short aliphatic amphiphiles, have been shown to exhibit hydrotropic activity, so the self-aggregation hypothesis needs to be completed.[152] In fact, it is now well-known that the presence of the hydrophobic solute itself can have a strong influence and even be the main driving force for hydrotropic aggregation, and that hydrotropy can thus be seen as a cooperative phenomenon.[162] Shimizu *et al.* also stated that this cooperative aggregation is enough to explain the typical sigmoidal shape of the hydrotropic solubilization curve (great increase above the MHC then a plateau is reached at high concentration), based on statistical thermodynamics[162], in agreement with Balasubramanian *et al.*[161]. The solute-hydrotrope preferential association as major force for the solubilization is also believed to apply to a multitude of drug molecules, similar to a complexation phenomenon.[157] Even if there is still no consensus on the main driving force of hydrotropy, it is fairly accepted that hydrotropes form weak aggregates. Figure III.2 depicts the idea of a solute-induced cooperative aggregation of hydrotropes molecules.

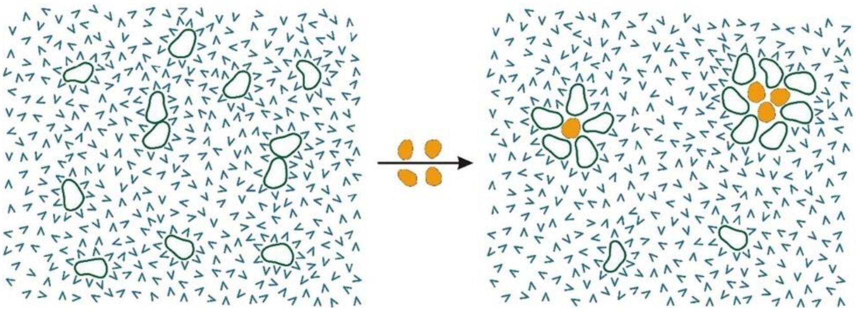

Figure III.2. Schematic representation of the clustering of hydrotrope molecules (green shapes) around a hydrophobic solute (orange). The blue “v” represents water molecules. Adapted with permission from reference [152].

Finally, through the use of the Fluctuation Theory of Solution (FTS), it has been suggested that self-aggregation of hydrotropes hinders solubilization, rather than increasing it.[157] The last hypothesis, stating that hydrotropes induce a water activity depression promoting solubilization, is now viewed as a secondary contribution compared to the accumulation of the hydrotrope around the solute.[154,156,157] One way of combining these views is to see the hydrotrope-solute association as a water-mediated interaction between the hydrophobic parts of both hydrotrope and solute[163] as depicted in Figure III.3.

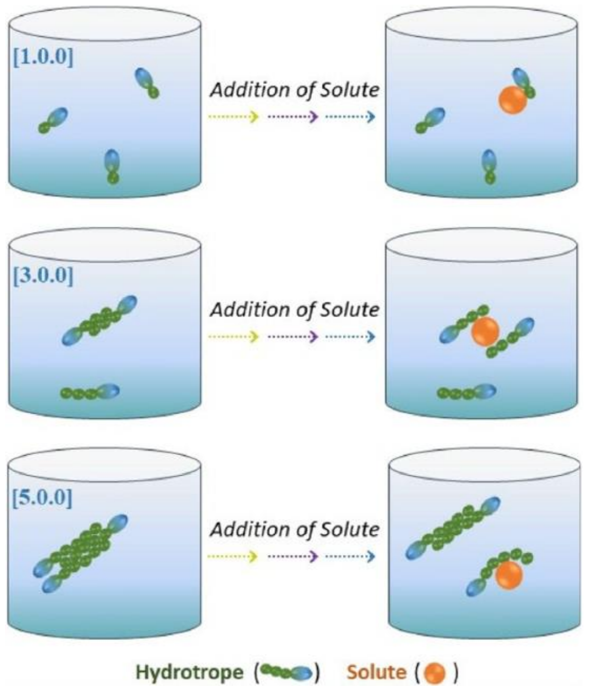

Figure III.3. Schematic representation of the hydrotropy mechanism with varying degrees of hydrophobicities. Reproduced with permission from reference [157].

Beyond the debate about the main driving force of hydrotropy, it is clear that several distinct and sometimes complementary phenomena can occur simultaneously, and that specific mechanisms arising from the particular structure of a hydrotropic agent, such as the π-stacking of aromatic compounds, can influence these contributions, making comparison between different hydrotropes families difficult and sometimes irrelevant.

Facilitated hydrotropy

Finally, one last concept to address is that of “facilitated hydrotropy”. It consists in increasing the water-solubility of the chosen hydrotropic agent by addition of another hydrotrope or a co-solvent.[164] Indeed, solubilizing agents often exhibit a preferential interaction towards the solute, but some of them are too poorly soluble in water to be described as hydrotropes, i.e. to exhibit a classical hydrotropic solubilization profile. The addition of a co-solvent or a hydrotrope to increase the solubility of the first hydrotrope may lead under optimum conditions to the formation of aggregates resulting in a great solubility enhancement of the solute.[165] Durand *et al.* for instance reported that the dimethyl isosorbide/ benzyl alcohol/ water system behaves according to the principle of facilitated hydrotropy for the solubilization of the hydrophobic dye Sudan red III, with benzyl alcohol as the facilitated hydrotrope and dimethyl isosorbide acting as the co-solvent.[165] They observed self-associating nanostructures, however they also reported a decrease in the overall hydrotropic solubilization efficacy at high co-solvent concentration, interpreted as a hinderance of the self-association process.

In the literature, a phenomenon similar to facilitated hydrotropy is also found and referred to as “mixed hydrotropy”[166]. However, this term rather applies to the use of several hydrotropes to increase the solute solubility or even to create a solubilization synergy, but not necessarily with the goal of enhancing the solubility of the first hydrotrope. Mixed hydrotropy is particularly used to solubilize poorly water-soluble drugs[166–168] but often just results from the combination of conventional hydrotropes as part of a screening process. It should also be noted that there is still a gap between theoretical studies focusing on water/organic solvent/hydrotrope ternary systems, or on the solubilization of a well-known hydrophobic test compound such as Disperse Red 13 on the one hand, and on the other hand highly empirical studies reporting the practical use of hydrotropic agents to increase the solubility of hydrophobic compounds of interest, mainly in the pharmaceutical field as an alternative to classical drug delivery systems.

III.2.2. Classical hydrotropes

Since Neuberg's first mention of hydrotropy over a century ago, a growing number of compounds have been qualified as hydrotropes. This is the case of short aliphatic amphiphiles (mainly C_iE_j and C_iP_j), which have been widely recognized as hydrotropes.[169] More recently, with the rise of green chemistry and the challenges associated with the bio-sourcing of chemical compounds, several structures derived from glycerol, notably glycerol mono- and dialkyl ethers (C_iGly and [x.y.z], respectively)[153,170,171], or from sugars such as alkyl glucosides (C_iGlu) or even sometimes short alkyl polyglucosides[172] (APGs), or mono alkyl ethers of isosorbide[173,174] (C_i-Iso), have emerged as bio-sourced hydrotropic compounds. Indeed, they can be synthesized partly from compounds recovered or derived from biomass, mostly acting as precursors.[170,173,175,176] However, large-scale industrial use of these compounds remains limited to a handful of alkyl polypentosides (*i*-C_5Xyl) and alkyl polyglucosides (C_4Glu, C_7Glu).[159] The chemical structures of the main classes of hydrotropes and are presented in Figure III.4. This categorization does not necessarily reflect particular hydrotropic properties like aggregation behavior, but rather a classification according to their structure and/or origin.

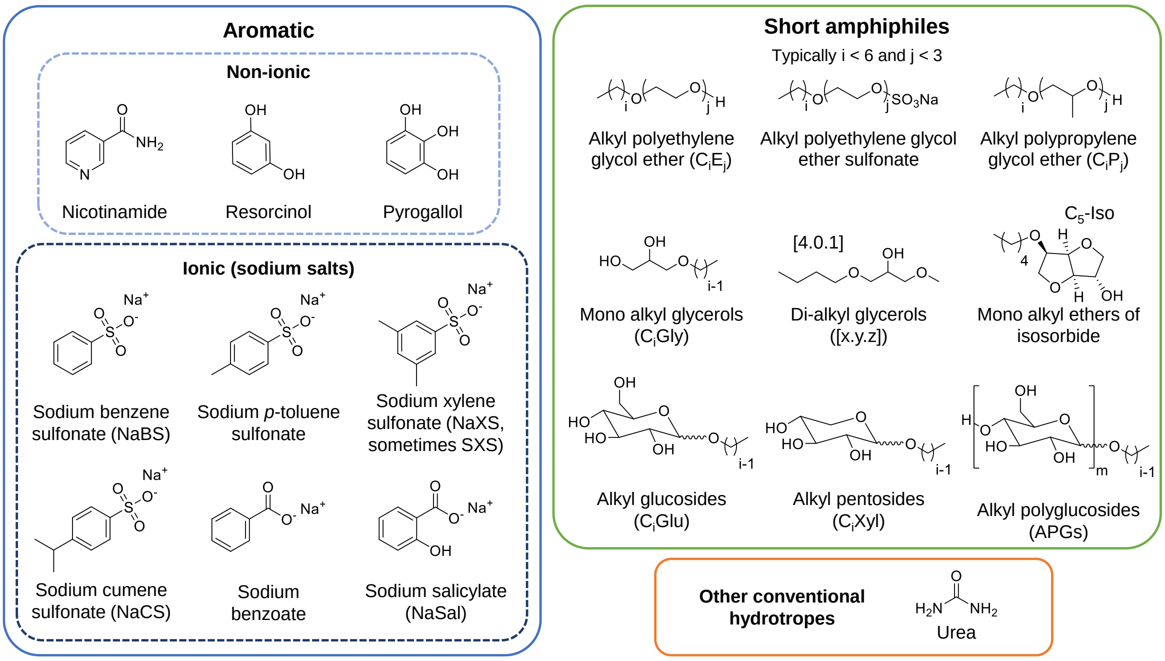
Aromatic
Non-ionic
Nicotinamide
Resorcinol
Pyrogallol
Ionic (sodium salts)
Sodium benzene sulfonate (NaBS)
Sodium p-toluene sulfonate
Sodium xylene sulfonate (NaXS, sometimes SXS)
Sodium cumene sulfonate (NaCS)
Sodium benzoate
Sodium salicylate (NaSal)
Short amphiphiles
Typically i < 6 and j < 3
Alkyl polyethylene glycol ether (CiEj)
Alkyl polyethylene glycol ether sulfonate
Alkyl polypropylene glycol ether (CiPj)
Mono alkyl glycerols (CiGly)
[4.0.1]
Di-alkyl glycerols ([x.y.z])
C5-Iso
Mono alkyl ethers of isosorbide
Alkyl glucosides (CiGlu)
Alkyl pentosides (CiXyl)
Alkyl polyglucosides (APGs)
Other conventional hydrotropes
Urea

Figure III.4. Chemical structures of main hydrotropes classes.

III.2.3. Pharmaceutical and biochemical literature research strategy

To find compounds with potential hydrotropic action, the strategy adopted was to browse the biological and pharmaceutical literature in search for “solubilizing agents” with little or no known mechanism of action. In fact, a large number of studies focuses on the biological activities of active ingredients, and water-solubilization remains a secondary issue. Others, notably in drug delivery, focus primarily on the solubilization of hydrophobic active ingredients, but are mainly empirical in their search for the most suitable solubilizing agent(s) (surfactants, cage molecules, hydrotropes, etc.).[3] There is often little to no care about the relation between the structures of the drug molecule and solubilizing agent on one side, and the effectiveness of the solubility increase on the other, notably in the case of hydrotropic agent, when micellization or encapsulation can be easily rooted out, or the hydrophobic effect appears less obvious. Meglumine for example has been reported as hydrotropic agent for a small number of drug molecules (see section I.2.4.1), however it was seen that this description does not really reflect its solubilization mechanism. This literature research approach also applied to food chemistry and aroma research, where familiar phenomena of hydrotropy such as π-stacking play an important role for instance in the altering or preserving of flavor and color upon solubilization process.

Keywords such as “solubilizer”, “solubilization agent”, “solubility enhancer”, or “hydrotropic agent” were used to scan mostly the drug and food literature from databases such as the Chemical Abstracts database (CAPLUS) and MEDLINE from SciFinder, or PubMed from the National Institutes of Health (NIH), which uses MEDLINE alongside with life science journals, and online books.

III.3. Experimental part

III.3.1. Materials

Naringenin (≥ 93 %), *trans*-resveratrol (≥ 98 %), phloroglucinol (> 99 %), and meglumine (> 99 %) were purchased from TCI Chemicals, phloretin (≥ 90 %) from Symrise, morin monohydrate (≥ 85 %), pyrogallol (≥ 98 %), cinnamaldehyde (> 98 %), triacetin (99 %), quercetin monohydrate (HPLC grade), L-pyroglutamic acid (≥ 99 %), and Disperse Red 13 (DR-13, > 95 %) from Merck. Deionized water from Milli-Q Millipore equipment was used to prepare all solutions (18.20 MΩ resistivity).

III.3.2. Methods

III.3.2.1. Solubilization measurements

Solubilization experiments of DR-13 and polyphenols were carried out by UV-vis spectroscopy. UV-vis spectra were recorded on an Agilent Technologies Cary 60 UV-vis spectrometer in 1 cm path-length quartz cells. For binary solvents mixtures, solvents were weighted to reach each selected ratio. For hydrotropy experiments, a stock solution of tested hydrotrope was prepared and diluted to chosen concentrations. Then samples were saturated by adding stepwise hydrophobic test compounds (polyphenol or DR-13) under constant stirring until visible precipitation occurred. The samples were then magnetically stirred for about 30 min to ensure proper saturation. Unsolubilized compound was removed by filtration (PTFE, 0.45 µm). Dilutions with organic solvents (methanol, ethanol, or acetone) were carried out prior to UV-vis spectroscopy measurements. Beer-Lambert calibration curves of each compound were used to calculate the amount of solubilized solute. When the signals of the hydrotrope and test compound were too close to one another and overlapped (with cinnamaldehyde for instance), a mathematical deconvolution was performed using the "*multiple peaks fit*" function of Origin software and fixing the peak value with the λ_{max} of the given polyphenol. The solubilization tests were carried out in triplicate for each solvents mixture and for each ratio to ensure reproducibility and statistical reliability, and the mean value was calculated.

For every solubilization experiment with oxidation sensitive polyphenol, protective measures were taken to prevent or slow down oxidation phenomena. Aluminium foil was used to protect samples from light, and UV-vis measurements were carried out directly after the dilution step to minimize experimentation time. Furthermore, for cinnamaldehyde, no noticeable oxidation was observed during experimentation, notably on the UV spectra. The concentration of cinnamaldehyde could moreover be confirmed by calculation from the peaks intensity and matched the initial concentrations, reinsuring that no consequent amount of cinnamaldehyde had deteriorated. In addition, cinnamaldehyde is not considered a particularly efficient antioxidant[177], which could mean that it does not easily oxidize. Finally, it should be stressed out that no reaction was observed between cinnamaldehyde and the studied polyphenols, as the UV-vis spectra were not modified (i.e. no new signal appeared, differences were only noticeable on the intensity of the characteristic peaks of each compound).

III.3.2.2. Solubilization behavior modeling with COSMO-RS

COSMO-RS software (see section I.3.3) was used to predict solubility profiles and potential synergies of solubilization of binary solvents mixtures. For each compound, its chemical potential of solvation μ_{solv} was calculated for each ratio of ethanol-triacetin and ethanol-cinnamaldehyde mixtures. A minimum of μ_{solv} is interpreted as a maximum of solubility. For solubilities prediction, equation (III. 1) is commonly used.[178]

$$\log_{10}\left(x_j^{SOL(0)}\right) = \frac{\left[\mu_j^{(p)} - \mu_j^{(\infty)} - \max\left(0, \Delta G_{fus}\right)\right]}{RT \ln 10} \tag{III. 1}$$

with $x_j^{SOL(0)}$ the molar concentration of the solute j at infinite dilution in solvent i, $\mu_j^{(p)}$the chemical potential of pure solute j, $\mu_j^{(\infty)}$ the chemical potential of solute j in solvent i, and $\Delta G_{fus}$the Gibbs free energy of fusion. As the solute is a solid, the Gibbs free energy of crystallization or fusion, respectively, has to be considered. However, the solubilities of the polyphenols were quite high in the binary solvents mixture that the approximation of infinite dilution could not be applied anymore. Therefore, equation (III. 2) was preferred to calculate solubilities.[178]

$$\log_{10}\left(x_j^{SOL(1)}\right) = \frac{\left[\mu_j^{(p)} - \mu_j^{(i)}\left(x_j^{SOL(0)}\right) - \max\left(0, \Delta G_{fus}\right)\right]}{RT \ln 10} \tag{III. 2}$$

The solubility of the solute j is then calculated in the solvent (or solvents mixture) i in a mole fraction concentration of $x_j^{SOL(0)}$ (which was obtained via eq. III. 1) to consider the non-negligible concentration of the solute in the mixture. This equation is solved iteratively until the difference $\left|x_j^{SOL(k)} - x_j^{SOL(k-1)}\right|$ is below a given threshold and was used for the calculation of solubilities in this work.

All calculations were performed on the TZVPD-FINE level with compounds from the COSMObase TZVPD-FINE 19.0 database. If the molecule was not part of the database, the charge distribution (COSMO-surface), was calculated via COSMOconf, also on TZVPD-FINE level (i.e. full geometry optimization and extended basis set).

III.4. Solubilization in binary solvents mixtures: study of polyphenols structure-low solubility relation

III.4.1. Solubilization trials of polyphenols in triacetin/ethanol and cinnamaldehyde/ethanol systems

All the studied polyphenols were solubilized in triacetin/ethanol binary mixtures, but only quercetin, xanthohumol, and morin exhibit a λ_{max} sufficiently distant from the one of cinnamaldehyde ($\lambda_{max} = 275$nm) to be quantified precisely enough with UV-visible spectroscopy without the need for time-consuming separation techniques, and were consequently the only ones solubilized in cinnamaldehyde/ethanol mixtures. Figure III.5 presents the chemical structures of the tested polyphenols. Morin and naringenin were chosen for their structural similarity with quercetin, as morin has one hydroxyl group in position 6’ instead of 3’, while naringenin has two hydroxyl groups less and is not completely conjugated (see Figure III.5), which makes it non-planar. Xanthohumol, phloretin, and *trans*-resveratrol (referred to as resveratrol in the following) were also selected because of their different structures (geometry, hydrophobicity, potential π-stacking), and the relevance of the comprehension of their solubilization mechanism, as they all exhibit potential beneficial biological activities (see section I.2.3.3.1).

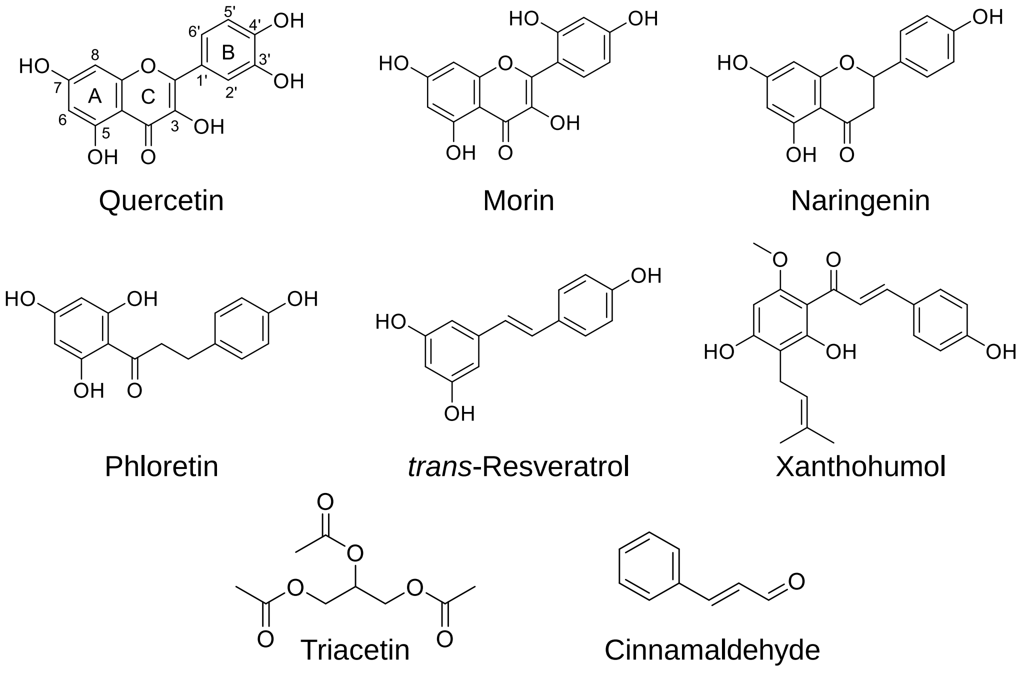

Figure III.5. Chemical structures of studied polyphenols and solvents.

Triacetin/ethanol mixtures

Solubilization profiles of investigated polyphenols in triacetin/ethanol binary mixtures are presented in Figure III.6. Quercetin, morin, and naringenin were drawn on a separate graph to highlight the potential different solubilization mechanisms of these structurally very similar compounds.

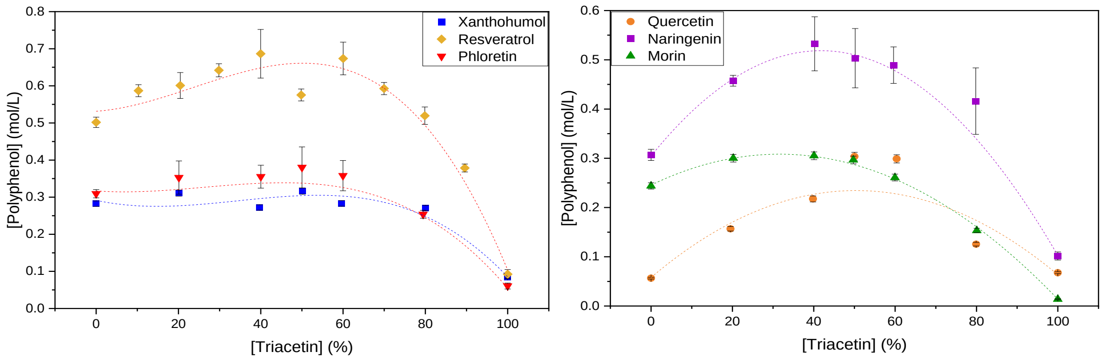

Figure III.6. Solubility profiles of studied polyphenols in triacetin/ethanol mixtures in wt%. A) Blue (squares): xanthohumol. Dark yellow (diamonds): trans-resveratrol. Red (inverted triangles): phloretin. B) Purple (stars): naringenin. Orange (circles): quercetin.

Some interesting observations can already be made by looking at the solubilization profiles. Indeed, resveratrol, quercetin, morin, and naringenin exhibit significant solubilization synergies behaviors, i.e. a significant solubility enhancement (more than 30-40 %) in the mixture compared to each pure solvent, where for xanthohumol and phloretin this is less pronounced (see Figure III.6). Furthermore, all polyphenols seem to be more soluble in pure ethanol than in pure triacetin, except for quercetin, which is rather poorly solubilized by ethanol (about 0.06 mol/L), and it also the least soluble polyphenol for almost every solvent mixture composition. Naringenin is not a planar molecule, and with two aromatic rings not situated in the same plane, it exhibits much less stacking than quercetin and morin, which could explain its overall greater solubility than quercetin and morin (see Figure III.18 and Figure A.5 in Appendix A.4).

Finally, the synergy seemingly exerted by quercetin is also much more significant than morin (the difference between the maximum solubility and the solubility in each pure solvent is far greater than for morin), which can come as a surprise when considering that their structures are highly similar. The only structural difference with quercetin is the ortho- and para-substituted B ring of morin, which could lead to the formation of an intramolecular hydrogen bond with the hydroxyl group in position 3 or the oxygen atom in the pyranyl ring, or the one from the ether group (see Figure III.5 and Figure III.18).

Triacetin/cinnamaldehyde mixtures

As previously mentioned, solubilization behavior of polyphenols for the cinnamaldehyde/ethanol mixtures could only be easily investigated with quercetin, morin, and xanthohumol. In addition, the mixtures could be analyzed only up to a cinnamaldehyde concentration of around 20 %, after which the absorbance of cinnamaldehyde is such that even at very high dilution it is experimentally difficult to obtain accurate results. Figure III.7 shows the solubilization profiles of the three tested compounds.

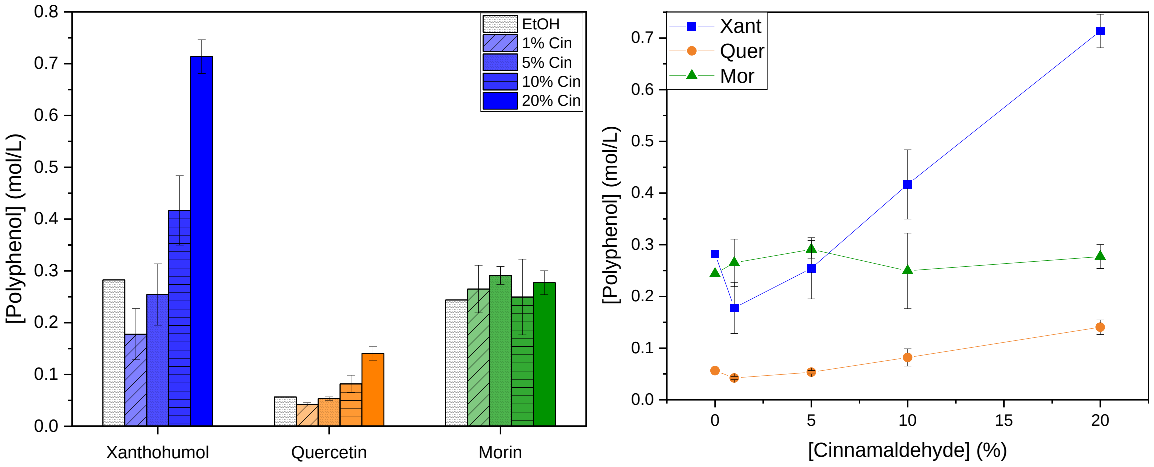

Figure III.7. Solubility profiles of studied polyphenols in cinnamaldehyde/ethanol mixtures. Blue: xanthohumol. Orange: quercetin. Green: morin.

Except in the case of morin, where it is difficult to identify a trend, the increase in the content of xanthohumol appears to be clearly correlated to the solubility enhancement of both quercetin and xanthohumol compared to pure ethanol, at least over a concentration range up to 20 wt% (see Figure III.7). However, this enhancement is significantly more pronounced for the latter. One major factor that can be emphasized is the hydrophobicity of solvents. Indeed, cinnamaldehyde is much more hydrophobic than triacetin, as shown by its octanol-water partition coefficient (log K_{ow} or log P), around 1.80-1.90 (estimated), against 0.20-0.25 for triacetin (estimated). This greater hydrophobicity of cinnamaldehyde may partially explain why it is able to better solubilize xanthohumol compared to triacetin (around 0.7 mol/L at 20 % cinnamaldehyde and around 0.3 mol/L with 20 % triacetin, see Figure III.6 andFigure III.7) which is very hydrophobic (log P around 5, estimated). However, hydrophobicity alone cannot account for all the observed solubilization behaviors, since quercetin and morin, which are also quite hydrophobic (log P about 1.5-1.6 for both, estimated), are not really better solubilized with cinnamaldehyde than with triacetin as secondary solvent (at least over the investigated concentration range). It seems therefore that hydrophobicity is the main factor hindering the solubilization of xanthohumol, but is only a secondary factor, or at least not unique regarding quercetin and morin.

Another phenomenon to consider is the formation of hydrogen bonds (HBs). Intuitively, molecules with numerous groups capable of forming such bonds with the solvent should exhibit better solubility, due to the stability of the solvated form. This should be the case for polyphenols, but it is well known that these molecules are generally not highly soluble in water, which is a particularly suitable solvent for the formation of HBs. Indeed, the stabilization of molecules in solution is a necessary but not sufficient condition to obtain successful solubilization. It also depends on the stability of the crystalline forms, among others. Thus, solute-solute intermolecular HBs can lower solubility. In addition, strong intramolecular HBs can inhibit the formation of intermolecular HB with the solvent. The hydroxyl group in position 5 on the A ring of flavonoids is for example well known to form a strong intramolecular HB with the ketone function of the same ring, which could explain the high pK_a of this hydroxyl group[83] (see structures in Figure III.5).

Finally, π-stacking should also be considered. This phenomenon has already been discussed in the first part of this work. Cinnamaldehyde could interact with the A-ring of flavonoids (see Figure III.5). However, one can see in Figure III.7 that cinnamaldehyde cannot efficiently break the stacking of quercetin and morin, judging by the very poor or even non-improvement of solubility with increasing concentration of cinnamaldehyde.

III.4.2. Solubilization modeling and synergetic effects predictions with COSMO-RS

To gain further insight into the reasons for the different solubilization behavior observed for polyphenols, and to screen the solubilization potential of cinnamaldehyde/ethanol binary mixture over the entire range of cinnamaldehyde concentration, COSMO-RS software was used to predict chemical potential μ_{solv} and solubilities of the studied polyphenols in both triacetin/ethanol and triacetin/cinnamaldehyde mixtures (Figure III.8 and Figure III.9).

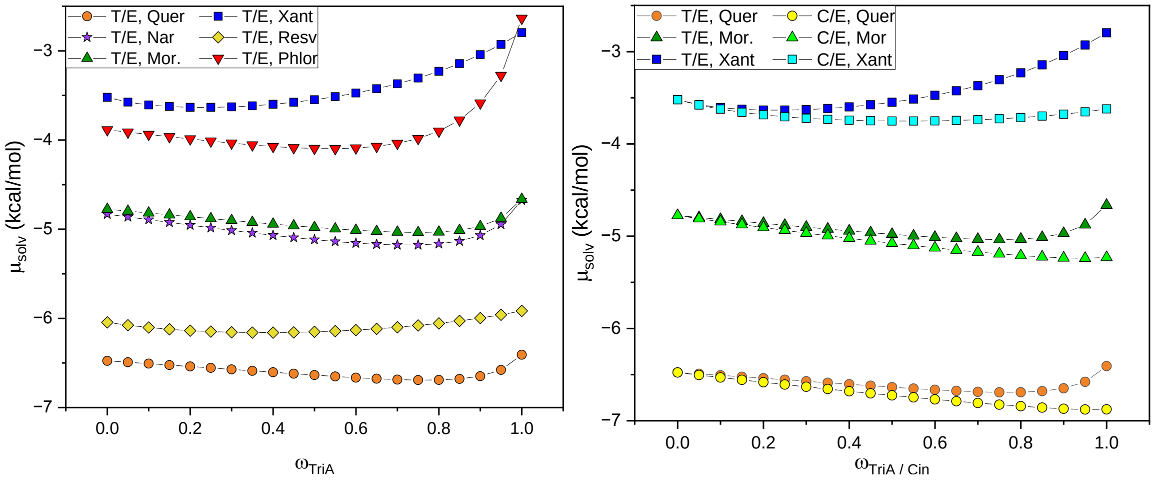

Figure III.8. Chemical potentials of solvation μ_{solv} in triacetin/ethanol mixtures of all studied compounds (left) and comparison of chemical potentials of solvation μ_{solv} in triacetin/ethanol and cinnamaldehyde/ethanol mixtures of xanthohumol, morin, and quercetin (right) calculated with COSMO-RS software. Orange circles: quercetin. Purple stars: naringenin. Green triangles: morin. Blue squares: xanthohumol. Yellow diamonds: trans-resveratrol. Red inverted triangles: phloretin. Lighter colors represent triacetin-ethanol mixtures while darker colors represent cinnamaldehyde/ethanol mixtures.

Solubility results from COSMO-RS are to be considered in comparison with experimental results shown in Figure III.6 and Figure III.7. Firstly, it is obvious from Figure III.8 that μ_{solv} of all studied polyphenols are predicted to be lower in ethanol than in triacetin. The opposite is observed with cinnamaldehyde, which according to COSMO-RS calculation, solubilizes quercetin, morin and xanthohumol better than ethanol. At high cinnamaldehyde/triacetin concentration however, one can observe that the difference of μ_{solv} is significantly more pronounced with xanthohumol compared to the other two flavonoids. This is consistent with experimental solubility profiles (see Figure III.7), showing a growing solubility gain with increasing cinnamaldehyde concentration for xanthohumol compared to quercetin and morin above 10 % cinnamaldehyde. Due to experimental limitations discussed above, cinnamaldehyde concentrations were limited at

20 wt%. The COSMO-RS calculations indicate, however, that an even greater increase in solubility could be expected at higher cinnamaldehyde concentrations.

The comparison between COSMO-RS predictions and experimental data can also be further examined by looking at possible synergies. Indeed, μ_{solv} calculations for triacetin/ethanol mixtures show a synergy for all studied compounds reflected by a minimum of μ_{solv} for a non-extreme concentration of one solvent (see Figure III.8). However, observed solubility synergies upon experimentation showed significant magnitude differences in the synergies between the investigated polyphenols, which are much less pronounced in μ_{solv} calculations (see Figure III.8). In fact, μ_{solv} is a well-suited criterium to investigate the existence of solubilization synergy between solvents synergies in terms of molecular interactions, but reflect poorly the intensity of the synergy. To further study this behavior, solubility values were predicted with COSMO-RS according to equation (III. 2) (see section III.3.2.2 for explanations). Figure III.9 shows the solubility predictions for all studied polyphenols in triacetin/ethanol mixtures.

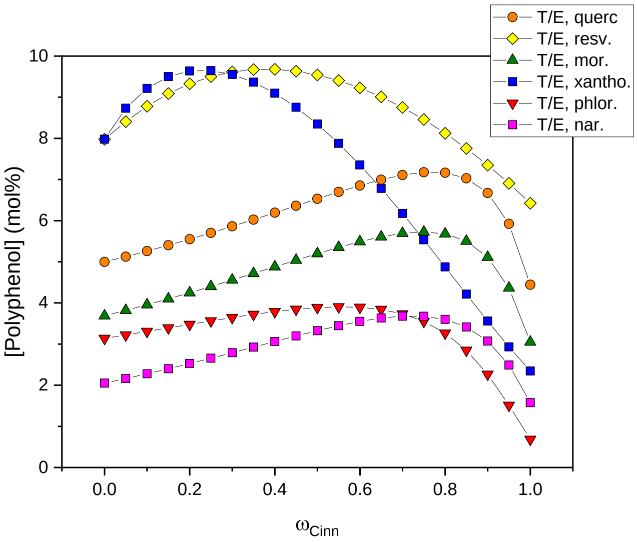

Figure III.9. COSMO-RS predictions for the solubility in molar fraction of studied polyphenols in triacetin/ethanol mixtures. Colors are the same as for Figure III.8.

Again, COSMO-RS predicted synergies for all the investigated compounds, however this time the magnitude differences between them are more clearly visible. Indeed, it can be seen in Figure III.9 phloretin exhibits a poor synergy, as well as xanthohumol to a lesser extent (the increase in solubility from the mixture compared to pure ethanol is not significant). The other polyphenols show much greater synergies, even if the overall solubility or the solubility gain compared to one pure solvent is much higher than the other, as seen for xanthohumol. These observations match the experimental results (see Figure III.6).

Moreover, although the predicted solubility values themselves are theoretical and therefore cannot be considered as such (see below COSMO-RS limitations), the solubility enhancement factors predicted with COSMO-RS are still relevant. For instance, resveratrol is predicted to have an increased solubility by a little over 20 % (in mol%) at the highest solubility compared to the one in pure ethanol (see Figure III.9), while the experimental increase is from approximately 0.50 mol/L to 0.68 mol/L (~12 % increase in mol%, see Figure III.6). Similarly, the highest solubility in a binary triacetin/ethanol mixture of naringenin is predicted to be almost 80 % higher (in mol%) than in pure ethanol, whilst the experiment shows an increase from 0.31 mol/L to 0.53 mol/L (~53 % increase in mol).

Another lead to understand these synergies arises from the disruption of ethanol HBs network by triacetin. Indeed, a pure ethanol solution can be viewed as three-dimensional regular intermolecular hydrogen bonds network. The idea of the disruption of that somewhat stable network is that, when triacetin is added, ethanol molecules bind less strongly with it than with themselves, and are therefore more available to form HBs with the solute upon addition of the latter. This hypothesis was suggested by Degot *et al.*, who reported that a mixture of triacetin and ethanol has the ability to solubilize curcumin, and that this phenomenon is maximized in a range of 60 % to 80 % triacetin.[126] This phenomenon, driven by the polarity of the solvents and the solutes, could explain why the synergies are observed more or less also in the same range (60 % to 80 % triacetin) for naringenin, phloretin, morin, and quercetin. Besides, it is complementary with the weaker solubilization of the very hydrophobic xanthohumol or the structures exhibiting strong stacking, i.e. quercetin and morin. However, this explanation alone is not sufficient to fully elucidate the differences in synergies observed at much lower triacetin concentration with resveratrol and xanthohumol (see Figure III.9). Indeed, this view is based on COSMO-RS calculations made at infinite dilution, which removes the influence of the solute. The addition of the solute could indeed significantly impact the structuring of the solvents, which makes the phenomenon even more challenging to understand.

To understand the origin of the solubilization synergies between ethanol and triacetin, COSMO-RS is once again a useful tool. To that end, σ-profiles of studied compounds and solvents were calculated. σ-profiles and σ-surfaces of triacetin, ethanol, and cinnamaldehyde are presented in Figure III.10, and the σ-profiles and σ-surfaces of the studied polyphenols are found in Appendix A.4. A σ-profile represents a histogram that displays the amount of surface segments with a specific screening charge density σ_i. Thus, it indicates to which extent a certain polarity can be found on the COSMO-surface of a molecule. The surface segments can be non-polar (green, $\sigma \sim 0$ e.Å^{-2}) or exhibit Lewis base (red, $\sigma > 0.01$ e.Å^{-2}) or Lewis donor (blue, $\sigma < -0.01$ e.Å^{-2}) character (for the colors, see Figure I.17 in chapter I).

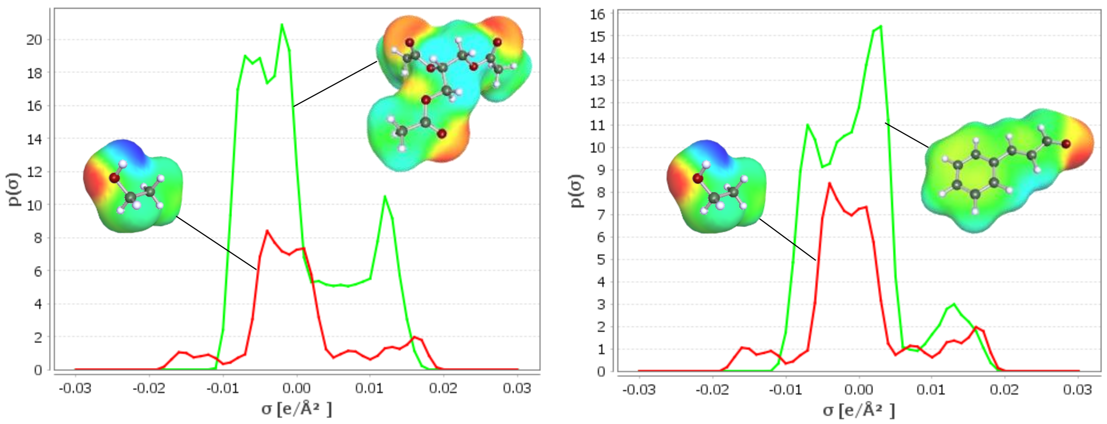

Figure III.10. σ-profiles and σ-surfaces of used solvents. Left: ethanol (red) and triacetin (green). Right: ethanol (red) and cinnamaldehyde (green).

As can be expected from its molecular structure and seen in its σ-profile, triacetin can form multiple HBs with polyphenols by offering hydrogen acceptor surface segments (see Figure III.10). In addition, significant van der Waals-interactions are possible due to a broad peak in the non-polar region of the σ-profile around 0 e.Å^{-2}. However, the σ-profile of triacetin does not show any surface segments with a screening charge density σ of ≤ -0.01 e.Å^{-2}, so triacetin lacks the ability to act as a Lewis acid. Ethanol, on the other hand is a very polar molecule exhibiting a smaller amount of non-polar surface segments while offering both surface segments with Lewis base and Lewis acid character relatively balanced. Ethanol is able to form strong HBs with polyphenols, as they all exhibit polar substituents (mostly hydroxyl groups) and also HBs acceptor (carbonyl moiety), except resveratrol. These hydrogen bonds can be considered as the main reason for the higher solubility of most studied polyphenols in pure ethanol than in pure triacetin (see Figure III.6). However, when looking at the σ-profiles of the polyphenols (see Figure A.4 in Appendix A.4), it appears that they are significantly less symmetrical than the σ-profile of ethanol. In fact, they all show quite strong Lewis acid character (presence of a region of the σ-profile ≤ -0.01 e.Å^{-2}, even ≤ -0.02 e.Å^{-2}) due to their hydroxyl groups, while the Lewis base character is less pronounced with almost none surface segments over 1.5 e.Å^{-2}. In this regard, ethanol could help reduce the electrostatic misfit of triacetin by providing hydrogen bond donors, while triacetin significantly increases the amount of van der Waals-interactions and also balances out the polar and hydrogen bonding interactions by providing almost exclusively polar surface segment with Lewis base character. One way of understanding the existence of solubilization synergies between triacetin and ethanol is therefore the optimized balance of van der Waals, polar and hydrogen bonding interactions compared to the respective pure solvents.

Predictions limitations

Although the absolute concentrations predicted by COSMO-RS cannot be taken at face value, it is in principle possible to compare them qualitatively to determine which compound is more soluble than another for a given solvent composition. However, it is obvious with the example of quercetin that this comparison is not possible for all compounds. Indeed, experimental results show that quercetin is the least soluble polyphenol of all for virtually any triacetin concentration (except in pure triacetin, see Figure III.6), however this observation is not reflected in the theoretical calculations as quercetin is predicted to be more soluble than naringenin, phloretin, and morin over the entire triacetin concentration range (see Figure III.8 and Figure III.9). This example clearly highlights some of COSMO-RS limitations. This can most likely be attributed to the inability of COSMO-RS to predict π-stacking, which is especially evident when comparing theoretical and experimental results for the three structurally very similar flavonoids quercetin, naringenin and morin (see structures in Figure III.5). Indeed, experimental data show that the trend in solubility is naringenin > morin > quercetin, as in the COSMO-RS predictions this trend is inverted. It has also already been seen in the first chapter of this work that π-stacking can be a major hinderance for flavonoids solubility, especially the highly conjugated and flat one, such as quercetin and morin. Naringenin on the other side is believed to be less prone to π-stacking due to its non-planar geometry (see Figure A.4 in Appendix A.4). Without any π-stacking breaking agent, it is then reasonable to think that the solubility trend observed for these structurally similar flavonoids can be explained mostly through π-stacking despite the additional HBs donor/acceptors hydroxyl groups of morin and quercetin compared to naringenin. COSMO-RS calculations, however, do not take these interactions into account and consequently fail to correctly predict the order of solubilities for these polyphenols.

Another limitation from solubility predictions comes from the conversion of chemical potential to solubility values. Indeed, this conversion depends on the accuracy of the ΔG_{fus} estimate (see eq. $III.1$ and $III.2$). Technically, literature ΔG_{fus} values can be found for all polyphenols, but these values are obtained by different methods from various publications and the amount of data (especially for the required value of ΔS_{fus}) is extremely scarce for all studied polyphenols. Thus, ΔG_{fus} estimates were used for solubility calculations. The inaccuracy of these estimates can be expected to be comparable for structurally similar compounds, such as quercetin, morin and naringenin. However, significant structural differences could potentially lead to an overall poor prediction of solubilities in terms of absolute values, like for xanthohumol. It should be stressed that an inaccurate value of ΔG_{fus} only affects the absolute solubility value, not the prediction of a synergy nor overall the shape of the solubility curve.

Finally, it is worth remembering that some of the polyphenols studied, in particular quercetin, are sensitive to oxidation phenomena. Yet, theoretical calculations are based on impurity-free mixtures. The possible presence of oxidation products of these polyphenols, which are structurally close to their native compounds, can influence total polyphenol solubilities, for example by acting as anti-stacking agents. This potential effect will be discussed in further details for the oxidation products of quercetin (see section III.6).

In summary, COSMO-RS calculations correctly predict the existence of synergies for all studied compounds, enhancement factors for most polyphenols and overall solubility ranges - given the (mostly) ab-initio nature of the calculations - quite well. However, limitations can clearly be observed with regard to the calculated relative solubilities of the polyphenols studied, especially due to the inability to predict π-stacking. Nevertheless, COSMO-RS remains a powerful tool for validating experimental results, as well as for predict synergies of solubilization in binary mixtures and to better understand their appearance.

III.5. Quercetin hydrotropic solubilization investigation

It was previously seen that different techniques can be used to solubilize quercetin in aqueous solution. Apart from classical drug delivery methods involving entrapment or encapsulation of quercetin into the hydrophobic core of highly structured aggregates or molecules (liposomes, micelles, cyclodextrins, etc.), the effective solubilization mechanism of quercetin had to involve the deprotonation of at least one or two hydroxyl groups and to hinder π-stacking. The use of meglumine was investigated to that end (see section I.4), but classical hydrotropes and compounds exhibiting hydrotropic properties could be an alternative in order to enhance quercetin aqueous solubility, especially if the π-stacking could be broken without deprotonation of its hydroxyl groups, which has been recognized as the driving force for quercetin oxidation. In this perspective, classical hydrotropes as well as some potential hydrotropic agents found in the pharmaceutical literature were investigated.

III.5.1. Solubilization trials with classical hydrotropes

The hydrotropes candidates were first tested for the solubilization of Disperse Red 13 (DR-13, see structure in Figure III.11), a hydrophobic dye classically used for hydrotropic estimation, and then used for quercetin solubilization.

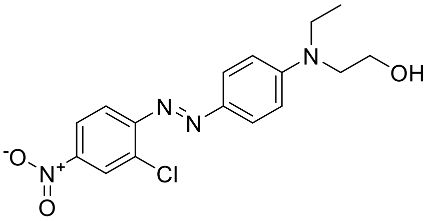

Figure III.11. Chemical structure of hydrophobic dye Disperse Red 13 (DR-13).

Quercetin solubilization was investigated with sodium salicylate (NaSal) and nicotinamide in comparison with ethanol. Solubilization profiles are presented in Figure III.12.

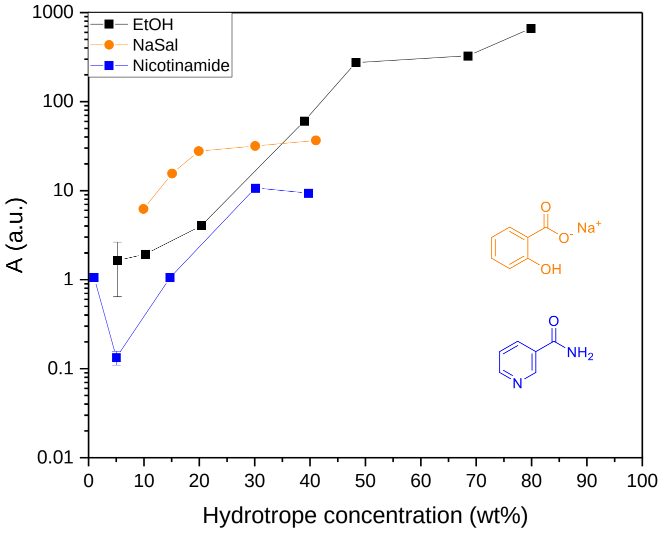

Figure III.12. Solubilization profiles in water of quercetin with ethanol (black), sodium salicylate (orange), and nicotinamide (blue).

Logarithmic scaling can sometimes be useful for comparing simultaneously several compounds that have different enhancement factors, as it allows a better visualization of these exponential effects. It can be seen in Figure III.12 that all three tested compounds behave as hydrotropes for quercetin. In addition, over a hydrotropic concentration range of up to around 40 %, where the three compounds can be compared, sodium salicylate appears to be the most effective.

III.5.2. Extension to potential hydrotropic agents

The compounds pre-selected as potential hydrotropic agents were the following: *N*,*N*-dimethylbenzamide (DMBA) and *N*,*N*-diethylnicotinamide (DENA), that have been reported to act as hydrotropes alone[179] or as functional groups providing polymers with hydrotropic properties[180], thymine, DL-tryptophan, ethenzamide, matrine, and oxybuprocaine. The structures of these compounds are presented in Figure III.13. Among these, oxybuprocaine and matrine were ruled out for the investigation as there were not easily commercially available or very expensive, and ethenzamide was finally not selected as its poor water-solubility (less than 1 g/L) prevents it from qualifying as a hydrotrope.

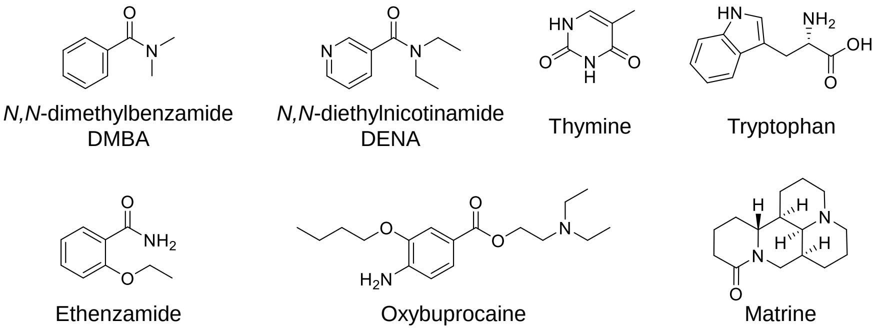

Figure III.13. Chemical structures of investigated (top) and ruled out (bottom) potential hydrotropic agents.

Figure III.14 presents the solubilization behaviors of DR-13 and quercetin with DENA, DMBA, thymine, and tryptophan.

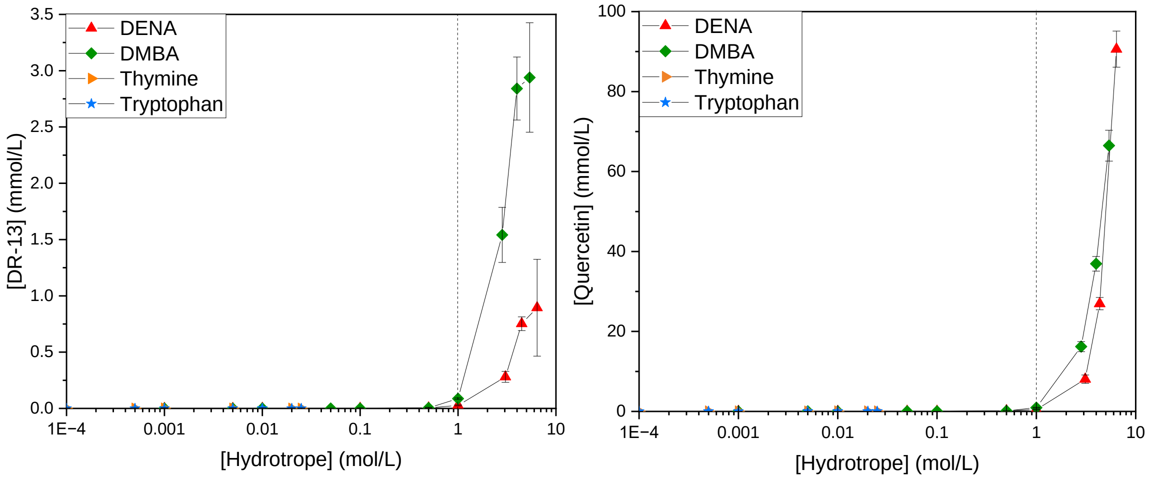

Figure III.14. Solubilization curves of Disperse Red 13 (left) and quercetin (right) with potential hydrotropic compounds DENA, DMBA, thymine, and DL-tryptophan.

It can be seen in Figure III.14 that both DENA and DMBA exhibit a classical sudden solubility enhancement at around 1 M, that can be considered as the MHC. In addition, a reduction of this solubility enhancement seems to be reached at the highest hydrotropes concentrations with DR-13 (see Figure III.14, left), indicating the probable existence of a plateau. Thymine and tryptophan however appear too poorly water-soluble to reach a concentration high enough to assess a potential influence on either DR-13 or quercetin solubility. These two compounds were therefore not further considered as hydrotropic agents.

Pyroglutamic acid

Another compound with potential hydrotropic properties towards quercetin has been investigated in greater detail: pyroglutamic acid (also known as pyrrolidone carboxylic acid, or PCA). PCA is already used as pharmaceutical ingredient as well as dietary supplement, and its sodium salt is used as humectant in the cosmetic industry. As a pharmaceutical ingredient, it was already used to enhance water-solubility of drug molecules, such as Vonoprazan[181] or as cocrystal builder[182]. However, to the best of our knowledge, PCA was never reported as a hydrotropic agent. Figure III.15 shows the solubilization trials of quercetin with PCA at two different pH values.

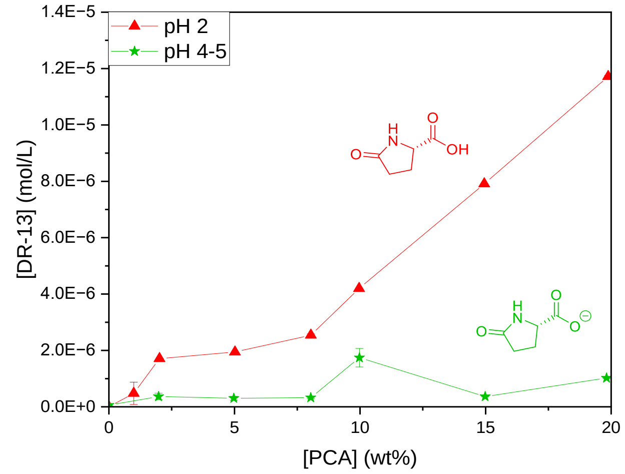

Figure III.15. Solubilization profiles of DR-13 with L-pyroglutamic acid (PCA) at two different pH values. pK_a of PCA was experimentally determined at 3.3 (see Figure A.5 in Appendix A.5).

PCA seems able to increase DR-13 water-solubility only significantly when fully protonated, i.e. at pH 2 and below (pKa of PCA was experimentally assessed at 3.3 with a standard spectroscopic method). PCA has indeed been reported to form salt with drug compound to enhance their solubility[183–185].

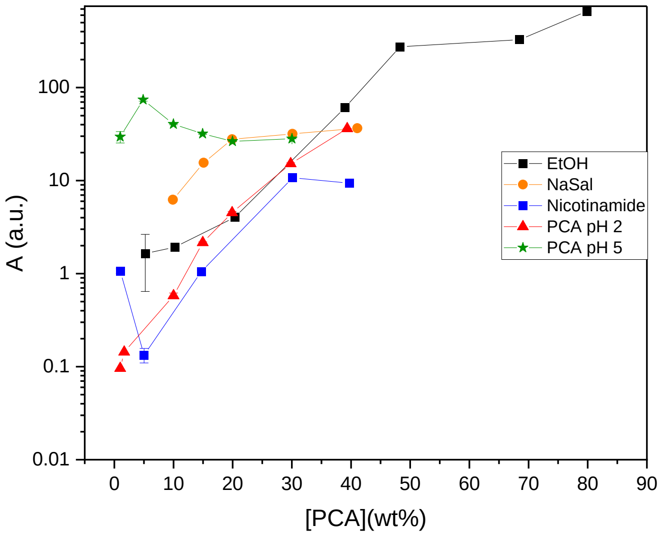

Figure III.16. Solubilization profiles of quercetin with L-pyroglutamic acid (PCA) at two different pH values compared to previous investigated hydrotropes.

Interestingly, PCA seems to be more potent in solubilizing quercetin at pH 5 than when fully protonated (up to around 30 wt%, see

Figure III.16). It can be hypothesized that at pH 5, when PCA is negatively charged, the interaction with the fully protonated quercetin (see section I.4.3) is strong enough to induce an increase in its solubility. However, contrary to pH 2 where quercetin solubility increases with PCA concentration, at pH 5 the solubility of quercetin seems almost independent of PCA concentration. As for DR-13, it is the fully protonated PCA that shows seemingly a hydrotropic behavior towards quercetin. PCA could therefore be able to hinder quercetin π-stacking (concentration-dependent phenomenon), but this property seems itself weaker than an electrostatic interaction.

III.6. Small phenol and π-stacking aggregation influence on quercetin solubility: phloroglucinol and pyrogallol

III.6.1. Solubilization enhancement comparison between phloroglucinol and pyrogallol

Based on the previous results, it is clear that an important stacking phenomenon prevents the optimal solubilization of certain flavonoids, notably quercetin and morin, even with the aromatic structure of cinnamaldehyde. It was thus decided to study the influence of two simple phenolic molecules on the π-stacking of quercetin and morin, as well as naringenin, which served as a reference flavonoid that should display less stacking as its structure is not entirely conjugated. Pyrogallol (benzene-1,2,3-triol) and phloroglucinol (benzene-1,3,5-triol) were investigated as potential hydrotropes. To better detect a potential anti-stacking effect of these structures on the studied flavonoids, water was chosen as the solvent, where the latter are particularly poorly soluble even though numerous hydrogen bonds between the hydroxyl groups of polyphenols and water molecules should, on the contrary, allow a good solubility. This shows the even stronger π-stacking in water. The Figure III.17 displays the solubilization profiles of the three selected flavonoids in water with different phloroglucinol concentrations.

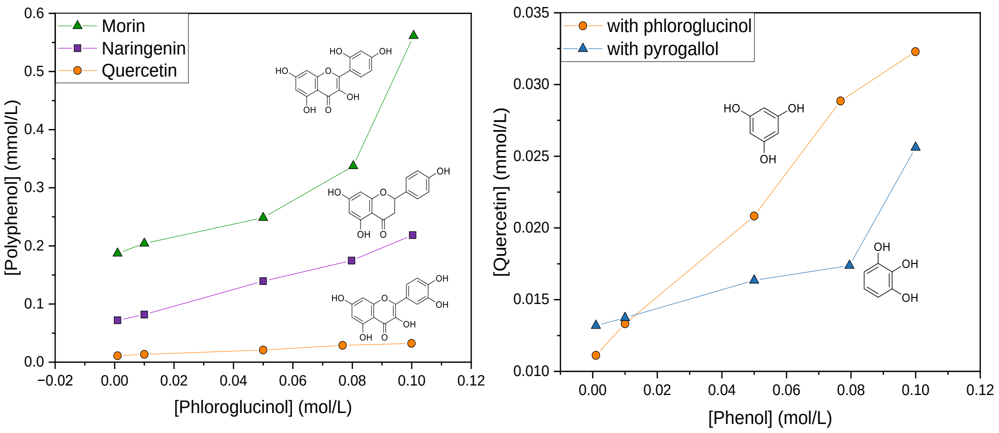

Figure III.17. Left: solubility profiles of studied polyphenols in water with phloroglucinol. Purple: naringenin. Orange: quercetin. Green: morin. Right: Comparison of solubilization of quercetin with pyrogallol (blue triangles) and phloroglucinol (orange circles).

A linear increase in solubility with increasing phloroglucinol concentration can be observed for naringenin in Figure III.17. What is most striking, however, is the almost exponential increase in the solubility of morin, compared to the very low evolution of quercetin. Contrary to pyrogallol, which is highly water-soluble and recognized as a hydrotrope[160], phloroglucinol appears too weakly soluble (about 1 wt% or around 10 mg/mL[186] which corresponds roughly to 0.08 mol/L) to qualify as a hydrotrope. In this experiment, phloroglucinol was successfully solubilized up to approximately 0.12 mol/L in pure water (0.10 mol/L was thus taken as a reasonable limit of solubility for the experiment). Furthermore, although pyrogallol is able to solubilize a significant amount of quercetin at high concentrations, due to its greater water solubility, when compared over the concentration range at which phloroglucinol is still soluble, the latter is still slightly better than pyrogallol at solubilizing quercetin (see Figure III.17, right).

Geometry

Another key factor for the solubility of polyphenols is their geometry. It is well-known that the conformation of aromatic compounds has a strong influence on π-stacking. Indeed, the planarity of a conformer facilitates (intermolecular) π-stacking, mainly for two reasons. Firstly, two planar molecules can more easily approach one another, and for an aromatic-aromatic interaction to take place, it is thought that the centroids of the phenyls must not be further apart than 7 Å[11] (at least in the case of the T-shape arrangement, but a minimal distance is still required for every kind of π-stacking). Secondly, in the case of the offset π-stack (i.e. parallel displaced), the flatness of the overall structure of a conformer allows the aggregation of several molecules on top of each other, forming piles or clusters. In other words, the aggregation of planar aromatic structures by π-stacking is less sterically hindered. This could explain the differences observed between morin and quercetin. Indeed, the two most energetically stable conformers of morin calculated by COSMO-RS (see Figure III.18) both feature an intramolecular HB of the hydroxyl group in position 2'.

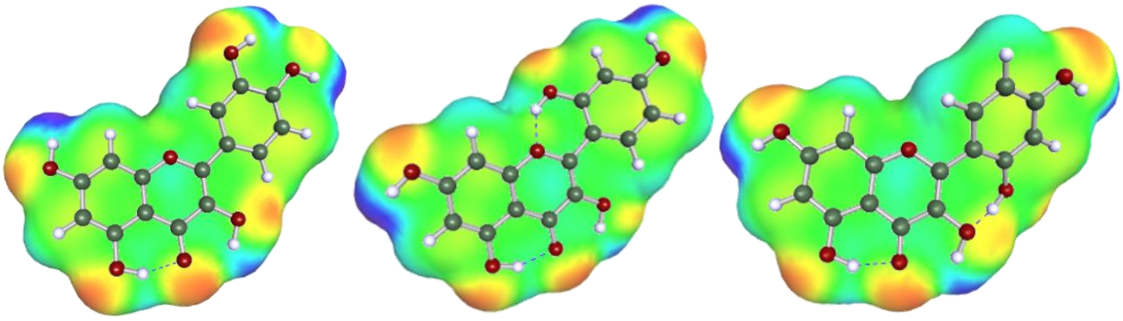

Figure III.18. Structures and σ-surfaces of the most stable conformers of quercetin (left) and morin (center and right) calculated with COSMO-RS software. Dotted line represents predicted hydrogen bonds.

This bond can be established either with the oxygen atom of the hydroxyl group in position 3, or with that of the ether function of the C ring. This HB tends to slightly break the planarity of morin conformers compared to those of quercetin, whose most energetically stable conformers are all nearly planar.

Overall, these higher solubilization results at low concentrations, along with the quick rise of solubility observed with morin even with low amounts of phloroglucinol, and the difference in trends for the three flavonoids solubilization profiles suggest that it would be interesting to investigate the anti-stacking activity[§] of phloroglucinol at higher concentrations. For this purpose, binary mixtures of ethanol and water were prepared to try to optimize phloroglucinol solubility.

[§] In this section, anti-stacking refers to the hinderance of π-stacking of quercetin molecules with one another. This mechanism is probably due to the somewhat preferential stacking of quercetin molecules with pyrogallol (or phloroglucinol) molecules, resulting in smaller aggregates easier to solvate, similar to the classical hydrotropic action with aromatic compounds.

III.6.2. Facilitated hydrotropy inspired enhancement of phloroglucinol water-solubility

Ethanol as co-solvent

Ethanol was firstly used as an obvious co-solvent to try to improve phloroglucinol water-solubility. Figure III.19 shows the quercetin solubilizing ability of the ternary system phloroglucinol/ethanol/water against ethanol/water binary mixtures as control.

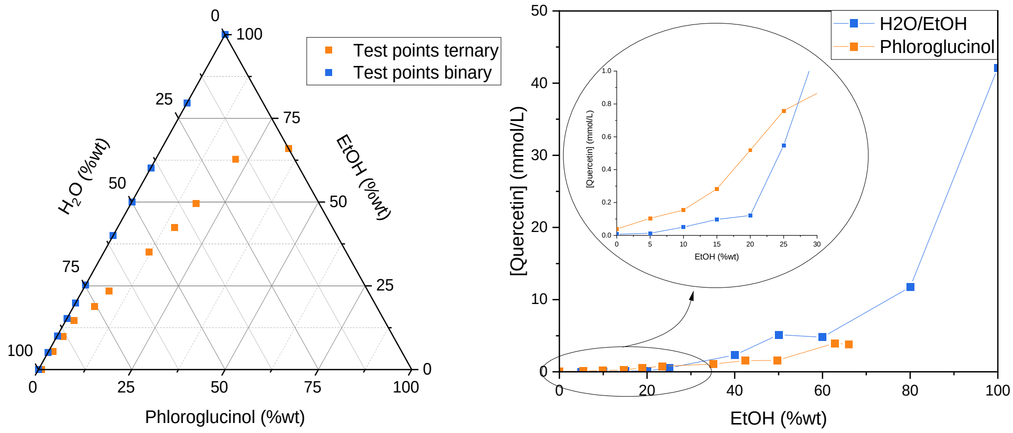

Figure III.19. Solubilization of quercetin as a proof of concept of facilitated hydrotropy of phloroglucinol with ethanol as co-solvent. Blue: reference solubility of quercetin in ethanol/water binary mixture. Orange: quercetin solubility in phloroglucinol/ethanol/water ternary mixture.

It can be seen that up to ca. 25 wt% ethanol, the ternary system, i.e. the one containing phloroglucinol, shows better quercetin solubility than the ethanol/water reference system (see Figure III.19). The logical next step was therefore to test the influence of the binary mixture phloroglucinol/pyrogallol on quercetin water-solubility.

Pyrogallol/phloroglucinol combination

Since pyrogallol is structurally very close to phloroglucinol and much more water-soluble, it might function as a hydrotrope for phloroglucinol. Figure III.20 shows a facilitated hydrotropy experiment in which samples of different pyrogallol concentrations were saturated with phloroglucinol and subsequently saturated with quercetin after filtration.

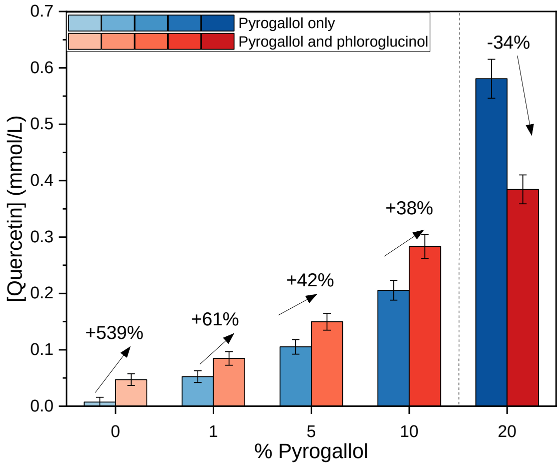

Figure III.20. Solubility profile of quercetin in water with pyrogallol alone (blue) or with pyrogallol and phloroglucinol (red). Percentages indicate quercetin solubility changes with combination of phloroglucinol and pyrogallol compared to pyrogallol alone.

Up to 10 %, it is clear that the samples containing phloroglucinol manage to solubilize quercetin better than the pyrogallol controls. Interestingly, at a high pyrogallol concentration (ca. 20 %, see Figure III.20), not only the sample with phloroglucinol does not solubilize more quercetin but on the contrary, it reduces the amount of quercetin in the aqueous solution. It should also be noted that it is difficult to precisely determine the amount of phloroglucinol contained in each sample. Indeed, to achieve maximum solubility, phloroglucinol was added in excess to the pyrogallol samples and these were then filtered. The added mass of phloroglucinol needed to reach precipitation was registered, so the concentration of phloroglucinol has an upper limit (< 0.2 M). Moreover, even if both compounds absorb at the same wavelength (λ_{max} = 268 nm), the UV-visible absorbance being additive, it is theoretically possible to determine the phloroglucinol concentration by deducting pyrogallol contribution. This being said, it is in practice rather challenging to obtain accurate results. Nevertheless, even without precisely knowing the phloroglucinol concentration, it is still possible to determine whether phloroglucinol is actually present in the final samples or not. This is the case for samples up to 10 % pyrogallol. At 20 %, it seems that the total phenol concentration (pyrogallol plus phloroglucinol) is nearly equal to, or even very slightly lower than the initial pyrogallol concentration. Thus, at high pyrogallol concentration, phloroglucinol seems to have an effect comparable to salting out (at 20 %, the solution is far from saturation with pyrogallol alone). Despite that, even with a decrease in the solubility of pyrogallol, it would not be sufficient to explain the drop of quercetin solubility by almost a third (see Figure III.20).

Anti-stacking

By considering all these factors, it is possible to better understand the different interactions at work between phloroglucinol or pyrogallol and quercetin under the tested conditions. Indeed, these two structures being composed of only one aromatic ring substituted by several hydroxyl groups, they should both be planar, be able to make several hydrogen bonds with the solvent (water and ethanol), and achieve strong stacking on the polyphenols. The conformers' calculations confirm the planarity of the two trihydroxybenzenes (see Figure V.4). However, there are important differences between them. Indeed, even if the lack of solubility of phloroglucinol is easily explained by the symmetry of its structure, its behavior regarding quercetin and pyrogallol is striking.

Cheng *et al*. showed the ability of simple phenols to adsorb onto ethylene glycol-substituted aromatic rings (polystyrene).[187] The adsorption of 1,3-dihydroxybenzene (resorcinol) increases with the number of ethylene glycol on the substrate, showing that adsorption is also driven by intermolecular hydrogen bonding in addition to hydrophobic interactions and π-stacking. But this adsorption also occurs without any substituents on the substrate, suggesting that hydrophobic interactions and π-stacking are the primary driven forces. Furthermore, they demonstrated that in the presence of HB-acceptor groups on the polystyrene rings (ethylene glycol units), multi-substituted phenols (di- and trihydroxybenzenes) whose hydroxyl groups are separated by one carbon on the ring (resorcinol and phloroglucinol) adsorb better than those with adjacent hydroxyl groups (catechol and pyrogallol, respectively).[187] Thus, two main hypotheses can be made about the superior results obtained with phloroglucinol over pyrogallol as an anti-stacking agent for quercetin. Firstly, the positioning of the hydroxyl groups of phloroglucinol is optimal since it prevents the formation of intramolecular HB that could occur in pyrogallol. Secondly, the repartition of the phloroglucinol substituents enables two possible geometries (assuming sandwich or parallel-displaced stacking, which seems to be a realistic assumption for quercetin[74]), one of which features the phloroglucinol hydroxyl groups between the ones of quercetin. This particular arrangement, where no hydroxyl faces another, which is not possible with pyrogallol, should minimize electrostatic repulsions. Obviously, this consideration alone does not fully explain the phenomenon, as electrostatic interactions are not necessarily predominant in π-stacking. However, this hypothesis remains reasonable when considering that the other interactions should not differ significantly from phloroglucinol to pyrogallol. As stated by Wheeler: *"In stacking interactions in which both rings bear substituents, the substituent effects depend on the relative position of the substituents"*[19]. It is therefore possible that this allows for better adsorption of phloroglucinol onto quercetin molecules. This could also mean that two phenol-substituted rings interact even more than one phenol with a slightly substituted ring like the one of cinnamaldehyde.

Synergy between phloroglucinol and pyrogallol

The observed synergy between phloroglucinol and pyrogallol in solubilizing quercetin (see Figure III.20) could therefore be explained by the greater aqueous solubility of phloroglucinol when combined with pyrogallol, which would then lead to a greater anti-stacking effect. Simultaneously, the presence of the strongly polarized pyrogallol could also bring more water molecules into the direct vicinity of the quercetin aggregates, thereby resulting in better solvation. Moreover, at equal pyrogallol concentration, there is an increase in the solubilization of quercetin in the presence of phloroglucinol, however, the increase generated by the latter declines with increasing pyrogallol concentration (see Figure III.20). As previously explained, the phloroglucinol concentrations of the first samples should not be significantly different from each other. In other words, the higher the share of phloroglucinol in the total phenol content (i.e. at low pyrogallol concentrations), the stronger the effect on quercetin solubilization. This shows the ability of phloroglucinol to effectively break the stacking of quercetin and thus serves as a proof of concept of the facilitated hydrotropy towards it. Furthermore, at high pyrogallol concentration, the decrease of quercetin solubilization (see Figure III.20) could be explained by a drop of the overall water-solubility of the pyrogallol-phloroglucinol aggregate, similar to a "salting out" phenomenon.

III.7. Conclusions: outlook for the search of hydrotropic compounds

In this chapter, the solubilization behavior of a set of polyphenolic compounds was investigated in binary solvents mixtures or towards selected hydrotropes in water. Although the low solubility (particularly in water, or in classical green/edible solvents) of polyphenols is well-known, choosing the appropriate solubilization strategy based on their structure does not yet seem to be standard practice in the pharmaceutical literature, where the search for solubilizing agents in often based on trial and error process.

Combinations of ethanol with triacetin or cinnamaldehyde and COSMO-RS calculations were used to highlight the effect of structural differences regarding apolarity, hydrogen bonding (inter- and intramolecular) capability, and π-stacking, as well as to detect possible synergetic behaviors. Resveratrol and naringenin were successfully solubilized in a mixture of ethanol and triacetin. For these compounds, the effects of the solvents are predominant, as triacetin creates a synergetic effect between 40 % and 60 %, presumably by breaking the structuring of ethanol, in agreement with Degot and coworkers[126], although the synergetic effect was found at lower triacetin concentrations. The strongly hydrophobic xanthohumol showed very promising solubility enhancement in the mixture ethanol/cinnamaldehyde, and could achieve even higher solubilization values at higher cinnamaldehyde concentrations. In addition, triacetin, cinnamaldehyde, and ethanol being food-agreed and edible, they can be used in end formulations or help design extraction strategies without necessarily having to remove the solvents.

Phloroglucinol, in combination with pyrogallol or ethanol, was used to study the influence of trihydroxybenzenes on the π-stacking of the flavonoids naringenin, morin, and quercetin. It showed promising results as it seems able to efficiently break the stacking of quercetin, provided it can be sufficiently solubilized in water. If this lack of solubility of phloroglucinol in water can be overcome, as it was shown with the addition of pyrogallol, or to a lesser extent with ethanol, then phloroglucinol could be consider as a hydrotropic agent for quercetin and similar compounds, like morin. Phloroglucinol is also an oxidation sub-product of many polyphenols, so this anti-stacking capacity could give an insight into why oxidized polyphenols tend to be more water-soluble than their native form. Furthermore, one can imagine how quercetin or similar flavonoids could be used in formulations as antioxidants which could then act as solubility enhancers upon degradation, a behavior one can describe as "sacrificial antioxidant/solubilizer".

To summarize, the polarity of solvents and solutes plays a key role. Software like COSMO-RS can be useful to predict trends and synergies in solubilizing behavior. However, π-stacking can also constitute a strong obstacle and the design of anti-stacking agents must be carefully considered as it is challenging to fully understand the effects of each substituent in the case of aromatic structures for example. Finally, although π-stacking is ubiquitous in biological research, in phenomena such as protein aggregation, co-pigmentation, co-crystallization and others, it seems to be less considered when hydrotropic behavior is suspected, perhaps because π-stacking is sometimes regarded as an organized structuring, in opposition with the conventional non-organized aggregation view of hydrotropes. It thus appears that there should be further research focusing on hydrotropic solubilization mechanism from the perspective of pro- and anti-stacking.

Chapter IV

—

Meglumine and metformin as new counterion for fatty acids: brief characterization and perspectives

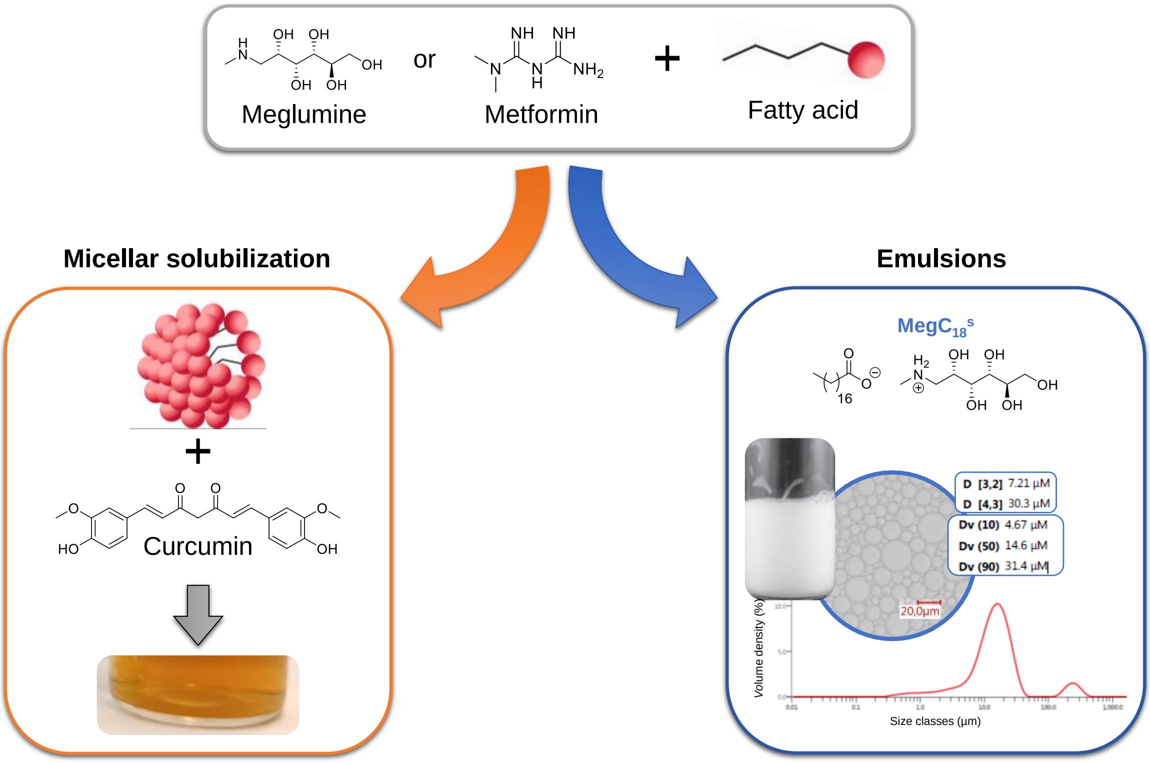
Meglumine
or
Metformin
+
Fatty acid
Micellar solubilization
Emulsions
MegC18s
16
Curcumin
D [3,2] 7.21 µM
D [4,3] 30.3 µM
Dv (10) 4.67 µM
Dv (50) 14.6 µM
Dv (90) 31.4 µM
20,0µm
Volume density (%)
Size classes (µm)

IV.1. Introduction

Traditional soaps, i.e. fatty acid salts (mostly sodium or potassium salts) have been used for ages, and are still widely spread today, especially because they are inexpensive, easy to formulate, and require only readily available raw materials. Furthermore, in addition to displaying great detergency properties, these molecules also have antimicrobial properties which could be interesting in various fields of application such as agriculture, medicine, and cosmetics[188,189]. However, they suffer multiple limitations as they are irritant, especially to the eyes, and give a bad taste to food formulation[189]. Moreover, their weak solubility in water at room temperature, reflected by relatively high Krafft points[190,191] reduces the field of their applications. The solubilization power of a surfactant tends to increase with the length of its hydrophobic part, but its solubility decreases simultaneously, this is why it is interesting to find ways to lower the Krafft point of surfactants with long carbon chains. For sodium laurate (NaC_{12}), the Krafft point is still about 25°C but it increases rapidly with longer alkyl chains and is about 71°C for sodium stearate[191] (NaC_{18}).

To increase their solubility, fatty acids are often chemically modified (mostly ethoxylated and sulfonated methyl esters derivatives[192]) but these techniques require synthesis steps and add complexity and cost to the formulation. The nature of the counterion also influences greatly the solubility of a surfactant[193]. Tetraalkylammoniums for example have proved to be efficient to lower the Krafft point of carboxylates[194,195]. Tetrabutylammonium (TBA) in particular can decrease Krafft temperature down to less than 3°C for carboxylates soaps with chain length up to C_{20}[194]. However, the known toxicity of tetraalkylammonium prevents them from being used in industry. Choline, formerly known as vitamin B_4, is another interesting lead. Choline is a quaternary ammonium but with a hydroxyl group that allows its physiological degradation. Choline soaps have the advantage of having low Krafft temperatures[196–198] while being totally biocompatible[199]. Nevertheless, despite their fine properties, these systems still suffer from several limitations, e.g. their unpleasant smell. Further, the current legislation also does not allow the use of choline in cosmetics.

All in all, several amino compounds have been demonstrated as potent counterions for soaps formation. Here we propose the study of meglumine and metformin as interesting amino-counterion for fatty acids soaps. Meglumine is already known to form adducts with carboxylic acids through salt formation (see section I.2.4) and has the possibility to form multiple hydrogen bonds with water. Metformin is particularly interesting for drug delivery applications, where it could benefit from being associated with hydrophobic fatty acids to possibly enhance its bioavailability.

IV.2. Bibliographic background

IV.2.1. Surfactants: definition and applications

Surfactants (or surface-active agents) are amphiphilic organic molecules, i.e. they possess both a hydrophilic and a hydrophobic moiety and are able to lower the interfacial tension (called surface tension in the case of a water-air system) between two immiscible phases. This is due to their adsorption at the interface resulting from their amphiphilic nature. They exhibit many unique properties, one of the most interesting being the ability to spontaneously form micelles at a given concentration in aqueous solution, the so-called Critical Micellar Concentration (CMC)[200,201]. Surfactants are often classified firstly according to their polar head, the main classes of surfactants thus being ionic, non-ionic, and zwitterionic surfactants, functional and structural groups accounting for the subclasses[201]. In addition, it is becoming increasingly common to also designate surfactants according to their origin, for example whether they are derived from petrochemicals or renewable resources[192,200,201]. However, the pertinence of the opposition between "synthetic" and "natural" surfactants is still subject to much debate, as it does not necessarily reflect an opposition in either their properties or their environmental impact[201].

Surfactants are ubiquitous in industrial and personal applications such as the such as the agricultural and pharmaceutical industries, personal care, household products or in food as emulsifiers.[201,202] They can as well be used for catalysis, or direct solubilization and therefore also extraction. In order to act as efficient solubilizing agents, surfactants have to be used at a higher concentration than their CMC (CMC $\approx 10^{-4} - 10^{-2}$ M) to form micelles. The formation of direct micelles for example (hydrophobic tail oriented towards the inner core and polar heads towards water) create hydrophobic cavities able to entrap poorly water-soluble compounds[203].

IV.2.2. Surface tension, micellization, and other phase behaviors

At equilibrium, attractive forces between solvent molecules are identical in all directions. This homogeneity is disrupted at the interface, i.e. at the boundary of an immiscible phase (air or oil in the case of water, for example). Consequently, molecules at the interface have a higher free potential energy than molecules in the bulk liquid (because of weaker or no attractive forces in the direction of the second phase)[200]. This excess of free energy per surface is called interfacial tension or surface tension γ in the case of liquids and can be assimilated to a force per unit length. Another representation is to consider surface tension as the minimum work required to expand the interface by migration of molecules from the bulk, at given temperature and pressure. When surfactant is added to a biphasic system, it adsorbs at the interface, and the newly created molecular interactions between the polar phase molecules and polar head of the surfactant on the one hand and between the non-polar phase molecules and the hydrophobic tail on the other are stronger than the one between the two phases (polar and non-polar)[200]. This weaker repulsion between the two phase translates into lower surface tension.

Micellization and CMC

Upon concentration increase and subsequent saturation of the interface with surfactant molecules, formation of aggregation structures occurs spontaneously. It results from the "hydrophobic effect", which arises from positive enthalpy generation (free energy) upon cavity creation in water that breaks strong hydrogen bonds, and from structuring of water surrounding the hydrophobic group, resulting in negative enthalpy and positive entropy that partially offset each other[204,205]. The positive free energy generated by cavity formation in water is significantly greater than the energy gain due to the structuring of water molecules around the hydrophobic group. Surfactant aggregation and hydrophobic interactions between non-polar solutes in water are thus primarily due to strong cohesive interactions between water molecules[206].

Many physico-chemical properties of aqueous surfactant solutions are concentration-dependent and undergo a sharp change at CMC[200] (see Figure IV.1). This makes the CMC value highly relevant. Subsequently, these abrupt changes in properties enable the measurement of CMC by a wide range of methods, the most common being surface tension or conductivity monitoring for ionic surfactants.

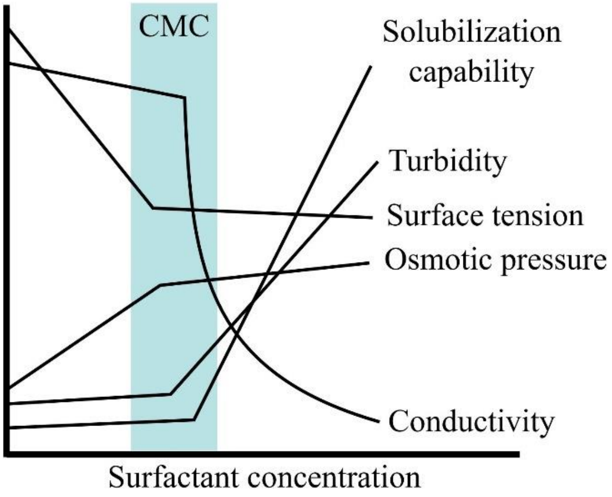

Figure IV.1. Schematic representation of physical properties of aqueous solution as a function of surfactant concentration. Inspired from reference [207].

Lastly, the size and shape of micelles can vary widely, depending in particular on the length and saturation of the hydrophobic tail, the nature of the counterion and the surfactant concentration. Micelle structure has a direct influence on surfactant properties, and is mainly characterized by the stacking parameter p described in equation (IV. 1)[208].

$$p = \frac{v_0}{a_0 \times l} \tag{IV. 1}$$

where v_0 is the volume of the hydrophobic part of the surfactant, l its length and a_0 the polar head surface (at the equilibrium at the interface).

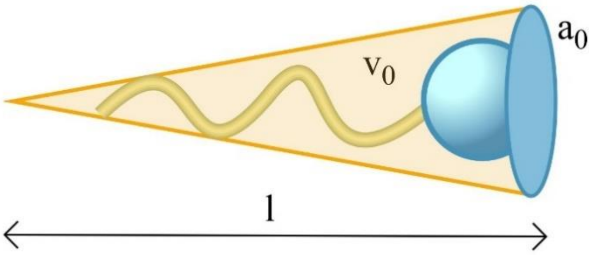

Figure IV.2. Schematic representation of a surfactant and associated parameters.

Mesophases

At high surfactant concentrations, the packing of micelles often leads to the formation of lyotropic liquid crystalline phases, also referred to as mesophases. Highly packed spherical micelles can induce cubic phase formation for example, whereas rod-like aggregates will generally tend to form hexagonal phase when packed[200]. Lamellar phases (Lα) are also common and originate from bilayers packing. All in all, a typical phases sequence for solution with increasing surfactant concentration is isotropic micellar (L_1), cubic, hexagonal (H_1), lamellar (Lα) and reverse phases. It should be stressed that these phases are highly temperature-dependent in the case of non-ionic surfactants, and that every surfactant exhibits a specific phase diagram, not necessarily containing all the mesophases.

IV.2.3. Krafft point

Like many other compounds, surfactant solubility is highly temperature-dependent. For non-ionic surfactants (for instance ethoxylated or propoxylated ones), hydrogen bonds with water molecules are greatly responsible for the aqueous solubility. As temperature increases, these bonds break and the overall solubility of the surfactants is subsequently reduced. In the case of ionic surfactants, thermal agitation of solvent molecules, known as Brownian motion[209], has an effect on the ion pair dissociation of the surfactant. A greater dissociation due to increased temperature enhances surfactant hydrophilicity. Furthermore, the aqueous solubility of ionic surfactant increases significantly above a certain temperature, known as Krafft temperature T_{Kr} or Krafft point (named after professor Friedrich Krafft). By definition, it is the temperature at which the solubility of the surfactant is equal to the CMC, or in other words, the Krafft point represents the intersection of the curves of solubility versus temperature and CMC versus temperature (see Figure IV.3). At temperatures lower than the Krafft point, an increase in surfactant concentration no longer leads to micellization but to surfactant crystallization. For this reason, determination of the Krafft point is experimentally essential. In addition, a greater hydrophobic tail increases a surfactant's solubilizing capacity, but at the same time leads to lower water solubility and a higher Krafft temperature[190,207]. It should be noted that the "solubility temperature" of soaps is not concentration-independent. In fact, it was observed that at low soap concentrations, the "solubility temperature" increases with decreasing concentrations of soaps, therefore T_{Kr} does not exactly correspond to the solubility temperature[207]. Nevertheless, this distinction is rarely done in literature and is only relevant at very low concentrations of soaps, so it will not be made in this study. However, it is important to measure T_{Kr} always at the same soap concentration for this reason. By convention, Krafft temperature is assessed as the clearing temperature of a 1 wt% aqueous surfactant solution. As crystallization is also a kinetic phenomenon, it is common to adjust the determination by cooling the clear surfactant solution.

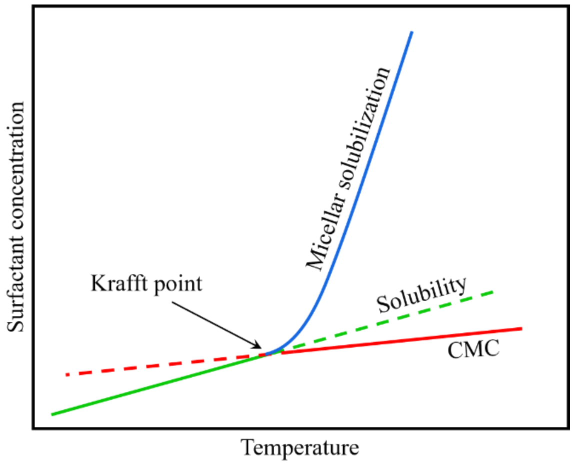

Figure IV.3. Schematic representation of the relation between surfactant solubility, CMC, and Krafft point. Based on reference [210].

IV.2.4. Emulsions

Any system composed of several immiscible compounds tends to reach a thermodynamically stable state through minimization of the interface between the two immiscible phases, i.e. towards phase separation. An emulsion is a monophasic oil/water system with colloidal droplets of one phase in the other (continuous phase). The emulsion state is commonly achieved by mixing the two phases (mechanical agitation, ultrasound, microfluidics, etc.). In the presence of surfactant (frequently referred to as emulsifier in industrial applications in this case), the thermodynamically inevitable dephasing is kinetically hindered[200]. The surfactant thus acts as an emulsion stabilizer. It should be mentioned that there exist stable emulsions without surfactants. One of the most common examples is Pickering emulsions, in which the droplet structure is stabilized by the adsorption on their surface of solid particles of various kinds (silica, clay, proteins, polysaccharides, etc.).[211,212]

The affinity of the surfactant, as well as the ratio between the two immiscible phases determine the nature of the emulsion, whether direct (apolar phase dispersed in polar phase), inverse (vice versa), or multiple. In 1910 already, Ostwald showed that for a water/oil system, the water-to-oil-ratio (WOR) is the predominant factor determining the nature of the emulsion if it is far from unity, independently of the surfactant affinity[213]. When this ratio is close to 1, it is conversely the nature of the surfactant that dictates emulsion morphology, as stated by Bancroft in the early 20th century[214,215]. There are several ways to characterize an emulsion, and to characterize surfactants according to the nature of the emulsion they can form. Griffin and later Davies attempted to construct an affinity scale for surfactants, the hydrophilic lipophilic balance (HLB)[216,217]. This semi-empirical scale uses the contributions of the various groups in the surfactant structure to estimate its ability to act as an oil-in-water or water-in-oil emulsifier, for example (see Figure IV.4). More advanced characterization methods, such as Winsor’s R-ratio[218], the HLD theory[219] or the phase inversion temperature[220] (PIT) and PIT-slope[221] helped rationalize the contributions of surfactants on SOW systems and are also very relevant for the study of microemulsions. This study however mainly focuses on the influence of amino counterion on simple carboxylate systems, so these theories will not be discussed extensively here.

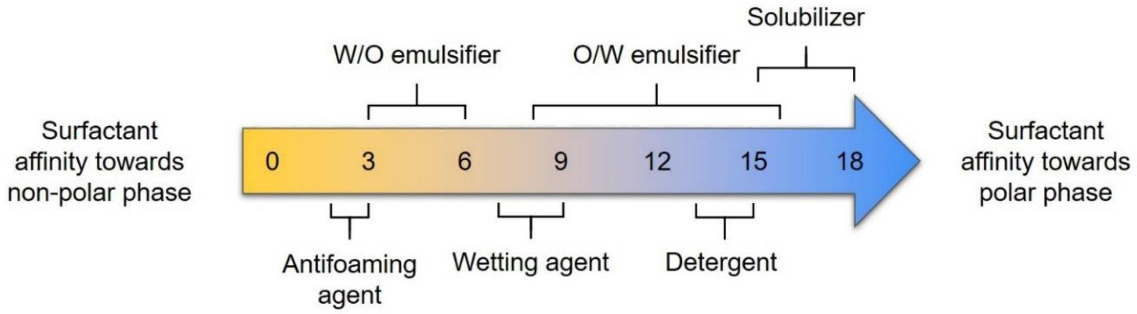

Figure IV.4. Representation of HLB scale and associated applications for surfactants.

IV.2.5. Soaps: carboxylic acid salts

The term soap refers to salts formed by the association of a negatively charged fatty acid carboxylate and a positively charged counterion, historically sodium or potassium. Soaps are the oldest man-made surfactants initially derived from animal fats, and are still today the most consumed surfactant class in the world[201]. Although soaps have lost much of their appeal since the second half of the 20th century in favor of “technical” surfactants (derived from petrochemicals, mostly sulfates and sulfonates), notably because they are irritating[222] and sensitive to pH and salt[201], there is currently a resurgence of these, mainly for ecological reasons. Indeed, soaps can be made from renewable sources, which makes them highly relevant to today's green chemistry issues. Furthermore, most of their disadvantages could yet be tackled through careful synthesis and formulation[189]. One of the most important property of soaps is the aqueous solubility, which is like for other surfactants highly dependent on its structure. A long hydrophobic tail (C_{18+}) will have a great solubilization capability but a reduced solubility, reflected by a high Krafft point (71°C for sodium stearate[191]). The length of the carbon chain can also influence other properties, like foaming generation capacity or stability[223]. The intended application often determines the carbon chain length (and saturation), and therefore the source of the materials. Finally, the nature of the counterion plays a major role in soap properties (see section IV.2.6). One example is the frequent substitution of sodium for potassium to improve aqueous solubility[190] (lower Krafft temperature for a given carbon chain).

Salinity and ionic force sensitivity

As salinity directly influences the activity of water, it subsequently impacts the affinity of the surfactant towards water. An increase of salinity will decrease the activity of water and thus the affinity of the surfactant for the aqueous phase[224]. For ionic surfactants, the increase of the ionic force, i.e. the concentration of free ions in aqueous solution, also leads to an enhanced screening of the ionic head charges, resulting in a decreased hydrophily of the surfactant (see Figure IV.5). This is particularly important for salts, which are easily disrupted by the presence of electrolytes such as Mg^{2+} or Ca^{2+} ions in tap water, or other counterions introduced in solution from the formulation. As counterion freely exchange with the ones initially associated with the carboxylate, new soaps are formed with different properties, such as a significantly low water-solubility of Mg^{2+} or Ca^{2+} carboxylate (high T_{Kr})[225].

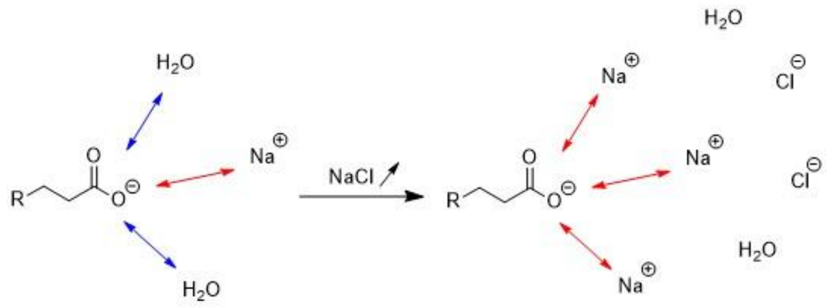

Figure IV.5. Representation of the charge screening of an anionic surfactant by increasing the ionic strength. Example of a carboxylate with increasing sodium chloride concentration.

pH sensitivity

Another factor to bear in mind when studying soaps is pH. Indeed, most soaps exhibit a relatively high pH value in aqueous solution (> 9 typically for long-chain carboxylate[226]) and are sensitive to pH change. At low pH values, it has been extensively reported that lamellar or crystalline phase formation for example disrupt the solution, making it unstable and turbid.[207,226,227] This pH dependence prevents the use of soaps in certain applications where the pH value must be fixed, such as in certain cosmetics or food formulations. Fatty acids are also often dispersed in aqueous solution at low pH value, but that does not qualify as solubilized soaps, which correspond to a macroscopic water-like clear solution with fatty acids acting as surfactants as the main components.

IV.2.6. Counterion influence and Hofmeister series

Counterion-to-headgroup association plays a major role in the properties of ionic surfactants. The nature of the counterion is known to influence for instance the surfactant solubility[190] as already mentioned with Na^+, K^+, Mg^{2+} or Ca^{2+} carboxylates with significant differences in their T_{Kr}, as well as many other properties. These salts effects are ubiquitous and of considerable importance in biology, chemistry and pharmacy and belong to the broad field of "specific ion effects". Hofmeister and co-workers pioneered the rationalization of these effects at the end of the 19th century. In a series of publications entitled "About the science of the effect of salts" ("*Zur Lehre von der Wirkung der Salze*"[228,229]), they thoroughly investigated the influence of different salts on the denaturation and solubility of proteins, sodium oleate and colloidal ferric oxide, which was generalized to ions years later to become what is nowadays known as the "Hofmeister series" (see Figure IV.6)[228]. This empirical classification linked the hydration of salts to their solubilization (salting-in) or precipitation (salting-out) impact independently of the considered solute.

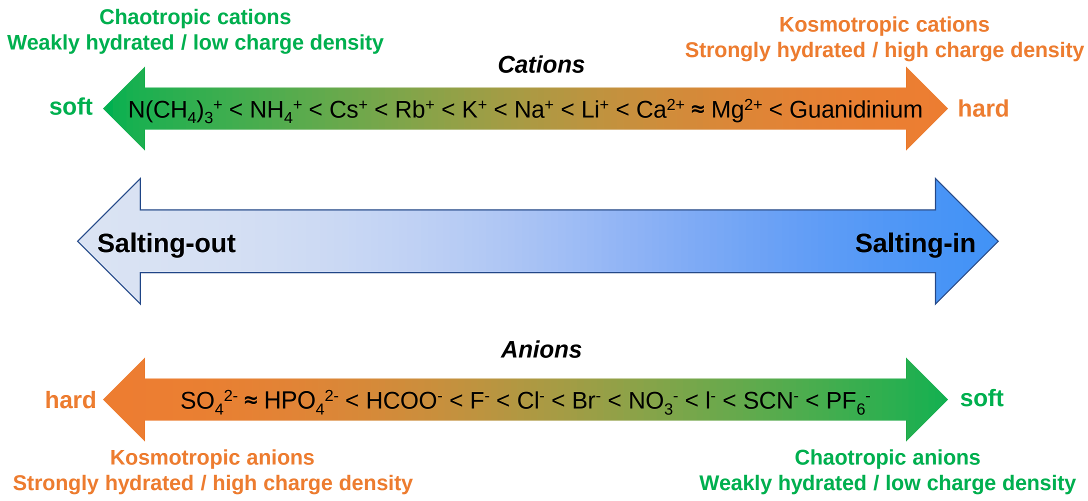
Chaotropic cations
Weakly hydrated / low charge density
Kosmotropic cations
Strongly hydrated / high charge density
Cations
soft
N(CH4)3+ < NH4+ < Cs+ < Rb+ < K+ < Na+ < Li+ < Ca2+ ≈ Mg2+ < Guanidinium
hard
Salting-out
Salting-in
Anions
hard
SO42- ≈ HPO42- < HCOO- < F- < Cl- < Br- < NO3- < I- < SCN- < PF6-
soft
Kosmotropic anions
Strongly hydrated / high charge density
Chaotropic anions
Weakly hydrated / low charge density

Figure IV.6. Hofmeister series ranging from salting-out to salting-in for cations and anions. Based on references [128,230].

The initial vision of the Hofmeister series consisted of ranking ions based on their influence on bulk water structure, by opposing "water structure makers" and "water structure breakers" in their ability to solubilize a third component. This alteration of the water structure is now though to only be involved in the direct vicinity of the ion, and not the bulk itself.[204,228,230] Indeed, instead of long-range electrostatic interactions, it is now fairly accepted that short-range ion-ion interactions are predominant[231]. The classification of the Hofmeister series is thus to be interpreted carefully, but still remains a powerful tool, mostly for biological systems or drug design for example.

In order to refine the comprehension of specific ion effects, Collins introduced in 2004 a "concept of matching water affinities" that order ions according to their interactions with water molecules, in respect to water-water interactions[232]. In this model, the size of the (monovalent) ions is crucial, as the charge density is believed to be the dominant force at play. It therefore predicts a strong interaction between "small" (in regard with the medium-sized water molecule) ions of high charge density highly hydrated (kosmotropes) referred to as "hard" (like sodium or carboxylate), and "large" ions of low charged density that are weakly hydrated (chaotropes) called "soft" (see Figure IV.6)[232,233]. The model states that the association of similar-sized ions will spontaneously lead to the formation of an inner-sphere ion pair, whereas the combination of two ions of different size causes dissociation due to the tendency of each ion to keep its own hydration shell, irrespective to their chaotropic or kosmotropic nature. A generalization of this concept to the ability of surfactant headgroups to form close pairs with counterion was proposed by Vlachy *et al.*[234] and is represented in Figure IV.7.

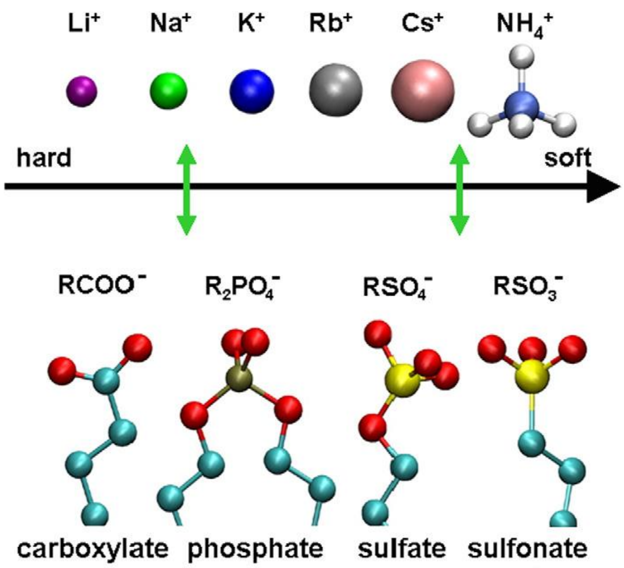
Li+
Na+
K+
Rb+
Cs+
NH4+
hard
soft
RCOO-
R2PO4-
RSO4-
RSO3-
carboxylate
phosphate
sulfate
sulfonate

Figure IV.7. Ordering of anionic surfactant headgroups and counterions regarding their capabilities to form close pairs. Reproduced with permission from reference [234].

IV.2.7. Guanidines and metformin

Guanidinium and guanidines

At the end of the 18th, medicinal plant *Galega officinalis* was used to treat symptoms of diabetes (thirst and frequent urination)[235] and this effect was later recognized to be due to the rich dose of guanidine in the plant. Guanidine (which gives its name to the family of compounds comprising all its derivatives, see structure Figure IV.8) has first been identified and synthesized in the middle of the 19th century by Strecker[235]. In 1918 Watanabe studied the metabolic influence of the injection of guanidine hydrochloride on blood sugar and showed that it induced a decrease in glucose in animals[236].

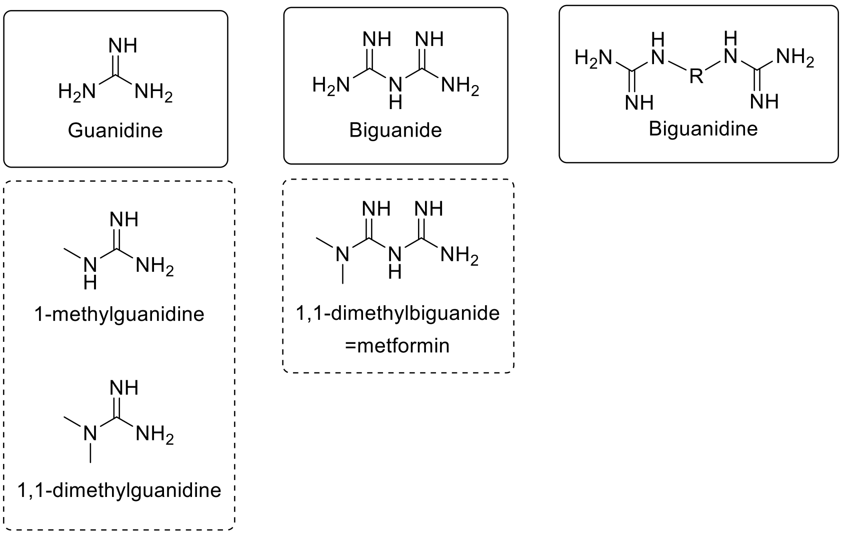
Guanidine
Biguanide
Biguanidine
1-methylguanidine
1,1-dimethylbiguanide
=metformin
1,1-dimethylguanidine

Figure IV.8. General chemical structures of guanidines, biguanidines, and biguanides as well as compounds belonging to these families.

The specificity of guanidine comes from the structure of its cationic form, the guanidinium (Gu^+) group. It is composed of three amino groups bound to a common carbon atom, and is thus a planar Y-conjugated quasi-aromatic compound. Its very high pK_a (13.6[237]) makes it fully protonated in aqueous solution. Its symmetry and conjugation create a uniform charge distribution. Gu^+ is a hydrogen bond donor, and one distinctive feature is its planarity, which makes it interact with water molecules only in its molecular plane, whereas both faces remain hydrophobic[237].

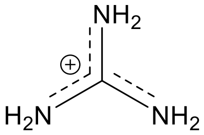

Figure IV.9. Chemical structure of the guanidinium cation.

Vazdar and co-workers studied the counter-intuitive pairing of two Gu^+ cations that they described as “weakly thermodynamically stable like-charge ion pairs”[237], as dispersion and cavitation forces could overwhelm the Coulomb repulsion. They propose that this phenomenon could be responsible for the arginine-arginine pairing or the frequently observed interaction between positively charged peptides and proteins.

Arginine “magic”, guanidinium ion

Arginine is an amino acid bearing a guanidinium cation as functional group (see structure in Figure IV.10), thereby exhibiting several of the interesting properties, the most remarkable being the ability of arginine-rich peptides (so highly positively charged compounds) to penetrate cellular membrane with ease[237,238]. This phenomenon is known as arginine “magic”[239]. This phenomenon is essential to better understand biological mechanisms and to design effective delivery methods able to penetrate biological barriers.

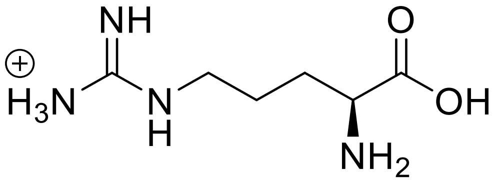

Figure IV.10. Chemical structure of amino acid arginine.

Biguanides and metformin

Some compounds have two "complete" guanidine groups directly linked and are called biguanidines. Another type of compound based on the guanidine group is the biguanide subclass, which regroups structures with two guanidine functions sharing a central nitrogen atom (see Figure IV.8). Among this group, there is one particularly interesting compound, 1,1-dimethylbiguanide, commonly known as metformin (see structure Figure IV.8), which has become central in type 2 diabetes treatment. The first synthesis of biguanidine was made in 1879 by Rathke[240], and metformin was synthesized by Werner and Bell for the first time in 1922[241] but not used for diabetes treatment. In the 1940s, academic interest for metformin raised again in the search of anti-malarial agents[242], but it was not until 1957 than metformin ability to lower blood glucose level was firstly reported by Jean Sterne[243].

In 2015 metformin had become the most prescribed glucose-lowering agent for treatment of type 2 diabetes worldwide[235]. In addition, metformin and other biguanides have been studied for several years for their demonstrated long-term cardiovascular benefits[244] and possible anti-cancer properties[245]. Metformin also exhibits chelating properties thanks to its imine groups. Furthermore, as reported by Bailey *et al.*, it does not appear to work according to one single pathway but rather impacts biological functions through multiple mechanisms[235].

Metformin is a very highly water-soluble compound, with pK$_a$s around 2.7-2.8 and 11.5-11.6[246,247] so it is positively charged at physiological pH. Its high hydrophily (log P = -1.43[235]) but low bioavailability mostly due to the lack of hydrophobic part in its structure makes it a BCS class III compound[235] (see section I.2.3.3.3). Furthermore, metformin has a dose-dependent uptake[248] and a quite rapid excretion mechanism (see pharmacokinetics of metformin in Figure IV.11) which makes it impractical to deliver alone, and metformin often requires drug delivery methods to be efficiently administered. For more details about the pharmacokinetics of metformin, the reader is referred to the work of Graham *et al.*[249]. Research focuses now on more lipophilic derivatives of metformin to overcome this issue. Moreover, other biguanides suffer the same limitations[245].

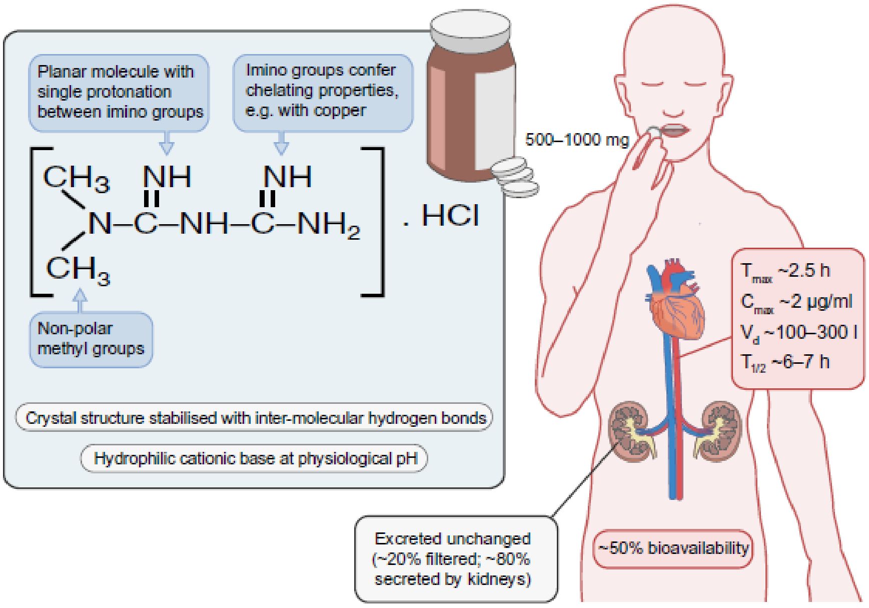
Planar molecule with single protonation between imino groups
Imino groups confer chelating properties, e.g. with copper
CH3 NH NH N–C–NH–C–NH2 CH3 . HCl
Non-polar methyl groups
Crystal structure stabilised with inter-molecular hydrogen bonds
Hydrophilic cationic base at physiological pH
500–1000 mg
T$_{max}$ ~2.5 h
C$_{max}$ ~2 µg/ml
V$_d$ ~100–300 l
T$_{1/2}$ ~6–7 h
Excreted unchanged (~20% filtered; ~80% secreted by kidneys)
~50% bioavailability

Figure IV.11. Metformin hydrochloride chemical structure and pharmacokinetics in human. Reproduced with permission from reference [235].

This may seem all the more surprising given that, as previously mentioned, arginine-rich peptides (and therefore guanidinium-rich peptides) easily permeate cell membranes. This can be understood as that the guanidinium group is partially responsible for the “arginine magic” phenomenon, but it not merely sufficient. Herce *et al*. have established the role of fatty acids and gradient pH in the cell membrane cellular in the penetration mechanism of guanidinium-rich molecules[238].

Interactions between fatty acids and guanidines

Guanidinium-rich peptides are able to cross directly cellular membrane in a non-endocytotic manner (without killing the cell), therefore the mechanism must consist in the reversible formation of a channel of some kind. Herce *et al.* have highlighted the role of deprotonation of cell membrane fatty acids in the passage of guanidine-rich peptides[238]. In fact, this deprotonation facilitates interaction with the positively charged Gu^+ group by lowering the free energy of the insertion. This interaction and the hydrophobic core of membrane fatty acids create a channel through the lipidic membrane that enable the transduction of the peptide into the cell[238]. pH-gradient across the membrane is also a key parameter for the release of the peptide in the cell and the protonation of fatty acids which can then diffuse back across the membrane[238].

However, positive charge of Gu^+ group is necessary but not sufficient, as lysine monomers or other polycations were shown to have poor cellular uptake in comparison[250]. Furthermore, another surprising property of this mechanism is the apparent lack of cell-type specificity[250]. It has been hypothesized that hydrogen bonding and membrane potential are major factors for the uptake mechanism of guanidinium-rich peptides. Thus, the bidentate charge-assisted hydrogen bonding occurring between Gu^+ group and HB-acceptors such as fatty acids has been demonstrated to be crucial for the partition of the ion pair into the membrane[250]. A representation of this particular ion pairing is shown in Figure IV.12.

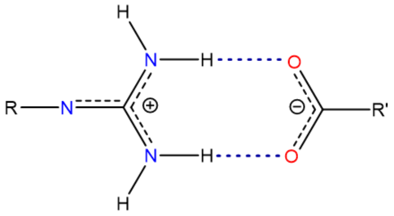

Figure IV.12. Representation of the guanidinium···carboxylate synthon with charge-assisted hydrogen bonding. Blue dashed lines represent hydrogen bonds. Inspired from reference [251].

IV.3. Materials and methods

IV.3.1. Materials

Naringenin (> 93 %), phloroglucinol anhydrous (> 99 %), docosanoic acid (behenic acid or BA) (≥ 99 %), guanidine hydrochloride (GuHCl) (> 98 %), 1-methylguanidine hydrochloride (mGuHCl) (> 98 %), *N*,*N*-dimethylbiguanide hydrochloride (metformin hydrochloride or MetHCl) (> 98 %), creatine monohydrate (> 98 %), and L-histidine (≥ 99 %) were purchased from TCI Chemicals. Meglumine (≥ 99 %), pyrogallol (≥ 98 %), dodecanoic acid (lauric acid or LA) (≥ 99 %), sodium myristate (NaC14) (> 98 %), tetradecanoic acid (myristic acid or MA) (≥ 99 %), sodium palmitate (NaC16) (≥ 99 %), hexadecanoic acid (palmitic or PA) (≥ 99 %), sodium stearate (NaC18) (≈ 99 %), cis-9-octadecanoic acid (oleic acid or OA) (≥ 99 %), L-arginine (Arg) (≥ 99 %), L-lysine monohydrate (Lys) (≥ 99 %), triacetin (99 %), isopropyl myristate (IPM) (> 98 %), and *n*-

octane (≥ 99 %) were purchased from Merck (Sigma-Aldrich). Octadecanoic acid (stearic acid or SA) (≥ 98.5 %) and sodium laurate (NaC12) (≈ 99 %) were purchased from Fluka, paraffin oil (PO) from Cooper, phloretin (≈ 90 %) from Symrise, *trans*-resveratrol (98 %) from Evolva, and xanthohumol (90 %) was kindly provided by HHV GmbH.

IV.3.2. Methods

IV.3.2.1. Samples preparation

Meglumine and guanidine derivatives carboxylates were synthesized using two different protocols. The procedure for synthesis in organic solvents inspired by the work of Cassimiro and colleagues is especially well suited to conventional compounds analyses such as NMR or IR spectroscopy, or thermal analysis[113–115,252], whereas *in situ* soap synthesis by bringing together the deprotonated fatty acid with a new counterion lends itself better to solution behavior analyses.

Protocol ex situ

Meglumine-carboxylic acid salts and metformin-carboxylic acid salts were synthesized according to the modified version of protocol of Cassimiro *et al.*[115]. Equimolar quantities of counterion (meglumine or MetHCl) (2.51 mmol for $MegC_{12}$) and carboxylic acid were solubilized separately in a solvent mixture composed of ethyl acetate/methanol (1:1 v/v) under constant stirring with moderate heating (~ 50°C). The solution containing the carboxylic acid was added dropwise to the counterion one, and the resulting solution was kept for one night at 5°C. The solvent was removed under reduced pressure with a rotary evaporator and the resulting paste was dried 72 hours under high vacuum at 50°C.

Protocol in situ

For *in situ* soap formation of amino carboxylates, the protocol of Douliez and coworkers was applied[253–255]. Two variants were tested, one involving the prior deprotonation of the carboxylic acid using NaOH, the second based on the direct use of commercially available sodium salts of carboxylic acids. Shortly, carboxylic acids were precisely weighed to obtain the desired concentration (10 or 20 g/L, corresponding to 1 % and 2 %, respectively) and adapted volume of an aqueous solution of metformin (MetHCl) or meglumine was added to reach equimolar ratio. According to a well-known dispersion technique for lipid compounds[253–255], the solutions were energetically stirred and heated to ~ 70°C until the fatty acids were completely dissolved (at least 30 min), then the solutions were frozen at - 20°C. This operation was repeated 3 to 5 times. After the last heating phase, samples were cooled down at room temperature. Poorly dispersed fatty acid soaps were heated at 60°C for about 5 min prior to be used.

IV.3.2.2. Soap synthesis assessment via ^1H NMR

The effective preparation of soap samples was confirmed by 1H NMR. Spectra were recorded on an Avance III 3 (Bruker, US) at 300MHz for ^1H and ^{13}C. D_2O was used for metformin and adducts solubilized in aqueous phase and DMSO-d_6 for pure carboxylic acids analysis.

IV.3.2.3. Krafft point measurement

It is commonly accepted to determine the Krafft point of a surfactant by measuring the temperature at which a 1 wt% surfactant solution becomes clear, as the CMC is usually much lower than 1 wt%. The Krafft temperatures were optically determined by slowly heating the solutions in closed vials in a water bath up to 70°C and subsequently cooling to -3°C.

IV.3.2.4. Surface tension and CMC measurement

Surface tension was measured with a Krüss K100 tensiometer equipped with an RI01 Du Noüy ring probe and results were statistically analyzed with Krüss Laboratory Desktop software version 3.1.0.2617. All measurements were carried out at 25°C regulated with a Huber water bath directly connected to the tensiometer. For CMC measurements, a highly concentrated solution of each studied surfactant was prepared, then an automatic dilution was carried out with a Dosino 700 from Metrohm. Appropriate agitation and rest time were applied between each dilution to ensure equilibrium. Each CMC measurement was carried out in duplicate with freshly prepared stock solution.

IV.3.2.5. Micellar solubilization

Solubilization procedure

Curcumin and quercetin were chosen as test compounds for solubilization experiments with amino-carboxylates, which were soluble in water at room temperature. $MegC_{12}$, $MegC_{14}$, GuC_{12}, $mGuC_{12}$, $mGuC_{14}$, and $MetC_{12}$ were tested with curcumin and GuC_{12}, $mGuC_{12}$, $mGuC_{14}$, and $MetC_{12}$ with quercetin. Concentrations were selected based on CMC of amino carboxylates, below the CMC value, at around the CMC value (ranging between 0.4 and 1.0 mmol/L) and in excess at around 20 times the CMC value (ranging between 0.8 and 2.0 mmol/L), and 3 mL samples were prepared in triplicate. Hydrophobic test compound curcumin or quercetin was then added to the solutions under continuous stirring until saturation was reached (visually assessed). After filtration of unsolubilized compound (PTFE, 0.2 µm) and dilution with methanol (dilution factor between 10 and 100 depending on the sample), the amount of solubilized test compound was asserted with UV-vis spectrophotometry.

UV-Vis spectrophotometry

A UV-vis double beam spectrophotometer (Lambda 18, Perkin Elmer) was used to quantify curcumin in micellar solutions. Samples were analyzed in 1 cm path length quartz cells at $\lambda = 426$ nm and $\lambda = 370$ nm for curcumin and quercetin, respectively. Calibration curves of curcumin and quercetin in pure methanol were used to calculate the concentrations of solubilized compound.

IV.3.2.6. Emulsification process

To assess the surfactant ability of $MegC_n$, emulsions were designed with a 50-50w/w oil-to-water ratio at 1 w% of MegCn. *n*-octane, paraffin oil (PO), or IPM were chosen for the oil phase, as *n*-octane saturation makes it well suited to compare emulsions and IPM is widely used in the industry, for cosmetics for instance. For the emulsification tests, all amino-carboxylate were prepared *in situ* according to the protocol described earlier (see section IV.3.2.1) with prior deprotonation of fatty acids via the addition of proper amount of sodium hydroxide. Two different protocols were tested for the emulsification with $MegC_n$ (summarized in Table IV.1), one using a classical mechanical high-speed dispersing device, an Ultra-Turrax®, the second using sonication. The first emulsification protocol was realized with an Ultra-Turrax® (IKA T 25) at 125000 rpm at room temperature for 2 min. 10 g of sample were prepared, at a 50-50 water-to-oil ratio and 1 wt% MegCn as emulsifier. The second emulsification process used a Hielscher UP200St ultrasonic processor (Hielscher Ultrasonics GmbH, Germany) equipped with an S26d2D titanium sonotrode (Ø = 7 mm, L = 95 mm). The sonotrode was set for continuous running (frequency of 26 kHz), with an immersion depth of 5 mm. The emulsification time was calculated for optimal emulsion stability in accordance with the other settings and following the recommendations of Sahota *et al.* for an optimized dispersion and emulsion stability[256]. Quickly, the power is defined by the device itself and the amplitude, and the target volumetric energy E_v is set at 80 W.s/mL according to recommendations Sahota *et al.* The emulsification time t was thus calculated at around 25 s from the sample volumes according to equation (IV. 2).

$$E_v = \frac{P.t}{V} \tag{IV. 2}$$

Table IV.1. Sum-up of the two emulsifications protocols used in this work. $MegC_{18}^s$ refers to meglumine stearate and $MegC_{18}^o$ to meglumine oleate.

Characteristics	Protocol 1	Protocol 2
Emulsification process	Ultra-Turrax (12000 rpm)	Sonication
Emulsification time	2 min	25 s
$MegC_n$	$MegC_{18}^s$, $MegC_{18}^o$, $MegC_{22}$	$MegC_{12}$, $MegC_{18}^s$, $MegC_{22}$
Preparation of $MegC_n$	*In situ*, 10:1 and 1:1	*In situ*, 1:1
%$MegC_n$	1	1
Non-polar phase	*n*-octane or IPM	Paraffin oil (PO) or IPM
WOR	0.5	0.5

IV.3.2.7. Emulsion properties assessment

IV.3.2.7.1. Emulsion morphology analysis

Laser granulometer

The granulometry of the obtained emulsions (droplet size, size distribution) was assessed directly after each emulsion was made. As every emulsion obtained was a direct oil-in-water emulsions, a laser granulometer could be used to assess droplet size and distribution. Mean diameter of emulsion droplets were characterized using a Mastersizer 3000 (Malvern Instrument, UK) laser granulometer. A few drops of emulsion are directly added into the water bath of the device under agitation (1800 rpm) and analyzed with Mastersizer 3000 software (v3.00).

Optical microscope

Optical microphotographs emulsion samples were obtained using a KEYENCE VHX-900F digital microscope equipped with a VH-Z100UR/W/T lens and analyzed using KEYENCE 1.6.1.0 software.

IV.3.2.7.2. Stability measurement

The stability of the emulsions was assessed via Static Multiple Light Scattering (SMLS) using an AGS Turbiscan® from Formulaction. This device measures the evolution of the transmitted T and backscattered BS light (detected at 180° and 45°, respectively) sent through the sample over time. Size and concentration of scattered objects, typically droplets in the case of emulsions, directly influence T and BS light. The variations of the transmitted ΔT and backscattered ΔBS signals can therefore be use to follow the different destabilization phenomena that can occur such as creaming, coalescence, or Ostwald ripening. The device scans the full length of the sample (≈ 25 mm). A schematic representation of the measurement principle is given in Figure IV.13. Every sample was analyzed in glass tubes at 25°C during 4 weeks with one scan every 6 h. Experimental data were processed using the TurbiSoft Lab software (2.3.1.125 FAnalyser).

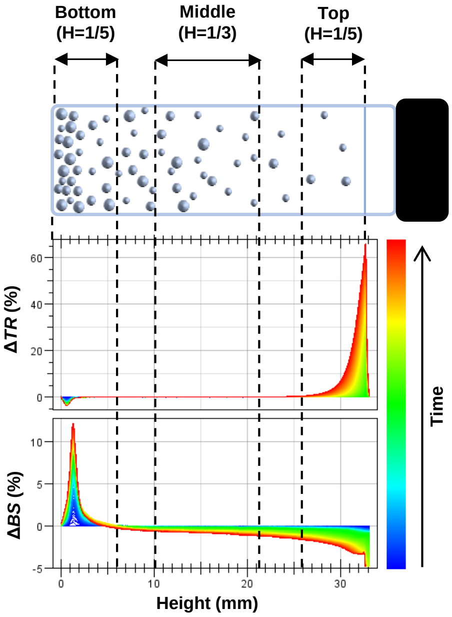

Figure IV.13. Representation of the evolution of transmitted ΔTR and backscattered light ΔBS measured with Turbiscan® for a partially sedimented dispersion. Reproduced with permission from reference [257].

IV.4. Synthesis and characterization of amino-carboxylate with meglumine or guanidine derivatives as counterion

Meglumine carboxylates

Following the protocol established by Cassimiro, Ferreira, and colleagues (see section IV.3.2.1), meglumine carboxylates ($\mathrm{MegC_n}$) were synthesized with different alkyl chains in organic solvents. However, unlike Cassimiro *et al.* who exploited meglumine's ability to make multiple hydrogen bonds with water via its hydroxyl groups to form hydrogels[**] at high $MegC_n$ concentration with diverse properties, our focus was primarily directed towards the surface-active characteristics of these $MegC_n$. Indeed, the formation of these “supra-amphiphiles” as described by Cassimiro *et al.*, is based on ion-pairing interaction, as the acid-base interaction between the carboxylic acids and the alkaline meglumine being the driven force. Irrespective of hydrogel formation, the association of the highly hydrophilic meglumine with fatty acids provide a simple and effective way of bringing these fatty acids into aqueous solution. This approach has also allowed the ionic strength influence to be removed in the formation process, as $MegC_n$ are recrystallized then isolated.

The feasibility of this combination naturally leads to the concept of soaps. However, $MegC_n$ with shorter-chain fatty acids (C_{12}, C_{14}) proved more difficult to synthesize using this method, as their solubility was very high in organic solvents (protocol had to be adapted with a step of solvent removal, which added time and energy consumption to the process). The next logical step was to test conventional soap protocols directly in aqueous solution. As meglumine is a fairly potent base ($pK_a = 9.5$), the use of pure carboxylic acid is possible without having to first use a sodium salt, for example. This *in situ* formation follow the procedure developed by Fameau *et al.* (see section IV.3.2.1).

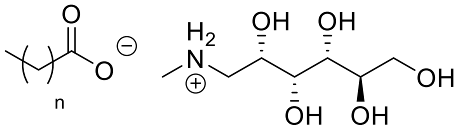

Figure IV.14. Chemical structure of meglumine soaps. n = 10, $MegC_{12}$; n = 12, $MegC_{14}$; n = 14, $MegC_{16}$; n = 16, $MegC_{18}{}^{s}$; n = 20, $MegC_{22}$.

Guanidine derivatives as counterion

As previously mentioned, the guanidinium group's ability to penetrate cell membranes does not extend to pure metformin. Furthermore, the preponderant role of the interaction of the guanidinium cation with fatty acids in the penetration mechanism was also established. As metformin is itself an active ingredient in the treatment of type II diabetes among others, metformin carboxylate formation using the same approach as with meglumine could be a way of increasing metformin bioavailability, which remains low because of the highly hydrophilic nature of metformin, which is highly water-solubility.

As metformin has a very specific structure (see Figure IV.8), it was decided to compare the $MetC_n$ obtained with other soaps formed with guanidine hydrochloride (GuHCl) or guanidine derivative as counterion. Methylguanidine hydrochloride (mGuHCl) was selected in this sense, as it is a fairly inexpensive and commonly available compound. Furthermore, since the charge repartition in biguanidine is not as straightforward as for the guanidinium cation, although metformin is also thought to be one time protonated at physiological pH, as its pK_as were reported at 2.8 and 11.5[247]. In order to better characterize the ionic interaction between metformin and the carboxylic acids, ^{13}C NMR was conducted.

[**] hydrogels based on amino compound interaction with fatty acids are widely reported, even without numerous HBs donor/acceptor groups.[258]

Figure IV.15 shows the spectra of pure metformin hydrochloride and MetC$_{12}$ in D_2O, and Table IV.2 the shifts in the signals upon association with the carboxylic acid.

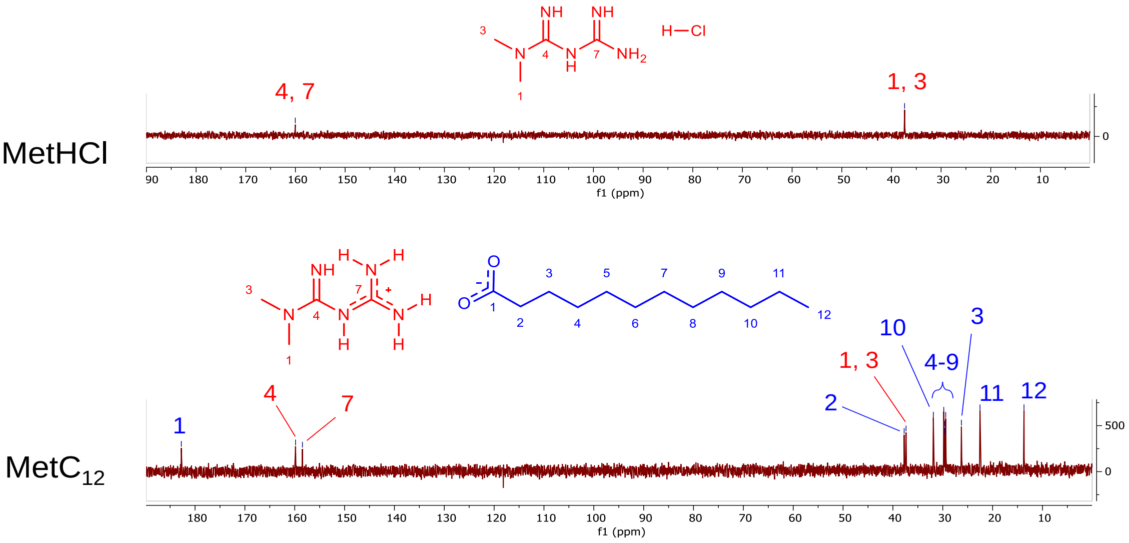

Figure IV.15. Chemical structures of studied amino acids.

Table IV.2. ^{13}C NMR Chemical shifts of MetHCl and MetC$_{12}$ in D_2O. Red refers to metformin and blue to sodium laurate. The carbon atoms numeration is based on Figure IV.15.

MetHCl			MetC$_{12}$			
Peak n°	Shift (ppm)	Assignment	Peak n°	Shift (ppm)	Assignment	Shifts/ MetHCl (ppm)
/	/	/	1	13.70	12	/
/	/	/	2	22.53	11	/
/	/	/	3	26.26	3	/
/	/	/	4	29.41	4-9	/
/	/	/	5	29.58		/
/	/	/	6	29.65		/
/	/	/	7	29.80		/
/	/	/	8	31.89	10	/
1	37.35	1, 3	9	37.36	1,3	+0.01
/	/	/	10	37.74	2	/
2	160.02	4, 7	11	158.46	7	**-1.56**
			12	159.84	4	-0.18
/	/	/	13	182.75	1	/

The strong shift (-1.56) of the central carbon of the guanidine group without methyl groups suggests that it is the one bearing the positive charge at non-extreme pH values (between 2.8 and 11.5), and the charge representation in Figure IV.15 can be deemed realistic.

MegC$_n$, GuC$_n$, mGuC$_n$, MetC$_n$ were investigated regarding their Krafft temperature, their CMC when it was possible, as well as their ability to solubilize hydrophobic compounds quercetin and curcumin or to form stable emulsions in the case of $MegC_n$. These tests served primarily as proof of concept for these applications with these particular amino-soaps.

Amino-acids as counterion

Finally, as the choice of counterions had focused on amino compounds, it was decided to test amino-acids as counterions as well. A few were selected for a series of quicker tests, notably on the Krafft temperature (see structures in Figure IV.16). Among them, arginine and creatine were particularly interesting, as they both bear a guanidine group. However, in the case of arginine, the guanidine group is independent of the amine group that makes arginine an amino-acid.

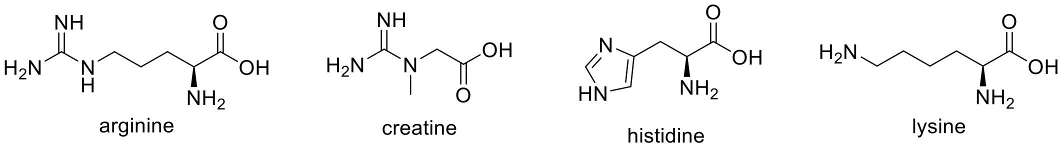

Figure IV.16. Chemical structures of studied amino acids.

IV.4.1. Krafft points determination

Table IV.3 lists the Krafft temperatures of soaps for the classical counterions (sodium and potassium), for tetrabutylammonium, known to have very low T_{Kr} but which use remains very limited due to its toxicity, as well as for choline chloride and the counterions studied in this work.

Table IV.3. Krafft temperatures of classical fatty acid soaps and fatty acid soaps prepared in this work. TBA refers to Tetrabutylammonium and Ch to Choline chloride. $MegC_n$, GuC_n, $mGuC_n$, and $MetC_n$ were prepared in situ using the sodium salts of correspondent carboxylic acids.

Counterion	C_{12}	C_{14}	C_{16}	C_{18}	C_{20}	C_{22}	Reference
				Krafft temperature (°C)			
Na	25	45	60	71	> 100	> 100	191
K	10	30	46	57	/	/	190
TBA	< 0	< 2-3	/	< 2-3	< 2-3	~ 12	195
Ch	< 0	1	12	40	/	/	196
Meg	< 5	16 < x < 20	/	~ 70	/	/	This work
Met	~ 6-7	40 < x < 50	/	> 70	/	/	This work
Gu	< 2-3	30 < x < 40	40 < x < 50	> 70	/	/	This work
mGu	< 0	20 < x < 30	40 < x < 50	~ 70-75	/	/	This work

Some compounds have lower T_{Kr} than what could be predicted with Collins' concept of "matching water affinities", for example ChC_n, as choline cation is even softer than NH_4^+ and should not be able to bond so efficiently with the very hard carboxylate (see Figure IV.6 and Figure IV.7). Wolfrum explained this behavior as the unsymmetrical and bulky structure of choline most likely increases the free energy of the crystal structure of ChCn and thereby decreases T_{Kr}[207]. Guanidinium on the other hand is a very hard cation and should therefore interact strongly with carboxylate according to Collins' concept. This seems to be true for GuC_{12}, $mGuC_{12}$, and $MetC_{12}$ which all have T_{Kr} below the one from potassium (see Table IV.3), but from C_{14} and longer chain the T_{Kr} do not seem to differ strongly from the sodium reference (apart for $mGuC_{14}$ which is still barely soluble at room temperature and could therefore be used at 25°C without major solubility issues). Metformin can also be viewed as fairly bulky and unsymmetrical, however it does not seem to exhibit a great T_{Kr} decrease compared to Na except for $MetC_{12}$. The T_{Kr} of $MetC_{16}$ was not reported either, as the sample remained unclear but not crystallized over the entire temperature range. Meglumine is quite different from other counterions in that it is capable of forming numerous hydrogen bonds with water, which could explain its relatively low T_{Kr} for $MegC_{12-14}$ as crystallization is hindered. On the other hand, increasing the concentration of $MegC_n$ leads, for the same reason, to rapid hydrogel formation (over 20 % $MegC_{12}$ for example). $MegC_{16}$ was also prone to the formation of mesophases and would need further investigation. Figure IV.17 presents pictures of some transitions to illustrate this section, and Figure IV.18 shows some amino-soaps under polarized light to highlight the formation of mesophases.

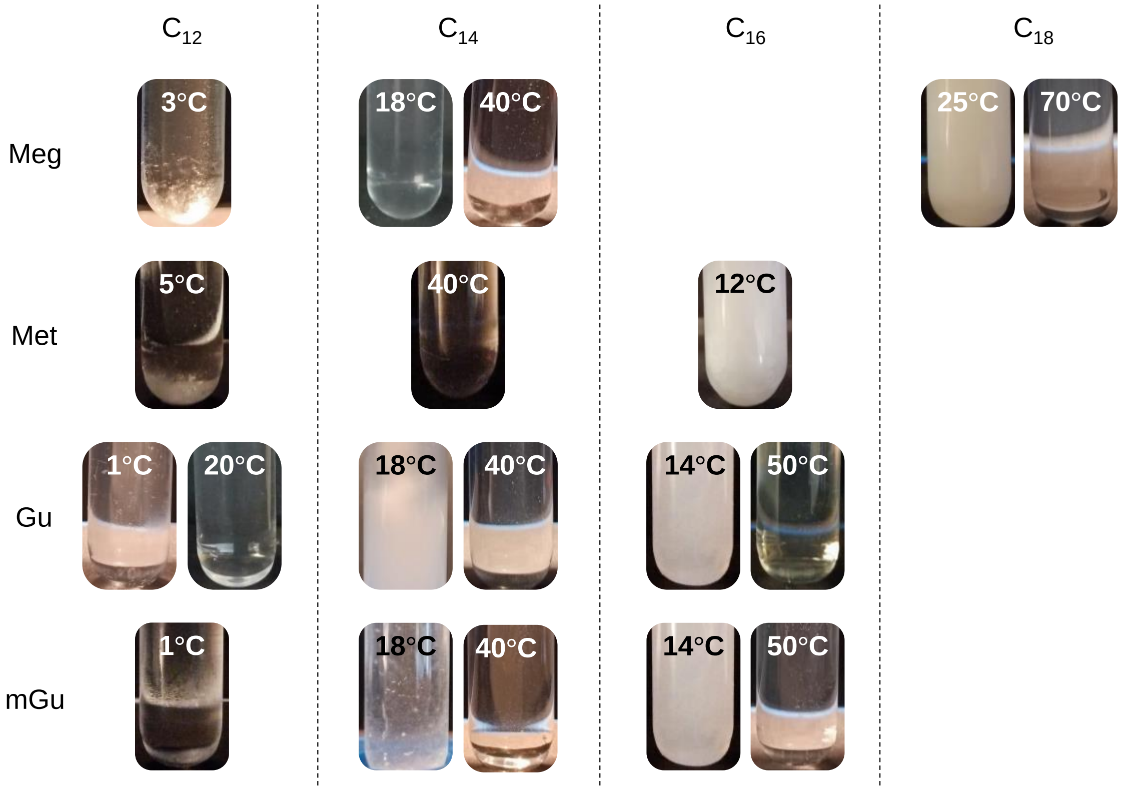

Figure IV.17. Photographs of Meg-, Met-, Gu-, and $mGuC_{12-16}$ at different temperatures. Gu- and $mGuC_{14}$ and Gu- and $mGuC_{16}$ are very viscous above 40°C and 50°C, respectively.

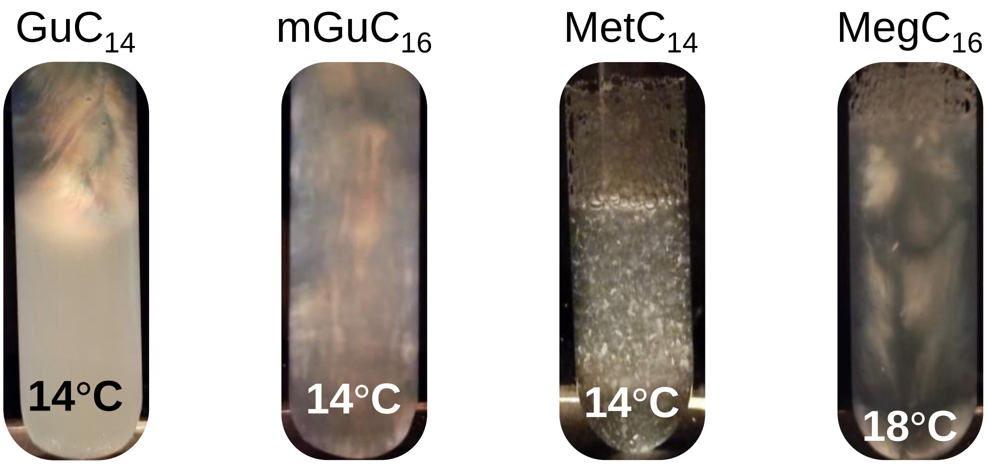

Figure IV.18. Examples of mesophases observation with polarized light.

Amino-acids

For amino-acids Krafft temperatures quick screening, amino-acids (see structures in Figure IV.16) were progressively added to a sodium salt carboxylate aqueous solution to reach different ratios in order to assess their influence on the T_{Kr} of the sodium carboxylate references. Figure IV.19 summarizes the results from this experiment.

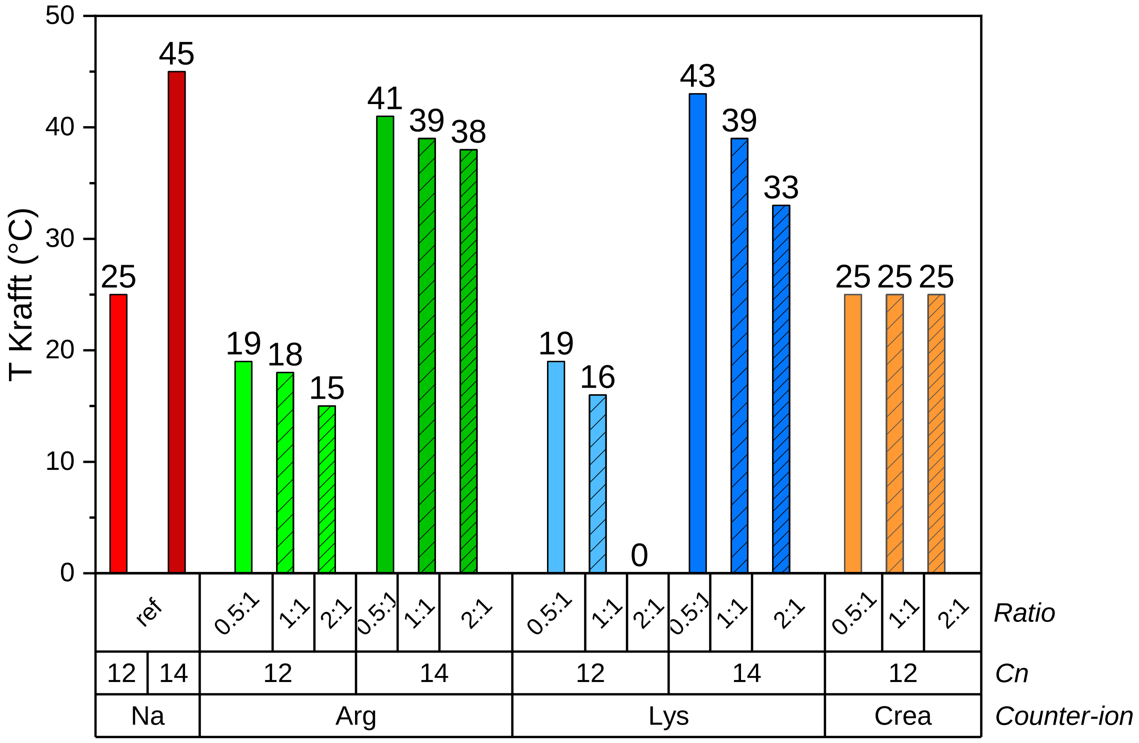

Figure IV.19. Screening of the influence of the addition of amino-acids on the Krafft temperature of sodium soaps. Arg refers to arginine, Lys to lysine, and Crea to creatine. Ratios represented are the amino-acids-to-carboxylate ratios.

Arginine and lysine were both able to somewhat decrease the T_{Kr} of the sodium soaps references, but interestingly creatine had no effect, probably because of the close proximity of its amine and acid groups, which could hinder an effective ion-pairing with another compound. Histidine results are not shown in Figure IV.19 as they all yielded T_{Kr} superior to 50°C and were subsequently not further determined. With a sidechain pK_a around 6, histidine is the only amino-acids among those studied which does not possess a positively charged sidechain at neutral pH (arginine sidechain $pK_a = 12.5$, lysine sidechain $pK_a = 10.9$). However, the exact nature of the phenomena at play with histidine and its subsequent phase behavior were not further investigated. Of all the studied amino-acids, lysine and arginine appear as the most promising, with a significant decrease of T_{Kr} with a C_{12}-Na ratio of 2:1 in comparison with NaC_{12}. A deeper study with a proper synthesis of $LysC_{12}$ and $ArgC_{12}$ may therefore be interesting to better understand the influence of the guanidinium group.

IV.4.2. Critical Micelle Concentrations

Critical Micelle Concentrations were measured for every amino soap with a sufficiently low T_{Kr}, i.e. for $MegC_{12-14}$, GuC_{12}, $mGuC_{12}$, and $MetC_{12}$ with surface tension measurements at 25°C. Table IV.4 summarizes these CMC as well as well as the values found in the literature for other soap counterions.

Table IV.4. CMC values for surfactants at 25°C. CMC determined in this work were measured by surface tension measurements.

Counterion	CMC values (mmol/L)		Reference
	C12	C14	
Na	24.4	6.9	[259]
K	23.4 – 25.5	6.6	[259]
TBA	5 – 7.4	1.7	[260]
Ch	25.5	6.4	[261]
Meg	~ 10	3 – 5	This work
Met	~ 9	/	This work
Gu	~ 6	/	This work
mGu	2 – 3	/	This work

As a mean of comparison, one can cite the work of Song *et al.*, who reported on the self-aggregation properties of alkylguanidinium surfactants (compounds where the alkyl chain is covalently bound to the guanidium headgroup)[262]. They reported, for alkyl chains of 12 carbons, a CMC of 6 mM and 0.7 mM for guanidinium and dimethylguanidinium headgroups, respectively. All in all, the CMC values of studied amino-carboxylates lie within the same order of magnitude. The insertion of a dimethyl group in the guanidinium cation increases slightly the hydrophobicity of the surfactant and facilitates the formation of micelles. That hypothesis can also be made for $mGuC_{12}$ which has a slightly lower CMC than GuC_{12} (see Table IV.4). Furthermore, the reported somewhat weak mutual repulsion of guanidinium cations could also explained the low CMC values observed with guanidine derivatives soaps.

IV.4.3. Micellar solubilization of quercetin and curcumin

Next, the solubilizing capacity of micellar solutions of $MegC_{12-14}$, GuC_{12}, $mGuC_{12-14}$, and $MetC_{12}$ was compared. Quercetin (Quer) and curcumin (Cur) were selected as hydrophobic test compounds, as they are both very insoluble in water but for distinct reasons and known for their potentially beneficial biological properties (see section I.2.3.3.1). Furthermore, in the case of the micellar solubilization of curcumin with $MetC_n$, both are thought to have biological activities, and thus their combined solubilization could be advantageous. The first experiment consisted in comparing the solubilization of Cur with $MetC_{12}$ and $MegC_{12}$ using MetHCl as a control. The goal was to differentiate between the chaotropic effect of the guanidinium groups of Met and the effective micellar solubilization. All surfactants were prepared *in situ* as 2 % stock solutions in water and were diluted to chosen concentrations. The concentrations were selected around the CMC (both $MetC_{12}$ and $MegC_{12}$ have a CMC around 10 mM) and in excess (around 20 times the CMC) and the solubilization procedure was the same as in chapter I and II (see section I.3.2.1). Table IV.5 summarizes the amount of curcumin effectively solubilized with $MetC_{12}$ and $MegC_{12}$.

Table IV.5. Amounts of solubilized curcumin with $MetC_{12}$ and $MegC_{12}$.

[Solubilizer] (mmol/L)	**[Curcumin] (mmol/L)**				
	Met·HCl	**$MetC_{12}$**		**$MegC_{12}$**	
1	-	0.001		0.003	
10	2×10^{-4}	0.008		0.013	
200	6×10^{-4}	0.586		0.817	

Both $MetC_{12}$ and $MegC_{12}$ were able to solubilize a fair amount of Cur at 200 mM compared to MetHCl alone. Interestingly, $MegC_{12}$ seems to be able to solubilize Cur slightly more efficiently than $MetC_{12}$.

The aim of the second experiment was to compare the soaps resulting from the three guanidine derivatives, GuC_{12}, $mGuC_{12}$, and $MetC_{12}$ at around 2 wt%, corresponding to roughly 90 mM. Cur and Quer were once again used as test solutes.

Table IV.6. Amounts of solubilized curcumin or quercetin with GuC_{12}, $mGuC_{12}$, and $MetC_{12}$.

Solute	**[Solute] (mmol/L)**		
	GuC_{12}	**$mGuC_{12}$**	**$MetC_{12}$**
Cur	0.12	0.15	0.34
Quer	0.61	0.77	1.53

$MetC_{12}$ seems to be the best candidate for solubilizing hydrophobic compounds among all the guanidine derivatives chosen as counterions.

The solubilizing power of amphiphilic compounds towards hydrophobic molecules tends to increase with the size of their hydrophobic part, i.e. in the case of linear carboxylic acids-based surfactants, the length of their carbon chain. So, the natural next step would be to test soaps with longer chains. However, neither GuC_{14} and $MetC_{14}$ were freely soluble at RT at the chosen concentrations, so $mGuC_{14}$ was only comparable with $MegC_{14}$. As the CMC of $MegC_{14}$ measured at around 4 mM, concentration for this test was chosen as for the first one, i.e. 20 times the CMC. As the CMC of $mGuC_{14}$ was not assessed, it was subsequently prepared at 80 mM as well. Table IV.7 presents the comparison of $mGuC_{14}$ and $MetC_{14}$ for the solubilization of Cur.

Table IV.7. Amounts of solubilized curcumin with $mGuC_{14}$ and $MetC_{14}$.

[Solubilizer] (mmol/L)	**[Curcumin] (mmol/L)**	
	$mGuC_{14}$	**$MegC_{14}$**
80	0.092	0.641

Once again, $MegC_{14}$ seems more efficient as its guanidine counterpart. A reason for that could be the solubilizing effect of free meglumine molecules in addition of the micelle solubilization. To gain more knowledge on that, the shape, size and organization of micelles could be investigated further, for example with Dynamic Light Scattering. However, this requires a more detailed and much longer study.

IV.5. Characterization of meglumine-carboxylates emulsification capacity

Surfactants are not only used as solubilizers or for detergency, they are also very often involved in stabilizing emulsions, and are therefore often referred to as "emulsifiers" by manufacturers, most notably in the food and cosmetics industries. As for soaps, even if they are approved for use in the food industry, they are rarely used by manufacturers, as they are notorious for imparting a bad taste to formulations[189], and well-known surfactants like glycerides, caseinates, lecithin or others are often preferred[263]. The same is true for cosmetics, but in recent years there has been a resurgence in their appreciation by the general public, mostly driven by environmental considerations. Indeed, one of the great appeals of soaps is the possibility of producing them from renewable natural resources (as opposed to the petrochemical industry), and thus the opportunity to label them as natural compounds. Meglumine is already used in cosmetics as an ingredient for hair conditioners and is accepted in food products[106]. In an attempt to establish the suitability of meglumine soaps as potential emulsifiers, and in order to compare the different soaps synthesized, the emulsification and emulsion stabilization capacity of meglumine fatty acid was investigated.

Two emulsification processes were used, the first one was a classical protocol with Ultra-Turrax® and the second one was optimized for emulsion stability, using sonication as emulsification method. A standard WOR ratio of 50-50 was applied to avoid any specific influence on the emulsion properties. Moreover, three different non-polar compounds were selected, *n*-octane, isopropyl myristate (IPM) and paraffin oil (noted PO, a commercial mixture of C_{14-18} saturated aliphatic alkanes and cyclic ones, and used in pharmaceutics). *n*-octane is a classical linear saturated alkane, as IPM and paraffin oil both are very common cosmetic oils. Fatty acids of different lengths were used for the formation of $MegC_n$, and the influence of saturation was assessed by comparing stearic and oleic acids for $MegC_{18}$. In the following, $MegC_{18}^s$ refers to meglumine stearate and $MegC_{18}^o$ to meglumine oleate. Emulsions of $MegC_{18}^s$, $MegC_{18}^o$, and $MegC_{22}$ from the first protocol were compared with Na derivatives as controls. More details about the emulsification process are found in section IV.3.2.6. It is well known that quantitative comparison of different emulsification protocols is impossible, therefore comparisons of the two procedures for the same $MegC_n$ will necessarily remain qualitative. It is also important to note that the emulsions were carried out at a 1 wt% $MegC_n$ concentration for a total mass of 10 g, which for $MegC_{12}$ for example represents approximately 2 mol/L, way above its CMC (around 10 mM, see Table IV.4). The CMC of $MegC_{18}$ and $MegC_{22}$ could not be measured due to their poor aqueous solubility, but their concentration in emulsion samples is most probably much higher than the value that might be expected for a CMC of a surfactant with the same chain length.

IV.5.1. Emulsions characterization

The microscopic observations and granulometry (size and distributions of droplets) of the emulsions obtained with Ultra-Turrax® are shown in Figure IV.20 and Figure IV.21 and those from emulsions prepared by sonication are presented in Figure IV.22. D_{10}, D_{50}, and D_{90} are given, where D_x is the maximum particle diameter below which x % of the sample volume exists, also known as the volume-average particle size. Monitoring these three parameters helps to track significant changes in particle size, as well as changes at the extremes of the distribution, which could be due to coalescence or Ostwald ripening for example[264]. In addition, the average diameters weighted by surface area $D_{[3,2]}$ and volume $D_{[4,3]}$ were also measured with a laser granulometer. As the number of droplets is not known, the measured diameters are influenced by the size of each population. $D_{[4,3]}$ is for instance more appropriate to characterize larger droplets than $D_{[3,2]}$. The evolution of $D_{[3,2]}$

and $D_{[4,3]}$ can reveal destabilization phenomena that arise from droplets size increase, e.g. coalescence or Ostwald ripening.

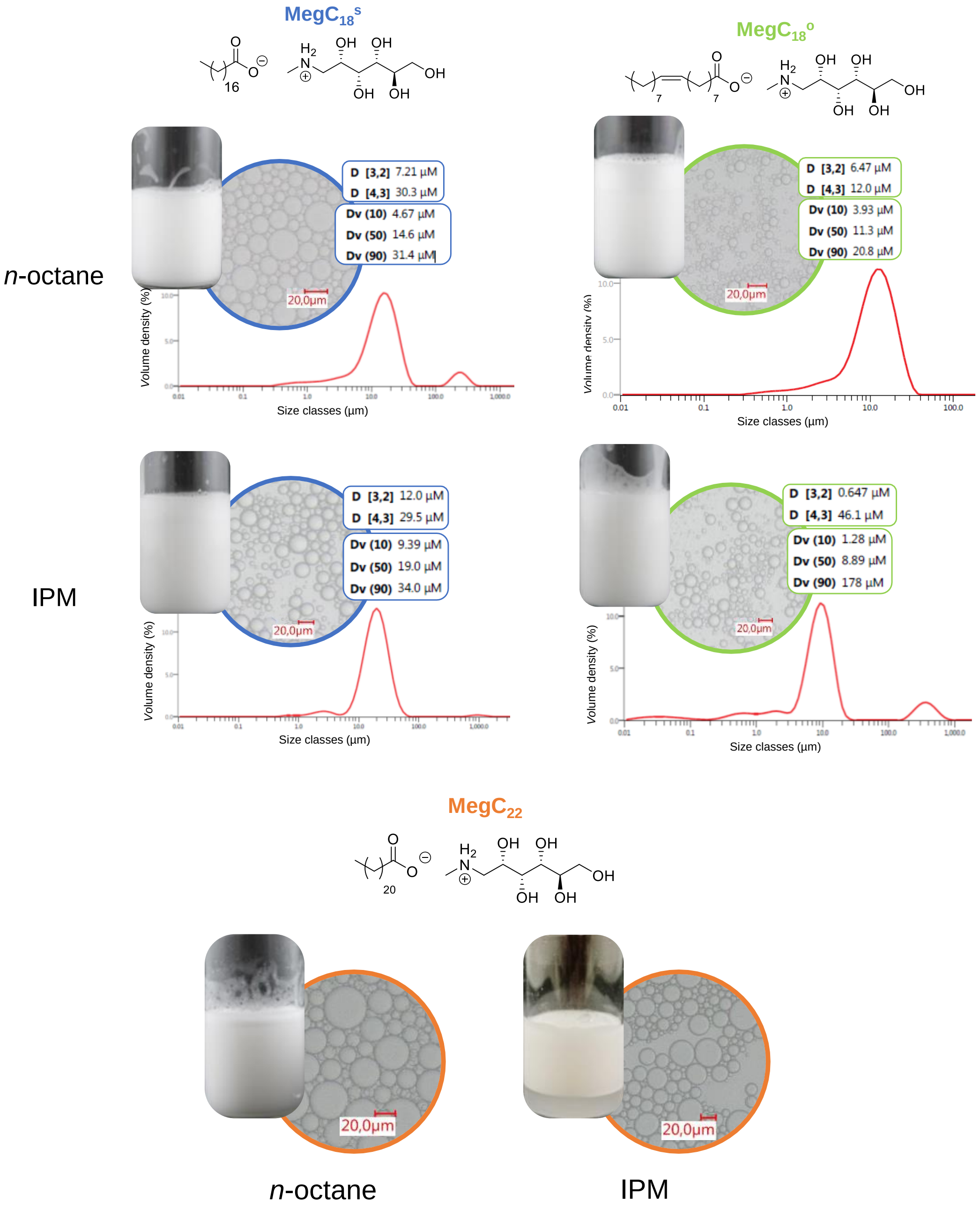

Figure IV.20. Macroscopic and microscopic pictures of n-octane/water and IPM/water emulsions from $MegC_{18}^{s}$, $MegC_{18}^{o}$, and $MegC_{22}$, as well as granulometry analysis for $MegC_{18}^{s}$ and $MegC_{18}^{o}$ emulsions. Emulsions prepared according to protocol 1.

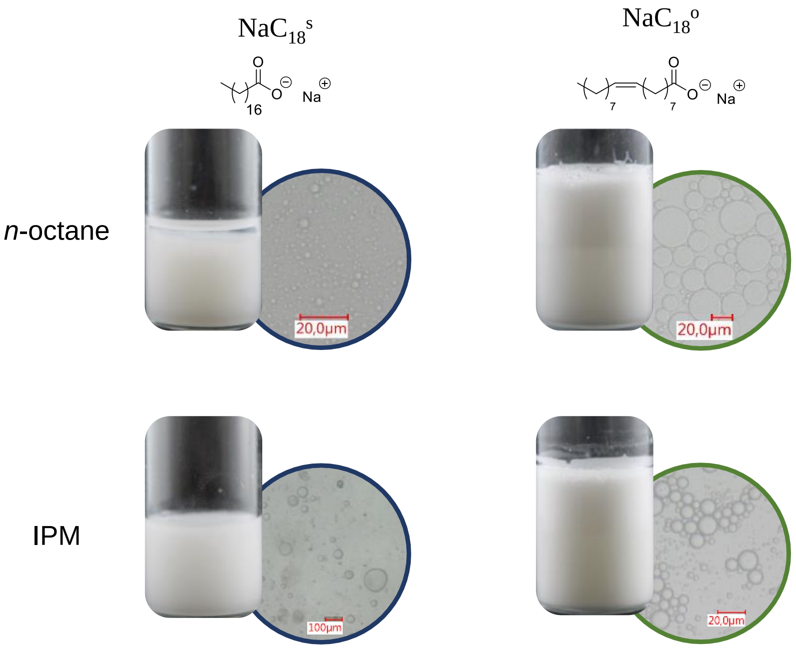

Figure IV.21. Macroscopic and microscopic pictures of NaC$_{18}^{s}$ and NaC$_{18}^{o}$ n-octane/water and IPM/water emulsions. Emulsions prepared according to protocol 1.

MegC$_{18}^{s}$ and MegC$_{18}^{o}$ both produced seemingly complete emulsions. Also, as might be expected, emulsions obtained with meglumine stearate produce larger droplets than those obtained with meglumine oleate, regardless of the oil phase, as chain saturation allows for optimum chain length. MegC$_{22}$ seems to produce even larger droplets, however its lack of solubility at room temperature probably makes emulsion formation less effective, as it is evident by macroscopic observations with IPM in Figure IV.20. Another observation to be made concerns the Droplet Size Distribution (DSD). All emulsions made with Ultra-Turrax® seem to be quite polydisperse, which can be detrimental not only to the desired applications (influencing physicochemical and sensory properties, such as appearance and texture for example[265]) but also more directly to emulsion stability. High polydispersity indeed promotes destabilization phenomena such as Ostwald ripening. The latter accounts for the passive diffusion of the dispersed phase from small to large droplets, and thus contributes to the general increase in droplet size. Nevertheless, MegC$_{18}$ emulsions appear to form emulsions more efficiently than their sodium counterparts (see Figure IV.20 and Figure IV.21). The influence of the non-polar phase is more difficult to unambiguously evaluate for this protocol.

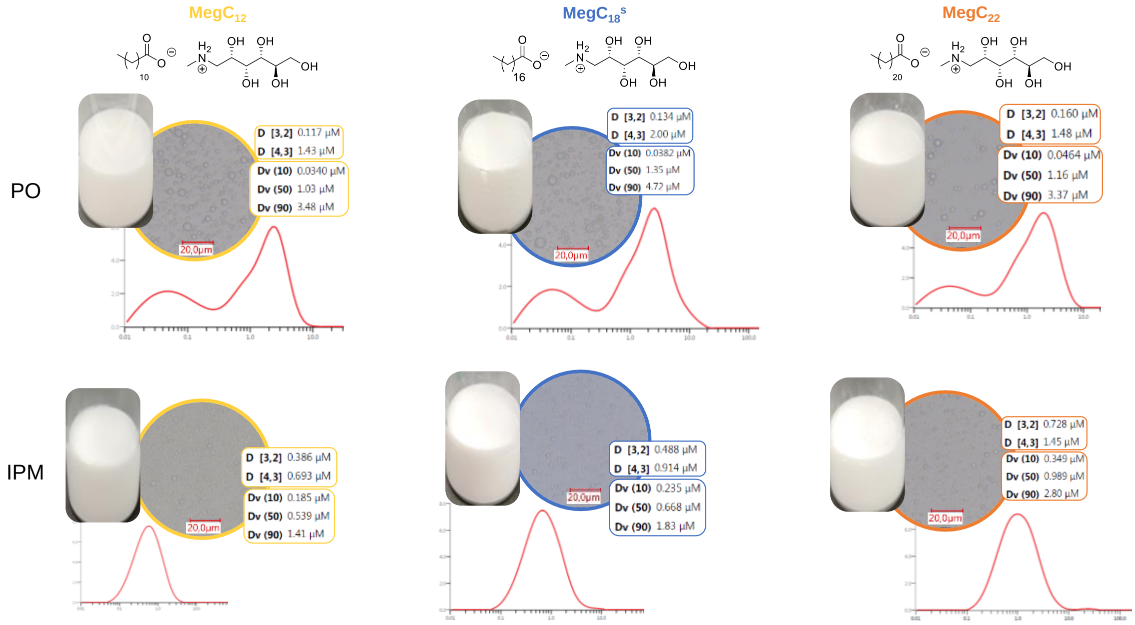

Figure IV.22. Macroscopic, microscopic pictures, and granulometry analysis of PO/water and IPM/water emulsions from MegC$_{12}$, MegC$_{18}^{s}$ and MegC$_{22}$. Emulsions prepared according to protocol 2.

Sonication proved to be a better adapted method to produce emulsions with small droplets. Furthermore, the influence of the choice of oil on the DSD is this time evident, as two major populations seem to visible in the PO emulsions, as for IPM the polydispersity could be described as monomodal, i.e. single-peaked. Furthermore, the chain-length seems to have a greater influence on the droplets size of the IPM emulsions than the PO ones, as there is a clear increase in all the measured diameters with increasing fatty acids chain length. The seemingly bimodal (double-peaked) DSD of the PO emulsions may be responsible for difficulty in assessing the influence of chain length on emulsions structure. All in all, meglumine soaps seem to be able to form standard emulsions quite efficiently. Emulsion stability is crucial for any application, and medium-term stabilization capacity of MegC$_n$ was further investigated via Multiple Light Scattering.

IV.5.2. Stability measurement: Multiple Light Scattering

To characterize the destabilization phenomena that can occur over time, samples from the second protocol were analyzed using Static Multiple Light Scattering with a Turbiscan®. The evolution of the transmitted ΔT and backscattered ΔBS light can provide information on droplet migration and size, as well as on the thickness of the emulsion phase. The evolution of ΔT and ΔBS signals over a one-month period is shown in Figure IV.23 for MegC$_{12}$. Profiles for other emulsions are found in Appendix A.7.

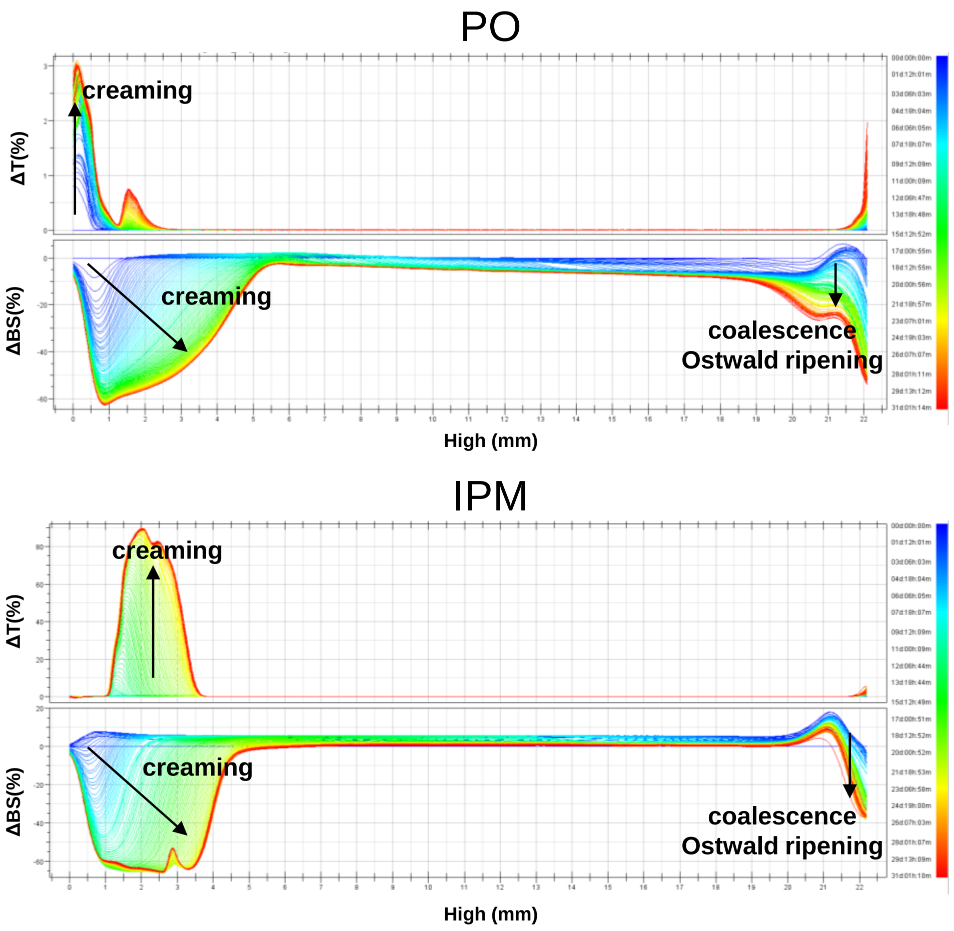

Figure IV.23. ΔT and ΔBS signals evolution for MegC$_{12}$ PO/water (top) and IPM/water emulsions prepared according to protocol 2.

It is clearly visible in Figure IV.23 that creaming occurs, as the ΔT increases at the bottom of the sample and ΔBS decreases simultaneously. Furthermore, some coalescence and/or Ostwald ripening can be observed at the top of the sample, as increase in droplet size slowly causes ΔBS to drop (fewer and larger droplets scatter light less than many small ones). Overall, almost no destabilization is observed in the middle of the emulsion over a one-month period, and creaming, Ostwald ripening, and coalescence remain relatively limited. The emulsions from MegC$_{18}^{s}$ and MegC$_{22}$ exhibit very similar profiles (see Appendix A.7), demonstrating the possibility of using MegC$_{n}$ as emulsifiers. These systems could be optimized by screening different WOR or testing other apolar phases, or by improving the emulsification process.

IV.6. Conclusions

The preparation of all these soaps, as well as their brief characterization in terms of Krafft temperature, CMC, ability to solubilize hydrophobic compounds and emulsifying capacity served as a proof of concept for the use of non-common amino counterions for soap formation and applications. Phase behavior and aqueous phenomena have not been studied in depth as it was not the main focus of this thesis. Furthermore, the combination of metformin with fatty acids, in the form of salts or as micelles, could have an impact on metformin's ability to cross cell membranes, and could therefore find applications in drug delivery. It should be emphasized that this is purely conjectural, and *in vitro* experiments should be carried out to further explore this possibility.

General conclusion

The objectives of this thesis were to identify compounds or to help establish guidelines for the identification of solubilizers from the biological and pharmaceutical literature as hydrotropic agents, and to rationalize the hydrotropic action towards polyphenols based on their structure. To address these challenges, solubilization behaviors of polyphenols were investigated in aqueous solution and in binary solvents systems, via spectroscopic methods, modeling software and for potential applications.

In the first chapter, investigation focused on meglumine as a potent solubilizer for the polyphenol quercetin, as well as its influence on the oxidation behavior of the latter. A method was also developed to predict deprotonation order of oxidation-sensitive polyphenols using the modeling software COSMO-RS. In the second chapter a practical application of this solubilization was presented through the liposomal encapsulation of quercetin directly from aqueous solution under optimized conditions. The study was extended in the third chapter to a set of polyphenols of different subclasses and their solubilization in two binary solvents systems, triacetin/ethanol and cinnamaldehyde/ethanol, as well as with conventional and potential hydrotropes. Finally, in the last chapter, a preliminary study of the possibility of using certain amino compounds as counterions for linear fatty acid systems was presented. This served as a proof of concept of the enhancement of the amphiphilic behavior of the very hydrophilic meglumine and metformin, among others.

The study of the solubilization of quercetin in aqueous solution by meglumine as a function of pH in the first chapter demonstrated a strong solubilization effect of meglumine at pH 8 and above. The amount of solubilized quercetin in aqueous solution at pH 8 was indeed increased by a factor of almost 7 (see Figure V.1). In addition, the oxidation monitoring via HPLC and H_2O_2 titration showed that the presence of meglumine did not affect significantly the rate of oxidation of quercetin, which allows the solubilization of quercetin in aqueous solution at mildly alkaline pH and applications based on short process time.

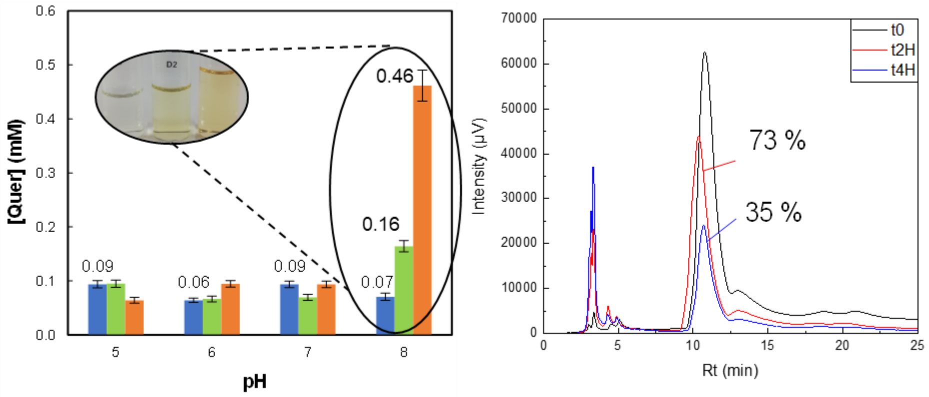

Figure V.1. Left: maximum solubility of quercetin in water as a function of pH and meglumine concentration. Blue: Ultrapure water (no meglumine). Green: 50 mM meglumine in ultrapure water. Orange: 250 mM in ultrapure water. Right: HPLC chromatogram of quercetin oxidative degradation at pH 8.4 in presence of 250 mM meglumine.

The interactions between meglumine and quercetin were investigated via NMR and resulted from a salt formation, most probably between one molecule of quercetin and one or two molecules of meglumine, and occurs when quercetin is at least one time negatively charged upon deprotonation, i.e. above its first pK_a. To gain further insights into this mechanism and identify which hydroxyl group(s) of quercetin were likely to interact with meglumine, the deprotonation order of quercetin was assessed using a specially developed method with the modeling software COSMO-RS. This method is based on the pK_a prediction ability of COSMO-RS and the selection of the hydroxyl group with the lowest predicted pK_a for each charge state to identify the most likely successive deprotonation path. This theoretical method, although not very accurate in terms of absolute pK_a values, allows to overcome the oxidation constraints that make the determination of pK_a 3, 4 and 5 for quercetin and other sensitive polyphenols virtually impossible using conventional spectroscopic techniques. The order of deprotonation determined in this work is presented in Figure V.2.

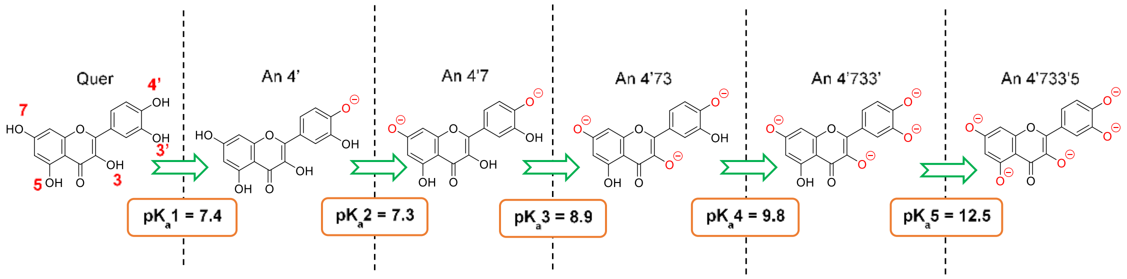

Figure V.2. pK_a calculations for the most probable deprotonation order of quercetin according to the COSMO-RS method.

The compromise between efficient solubilization and reasonable oxidation at pH around 8 was then tested on other polyphenols to confirm the conditions required for this interaction. Curcumin, *trans*-resveratrol, gallic acid, naringenin, and phloretin were solubilized at pH 8 in the presence of meglumine, and only the compounds exhibits pK_a values sufficiently lower than 8 showed a solubility enhancement effect with increasing meglumine concentration. These results have been published in the *Journal of Molecular Liquids* (see Appendix A.8).

The deprotonation method appears ideal for many oxidation-sensitive compounds, especially natural phenolic antioxidants, but has yet to be tested on a significant number of compounds. Lastly, the pK_a dependence of the solubilization mechanism of meglumine could be exploited to enable selective solubilization of certain polyphenols according to their pK_a, which could have applications in extraction of natural compounds in aqueous solution in the context of green chemistry. Once solubilized and separated, the compounds of interest could be precipitated once again by reducing the pH.

In chapter II, the ability of meglumine was assessed in a practical application, for the encapsulation of quercetin in liposomes. A modified version of the standard thin-film method, inspired by the pH-driven method, was applied to entrap quercetin in liposomes directly from aqueous solution. Quercetin was solubilized with meglumine at pH around 9 and a minimum of organic solvents was used to form the thin film of lipids. After removing the solvents, the aqueous solution of quercetin could be added directly and liposomes self-assembled. An electro-chemical method using Differential Pulse Voltammetry was used to detect liposomal quercetin and to ensure the absence of leakage of quercetin from the liposomes. However, this method revealed not to be able to discriminate between quercetin and its oxidation products. HPLC measurements were therefore conducted and proved perfectly suitable to quantify native quercetin as well as its oxidation (see Figure V.3).

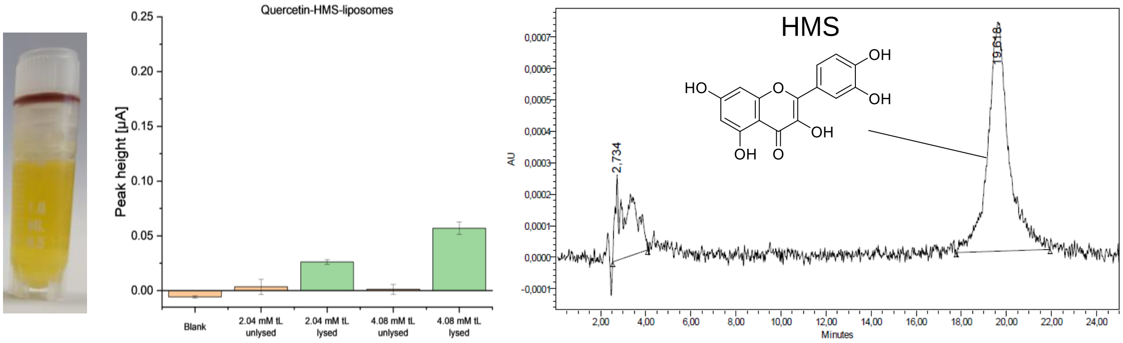

Figure V.3. Left: photograph of the HMS (high fraction) liposome sample after dialysis. Center left: DPV measurements signals of lysed (green) and unlysed (orange) HMS liposomes as a function of the total lipid concentration. Right: HPLC chromatogram of the HMS liposomes batch showing the clear signal for quercetin at R_t around 20 min.

As seen in Figure V.3, unoxidized quercetin was successfully encapsulated into the liposomes, proving that a fast process with a final step of pH-reduction was indeed well-suited for the solubilization of quercetin with meglumine. Moreover, the presence of meglumine did not affect the properties of liposomes, including size, size distribution, and surface charge.

The panel of investigated polyphenols was expanded in chapter III to include two flavonoids structurally closed to quercetin, morin and naringenin, as well as phloretin, *trans*-resveratrol, and xanthohumol. In order to identify the factors behind the low aqueous solubility of these compounds, and to establish a relation between their structure and the efficacy of hydrotropic mechanisms, COSMO-RS modeling software was once again used, this time for the prediction of chemical potentials, relative solubility, and potential solubilization synergies between the studied binary solvents. Comparison with experimental data demonstrated that COSMO-RS predictions of synergies were fairly accurate, and that calculations for relative solubility within the set of studied polyphenols was also quite successful, except for compounds prone to π-stacking, for which solubility was significantly overestimated by COSMO-RS due to its inability to automatically predict π-stacking, e.g. quercetin and morin. Both solvents systems proved to be prone to solubilization synergies, which can be understood for example in the case of ethanol/triacetin as an optimized balance of van der Waals forces, polar interactions and hydrogen bonding compared to the respective pure solvents. Similar synergies were found in ethanol/cinnamaldehyde mixtures. However, these synergies were found to be also dependent of the solute, as quercetin, naringenin, morin, and phloretin were predicted to exert a maximum solubility around 60 % to 80 % cinnamaldehyde, where xanthohumol and resveratrol showed the opposite trend with a synergy expected around 20 % to 40 % cinnamaldehyde.

Finally, the solubilization behavior of the three flavonoids quercetin, morin, and naringenin were compared regarding the hydrotropic action of pyrogallol and phloroglucinol. It was shown that these small phenols were able to increase the aqueous solubility of the flavonoids by braking the π-stacking, or more probably by promoting a preferential π-stacking interaction between flavonoid and the less bulky phloroglucinol or pyrogallol. The combination of these two phenols was also assessed as a mean to overcome the poor water-solubility of phloroglucinol (see Figure V.4).

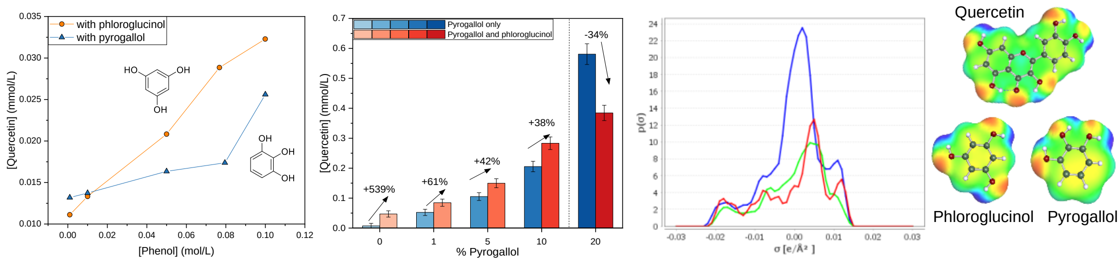

Figure V.4. Left: comparison of solubilization of quercetin with pyrogallol (blue triangles) and phloroglucinol (orange circles). Center left: solubility profiles of quercetin in water with pyrogallol alone (blue) or with pyrogallol and phloroglucinol (red). Percentages indicate quercetin solubility changes with combination of phloroglucinol and pyrogallol compared to pyrogallol alone. Right: σ-profiles and σ-surfaces of the most stable conformers of quercetin (blue), phloroglucinol (red), and pyrogallol (green) calculated with COSMO-RS software.

As such, even if phloroglucinol cannot be considered as a hydrotrope according to the definitions quoted in this work, it could be argued that the possibility of using facilitated hydrotropy concepts with a co-solvent (e.g. ethanol) or a second hydrotrope (pyrogallol), provides additional evidence of the potential hydrotropic properties of phloroglucinol. This example could help the search for other aromatic compounds whose solubility is too low to be considered as hydrotropes, but which could still prove useful in combination with others. Finally, since phloroglucinol is one of the main oxidation products of quercetin and numerous other flavonoids, this interaction could partially explain the observed solubility increase of polyphenols with oxidation, and could be used to design formulations where solubilizing properties could arise from the degradation of a polyphenolic antioxidant.

The study presented in the last chapter examined the ability of meglumine and other highly hydrophilic amino molecules, the antidiabetic agent metformin as well as guanidine derivatives, to act as counterions for linear fatty acids, therefore forming “soaps”. The double challenge was to increase both the aqueous solubility of fatty acids and the permeability of amino compounds by increasing their hydrophobicity. Soaps of meglumine, guanidine, methyl guanidine and metformin were therefore prepared according to two protocols, one *in situ* and the other *ex situ*, and characterized according to conventional criteria for surfactants. Thus, the CMCs of these compounds were shown to fall within the standard order of magnitude of a few millimolar for C_{12} chains. The Krafft points of these compounds proved to be advantageous compared to sodium and potassium soaps, up to a chain length of C_{14}, as summarized in Table V.1.

Table V.1. Krafft temperatures (°C) of classical fatty acid soaps and fatty acid soaps prepared in this work.

Counterion	C_{12}	C_{14}	Reference
Na	25	45	[191]
K	10	30	[190]
Meg	< 5	16 < x < 20	This work
Met	~ 6-7	40 < x < 50	This work
Gu	< 2-3	30 < x < 40	This work
mGu	< 0	20 < x < 30	This work

In addition, micellar solubilization of quercetin and curcumin has been shown to be achievable with these systems, which could enable increased drug delivery of both encapsulated actives and metformin, for example, for a complementary or reinforced biological activity. Finally, meglumine soaps proved to be suitable to form and stabilize emulsions with classical oils such as isopropyl myristate. The characteristics of these emulsions (WOR, choice of oil, emulsification process, etc.) could moreover be optimized to achieve even more stable emulsions for applications in cosmetics, e.g. in skin care or hair conditioning where meglumine is already used.

A final issue which has not been raised in details in this work is the importance of the amine function, which is present in many solubilizing agents and could have a significant influence on the hydrotropic action, particularly considering their interactions with phenols.

References

(1) Nikolakakis, I.; Partheniadis, I. Self-Emulsifying Granules and Pellets: Composition and Formation Mechanisms for Instant or Controlled Release. *Pharmaceutics* **2017**, *9* (4), 50. https://doi.org/10.3390/pharmaceutics9040050.

(2) Häckl, K.; Kunz, W. Some Aspects of Green Solvents. *CR Chim.* **2018**, *21* (6), 572–580. https://doi.org/10.1016/j.crci.2018.03.010.

(3) Jouyban, A.; A. Fakhree, M. A. Experimental and Computational Methods Pertaining to Drug Solubility. In *Toxicity and Drug Testing*; Acree, B., Ed.; InTech, 2012. https://doi.org/10.5772/19206.

(4) Description and Solubility - Description and Relative Solubility of USP and NF Articles. *Second Supplement to USP 35–NF 30* **2012**, 5805.

(5) Skyner, R. E.; McDonagh, J. L.; Groom, C. R.; van Mourik, T.; Mitchell, J. B. O. A Review of Methods for the Calculation of Solution Free Energies and the Modelling of Systems in Solution. *Phys. Chem. Chem. Phys.* **2015**, *17* (9), 6174–6191. https://doi.org/10.1039/C5CP00288E.

(6) Gamsjäger, H.; Lorimer, J. W.; Scharlin, P.; Shaw, D. G. Glossary of Terms Related to Solubility (IUPAC Recommendations 2008). *Pure and Applied Chemistry* **2008**, *80* (2), 233–276. https://doi.org/10.1351/pac200880020233.

(7) Crafts, P. The Role of Solubility Modeling and Crystallization in the Design of Active Pharmaceutical Ingredients. In *Computer Aided Chemical Engineering*; Elsevier, 2007; Vol. 23, pp 23–85. https://doi.org/10.1016/S1570-7946(07)80005-8.

(8) Augustijns, P.; Brewster, M. E. Supersaturating Drug Delivery Systems: Fast Is Not Necessarily Good Enough. *J. Pharm. Sci.* **2012**, *101* (1), 7–9. https://doi.org/10.1002/jps.22750.

(9) Bevernage, J.; Brouwers, J.; Brewster, M. E.; Augustijns, P. Evaluation of Gastrointestinal Drug Supersaturation and Precipitation: Strategies and Issues. *Int. J. Pharm.* **2013**, *453* (1), 25–35. https://doi.org/10.1016/j.ijpharm.2012.11.026.

(10) Völgyi, G.; Baka, E.; Box, K. J.; Comer, J. E. A.; Takács-Novák, K. Study of PH-Dependent Solubility of Organic Bases. Revisit of Henderson-Hasselbalch Relationship. *Anal. Chim. Acta* **2010**, *673* (1), 40–46. https://doi.org/10.1016/j.aca.2010.05.022.

(11) Burley, S. K.; Petsko, G. A. Aromatic-Aromatic Interaction: A Mechanism of Protein Structure Stabilization. *Science* **1985**, *229* (4708), 23–28. https://doi.org/10.1126/science.3892686.

(12) Hunter, C. A.; Sanders, J. K. M. The Nature of .Pi.-.Pi. Interactions. *J. Am. Chem. Soc.* **1990**, *112* (14), 5525–5534. https://doi.org/10.1021/ja00170a016.

(13) Wheeler, S. E.; Houk, K. N. Substituent Effects in the Benzene Dimer Are Due to Direct Interactions of the Substituents with the Unsubstituted Benzene. *J. Am. Chem. Soc.* **2008**, *130* (33), 10854–10855. https://doi.org/10.1021/ja802849j.

(14) Ringer, A. L.; Sinnokrot, M. O.; Lively, R. P.; Sherrill, C. D. The Effect of Multiple Substituents on Sandwich and T-Shaped π–π Interactions. *Chem. Eur. J.* **2006**, *12* (14), 3821–3828. https://doi.org/10.1002/chem.200501316.

(15) Sinnokrot, M. O.; Sherrill, C. D. Substituent Effects in Π−π Interactions: Sandwich and T-Shaped Configurations. *J. Am. Chem. Soc.* **2004**, *126* (24), 7690–7697. https://doi.org/10.1021/ja049434a.

(16) Parrish, R. M.; Sherrill, C. D. Quantum-Mechanical Evaluation of π–π versus Substituent−π Interactions in π Stacking: Direct Evidence for the Wheeler–Houk Picture. *J. Am. Chem. Soc.* **2014**, *136* (50), 17386–17389. https://doi.org/10.1021/ja5101245.

(17) Ringer, A. L.; Sherrill, C. D. Substituent Effects in Sandwich Configurations of Multiply Substituted Benzene Dimers Are Not Solely Governed By Electrostatic Control. *J. Am. Chem. Soc.* **2009**, *131* (13), 4574–4575. https://doi.org/10.1021/ja809720r.

(18) Watt, M.; Hardebeck, L. K. E.; Kirkpatrick, C. C.; Lewis, M. Face-to-Face Arene−Arene Binding Energies: Dominated by Dispersion but Predicted by Electrostatic and Dispersion/Polarizability Substituent Constants. *J. Am. Chem. Soc.* **2011**, *133* (11), 3854–3862. https://doi.org/10.1021/ja105975a.

(19) Wheeler, S. E. Local Nature of Substituent Effects in Stacking Interactions. *J. Am. Chem. Soc.* **2011**, *133* (26), 10262–10274. https://doi.org/10.1021/ja202932e.

(20) Kalepu, S.; Nekkanti, V. Insoluble Drug Delivery Strategies: Review of Recent Advances and Business Prospects. *Acta Pharmaceutica Sinica B* **2015**, *5* (5), 442–453. https://doi.org/10.1016/j.apsb.2015.07.003.

(21) Wang, W.; Sun, C.; Mao, L.; Ma, P.; Liu, F.; Yang, J.; Gao, Y. The Biological Activities, Chemical Stability, Metabolism and Delivery Systems of Quercetin: A Review. *Trends Food Sci. Technol.* **2016**, *56*, 21–38. https://doi.org/10.1016/j.tifs.2016.07.004.

(22) Thakuria, R.; Delori, A.; Jones, W.; Lipert, M. P.; Roy, L.; Rodríguez-Hornedo, N. Pharmaceutical Cocrystals and Poorly Soluble Drugs. *Int. J. Pharm.* **2013**, *453* (1), 101–125. https://doi.org/10.1016/j.ijpharm.2012.10.043.

(23) Grothe, E.; Meekes, H.; Vlieg, E.; ter Horst, J. H.; de Gelder, R. Solvates, Salts, and Cocrystals: A Proposal for a Feasible Classification System. *Cryst. Growth Des.* **2016**, *16* (6), 3237–3243. https://doi.org/10.1021/acs.cgd.6b00200.

(24) Jacobo-Velázquez, D. A.; Cisneros-Zevallos, L. Bioactive Phenolics and Polyphenols: Current Advances and Future Trends. *Int. J. Mol. Sci.* **2020**, *21* (17), 6142. https://doi.org/10.3390/ijms21176142.

(25) Cutrim, C. S.; Cortez, M. A. S. A Review on Polyphenols: Classification, Beneficial Effects and Their Application in Dairy Products. *Int. J. Dairy Technol.* **2018**, *71* (3), 564–578. https://doi.org/10.1111/1471-0307.12515.

(26) Del Rio, D.; Rodriguez-Mateos, A.; Spencer, J. P. E.; Tognolini, M.; Borges, G.; Crozier, A. Dietary (Poly)Phenolics in Human Health: Structures, Bioavailability, and Evidence of Protective Effects Against Chronic Diseases. *Antioxid. Redox Signaling* **2013**, *18* (14), 1818–1892. https://doi.org/10.1089/ars.2012.4581.

(27) Radtke, J. Zufuhr und Absorption ausgewählter Flavonoide, Technische Universität München, **2001**.

(28) Kühnau, J. The Flavonoids. A Class of Semi-Essential Food Components: Their Role in Human Nutrition. In *World Review of Nutrition and Dietetics*; Bourne, G. H., Ed.; S. Karger AG, 1976; Vol. 24, pp 117–191. https://doi.org/10.1159/000399407.

(29) Sharma, N.; Dobhal, M.; Joshi, Y.; Chahar, M. Flavonoids: A Versatile Source of Anticancer Drugs. *Phcog. Rev.* **2011**, *5* (9), 1. https://doi.org/10.4103/0973-7847.79093.

(30) Cook, N. C.; Samman, S. Flavonoids - Chemistry, Metabolism, Cardioprotective Effects, and Dietary Sources. *J. Nutr. Biochem.* **1996**, *7* (2), 66–76. https://doi.org/10.1016/S0955-2863(95)00168-9

(31) Manach, C.; Scalbert, A.; Morand, C.; Rémésy, C.; Jiménez, L. Polyphenols: Food Sources and Bioavailability. *Am. J. Clin. Nutr.* **2004**, *79* (5), 727–747. https://doi.org/10.1093/ajcn/79.5.727.

(32) Brewer, M. S. Natural Antioxidants: Sources, Compounds, Mechanisms of Action, and Potential Applications. *Compr. Rev. Food Sci Food Saf.* **2011**, *10* (4), 221–247. https://doi.org/10.1111/j.1541-4337.2011.00156.x.

(33) Muhammad, D. R. A.; Praseptiangga, D.; Van de Walle, D.; Dewettinck, K. Interaction between Natural Antioxidants Derived from Cinnamon and Cocoa in Binary and Complex Mixtures. *Food Chem.* **2017**, *231*, 356–364. https://doi.org/10.1016/j.foodchem.2017.03.128.

(34) Jangid, A. K.; Pooja, D.; Kulhari, H. Determination of Solubility, Stability and Degradation Kinetics of Morin Hydrate in Physiological Solutions. *RSC Adv.* **2018**, *8* (50), 28836–28842. https://doi.org/10.1039/C8RA04139C.

(35) Rajput, S. A.; Wang, X.; Yan, H.-C. Morin Hydrate: A Comprehensive Review on Novel Natural Dietary Bioactive Compound with Versatile Biological and Pharmacological Potential. *Biomed. Pharmacother.* **2021**, *138*, 111511. https://doi.org/10.1016/j.biopha.2021.111511.

(36) Zhang, L.; Song, L.; Zhang, P.; Liu, T.; Zhou, L.; Yang, G.; Lin, R.; Zhang, J. Solubilities of Naringin and Naringenin in Different Solvents and Dissociation Constants of Naringenin. *J. Chem. Eng. Data* **2015**, *60* (3), 932–940. https://doi.org/10.1021/je501004g.

(37) Barreca, D.; Gattuso, G.; Bellocco, E.; Calderaro, A.; Trombetta, D.; Smeriglio, A.; Laganà, G.; Daglia, M.; Meneghini, S.; Nabavi, S. M. Flavanones: Citrus Phytochemical with Health-Promoting Properties: Citrus Phytochemical with Health-Promoting Properties. *BioFactors* **2017**, *43* (4), 495–506. https://doi.org/10.1002/biof.1363.

(38) Renaud, S.; de Lorgeril, M. Wine, Alcohol, Platelets, and the French Paradox for Coronary Heart Disease. *The Lancet* **1992**, *339* (8808), 1523–1526. https://doi.org/10.1016/0140-6736(92)91277-F.

(39) Mariadoss, A. V. A.; Vinyagam, R.; Rajamanickam, V.; Sankaran, V.; Venkatesan, S.; David, E. Pharmacological Aspects and Potential Use of Phloretin: A Systemic Review.

Mini Rev. Med. Chem. **2019**, *19* (13), 1060–1067. https://doi.org/10.2174/1389557519666190311154425.

(40) de Oliveira, M. R. Phloretin-induced Cytoprotective Effects on Mammalian Cells: A Mechanistic View and Future Directions. *BioFactors* **2016**, *42* (1), 13–40. https://doi.org/10.1002/biof.1256.

(41) Anunciato Casarini, T. P.; Frank, L. A.; Pohlmann, A. R.; Guterres, S. S. Dermatological Applications of the Flavonoid Phloretin. *Eur. J. Pharmacol.* **2020**, *889*, 173593. https://doi.org/10.1016/j.ejphar.2020.173593.

(42) Yao, J.; Zhang, B.; Ge, C.; Peng, S.; Fang, J. Xanthohumol, a Polyphenol Chalcone Present in Hops, Activating Nrf2 Enzymes To Confer Protection against Oxidative Damage in PC12 Cells. *J. Agric. Food Chem.* **2015**, *63* (5), 1521–1531. https://doi.org/10.1021/jf505075n.

(43) Constant, J. Alcohol, Ischemic Heart Disease, and the French Paradox. *Clin. Cardiol.* **1997**, *20* (5), 420–424. https://doi.org/10.1002/clc.4960200504.

(44) Beretz, A.; Cazenave, J.-P.; Anton, R. Inhibition of Aggregation and Secretion of Human Platelets by Quercetin and Other Flavonoids: Structure-Activity Relationships. *Agents Actions* **1982**, *12* (3), 382–387. https://doi.org/10.1007/BF01965408.

(45) Conquer, J. A.; Maiani, G.; Azzini, E.; Raguzzini, A.; Holub, B. J. Supplementation with Quercetin Markedly Increases Plasma Quercetin Concentration without Effect on Selected Risk Factors for Heart Disease in Healthy Subjects. *J. Nutr.* **1998**, *128* (3), 593–597. https://doi.org/10.1093/jn/128.3.593.

(46) Bahar, E.; Kim, J.-Y.; Yoon, H. Quercetin Attenuates Manganese-Induced Neuroinflammation by Alleviating Oxidative Stress through Regulation of Apoptosis, INOS/NF-KB and HO-1/Nrf2 Pathways. *Int. J. Mol. Sci.* **2017**, *18* (9), 1989. https://doi.org/10.3390/ijms18091989.

(47) Guitard, R. Oxidation of Omega-3 Oil and Preservation by Natural Phenolic Antioxidants, University Lille 1 - Sciences and Technologies, **2016**.

(48) da Silva, E. L.; Piskula, M. K.; Yamamoto, N.; Moon, J.-H.; Terao, J. Quercetin Metabolites Inhibit Copper Ion-Induced Lipid Peroxidation in Rat Plasma ^{1}. *FEBS Letters* **1998**, *430* (3), 405–408. https://doi.org/10.1016/S0014-5793(98)00709-1.

(49) Lotito, S. B.; Zhang, W.-J.; Yang, C. S.; Crozier, A.; Frei, B. Metabolic Conversion of Dietary Flavonoids Alters Their Anti-Inflammatory and Antioxidant Properties. *Free Rad. Biol. Med.* **2011**, *51* (2), 454–463. https://doi.org/10.1016/j.freeradbiomed.2011.04.032.

(50) Day, A. J.; Bao, Y.; Morgan, M. R. A.; Williamson, G. Conjugation Position of Quercetin Glucuronides and Effect on Biological Activity. *Free Rad. Biol. Med.* **2000**, *29* (12), 1234–1243. https://doi.org/10.1016/S0891-5849(00)00416-0.

(51) Basaga, H. S. Biochemical Aspects of Free Radicals. *Biochem. Cell Biol.* **1990**, *68* (7–8), 989–998. https://doi.org/10.1139/o90-146.

(52) Leopoldini, M.; Marino, T.; Russo, N.; Toscano, M. Antioxidant Properties of Phenolic Compounds: H-Atom versus Electron Transfer Mechanism. *J. Phys. Chem. A* **2004**, *108* (22), 4916–4922. https://doi.org/10.1021/jp037247d.

(53) Leopoldini, M.; Russo, N.; Toscano, M. The Molecular Basis of Working Mechanism of Natural Polyphenolic Antioxidants. *Food Chem.* **2011**, *125* (2), 288–306. https://doi.org/10.1016/j.foodchem.2010.08.012.

(54) Litwinienko, G.; Ingold, K. U. Abnormal Solvent Effects on Hydrogen Atom Abstraction. 2. Resolution of the Curcumin Antioxidant Controversy. The Role of Sequential Proton Loss Electron Transfer. *J. Org. Chem.* **2004**, *69* (18), 5888–5896. https://doi.org/10.1021/jo049254j.

(55) Litwinienko, G.; Ingold, K. U. Abnormal Solvent Effects on Hydrogen Atom Abstraction. 3. Novel Kinetics in Sequential Proton Loss Electron Transfer Chemistry. *J. Org. Chem.* **2005**, *70* (22), 8982–8990. https://doi.org/10.1021/jo051474p.

(56) Brigati, G.; Lucarini, M.; Mugnaini, V.; Pedulli, G. F. Determination of the Substituent Effect on the O−H Bond Dissociation Enthalpies of Phenolic Antioxidants by the EPR Radical Equilibration Technique. *J. Org. Chem.* **2002**, *67* (14), 4828–4832. https://doi.org/10.1021/jo025755y.

(57) Huang, D.; Ou, B.; Prior, R. L. The Chemistry behind Antioxidant Capacity Assays. *J. Agric. Food Chem.* **2005**, *53* (6), 1841–1856. https://doi.org/10.1021/jf030723c.

(58) Pietta, P.-G. Flavonoids as Antioxidants. *J. Nat. Prod.* **2000**, *63* (7), 1035–1042. https://doi.org/10.1021/np9904509.

(59) Rice-Evans, C. A.; Miller, N. J.; Paganga, G. Structure-Antioxidant Activity Relationships of Flavonoids and Phenolic Acids. *Free Rad. Biol. Med.* **1996**, *20* (7), 933–956. https://doi.org/10.1016/0891-5849(95)02227-9.

(60) Wang, J.; Zhao, X.-H. Degradation Kinetics of Fisetin and Quercetin in Solutions Affected by Medium PH, Temperature and Co-Existed Proteins. *J. Serb. Chem. Soc.* **2016**, *81* (3), 243–253. https://doi.org/10.2298/JSC150706092W.

(61) Buchner, N.; Krumbein, A.; Rohn, S.; Kroh, L. W. Effect of Thermal Processing on the Flavonols Rutin and Quercetin. *Rapid Commun. Mass Spectrom.* **2006**, *20* (21), 3229–3235. https://doi.org/10.1002/rcm.2720.

(62) Jørgensen, L. V.; Cornett, C.; Justesen, U.; Skibsted, L. H.; Dragsted, L. O. Two-Electron Electrochemical Oxidation of Quercetin and Kaempferol Changes Only the Flavonoid C-Ring. *Free Rad. Res.* **1998**, *29* (4), 339–350. https://doi.org/10.1080/10715769800300381.

(63) Zenkevich, I.; Eshchenko, A.; Makarova, S.; Vitenberg, A.; Dobryakov, Y.; Utsal, V. Identification of the Products of Oxidation of Quercetin by Air Oxygenat Ambient Temperature. *Molecules* **2007**, *12* (3), 654–672. https://doi.org/10.3390/12030654.

(64) Brown, S. B.; Rajananda, V.; Holroyd, J. A.; EVANSt, E. G. V. A Study of the Mechanism of Quercetin Oxygenation by 18Q Labelling. **1982**, *205* (1) 239–244.

(65) Hajji, H. E.; Nkhili, E.; Tomao, V.; Dangles, O. Interactions of Quercetin with Iron and Copper Ions: Complexation and Autoxidation. *Free Rad. Res.* **2006**, *40* (3), 303–320. https://doi.org/10.1080/10715760500484351.

(66) Amidon, G. L.; Lennernäs, H.; Shah, V. P.; Crison, J. R. A Theoretical Basis for a Biopharmaceutic Drug Classification: The Correlation of in Vitro Drug Product Dissolution and in Vivo Bioavailability. *Pharm. Res.* **1995**, *12* (3), 413–420. https://doi.org/10.1023/a:1016212804288.

(67) Chavda, H.; Patel, C.; Anand, I. Biopharmaceutics Classification System. *Syst. Rev. Pharm.* **2010**, *1* (1), 62. https://doi.org/10.4103/0975-8453.59514.

(68) Tsume, Y.; Mudie, D. M.; Langguth, P.; Amidon, G. E.; Amidon, G. L. The Biopharmaceutics Classification System: Subclasses for in Vivo Predictive Dissolution (IPD) Methodology and IVIVC. *Eur. J. Clin. Pharmacol.* **2014**, *57*, 152–163. https://doi.org/10.1016/j.ejps.2014.01.009.

(69) M9 Biopharmaceutics Classification System- Based Biowaivers; U.S. Department of Health and Human Services Food and Drug Administration Center for Drug Evaluation and Research (CDER) Center for Biologics Evaluation and Research (CBER), **2021**.

(70) Kim, M. K.; Park, K.; Yeo, W.; Choo, H.; Chong, Y. In Vitro Solubility, Stability and Permeability of Novel Quercetin–Amino Acid Conjugates. *Bioorg. Med. Chem.* **2009**, *17* (3), 1164–1171. https://doi.org/10.1016/j.bmc.2008.12.043.

(71) Gugler, R.; Leschik, M.; Dengler, H. J. Disposition of Quercetin in Man after Single Oral and Intravenous Doses. *Eur. J. Clin. Pharmacol.* **1975**, *9* (2–3), 229–234. https://doi.org/10.1007/BF00614022.

(72) Moon, Y. J.; Wang, L.; DiCenzo, R.; Morris, M. E. Quercetin Pharmacokinetics in Humans. *Biopharm. Drug Dispos.* **2008**, *29* (4), 205–217. https://doi.org/10.1002/bdd.605.

(73) Cione, E.; La Torre, C.; Cannataro, R.; Caroleo, M. C.; Plastina, P.; Gallelli, L. Quercetin, Epigallocatechin Gallate, Curcumin, and Resveratrol: From Dietary Sources to Human MicroRNA Modulation. *Molecules* **2019**, *25* (1), 63. https://doi.org/10.3390/molecules25010063.

(74) Klitou, P.; Rosbottom, I.; Simone, E. Synthonic Modeling of Quercetin and Its Hydrates: Explaining Crystallization Behavior in Terms of Molecular Conformation and Crystal Packing. *Cryst. Growth Des.* **2019**, *19* (8), 4774–4783. https://doi.org/10.1021/acs.cgd.9b00650.

(75) Tawani, A.; Mishra, S. K.; Kumar, A. Structural Insight for the Recognition of G-Quadruplex Structure at Human c-Myc Promoter Sequence by Flavonoid Quercetin. *Sci. Rep.* **2017**, *7* (1), 3600. https://doi.org/10.1038/s41598-017-03906-3.

(76) Di Meo, F.; Sancho Garcia, J. C.; Dangles, O.; Trouillas, P. Highlights on Anthocyanin Pigmentation and Copigmentation: A Matter of Flavonoid π-Stacking Complexation To Be Described by DFT-D. *J. Chem. Theory Comput.* **2012**, *8* (6), 2034–2043. https://doi.org/10.1021/ct300276p.

(77) Herrero-Martínez, J. M.; Sanmartin, M.; Rosés, M.; Bosch, E.; Ràfols, C. Determination of Dissociation Constants of Flavonoids by Capillary Electrophoresis. *Electrophoresis* **2005**, *26* (10), 1886–1895. https://doi.org/10.1002/elps.200410258.

(78) Sauerwald, N.; Schwenk, M.; Polster, J.; Bengsch, E. Spectrometric PK Determination of Daphnetin, Chlorogenic Acid and Quercetin. *Zeitschrift für Naturforschung B* **1998**, *53* (3), 315–321. https://doi.org/10.1515/znb-1998-0310.

(79) Escandar, G. M.; Sala, L. F. Complexing Behavior of Rutin and Quercetin. *Can. J. Chem.* **1991**, *69* (12), 1994–2001. https://doi.org/10.1139/v91-288.

(80) Musialik, M.; Kuzmicz, R.; Pawłowski, T. S.; Litwinienko, G. Acidity of Hydroxyl Groups: An Overlooked Influence on Antiradical Properties of Flavonoids. *J. Org. Chem.* **2009**, *74* (7), 2699–2709. https://doi.org/10.1021/jo802716v.

(81) Herrero-Martínez, J. M.; Repollés, C.; Bosch, E.; Rosés, M.; Ràfols, C. Potentiometric Determination of Aqueous Dissociation Constants of Flavonols Sparingly Soluble in Water. *Talanta* **2008**, *74* (4), 1008–1013. https://doi.org/10.1016/j.talanta.2007.08.007.

(82) Kuntić, V.; Pejić, N.; Mićić, S.; Malešev, D.; Vujić, Z. Determination of Dissociation Constants of Quercetin. *Die Pharmazie* **2003**, *58* (6), 439–440.

(83) Lemańska, K.; Szymusiak, H.; Tyrakowska, B.; Zieliński, R.; Soffers, A. E. M. F.; Rietjens, I. M. C. M. The Influence of PH on Antioxidant Properties and the Mechanism of Antioxidant Action of Hydroxyflavones. *Free Rad. Biol. Med.* **2001**, *31* (7), 869–881. https://doi.org/10.1016/S0891-5849(01)00638-4.

(84) Álvarez-Diduk, R.; Ramírez-Silva, M. T.; Galano, A.; Merkoçi, A. Deprotonation Mechanism and Acidity Constants in Aqueous Solution of Flavonols: A Combined Experimental and Theoretical Study. *J. Phys. Chem. B* **2013**, *117* (41), 12347–12359. https://doi.org/10.1021/jp4049617.

(85) Milane, H. A.; Ubeaud, G.; Vandamme, T. F.; Jung, L. Isolation of Quercetin's Salts and Studies of Their Physicochemical Properties and Antioxidant Relationships. *Bioorg. Med. Chem.* **2004**, *12* (13), 3627–3635. https://doi.org/10.1016/j.bmc.2004.04.028.

(86) Protsenko, I. O.; Bulavin, L. A.; Hovorun, D. M. Investigation of Structural Properties of Quercetin by Quantum Chemistry Methods. *WDS'10 Proceedings of Contributed Papers 4* **2010**.

(87) Brovarets', O. O.; Hovorun, D. M. Intramolecular Tautomerization of the Quercetin Molecule Due to the Proton Transfer: QM Computational Study. *PLoS ONE* **2019**, *14* (11), e0224762. https://doi.org/10.1371/journal.pone.0224762.

(88) Barvinchenko, V. N.; Lipkovskaya, N. A.; Fedyanina, T. V. Keto-Enol Tautomerization of Quercetin in Solutions of a Cationic Surfactant, Miramistin. *Colloid J.* **2014**, *76* (1), 1–5. https://doi.org/10.1134/S1061933X13060021.

(89) Ishiguchi, T.; Takahashi, S. Safety of Gadoterate Meglumine (Gd-DOTA) as a Contrast Agent for Magnetic Resonance Imaging. *Drugs R D* **2010**, 13.

(90) Kheirandish, F.; Delfan, B.; Mahmoudvand, H.; Moradi, N.; Ezatpour, B.; Ebrahimzadeh, F.; Rashidipour, M. Antileishmanial, Antioxidant, and Cytotoxic Activities of Quercus Infectoria Olivier Extract. *Biomed. Pharmacother.* **2016**, *82*, 208–215. https://doi.org/10.1016/j.biopha.2016.04.040.

(91) Plungian, M. B. Solubilization of Rutin with Methyl Glucamine. 2,451,772, October 19, **1948**.

(92) Veronesi, Paolo. A. Water Soluble Salts of an NSAID with Meglumine/Glucamine. 4,748,174, **1988**.

(93) Grove, C.; Liebenberg, W.; Du Preez, J.; Yang, W.; de Villiers, M. M. Improving the Aqueous Solubility of Triclosan by Solubilization, Complexation and in Situ Salt Formation. *J. Cosmet. Sci.* **2003**, *54*, 537–550.

(94) Gupta, P.; Bansal, A. K. Ternary Amorphous Composites of Celecoxib, Poly(Vinyl Pyrrolidone) and Meglumine with Enhanced Solubility. **2005**, 8.

(95) Aloisio, C.; Gomes de Oliveira, A.; Longhi, M. Characterization, Inclusion Mode, Phase-Solubility and *in Vitro* Release Studies of Inclusion Binary Complexes with Cyclodextrins and Meglumine Using Sulfamerazine as Model Drug. *Drug Dev. Indus. Pharm.* **2014**, *40* (7), 919–928. https://doi.org/10.3109/03639045.2013.790408.

(96) Aloisio, C.; de Oliveira, A. G.; Longhi, M. Solubility and Release Modulation Effect of Sulfamerazine Ternary Complexes with Cyclodextrins and Meglumine. *J. Pharm. Biomed. Anal.* **2014**, *100*, 64–73. https://doi.org/10.1016/j.jpba.2014.07.008.

(97) Aloisio, C.; G. de Oliveira, A.; Longhi, M. Cyclodextrin and Meglumine-Based Microemulsions as a Poorly Water-Soluble Drug Delivery System. *J. Pharm. Sci.* **2016**, *105* (9), 2703–2711. https://doi.org/10.1016/j.xphs.2015.11.045.

(98) He, X.; Wei, Y.; Wang, S.; Zhang, J.; Gao, Y.; Qian, S.; Pang, Z.; Heng, W. Improved Pharmaceutical Properties of Honokiol via Salification with Meglumine: An Exception to Oft-Quoted ΔpK$_a$ Rule. *Pharm. Res.* **2022**, *39* (9), 2263–2276. https://doi.org/10.1007/s11095-022-03335-6.

(99) Basavaraj, S.; Sihorkar, V.; Shantha Kumar, T. R.; Sundaramurthi, P.; Srinivas, N. R.; Venkatesh, P.; Ramesh, M.; Kumar Singh, S. Bioavailability Enhancement of Poorly Water Soluble and Weakly Acidic New Chemical Entity with 2-Hydroxy Propyl-β-Cyclodextrin: Selection of Meglumine, a Polyhydroxy Base, as a Novel Ternary Component. *Pharm. Dev. Technol.* **2006**, *11* (4), 443–451. https://doi.org/10.1080/10837450600770577.

(100) Frézard, F.; Martins, P. S.; Bahia, A. P. C. O.; Le Moyec, L.; de Melo, A. L.; Pimenta, A. M. C.; Salerno, M.; Silva, J. B. B. da; Demicheli, C. Enhanced Oral Delivery of Antimony from Meglumine Antimoniate/β-Cyclodextrin Nanoassemblies. *Int. J. Pharm.* **2008**, *347* (1–2), 102–108. https://doi.org/10.1016/j.ijpharm.2007.06.029.

(101) Li, H.; Ma, L.; Li, X.; Cui, X.; Yang, W.; Shen, S.; Chen, M. A Simple and Effective Method to Improve Bioavailability of Glimepiride by Utilizing Hydrotropy Technique. *Eur. J. Pharm. Sci.* **2015**, *77*, 154–160. https://doi.org/10.1016/j.ejps.2015.06.016.

(102) Degot, P.; Funkner, D.; Huber, V.; Köglmaier, M.; Touraud, D.; Kunz, W. Extraction of Curcumin from Curcuma Longa Using Meglumine and Pyroglutamic Acid, Respectively, as Solubilizer and Hydrotrope. *J. Mol. Liq.* **2021**, *334*, 116478. https://doi.org/10.1016/j.molliq.2021.116478.

(103) Guo, R.-Y.; An, Z.-M.; Mo, L.-P.; Wang, R.-Z.; Liu, H.-X.; Wang, S.-X.; Zhang, Z.-H. Meglumine: A Novel and Efficient Catalyst for One-Pot, Three-Component Combinatorial Synthesis of Functionalized 2-Amino-4H-pyrans. *ACS Comb. Sci.* **2013**, 7.

(104) Nemallapudi, B. R.; Zyryanov, G. V.; Avula, B.; Guda, M. R.; Cirandur, S. R.; Venkataramaiah, C.; Rajendra, W.; Gundala, S. Meglumine as a Green, Efficient and Reusable Catalyst for Synthesis and Molecular Docking Studies of Bis(Indolyl)Methanes as Antioxidant Agents. *Bioorg. Chem.* **2019**, *87*, 465–473. https://doi.org/10.1016/j.bioorg.2019.03.005.

(105) Sravya, G.; Suresh, G.; Zyryanov, G. V.; Balakrishna, A.; Madhu Kumar Reddy, K.; Suresh Reddy, C.; Venkataramaiah, C.; Rajendra, W.; Bakthavatchala Reddy, N. A Meglumine Catalyst–Based Synthesis, Molecular Docking, and Antioxidant Studies of Dihydropyrano[3, 2- *B*]Chromenedione Derivatives. *J. Heterocycl. Chem.* **2020**, *57* (1), 355–369. https://doi.org/10.1002/jhet.3786.

(106) Manley, K.; Bravo-Nuevo, A.; Minton, A. R.; Sedano, S.; Marcy, A.; Reichman, M.; Tobia, A.; Artlett, C. M.; Gilmour, S. K.; Laury-Kleintop, L. D.; Prendergast, G. C. Preclinical Study of the Long-Range Safety and Anti-Inflammatory Effects of High-Dose Oral Meglumine. *J. Cell. Biochem.* **2019**. https://doi.org/10.1002/jcb.28492.

(107) Gay, C. A.; Gebicki, J. M. Perchloric Acid Enhances Sensitivity and Reproducibility of the Ferric–Xylenol Orange Peroxide Assay. *Anal. Biochem.* **2002**, *304* (1), 42–46. https://doi.org/10.1006/abio.2001.5566.

(108) Klamt, A. Conductor-like Screening Model for Real Solvents: A New Approach to the Quantitative Calculation of Solvation Phenomena. *J. Phys. Chem.* **1995**, *99* (7), 2224–2235. https://doi.org/10.1021/j100007a062.

(109) Klamt, A.; Eckert, F.; Diedenhofen, M.; Beck, M. E. First Principles Calculations of Aqueous pK_a Values for Organic and Inorganic Acids Using COSMO−RS Reveal an Inconsistency in the Slope of the pK_a Scale. *J. Phys. Chem. A* **2003**, *107* (44), 9380–9386. https://doi.org/10.1021/jp034688o.

(110) Eckert, F.; Diedenhofen, M.; Klamt, A. Towards a First Principles Prediction of pK_a: COSMO-RS and the Cluster-Continuum Approach. *Mol. Phys.* **2010**, *108* (3–4), 229–241. https://doi.org/10.1080/00268970903313667.

(111) Gao, Y.; Wang, Y.; Ma, Y.; Yu, A.; Cai, F.; Shao, W.; Zhai, G. Formulation Optimization and in Situ Absorption in Rat Intestinal Tract of Quercetin-Loaded Microemulsion. *Colloids Surf. B* **2009**, *71* (2), 306–314. https://doi.org/10.1016/j.colsurfb.2009.03.005.

(112) Cao, X.-J.; Sun, C.-R.; Pan, Y.-J. The Complex of Flunixin and Meglumine. *Acta Crystallogr. E Struct. Rep. Online* **2003**, *59* (10), o1471–o1473. https://doi.org/10.1107/S1600536803019470.

(113) Cassimiro, D. L.; Kobelnik, M.; Ribeiro, C. A.; Crespi, M. S.; Boralle, N. Structural Aspects, Thermal Behavior, and Stability of a Self-Assembled Supramolecular Polymer Derived from Flunixin–Meglumine Supramolecular Adducts. *Thermochimica Acta* **2012**, *529*, 59–67. https://doi.org/10.1016/j.tca.2011.11.030.

(114) Ferreira, L. M. B.; Kurokawa, S. S. S.; Alonso, J. D.; Cassimiro, D. L.; Souza, A. L. R. de; Fonseca, M.; Sarmento, V. H. V.; Regasini, L. O.; Ribeiro, C. A. Structural and Thermal Behavior of Meglumine-Based Supra-Amphiphiles in Bulk and Assembled in Water. *Langmuir* **2016**, *32* (45), 11878–11887. https://doi.org/10.1021/acs.langmuir.6b03176.

(115) Cassimiro, D. L.; Ferreira, L. M. B.; de Souza, A. L. R.; Fonseca, M.; Kurokawa, S. S. S.; Alonso, J. D.; Sarmento, V. H. V.; Ribeiro, C. A. On the Influence of Fatty Acid Chain Unsaturation on Supramolecular Gelation of Aminocarbohydrate-Based Supra-Amphiphiles. *J. Therm. Anal. Calorim.* **2018**, *134* (3), 1599–1609. https://doi.org/10.1007/s10973-018-7333-5.

(116) Cruz-Cabeza, A. J. Acid–Base Crystalline Complexes and the PKa Rule. *Cryst. Eng. Commun.* **2012**, *14* (20), 6362. https://doi.org/10.1039/c2ce26055g.

(117) Gerhäuser, C.; Frank, N. Xanthohumol, a New All-Rounder? *Mol. Nutr. Food Res.* **2005**, *49* (9), 821–823. https://doi.org/10.1002/mnfr.200590033.

(118) Arczewska, M.; Kamiński, D. M.; Gieroba, B.; Gagoś, M. Acid–Base Properties of Xanthohumol: A Computational and Experimental Investigation. *J. Nat. Prod.* **2017**, *80* (12), 3194–3202. https://doi.org/10.1021/acs.jnatprod.7b00530.

(119) Eslami, A. C.; Pasanphan, W.; Wagner, B. A.; Buettner, G. R. Free Radicals Produced by the Oxidation of Gallic Acid: An Electron Paramagnetic Resonance Study. *Chem.Cent. J.* **2010**, *4* (1), 15. https://doi.org/10.1186/1752-153X-4-15.

(120) Bernabé-Pineda, M.; Ramírez-Silva, M. T.; Romero-Romo, M.; González-Vergara, E.; Rojas-Hernández, A. Determination of Acidity Constants of Curcumin in Aqueous Solution and Apparent Rate Constant of Its Decomposition. *Spectrochim. Acta A* **2004**, *60* (5), 1091–1097. https://doi.org/10.1016/S1386-1425(03)00342-1.

(121) Priyadarsini, K. The Chemistry of Curcumin: From Extraction to Therapeutic Agent. *Molecules* **2014**, *19* (12), 20091–20112. https://doi.org/10.3390/molecules191220091.

(122) Jennings, M. L.; Solomon, A. K. Interaction between Phloretin and the Red Blood Cell Membrane. *J. Gen. Physiol.* **1976**, *67* (4), 381–397. https://doi.org/10.1085/jgp.67.4.381.

(123) Kron, I.; Pudychová-Chovanová, Z.; Veliká, B.; Guzy, J.; Perjési, P. (E)-2-Benzylidenebenzocyclanones, Part VIII: Spectrophotometric Determination of PK a Values of Some Natural and Synthetic Chalcones and Their Cyclic Analogues. *Monatsh. Chem.* **2012**, *143* (1), 13–17. https://doi.org/10.1007/s00706-011-0633-0.

(124) López-Nicolás, J. M.; García-Carmona, F. Aggregation State and p *K* $_a$ Values of (*E*)-Resveratrol As Determined by Fluorescence Spectroscopy and UV−Visible

Absorption. *J. Agric. Food Chem.* **2008**, *56* (17), 7600–7605. https://doi.org/10.1021/jf800843e.

(125) Zimányi, L.; Thekkan, S.; Eckert, B.; Condren, A. R.; Dmitrenko, O.; Kuhn, L. R.; Alabugin, I. V.; Saltiel, J. Determination of the p K_a Values of *Trans* -Resveratrol, a Triphenolic Stilbene, by Singular Value Decomposition. Comparison with Theory. *J. Phys. Chem. A* **2020**, *124* (31), 6294–6302. https://doi.org/10.1021/acs.jpca.0c04792.

(126) Degot, P. Solubilization and Extraction of Curcumin from Curcuma Longa Using Green, Sustainable, and Food-Approved Surfactant-Free Microemulsions. *Food Chem.* **2021**, 8.

(127) Mehringer, J.; Do, T.-M.; Touraud, D.; Hohenschutz, M.; Khoshsima, A.; Horinek, D.; Kunz, W. Hofmeister versus Neuberg: Is ATP Really a Biological Hydrotrope? *Cell Rep. Phys. Sci.* **2021**, *2* (2), 100343. https://doi.org/10.1016/j.xcrp.2021.100343.

(128) Mehringer, J. Stability of Proteins in the Presence of Anionic Additives, Universität Regensburg, **2021**.

(129) Pan, K.; Luo, Y.; Gan, Y.; Baek, S. J.; Zhong, Q. PH-Driven Encapsulation of Curcumin in Self-Assembled Casein Nanoparticles for Enhanced Dispersibility and Bioactivity. *Soft Matter* **2014**, *10* (35), 6820. https://doi.org/10.1039/C4SM00239C.

(130) Peng, S.; Zou, L.; Zhou, W.; Liu, W.; Liu, C.; McClements, D. J. Encapsulation of Lipophilic Polyphenols into Nanoliposomes Using PH-Driven Method: Advantages and Disadvantages. *J. Agric. Food Chem.* **2019**, *67* (26), 7506–7511. https://doi.org/10.1021/acs.jafc.9b01602.

(131) Bozzuto, G.; Molinari, A. Liposomes as Nanomedical Devices. *Int. J. Nanomed.* **2015**, 975. https://doi.org/10.2147/IJN.S68861.

(132) Sercombe, L.; Veerati, T.; Moheimani, F.; Wu, S. Y.; Sood, A. K.; Hua, S. Advances and Challenges of Liposome Assisted Drug Delivery. *Front. Pharmacol.* **2015**, *6*. https://doi.org/10.3389/fphar.2015.00286.

(133) Nsairat, H.; Khater, D.; Sayed, U.; Odeh, F.; Al Bawab, A.; Alshaer, W. Liposomes: Structure, Composition, Types, and Clinical Applications. *Heliyon* **2022**, *8* (5), e09394. https://doi.org/10.1016/j.heliyon.2022.e09394.

(134) Bulbake, U.; Doppalapudi, S.; Kommineni, N.; Khan, W. Liposomal Formulations in Clinical Use: An Updated Review. *Pharmaceutics* **2017**, *9* (4), 12. https://doi.org/10.3390/pharmaceutics9020012.

(135) Olusanya, T.; Haj Ahmad, R.; Ibegbu, D.; Smith, J.; Elkordy, A. Liposomal Drug Delivery Systems and Anticancer Drugs. *Molecules* **2018**, *23* (4), 907. https://doi.org/10.3390/molecules23040907.

(136) Sultana, F.; Neog, M. K.; Rasool, M. Targeted Delivery of Morin, a Dietary Bioflavanol Encapsulated Mannosylated Liposomes to the Macrophages of Adjuvant-Induced Arthritis Rats Inhibits Inflammatory Immune Response and Osteoclastogenesis.

Eur. J. Pharma. Biopharma. **2017**, *115*, 229–242. https://doi.org/10.1016/j.ejpb.2017.03.009.

(137) Tran, H.-M.; Yang, C.-Y.; Wu, T.-H.; Yen, F.-L. Liposomes Encapsulating Morin: Investigation of Physicochemical Properties, Dermal Absorption Improvement and Anti-Aging Activity in PM-Induced Keratinocytes. *Antioxidants* **2022**, *11* (6), 1183. https://doi.org/10.3390/antiox11061183.

(138) Mandal, A. K.; Sinha, J.; Mandal, S.; Mukhopadhyay, S.; Das, N. Targeting of Liposomal Flavonoid to Liver in Combating Hepatocellular Oxidative Damage. *Drug Delivery* **2002**, *9* (3), 181–185. https://doi.org/10.1080/15227950290097615.

(139) Ferreira-Silva, M.; Faria-Silva, C.; Carvalheiro, M. C.; Simões, S.; Marinho, H. S.; Marcelino, P.; Campos, M. C.; Metselaar, J. M.; Fernandes, E.; Baptista, P. V.; Fernandes, A. R.; Corvo, M. L. Quercetin Liposomal Nanoformulation for Ischemia and Reperfusion Injury Treatment. *Pharmaceutics* **2022**, *14* (1), 104. https://doi.org/10.3390/pharmaceutics14010104.

(140) Gang, W.; Jie, W. J.; Ping, Z. L.; Ming, D. S.; Ying, L. J.; Lei, W.; Fang, Y. Liposomal Quercetin: Evaluating Drug Delivery *in Vitro* and Biodistribution *in Vivo*. *Expert Opin. Drug Deliv.* **2012**, *9* (6), 599–613. https://doi.org/10.1517/17425247.2012.679926.

(141) Cheng, C.; Peng, S.; Li, Z.; Zou, L.; Liu, W.; Liu, C. Improved Bioavailability of Curcumin in Liposomes Prepared Using a PH-Driven, Organic Solvent-Free, Easily Scalable Process. *RSC Adv.* **2017**, *7* (42), 25978–25986. https://doi.org/10.1039/C7RA02861J.

(142) Edwards, K. A.; Curtis, K. L.; Sailor, J. L.; Baeumner, A. J. Universal Liposomes: Preparation and Usage for the Detection of MRNA. *Anal. Bioanal. Chem.* **2008**, *391* (5), 1689–1702. https://doi.org/10.1007/s00216-008-1992-1.

(143) Rink, S.; Kaiser, B.; Steiner, M.-S.; Duerkop, A.; Baeumner, A. J. Highly Sensitive Interleukin 6 Detection by Employing Commercially Ready Liposomes in an LFA Format. *Anal. Bioanal. Chem.* **2022**, *414* (10), 3231–3241. https://doi.org/10.1007/s00216-021-03750-5.

(144) Peng, S.; Li, Z.; Zou, L.; Liu, W.; Liu, C.; McClements, D. J. Improving Curcumin Solubility and Bioavailability by Encapsulation in Saponin-Coated Curcumin Nanoparticles Prepared Using a Simple PH-Driven Loading Method. *Food Funct.* **2018**, *9* (3), 1829–1839. https://doi.org/10.1039/C7FO01814B.

(145) Arvand, M.; Anvari, M. A Graphene-Based Electrochemical Sensor for Sensitive Detection of Quercetin in Foods. *J. Iran. Chem. Soc.* **2013**, *10* (5), 841–849. https://doi.org/10.1007/s13738-013-0219-3.

(146) Singh, G.; Maurya, S.; deLampasona, M. P.; Catalan, C. A. N. A Comparison of Chemical, Antioxidant and Antimicrobial Studies of Cinnamon Leaf and Bark Volatile Oils, Oleoresins and Their Constituents. *Food Chem. Toxicol.* **2007**, *45* (9), 1650–1661. https://doi.org/10.1016/j.fct.2007.02.031.

(147) Huang, B.; Yuan, H. D.; Kim, D. Y.; Quan, H. Y.; Chung, S. H. Cinnamaldehyde Prevents Adipocyte Differentiation and Adipogenesis via Regulation of Peroxisome Proliferator-Activated Receptor-γ (PPARγ) and AMP-Activated Protein Kinase (AMPK) Pathways. *J. Agric. Food Chem.* **2011**, *59* (8), 3666–3673. https://doi.org/10.1021/jf104814t.

(148) Williamson, E. M. Synergy and Other Interactions in Phytomedicines. *Phytomed.* **2001**, *8* (5), 401–409. https://doi.org/10.1078/0944-7113-00060

(149) Mehringer, J.; Kunz, W. Carl Neuberg's Hydrotropic Appearances (1916). *Adv. Colloid Interface Sci.* **2021**, *294*, 102476. https://doi.org/10.1016/j.cis.2021.102476.

(150) Patel, A.; Malinovska, L.; Saha, S.; Wang, J.; Alberti, S.; Krishnan, Y.; Hyman, A. A. ATP as a Biological Hydrotrope. *Science* **2017**, *356* (6339), 753–756. https://doi.org/10.1126/science.aaf6846.

(151) Zemb, T. N.; Klossek, M.; Lopian, T.; Marcus, J.; Schoettl, S.; Horinek, D.; Prevost, S. F.; Touraud, D.; Diat, O.; Marčelja, S.; Kunz, W. How to Explain Microemulsions Formed by Solvent Mixtures without Conventional Surfactants. *Proc. Natl. Acad. Sci. U.S.A.* **2016**, *113* (16), 4260–4265. https://doi.org/10.1073/pnas.1515708113.

(152) Kunz, W.; Holmberg, K.; Zemb, T. Hydrotropes. *Curr. Opin. Colloid Interface Sci.* **2016**, *22*, 99–107. https://doi.org/10.1016/j.cocis.2016.03.005.

(153) Queste, S.; Michina, Y.; Dewilde, A.; Neueder, R.; Kunz, W.; Aubry, J.-M. Thermophysical and Bionotox Properties of Solvo-Surfactants Based on Ethylene Oxide, Propylene Oxide and Glycerol. *Green Chem.* **2007**, *9* (5), 491. https://doi.org/10.1039/b617852a.

(154) Booth, J. J.; Abbott, S.; Shimizu, S. Mechanism of Hydrophobic Drug Solubilization by Small Molecule Hydrotropes. *J. Phys. Chem. B* **2012**, *116* (51), 14915–14921. https://doi.org/10.1021/jp309819r.

(155) Shimizu, S.; Booth, J. J.; Abbott, S. Hydrotropy: Binding Models vs. Statistical Thermodynamics. *Phys. Chem. Chem. Phys.* **2013**, *15* (47), 20625. https://doi.org/10.1039/c3cp53791a.

(156) Booth, J. J.; Omar, M.; Abbott, S.; Shimizu, S. Hydrotrope Accumulation around the Drug: The Driving Force for Solubilization and Minimum Hydrotrope Concentration for Nicotinamide and Urea. *Phys. Chem. Chem. Phys.* **2015**, *17* (12), 8028–8037. https://doi.org/10.1039/C4CP05414H.

(157) Paul, R.; Chattaraj, K. G.; Paul, S. Role of Hydrotropes in Sparingly Soluble Drug Solubilization: Insight from a Molecular Dynamics Simulation and Experimental Perspectives. *Langmuir* **2021**, *37* (16), 4745–4762. https://doi.org/10.1021/acs.langmuir.1c00169.

(158) Cui, Y.; Xing, C.; Ran, Y. Molecular Dynamics Simulations of Hydrotropic Solubilization and Self-Aggregation of Nicotinamide. *J. Pharm. Sci.* **2010**, *99* (7), 3048–3059. https://doi.org/10.1002/jps.22077.

(159) Mazaud, A. Aqueous Plant Extraction Using Glycerol and Sugar-Based Hydrotropes: Physicochemical Approach and Application to Rosemary, Université de Lille, **2020**.

(160) Saleh, A. M.; El-Khordagui, L. K. Hydrotropic Agents: A New Definition. *Int. J. Pharm.* **1985**, *24* (2–3), 231–238. https://doi.org/10.1016/0378-5173(85)90023-7.

(161) Balasubramanian, D.; Srinivas, V.; Gaikar, V. G.; Sharma, M. M. Aggregation Behavior of Hydrotropic Compounds in Aqueous Solution. *J. Phys. Chem.* **1989**, *93* (9), 3865–3870. https://doi.org/10.1021/j100346a098.

(162) Shimizu, S.; Matubayasi, N. The Origin of Cooperative Solubilisation by Hydrotropes. *Phys. Chem. Chem. Phys.* **2016**, *18* (36), 25621–25628. https://doi.org/10.1039/C6CP04823D.

(163) Abranches, D. O.; Benfica, J.; Soares, B. P.; Leal-Duaso, A.; Sintra, T. E.; Pires, E.; Pinho, S. P.; Shimizu, S.; Coutinho, J. A. P. Unveiling the Mechanism of Hydrotropy: Evidence for Water-Mediated Aggregation of Hydrotropes around the Solute. *Chem. Commun.* **2020**, *56* (52), 7143–7146. https://doi.org/10.1039/D0CC03217D.

(164) Klossek, M. L.; Touraud, D.; Kunz, W. Eco-Solvents – Cluster-Formation, Surfactantless Microemulsions and Facilitated Hydrotropy. *Phys. Chem. Chem. Phys.* **2013**, *15* (26), 10971. https://doi.org/10.1039/c3cp50636c.

(165) Durand, M.; Stoppa, A.; Molinier, V.; Touraud, D.; Aubry, J.-M. Toward the Rationalization of Facilitated Hydrotropy: Investigation with the Ternary Dimethyl Isosorbide / Benzyl Alcohol / Water System. *J. Solution Chem.* **2012**, *41* (3), 555–565. https://doi.org/10.1007/s10953-012-9814-7.

(166) Maheshwari, R.; Jagwani, Y. Mixed Hydrotropy: Novel Science of Solubility Enhancement. *Indian. J. Pharm. Sci.* **2011**, *73* (2), 179. https://doi.org/10.4103/0250-474X.91585.

(167) Madan, J.; Pawar, K.; Dua, K. Solubility Enhancement Studies on Lurasidone Hydrochloride Using Mixed Hydrotropy. *Int. J. Pharm. Investig.* **2015**, *5* (2), 114. https://doi.org/10.4103/2230-973X.153390.

(168) Jain, R.; Jain, N.; Jain, D. K.; Patel, V. K.; Rajak, H.; Jain, S. K. Novel UV Spectrophotometer Methods for Quantitative Estimation of Metronidazole and Furazolidone Using Mixed Hydrotropy Solubilization. *Arab. J. Chem.* **2017**, *10* (2), 151–156. https://doi.org/10.1016/j.arabjc.2013.09.003.

(169) Bauduin, P.; Renoncourt, A.; Kopf, A.; Touraud, D.; Kunz, W. Unified Concept of Solubilization in Water by Hydrotropes and Cosolvents. *Langmuir* **2005**, *21* (15), 6769–6775. https://doi.org/10.1021/la050554l.

(170) Lebeuf, R.; Illous, E.; Dussenne, C.; Molinier, V.; Silva, E. D.; Lemaire, M.; Aubry, J.-M. Solvo-Surfactant Properties of Dialkyl Glycerol Ethers: Application as Eco-Friendly Extractants of Plant Material through a Novel Hydrotropic Cloud Point Extraction (HCPE) Process. *ACS Sustainable Chem. Eng.* **2016**, *4* (9), 4815–4823. https://doi.org/10.1021/acssuschemeng.6b01101.

(171) Moity, L.; Shi, Y.; Molinier, V.; Dayoub, W.; Lemaire, M.; Aubry, J.-M. Hydrotropic Properties of Alkyl and Aryl Glycerol Monoethers. *J. Phys. Chem. B* **2013**, *117* (31), 9262–9272. https://doi.org/10.1021/jp403347u.

(172) Matero, A.; Mattsson, Å.; Svensson, M. Alkyl Polyglucosides as Hydrotropes. *J. Surfactants Deterg.* **1998**, *1* (4), 485–489. https://doi.org/10.1007/s11743-998-0046-y.

(173) Zhu, Y.; Durand, M.; Molinier, V.; Aubry, J.-M. Isosorbide as a Novel Polar Head Derived from Renewable Resources. Application to the Design of Short-Chain Amphiphiles with Hydrotropic Properties. *Green Chem.* **2008**, *10* (5), 532. https://doi.org/10.1039/b717203f.

(174) Durand, M.; Zhu, Y.; Molinier, V.; Féron, T.; Aubry, J.-M. Solubilizing and Hydrotropic Properties of Isosorbide Monoalkyl- and Dimethyl-Ethers. *J. Surfactants Deterg.* **2009**, *12* (4), 371–378. https://doi.org/10.1007/s11743-009-1128-4.

(175) Herbinski, A.; Métay, E.; Da Silva, E.; Illous, E.; Aubry, J.-M.; Lemaire, M. An Eco-Compatible Pathway to New Hydrotropes from Tetraols. *Green Chem.* **2018**, *20* (6), 1250–1261. https://doi.org/10.1039/C7GC02990J.

(176) Estrine, B.; Marinkovic, S.; Jérome, F. Synthesis of Alkyl Polyglycosides From Glucose and Xylose for Biobased Surfactants: Synthesis, Properties, and Applications. In *Biobased Surfactants*; Elsevier, 2019; pp 365–385. https://doi.org/10.1016/B978-0-12-812705-6.00011-3.

(177) Yu, C.; Li, Y.-L.; Liang, M.; Dai, S.-Y.; Ma, L.; Li, W.-G.; Lai, F.; Liu, X.-M. Characteristics and Hazards of the Cinnamaldehyde Oxidation Process. *RSC Adv.* **2020**, *10* (32), 19124–19133. https://doi.org/10.1039/C9RA10820C.

(178) Eckert, F. COSMOtherm Reference Manual.

(179) Kim, J. Y.; Kim, S.; Papp, M.; Park, K.; Pinal, R. Hydrotropic Solubilization of Poorly Water-Soluble Drugs. *J. Pharm. Sci.* **2010**, *99* (9), 3953–3965. https://doi.org/10.1002/jps.22241.

(180) Kim, J. Y.; Kim, S.; Pinal, R.; Park, K. Hydrotropic Polymer Micelles as Versatile Vehicles for Delivery of Poorly Water-Soluble Drugs. *J. Controlled Release* **2011**, *152* (1), 13–20. https://doi.org/10.1016/j.jconrel.2011.02.014.

(181) Qiao, Y.; Zhao, J.; Yue, X.; Zhang, Y.; Zhang, R.; Xu, Y.; Tang, X.; Liu, X.; Wang, Q. Study on Pharmacokinetics and Bioequivalence of Vonoprazan Pyroglutamate in Rats by Liquid Chromatography with Tandem Mass Spectrometry. *J. Chromatogr. B* **2017**, *1059*, 56–65. https://doi.org/10.1016/j.jchromb.2017.05.013.

(182) Mascitti, V.; Maurer, T. S.; Robinson, R. P.; Bian, J.; Boustany-Kari, C. M.; Brandt, T.; Collman, B. M.; Kalgutkar, A. S.; Klenotic, M. K.; Leininger, M. T.; Lowe, A.; Maguire, R. J.; Masterson, V. M.; Miao, Z.; Mukaiyama, E.; Patel, J. D.; Pettersen, J. C.; Préville, C.; Samas, B.; She, L.; Sobol, Z.; Steppan, C. M.; Stevens, B. D.; Thuma, B. A.; Tugnait, M.; Zeng, D.; Zhu, T. Discovery of a Clinical Candidate from the Structurally Unique Dioxa-Bicyclo[3.2.1]Octane Class of Sodium-Dependent Glucose Cotransporter 2 Inhibitors. *J. Med. Chem.* **2011**, *54* (8), 2952–2960. https://doi.org/10.1021/jm200049r.

(183) Chen, J.-R.; Shinal, E. C. Water-Soluble Formulations of m-AMSA with Pyroglutamic Acid. US4575509, March 11, **1986**.

(184) Youn, Y. S.; Cho, S. H.; Park, C. S.; Kim, Y. C.; Lim, D. K.; Jung, S. H.; Lee, S. H.; Kang, H. S. Pyroglutamic Acid Salt of Amlodipine. EP1391453A1, February 25, **2004**.

(185) Molino, M. Creatine Pyroglutamic Acid Salts and Methods for Their Production and Use in Individuals. WO2008/031184, March 20, **2008**.

(186) Fiege, H.; Voges, H.-W.; Hamamoto, T.; Umemura, S.; Iwata, T.; Miki, H.; Fujita, Y.; Buysch, H.-J.; Garbe, D.; Paulus, W. Phenol Derivatives. In *Ullmann's Encyclopedia of Industrial Chemistry*; Wiley-VCH Verlag GmbH & Co. KGaA, Ed.; Wiley-VCH Verlag GmbH & Co. KGaA: Weinheim, Germany, 2000; p a19_313. https://doi.org/10.1002/14356007.a19_313.

(187) Cheng, S.; Tang, H.; Yan, H. Effects of Multiple Weak Interactions on the Binding of Phenolic Compounds by Polymeric Adsorbents. *J. Appl. Polym. Sci.* **2006**, *102* (5), 4652–4658. https://doi.org/10.1002/app.24702.

(188) Arnould, A.; Cousin, F.; Chabas, L.; Fameau, A.-L. Impact of the Molar Ratio and the Nature of the Counter-Ion on the Self-Assembly of Myristic Acid. *J. Colloid Interface Sci.* **2018**, *510*, 133–141. https://doi.org/10.1016/j.jcis.2017.09.058.

(189) Wolfrum, S.; Marcus, J.; Touraud, D.; Kunz, W. A Renaissance of Soaps? — How to Make Clear and Stable Solutions at Neutral PH and Room Temperature. *Adv. Colloid Interface Sci.* **2016**, *236*, 28–42.

(190) McBain, J. W.; Sierichs, W. C. The Solubility of Sodium and Potassium Soaps and the Phase Diagrams of Aqueous Potassium Soaps. *J. Am. Oil Chem. Soc.* **1948**, *25* (6), 221–225. https://doi.org/10.1007/BF02645899.

(191) Lin, B.; McCormick, A. V.; Davis, H. T.; Strey, R. Solubility of Sodium Soaps in Aqueous Salt Solutions. *J. Colloid Interface Sci.* **2005**, *291* (2), 543–549. https://doi.org/10.1016/j.jcis.2005.05.036.

(192) Johansson, I.; Svensson, M. Surfactants Based on Fatty Acids and Other Natural Hydrophobes. *Curr. Opin. Colloid Interface Sci.* **2001**, *6* (2), 178–188. https://doi.org/10.1016/S1359-0294(01)00076-0.

(193) Kunieda, H.; Shinoda, K. Krafft Points, Critical Micelle Concentrations, Surface Tension, and Solubilizing Power of Aqueous Solutions of Fluorinated Surfactants. *J. Phys. Chem.* **1976**, *80* (22), 2468–2470. https://doi.org/10.1021/j100563a007.

(194) Yu, Z.; Zhang, X.; Xu, G.; Zhao, G. Physicochemical Properties of Aqueous Mixtures of Tetrabutylammonium Bromide and Anionic Surfactants. 3. Effects of Surfactant Chain Length and Salinity. *J. Phys. Chem.* **1990**, *94*, 3675–3681.

(195) Zana, R. Partial Phase Behavior and Micellar Properties of Tetrabutylammonium Salts of Fatty Acids: Unusual Solubility in Water and Formation of Unexpectedly Small Micelles. *Langmuir* **2004**, *20* (14), 5666–5668. https://doi.org/10.1021/la040033i.

(196) Klein, R.; Touraud, D.; Kunz, W. Choline Carboxylate Surfactants: Biocompatible and Highly Soluble in Water. *Green Chem.* **2008**, *10* (4), 433. https://doi.org/10.1039/b718466b.

(197) Klein, R.; Kellermeier, M.; Drechsler, M.; Touraud, D.; Kunz, W. Solubilisation of Stearic Acid by the Organic Base Choline Hydroxide. *Colloids Surf. A* **2009**, *338* (1–3), 129–134. https://doi.org/10.1016/j.colsurfa.2008.04.049.

(198) Klein, R.; Kellermeier, M.; Touraud, D.; Müller, E.; Kunz, W. Choline Alkylsulfates – New Promising Green Surfactants. *J. Colloid Interface Sci.* **2013**, *392*, 274–280. https://doi.org/10.1016/j.jcis.2012.10.003.

(199) Klein, R.; Müller, E.; Kraus, B.; Brunner, G.; Estrine, B.; Touraud, D.; Heilmann, J.; Kellermeier, M.; Kunz, W. Biodegradability and Cytotoxicity of Choline Soaps on Human Cell Lines: Effects of Chain Length and the Cation. *RSC Adv.* **2013**, *3* (45), 23347. https://doi.org/10.1039/c3ra42812e.

(200) Bernstein, M.; Bognolo, G.; Clark, P. E.; Driedger, A.; Farn, R. J.; Gadberry, J. F.; Gecol, H.; Hattori, Y.; Hepworth, P.; Hibbs, J.; Houston, J.; Issa, J.; Karsa, D. R.; Otterson, R., Schmiedel, P.; Slater, P. J.; Thomas, R. R.; von Rybinski, W. *Chemistry and Technology of Surfactants*. Farn, R. J., Blackwell. **2006**.

(201) Myers, D. *Surfactant Science and Technology*, 3rd ed.; J. Wiley: Hoboken, N.J, **2006**.

(202) *Handbook of Applied Surface and Colloid Chemistry*; Holmberg, K., Shah, D. O., Schwuger, M. J., Eds.; Wiley: Chichester, England ; New York, 2002.

(203) Petigny, L.; Özel, M. Z.; Périno, S.; Wajsman, J.; Chemat, F. Water as Green Solvent for Extraction of Natural Products. In *Green Extraction of Natural Products*; Chemat, F., Strube, J., Eds.; Wiley-VCH Verlag GmbH & Co. KGaA: Weinheim, Germany, 2015; pp 237–264. https://doi.org/10.1002/9783527676828.ch7.

(204) Evans, D. F. Self-Organization of Amphiphiles. *Langmuir* **1988**, *4* (1), 3–12. https://doi.org/10.1021/la00079a002.

(205) Kronberg, B.; Castas, M.; Silvestonti, R. Understanding the Hydrophobic Effect *J. Dispers. Sci. Technol.* **1994**, *15* (3), 333–351. https://doi.org/10.1080/01932699408943561.

(206) Shinoda, K. "Iceberg" Formation and Solubility. *J. Phys. Chem.* **1977**, *81* (13), 1300–1302. https://doi.org/10.1021/j100528a016.

(207) Wolfrum, S. Long Chain Soaps and Alkyl Sulfates in Aqueous Solutions at Room Temperature, Universität Regensburg, **2017**.

(208) Israelachvili, J. N.; Mitchell, D. J.; Ninham, B. W. Theory of Self-Assembly of Hydrocarbon Amphiphiles into Micelles and Bilayers. *J. Chem. Soc., Faraday Trans. 2* **1976**, *72*, 1525. https://doi.org/10.1039/f29767201525.

(209) Brown, R. XXVII. A Brief Account of Microscopical Observations Made in the Months of June, July and August 1827, on the Particles Contained in the Pollen of Plants;

and on the General Existence of Active Molecules in Organic and Inorganic Bodies. *The Philosophical Magazine* **1828**, *4* (21), 161–173. https://doi.org/10.1080/14786442808674769.

(210) *Prof Steven Abbott. Cloud and Krafft points | Practical Surfactants Science.* https://www.stevenabbott.co.uk/practical-surfactants/cloud-krafft.php (accessed 2023-09-24).

(211) Ramsden, W. Separation of Solids in the Surface-Layers of Solutions and ‘Suspensions’ (Observations on Surface-Membranes, Bubbles, Emulsions, and Mechanical Coagulation).—Preliminary Account. *Proc. R. Soc. Lond.* **1904**, *72* (477–486), 156–164. https://doi.org/10.1098/rspl.1903.0034.

(212) Pickering, S. U. CXCVI.—Emulsions. *J. Chem. Soc., Trans.* **1907**, *91* (0), 2001–2021. https://doi.org/10.1039/CT9079102001.

(213) Ostwald, Wa. Beiträge zur Kenntnis der Emulsionen. *Zeitschr. Chem. Ind. Kolloide* **1910**, *6* (2), 103–109. https://doi.org/10.1007/BF01465754.

(214) Bancroft, W. D. The Theory of Emulsification, V. *J. Phys. Chem.* **1913**, *17* (6), 501–519.

(215) Bancroft, W. D. The Theory of Emulsification, VI. *J. Phys. Chem.* **1915**, *19* (4), 275–309. https://doi.org/10.1021/j150157a002.

(216) Griffin, W. C. Classification of Surface-Active Agents by “HLB. *J. Soc. Cosmet. Chem.* **1949**, *1* (5), 311–326.

(217) Davies, J. T. A Quantitative Kinetic Theory of Emulsion Type. I. Physical Chemistry of the Emuslifying Agent. In *Gas/Liquid and Liquid/Liquid Interfaces.* 2nd Int. Cong. of Surface Activity, Butterworths, London, **1957**.

(218) Winsor, P. A. Hydrotropy, Solubilisation and Related Emulsification Processes. *Trans. Faraday Soc.* **1948**, *44*, 376. https://doi.org/10.1039/tf9484400376.

(219) Salager, J. L.; Morgan, J. C.; Schechter, R. S.; Wade, W. H.; Vasquez, E. Optimum Formulation of Surfactant/Water/Oil Systems for Minimum Interfacial Tension or Phase Behavior. *Soc. Pet. Eng.* **1979**, *19* (02), 107–115. https://doi.org/10.2118/7054-PA.

(220) Shinoda, K.; Arai, H. The Correlation between Phase Inversion Temperature In Emulsion and Cloud Point in Solution of Nonionic Emulsifier. *J. Phys. Chem.* **1964**, *68* (12), 3485–3490. https://doi.org/10.1021/j100794a007.

(221) Ontiveros, J. F.; Pierlot, C.; Catté, M.; Molinier, V.; Salager, J.-L.; Aubry, J.-M. A Simple Method to Assess the Hydrophilic Lipophilic Balance of Food and Cosmetic Surfactants Using the Phase Inversion Temperature of C10E4/n-Octane/Water Emulsions. *Colloids Surf. A* **2014**, *458*, 32–39. https://doi.org/10.1016/j.colsurfa.2014.02.058.

(222) Landeck, L.; Baden, L. A.; John, S.-M. Detergents. In *Kanerva’s Occupational Dermatology*; Rustemeyer, T., Elsner, P., John, S.-M., Maibach, H. I., Eds.; Springer: Berlin, Heidelberg, 2012; pp 847–857. https://doi.org/10.1007/978-3-642-02035-3_75.

(223) Miles, G. D.; Ross, J. Foam Stability of Solutions of Soaps of Pure Fatty Acids. *J. Phys. Chem.* **1944**, *48* (5), 280–290. https://doi.org/10.1021/j150437a006.

(224) Salager, J.-L.; Antón, R.; Andérez, J. M.; Aubry, J.-M. Formulation des microémulsions par la méthode du HLD. *Formulation* **2001**. https://doi.org/10.51257/a-v1-j2157.

(225) Pereira, R. F. P.; Valente, A. J. M.; Fernandes, M.; Burrows, H. D. What Drives the Precipitation of Long-Chain Calcium Carboxylates (Soaps) in Aqueous Solution? *Phys. Chem. Chem. Phys.* **2012**, *14* (20), 7517. https://doi.org/10.1039/c2cp24152h.

(226) Cistola, D. P.; Jackson, D.; Small, D. M. Ionization and Phase Behavior of Fatty Acids in Water: Application of the Gibbs Phase Rulet.

(227) Hirai, A.; Kawasaki, H.; Tanaka, S.; Nemoto, N.; Suzuki, M.; Maeda, H. Effects of L-Arginine on Aggregates of Fatty-Acid/Potassium Soap in the Aqueous Media. *Colloid Polym. Sci.* **2006**, *284* (5), 520–528. https://doi.org/10.1007/s00396-005-1423-1.

(228) Kunz, W.; Henle, J.; Ninham, B. W. 'Zur Lehre von der Wirkung der Salze' (about the Science of the Effect of Salts): Franz Hofmeister's Historical Papers. *Curr. Opin. Colloid Interface Sci.* **2004**, *9* (1–2), 19–37. https://doi.org/10.1016/j.cocis.2004.05.005.

(229) Kunz, W.; Neueder, R. An Attempt of a General Overview. In *Specific Ion Effects*; WORLD SCIENTIFIC, 2009; pp 3–54. https://doi.org/10.1142/9789814271585_0001.

(230) Kunz, W. Specific Ion Effects in Colloidal and Biological Systems. *Curr. Opin. Colloid Interface Sci.* **2010**, *15* (1–2), 34–39. https://doi.org/10.1016/j.cocis.2009.11.008.

(231) Zhang, Y.; Cremer, P. Interactions between Macromolecules and Ions: The Hofmeister Series. *Curr. Opin. Chem. Biol.* **2006**, *10* (6), 658–663. https://doi.org/10.1016/j.cbpa.2006.09.020.

(232) Collins, K. Ions from the Hofmeister Series and Osmolytes: Effects on Proteins in Solution and in the Crystallization Process. *Methods* **2004**, *34* (3), 300–311. https://doi.org/10.1016/j.ymeth.2004.03.021.

(233) Collins, K. D.; Neilson, G. W.; Enderby, J. E. Ions in Water: Characterizing the Forces That Control Chemical Processes and Biological Structure. *Biophy. Chem.* **2007**, *128* (2–3), 95–104. https://doi.org/10.1016/j.bpc.2007.03.009.

(234) Vlachy, N.; Jagoda-Cwiklik, B.; Vácha, R.; Touraud, D.; Jungwirth, P.; Kunz, W. Hofmeister Series and Specific Interactions of Charged Headgroups with Aqueous Ions. *Adv. Colloid Interface Sci.* **2009**, *146* (1–2), 42–47. https://doi.org/10.1016/j.cis.2008.09.010.

(235) Bailey, C. J. Metformin: Historical Overview. *Diabetologia* **2017**, *60* (9), 1566–1576. https://doi.org/10.1007/s00125-017-4318-z.

(236) Watanabe, C. K. Studies in the Metabolic Changes Induced by Administration of Guanidine Bases. Influence of Injected Guanidine Hydrochloride upon Blood Sugar Content. *J. Biol. Chem.* **1918**, *33*, 253–265.

(237) Vazdar, M.; Heyda, J.; Mason, P. E.; Tesei, G.; Allolio, C.; Lund, M.; Jungwirth, P. Arginine “Magic”: Guanidinium Like-Charge Ion Pairing from Aqueous Salts to Cell Penetrating Peptides. *Acc. Chem. Res.* **2018**, *51* (6), 1455–1464. https://doi.org/10.1021/acs.accounts.8b00098.

(238) Herce, H. D.; Garcia, A. E.; Cardoso, M. C. Fundamental Molecular Mechanism for the Cellular Uptake of Guanidinium-Rich Molecules. *J. Am. Chem. Soc.* **2014**, *136* (50), 17459–17467. https://doi.org/10.1021/ja507790z.

(239) Sakai, N.; Matile, S. Anion-Mediated Transfer of Polyarginine across Liquid and Bilayer Membranes. *J. Am. Chem. Soc.* **2003**, *125* (47), 14348–14356. https://doi.org/10.1021/ja037601l.

(240) Rathke, B. Ueber die Einwirkung von Phenylsenföl auf Diphenylguanidin. *Ber. Dtsch. Chem. Ges.* **1879**, *12* (1), 774–776. https://doi.org/10.1002/cber.187901201218.

(241) Werner, E. A.; Bell, J. The Preparation of Methylguanidine, and of Pp-Dimethylguanidine by the Interaction of Di- Cyanodiamide, and Methylammonium and Dimethyl- Ammonium Chlorides Respectively. *J. Chem. Soc. Trans.* **1922**, *121*, 1790-1794.

(242) Curd, F. H. S.; Davey, D. G.; Rose, F. L. Studies on Synthetic Antimalarial Drugs: X.—Some Biguanide Derivatives as New Types of Antimalarial Substances with Both Therapeutic and Causal Prophylactic Activity. *Ann. Trop. Med. Parasitol.* **1945**, *39* (3–4), 208–216. https://doi.org/10.1080/00034983.1945.11685237.

(243) Sterne, J. Du Nouveau Dans Les Antidiabétiques. La N,N-Diméthylamine Guanyl Guanidine (N.N.D.G.). *Maroc. Med.* **1957**, *36*, 1295–1296.

(244) Kinaan, M.; Ding, H.; Triggle, C. R. Metformin: An Old Drug for the Treatment of Diabetes but a New Drug for the Protection of the Endothelium. *Med. Princ. Pract.* **2015**, *24* (5), 401–415. https://doi.org/10.1159/000381643.

(245) Fortun, S.; Schmitzer, A. R. Synthesis and Characterization of Biguanide and Biguanidium Surfactants for Efficient and Recyclable Application in the Suzuki–Miyaura Reaction. *ACS Omega* **2018**, *3* (2), 1889–1896. https://doi.org/10.1021/acsomega.7b01962.

(246)Khalid Waleed S. Al-Janabi; Ali Khalil Mahmood; Hasan M. Luaibi. Determination of the Dissociation Constants of Metformin from a Second Derivative UV Spectrum. *Int. J. Res. Pharm. Sci.* **2020**, *11* (1), 790–796. https://doi.org/10.26452/ijrps.v11i1.1896.

(247) Desai, D.; Wong, B.; Huang, Y.; Ye, Q.; Tang, D.; Guo, H.; Huang, M.; Timmins, P. Surfactant-Mediated Dissolution of Metformin Hydrochloride Tablets: Wetting Effects Versus Ion Pairs Diffusivity. *J. Pharm. Sci.* **2014**, *103* (3), 920–926. https://doi.org/10.1002/jps.23852.

(248) Zhou, M.; Xia, L.; Wang, J. Metformin Transport by a Newly Cloned Proton-Stimulated Organic Cation Transporter (Plasma Membrane Monoamine Transporter) Expressed in Human Intestine. *Drug Metab. Dispos.* **2007**, *35* (10), 1956–1962. https://doi.org/10.1124/dmd.107.015495.

(249) Graham, G. G.; Punt, J.; Arora, M.; Day, R. O.; Doogue, M. P.; Duong, J. K.; Furlong, T. J.; Greenfield, J. R.; Greenup, L. C.; Kirkpatrick, C. M.; Ray, J. E.; Timmins, P.; Williams, K. M. Clinical Pharmacokinetics of Metformin. *Clin. Pharmacokinet.* **2011**.

(250) Rothbard, J. B.; Jessop, T. C.; Lewis, R. S.; Murray, B. A.; Wender, P. A. Role of Membrane Potential and Hydrogen Bonding in the Mechanism of Translocation of Guanidinium-Rich Peptides into Cells. *J. Am. Chem. Soc.* **2004**, *126* (31), 9506–9507. https://doi.org/10.1021/ja0482536.

(251) Nanubolu, J. B.; Sridhar, B.; Ravikumar, K.; Sawant, K. D.; Naik, T. A.; Patkar, L. N.; Cherukuvada, S.; Sreedhar, B. Polymorphism in Metformin Embonate Salt – Recurrence of Dimeric and Tetrameric Guanidinium–Carboxylate Synthons. *Cryst. Eng. Commun.* **2013**, *15* (22), 4448. https://doi.org/10.1039/c3ce26986h.

(252) Cassimiro, D. L.; Ferreira, L. M. B.; Capela, J. M. V.; Crespi, M. S.; Ribeiro, C. A. Kinetic Parameters for Thermal Decomposition of Supramolecular Polymers Derived from Diclofenac–Meglumine Supramolecular Adducts. *J. Pharm. Biomed. Anal.* **2013**, *73*, 24–28. https://doi.org/10.1016/j.jpba.2012.04.019.

(253) Douliez, J.-P.; Houinsou-Houssou, B.; Fameau, A.-L.; Novales, B.; Gaillard, C. Self Assembly of Anastomosis-like Superstructures in Fatty Acid/Guanidine Hydrochloride Aqueous Dispersions. *J. Colloid Interface Sci.* **2010**, *341* (2), 386–389. https://doi.org/10.1016/j.jcis.2009.09.061.

(254) Fameau, A.-L.; Ventureira, J.; Novales, B.; Douliez, J.-P. Foaming and Emulsifying Properties of Fatty Acids Neutralized by Tetrabutylammonium Hydroxide. *Colloids Surf. A* **2012**, *403*, 87–95. https://doi.org/10.1016/j.colsurfa.2012.03.059.

(255) Fameau, A.-L.; Houinsou-Houssou, B.; Ventureira, J. L.; Navailles, L.; Nallet, F.; Novales, B.; Douliez, J.-P. Self-Assembly, Foaming, and Emulsifying Properties of Sodium Alkyl Carboxylate/Guanidine Hydrochloride Aqueous Mixtures. *Langmuir* **2011**, *27* (8), 4505–4513. https://doi.org/10.1021/la2002404.

(256) Sahota, R. S.; M. Dakka, S. Investigation the Stability of Water in Oil Biofuel Emulsions Using Sunflower Oil. *Chem. Eng.* **2020**, *4* (2), 36. https://doi.org/10.3390/chemengineering4020036.

(257) Delforce, L. New Methodologies for Characterizing Particles, Complex Oils and Surfactants : Relations between Chemical Structure, Physicochemical Properties and Applicative Properties. phdthesis, Université de Lille, **2022**.

(258) Basit, H.; Pal, A.; Sen, S.; Bhattacharya, S. Two-Component Hydrogels Comprising Fatty Acids and Amines: Structure, Properties, and Application as a Template for the Synthesis of Metal Nanoparticles. *Chem. Eur. J.* **2008**, *14* (21), 6534–6545. https://doi.org/10.1002/chem.200800374.

(259) Mukerjee, P.; Mysels, K. J. *Critical Micelle Concentrations of Aqueous Surfactant Systems*, Nat. Stand. Ref. Data. Ser., Nat. Bur. Stand. 36, **1971**.

(260) Jansson, M.; Jönsson, A.; Li, P.; Stilbs, P. Aggregation in Tetraalkylammonium Dodecanoate Systems. *Colloids Surf.* **1991**, *59*, 387–397. https://doi.org/10.1016/0166-6622(91)80261-L.

(261) Klein, R. Choline Applied as Counterion – A Strategy for the Design of Biocompatible Surfactants and Green Ionic Liquids, Universität Regensburg, **2011**.

(262) Song, Y.; Li, Q.; Li, Y. Self-Aggregation and Antimicrobial Activity of Alkylguanidium Salts. *Colloids and Surfaces A: Physicochemical and Engineering Aspects* **2012**, *393*, 11–16. https://doi.org/10.1016/j.colsurfa.2011.10.015.

(263) Kralova, I.; Sjöblom, J. Surfactants Used in Food Industry: A Review. *J. Dispers. Sci. Technol.* **2009**, *30* (9), 1363–1383. https://doi.org/10.1080/01932690902735561.

(264) Hutin, A. Analyse de la taille des dispersions en phase liquide. **2022**. https://doi.org/10.5281/ZENODO.6410230.

(265) McClements, D. J. Biopolymers in Food Emulsions. In *Modern Biopolymer Science*; Elsevier, 2009; pp 129–166. https://doi.org/10.1016/B978-0-12-374195-0.00004-5.

Appendix

A.1. List of Abbreviations

ABTS	2,2'-azino-bis(3-ethylbenzothiazoline-6-sulfonic acid
API	Active Pharmaceutical Ingredient
Arg	L-Arginine
BA	Behenic acid
BCS	Biopharmaceutics Classification System
BDE	Bond Dissociation Enthalpy
BS, ΔBS	Backscattered and variation of backscattered light, respectively
CAC	Critical Aggregation Concentration
Ch	Choline
CHD	Coronary heart disease
CMC	Critical Micelle Concentration
COSMO-RS	Conductor-like Screening Model, Realistic Solvation
Crea	Creatine
D	Distribution coefficient
$D_{[3,2]}$	Average diameters weighted by area
$D_{[4,3]}$	Average diameters weighted by volume
DENA	*N,N*-diethylnicotinamide
DLS	Dynamic Light Scattering
DMBA	*N,N*-dimethylbenzamide
DMPE	Dimyristoylphosphatidylethanolamine
DMSO	Dimethyl sulfoxide
DMSO-d_6	Hexadeutero Dimethyl sulfoxide
DPPC	Dipalmitoylphosphatidylcholine
DPPG	Dipalmitoylphosphatidylglycerol
DPPH	Diphenylpicrylhydrazyl

DPV	Differential Pulse Voltammetry
DR-13	Disperse Red 13
DSD	Droplet Size Distribution
EE	Entrapment Efficacy
E_v	Volumetric energy
FDA	Food and Drug Administration
FOX	Ferrous Oxidation-Xylenol orange
FRAP	Ferric Reducing Antioxidant Power
FTS	Fluctuation Theory of Solution
Gu	Guanidine
Gu^+	Guanidinium cation
HAT	Hydrogen Atom Transfer
HB	Hydrogen bond
HEPES	4-(2-hydroxyethyl)-1-piperazineethanesulfonic acid
HH	Henderson–Hasselbalch
HLB	Hydrophilic Lipophilic Balance
HLD	Hydrophilic-Lipophilic Difference
HMS	HEPES, Meglumine, Sodium azide
HPLC	High Performance Liquid Chromatography
HS	Hunter-Sanders theory
HSS	HEPES, Sucrose, Sodium azide
I	Ionic strength
ICP-OES	Inductively Coupled Plasma-Optical Emission Spectrometry
IPM	Isopropyl myristate
IUPAC	International Union of Pure and Applied Chemistry
L	Length
LUV	Large unilamellar vesicle
Lys	L-Lysine
MA	Myristic acid

Meg	Meglumine
MeOH	Methanol
Met	Metformin
mGu	Methylguanidine
MHC	Minimum Hydrotropic Concentration
MLS	Multiple Light Scattering
MLV	Multilamellar vesicle
MVV	Multivesicular vesicle
NaSal	Sodium salicylate
NaSX (or SXS)	Sodium xylene sulfonate
NLC	Nanostructure Lipid Carrier
NMR	Nuclear Magnetic Resonance
NSAID	Nonsteroidal anti-inflammatory and analgesic drug
OA	Oleic acid
P or K_{ow}	Octane-water partition coefficient
p	Packing parameter
P	Power
PA	Palmitic acid
PCA	Pyrrolidone Carboxylic Acid, *a.k.a.* L-Pyroglutamic acid
PDM	pH-driven method
PEG	Polyethylene glycol
PI	Polydispersity index
PIT	Phase inversion temperature
pK_a	Negative logarithm of the acidic dissociation constant K_a
PO	Paraffin oil
PTFE	Polytetrafluoroethylene
ROS	Reacting Oxygen Specie
R_t	Retention time (HPLC)
RT	Room temperature

S_0	Intrinsic solubility
SA	Stearic acid
SDDS	Supersaturation Drug Delivery Systems.
SEC	Size Exclusion Chromatography
SET	Single Electron Transfer
SLN	Solid Lipid Nanoparticle
SOW	Surfactant/Oil/Water
SPLET	Sequential Proton Loss Electron Transfer
SUV	Small unilamellar vesicle
$T, \Delta T$	Transmitted and variation of transmitted light, respectively.
TBA	Tetrabutylammonium
TEAC	Trolox Equivalent Antioxidant Capacity
TFA	Trifluoroacetic acid
TFM	Thin-film method
T_{Kr}	Krafft temperature
tL	Total Lipid
TMC	Transition Metal Chelation
TMSP-d_4	3-(Trimethylsilyl)propionic-2,2,3,3-d_4 acid sodium salt
TZVPD-FINE	Triple Zeta Valence Polarized with Diffuse function refined
UV-Vis	Ultraviolet-visible
V	Volume
WH	Wheeler-Houk theory
WOR	Water-to-oil ratio
XO	Xylenol Orange
γ	Surface tension
ΔG_{fus}	Gibbs free energy of fusion
ΔG_{solv}	Gibbs free energy of solvation
ΔpK_a	pKa difference
ΔS_{fus}	Entropy of fusion

ζ-potential	Zeta potential
λ	Wavelength
λ_{max}	Wavelength of maximal UV-Vis absorption
μ	Chemical potential
μ_{solv}	Chemical potential of solvation
σ	Charge density

A.2. pK$_a$ calculations for quercetin deprotonation order determination

Table A.1. pK$_a$ calculations for the first deprotonation of quercetin. In this table and the following, the anionic forms of quercetin are designated according to the deprotonated hydroxyl group(s).

pK$_a$1		
Protonated form	**Deprotonated form**	**Calculated pK$_a$ value**
Quer	An1_4'	7.4
	An1_7	7.6
	An1_3'	8.0
	An1_3	8.0
	An1_5	10.2

Table A.2. pK$_a$ calculations for the second deprotonation of quercetin.

pK$_a$2		
Protonated form	**Deprotonated form**	**Calculated pK$_a$ value**
An1_4'	An2_4'3'	10.2
	An2_4'3	8.2
	An2_4'5	10.0
	An2_74'	7.3
An1_7	An2_73'	8.0
	An2_73	8.8
	An2_75	/
	An2_74'	7.2
An1_3'	An2_4'3'	9.6
	An2_3'5	9.9
	An2_73'	7.5
	An2_3'3	8.1
An1_3	An2_3'3	8.1
	An2_4'3	7.6
	An2_73	8.3
	An2_35	12.9
An1_5	An2_35	10.6
	An2_4'5	7.2

	An2_75	/
	An2_3'5	7.8

Table A.3. pK_a calculations for the third deprotonation of quercetin.

pK_a3		
Protonated form	**Deprotonated form**	**Calculated pK_a value**
An2_4'3'	An3_4'3'3	9.2
	An3_4'3'5	10.0
	An3_74'3'	7.3
An2_4'3	An3_4'3'3	11.2
	An3_4'35	12.5
	An3_74'3	8.0
An2_4'5	An3_74'5	8.4
	An3_4'3'5	10.2
	An3_4'35	10.7
An2_73'	An3_73'5	11.0
	An3_73'3	8.4
	An3_74'3'	9.4
An2_73	An3_735	/
	An3_74'3	7.3
	An3_73'3	7.6
An2_75	An3_735	/
	An3_74'5	/
	An3_73'5	/
An2_3'3	An3_4'3'3	10.7
	An3_73'3	7.8
	An3_3'35	12.2
An2_3'5	An3_4'3'5	9.6
	An3_73'5	8.5
	An3_3'35	10.3
An2_35	An3_735	/
	An3_4'35	7.3
	An3_3'35	7.5
An2_74'	An3_74'5	11.1
	An3_74'3	8.9
	An3_74'3'	10.2

Table A.4. pK_a calculations for the fourth deprotonation of quercetin.

pK_a4		
Protonated form	**Deprotonated form**	**Calculated pK_a value**
An3_735	An4_3'357	/

	An4_3574'	/
An3_74'5	An4_3574'	10.2
	An4_574'3'	9.7
An3_73'5	An4_3'357	9.9
	An4_574'3'	9.0
An3_4'3'3	An4_4'3'35	/
	An4_74'3'3	6.6
An3_4'3'5	An4_4'3'35	/
	An4_574'3'	7.9
An3_4'35	An4_4'3'35	/
	An4_3574'	7.8
An3_3'35	An4_4'3'35	/
	An4_3'357	8.1
An3_73'3	An4_3'357	12.5
	An4_74'3'3	9.4
An3_74'3'	An4_74'3'3	8.5
	An4_574'3'	10.6
An3_74'3	An4_74'3'3	9.8
	An4_3574'	12.4

Table A.5. pK$_a$ calculations for the fifth deprotonation of quercetin.

pK$_a$5		
Protonated form	**Deprotonated form**	**Calculated pK$_a$ value**
An4_4'3'35	An5	/
An4_3'357		9.4
An4_3574'		9.9
An4_574'3'		10.3
An4_74'3'3		12.5

A.3. HPLC calibration method for quercetin quantification

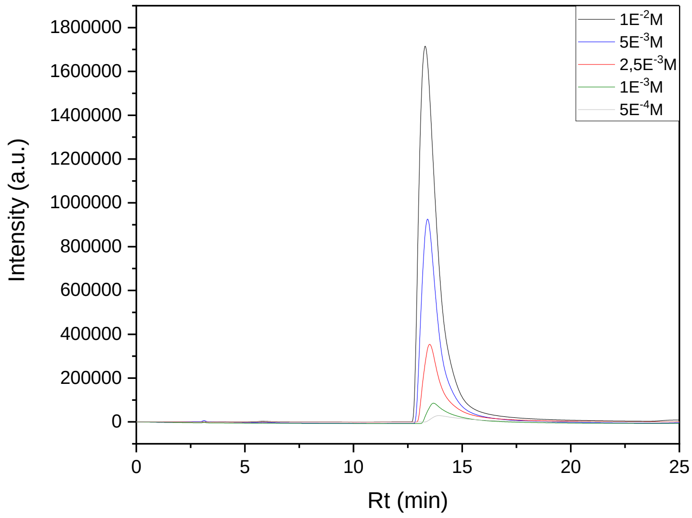

Figure A.1. Quercetin pure samples in MeOH for establishing the calibration curve of area under the curve versus quercetin concentration.

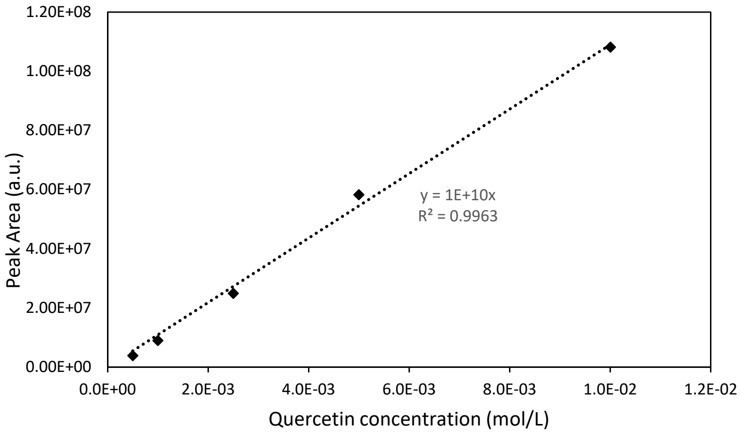

Figure A.2. Quercetin calibration curve of peak area as a function of concentration.

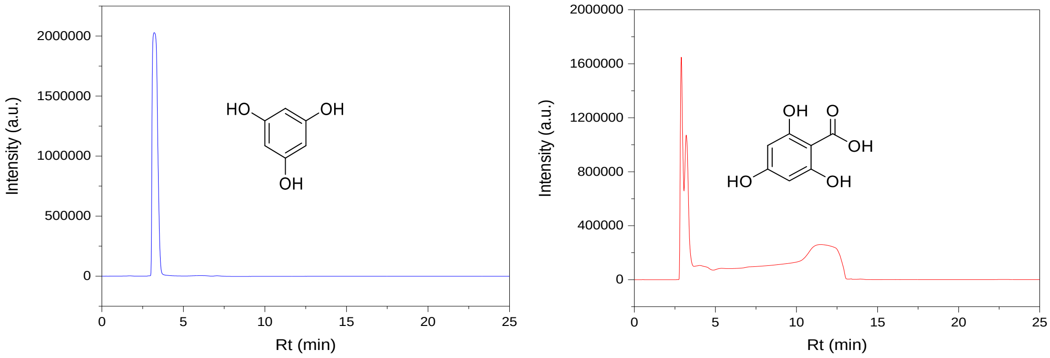

Figure A.3. Chromatograms of two major oxidation products of quercetin as pure compound. Left phloroglucinol, right phloroglucinic acid. Both recorded at λ = 210 nm.

A.4. COSMO-RS calculations for the polyphenols set

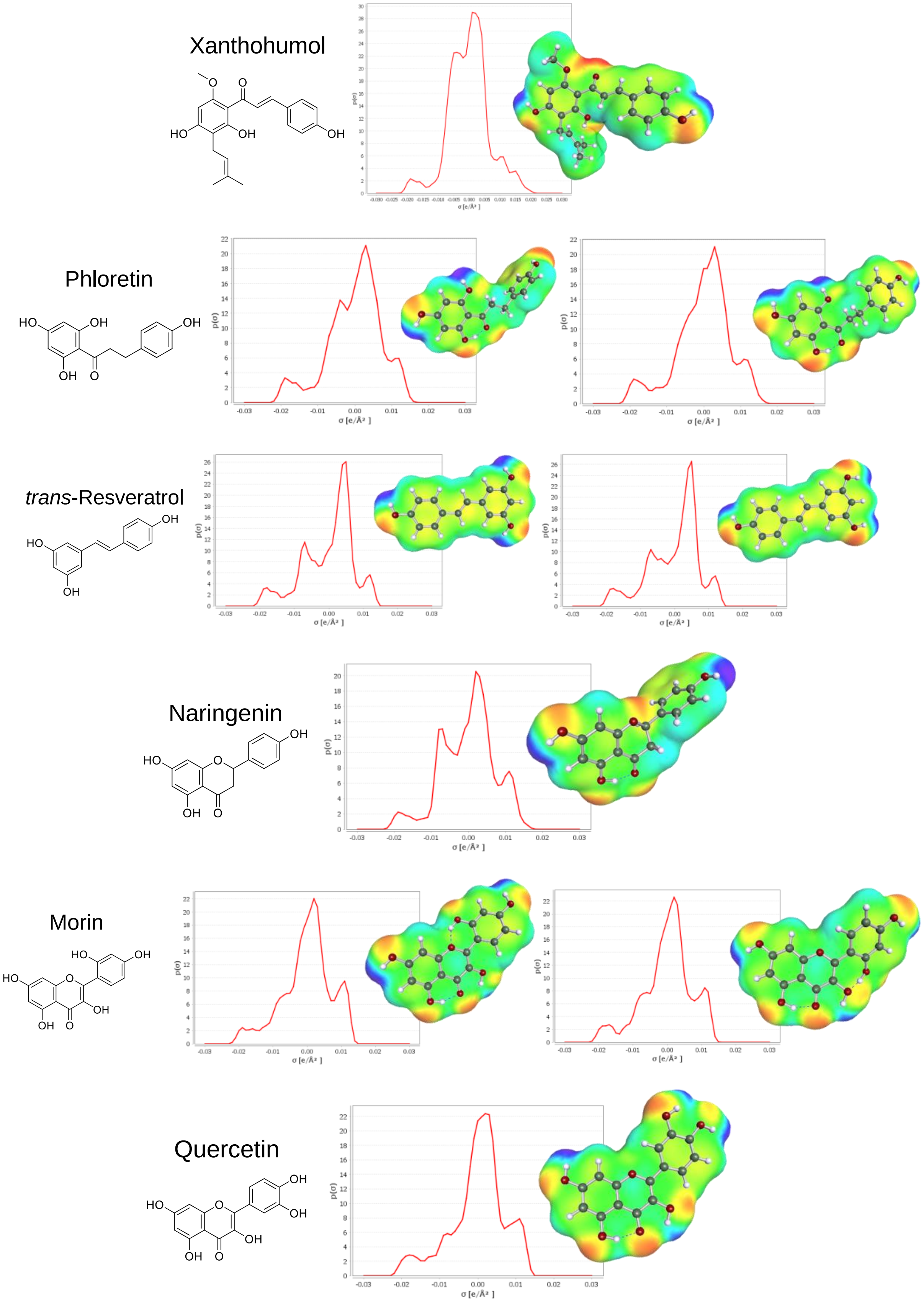

Figure A.4. Chemical structures, σ-profiles, and σ-surfaces of studied polyphenols.

A.5. Experimental pK$_a$ determination of pyroglutamic acid

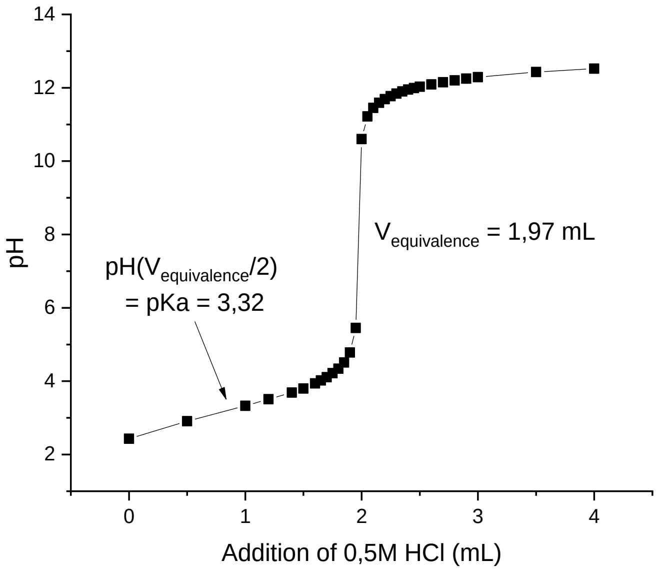

Figure A.5. Titration of a water solution of PCA (5.02 x10^{-2} mol/L) with a NaOH solution (0.50 mol/L).

A.6. Micrograph of phase behavior of guanidine soaps

Polarization microscopy was performed using a Leitz Orthoplan polarizing microscope (Wetzlar, Germany) equipped with a JVC (Yokohama, Japan) digital camera (TK-C1380) and a Linkam (Epsom, UK) LTS350 heating/freezing stage comprising a TMS90 temperature controller (± 0.5°C) and a CS196 cooling system.

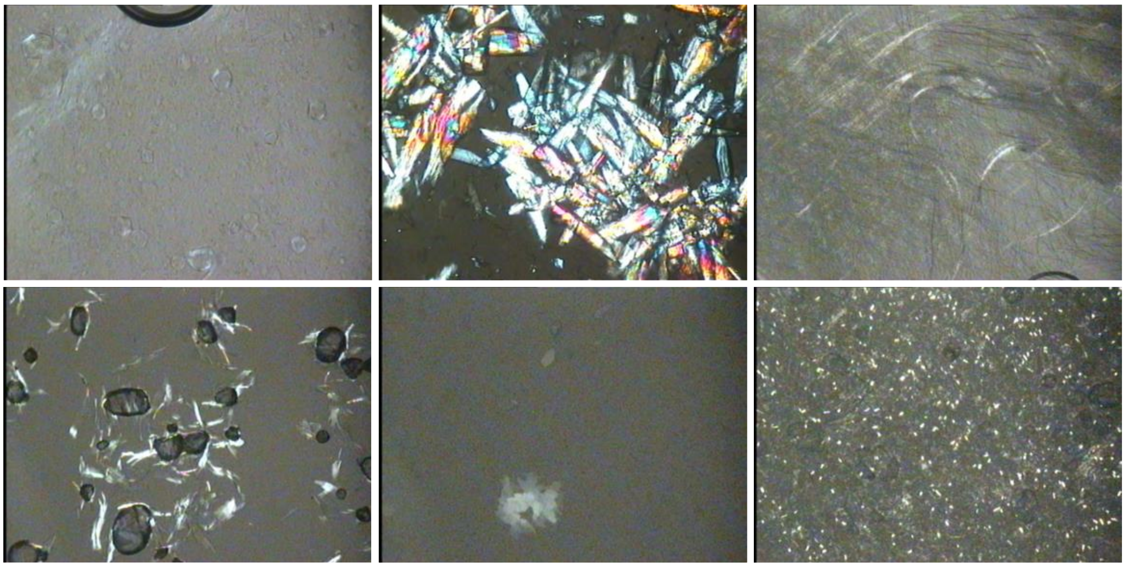

Figure A.6. Polarized micrographic pictures of GuC$_{16}$ (top left), mGuC$_{16}$ (top center), MetC$_{16}$ (top right), GuC$_{18}$ (bottom left), mGuC$_{18}$ (bottom center), and MetC$_{18}$ (bottom right) at 20°C. Magnification x100.

A.7. Turbiscan profiles of MegC$_n$ emulsions

Variations of transmitted (*ΔT*) and backscattered (*ΔBS*) signals of MegC$_n$ emulsions with a WOR of 50:50 in paraffin oil (PO) and isopropyl myristate (IPM). Turbiscan profiles were recorded from 0 (blue curve) to 30 days (red curve).

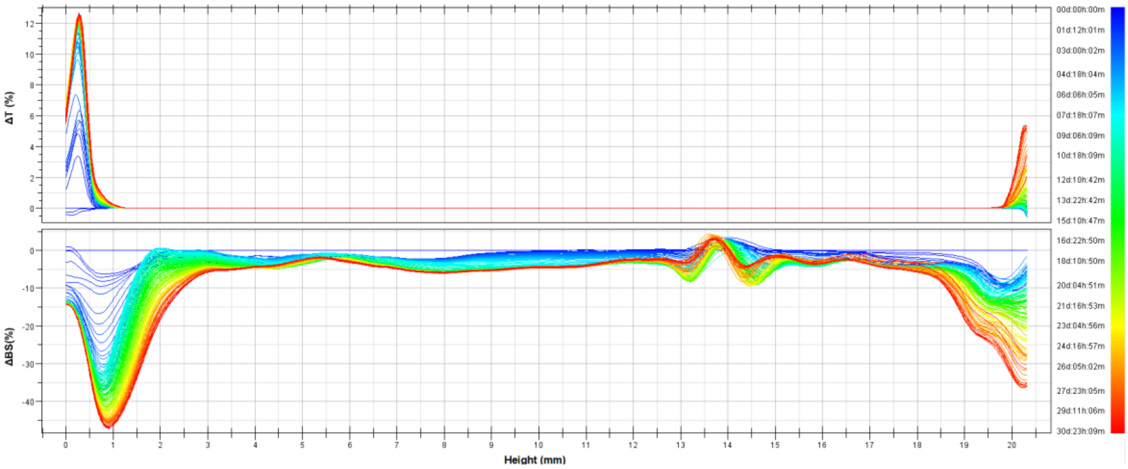

Figure A.7. Turbiscan profile of MegC$_{18}$^{s} with PO.

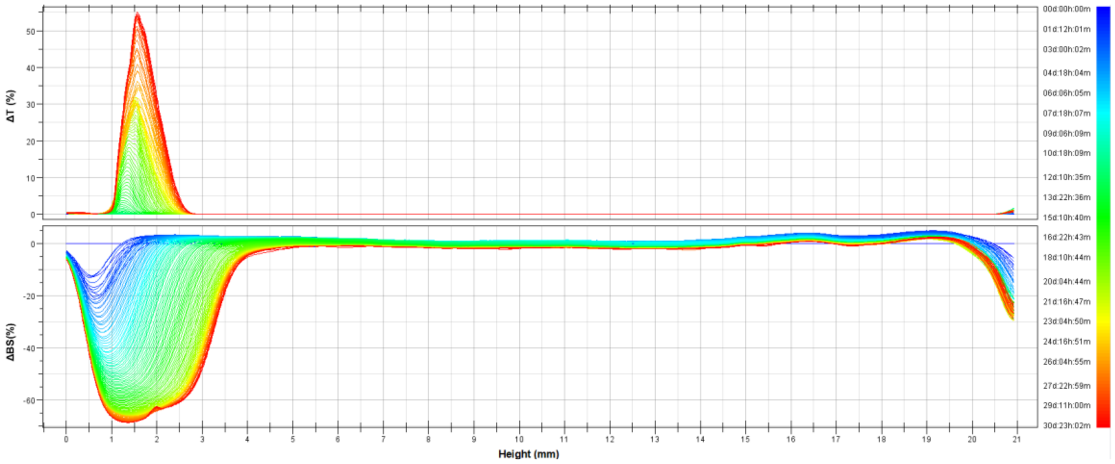

Figure A.8. Turbiscan profile of MegC$_{18}$^{s} with IPM.

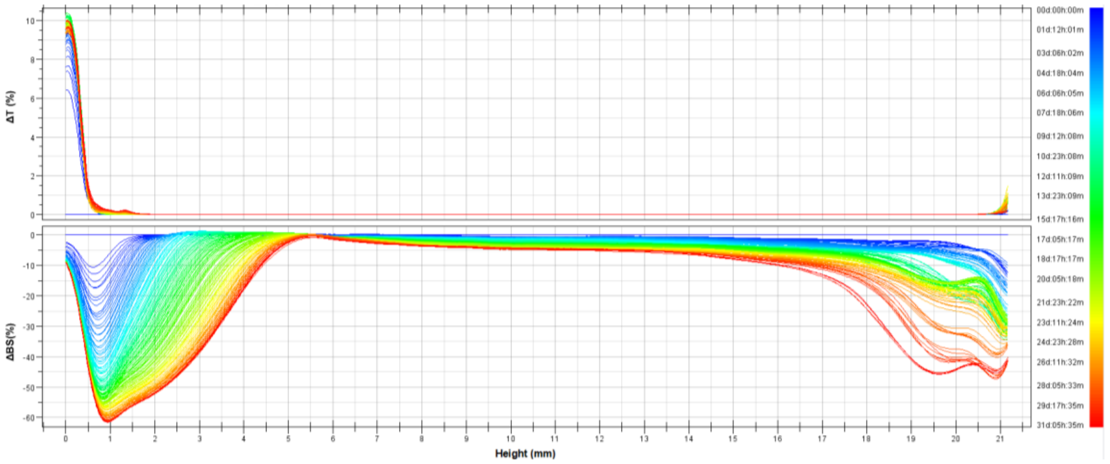

Figure A.9. Turbiscan profile of MegC$_{22}$ with PO.

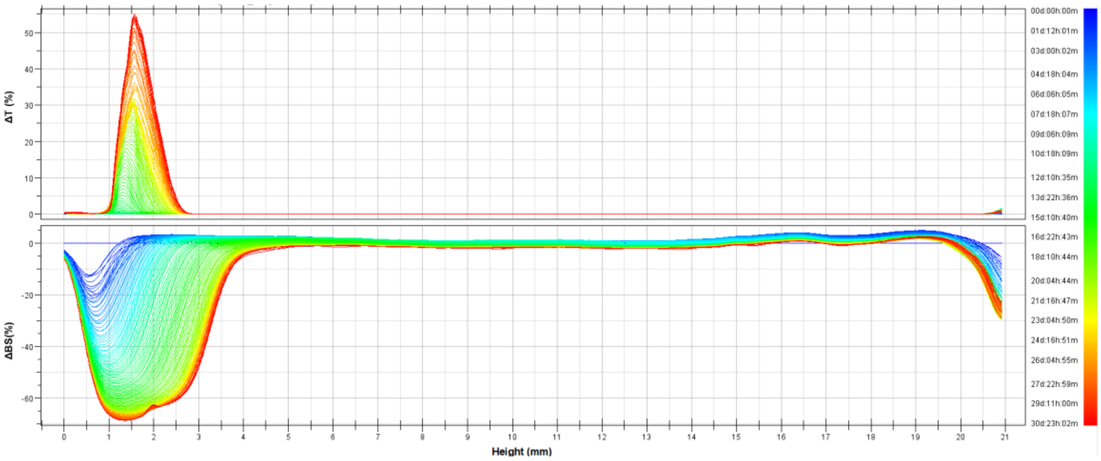

Figure A.10. Turbiscan profile of $MegC_{22}$ with IPM.

A.8. Publication – Enhancement of water solubilization of quercetin by meglumine and application of the solubilization concept to a similar system

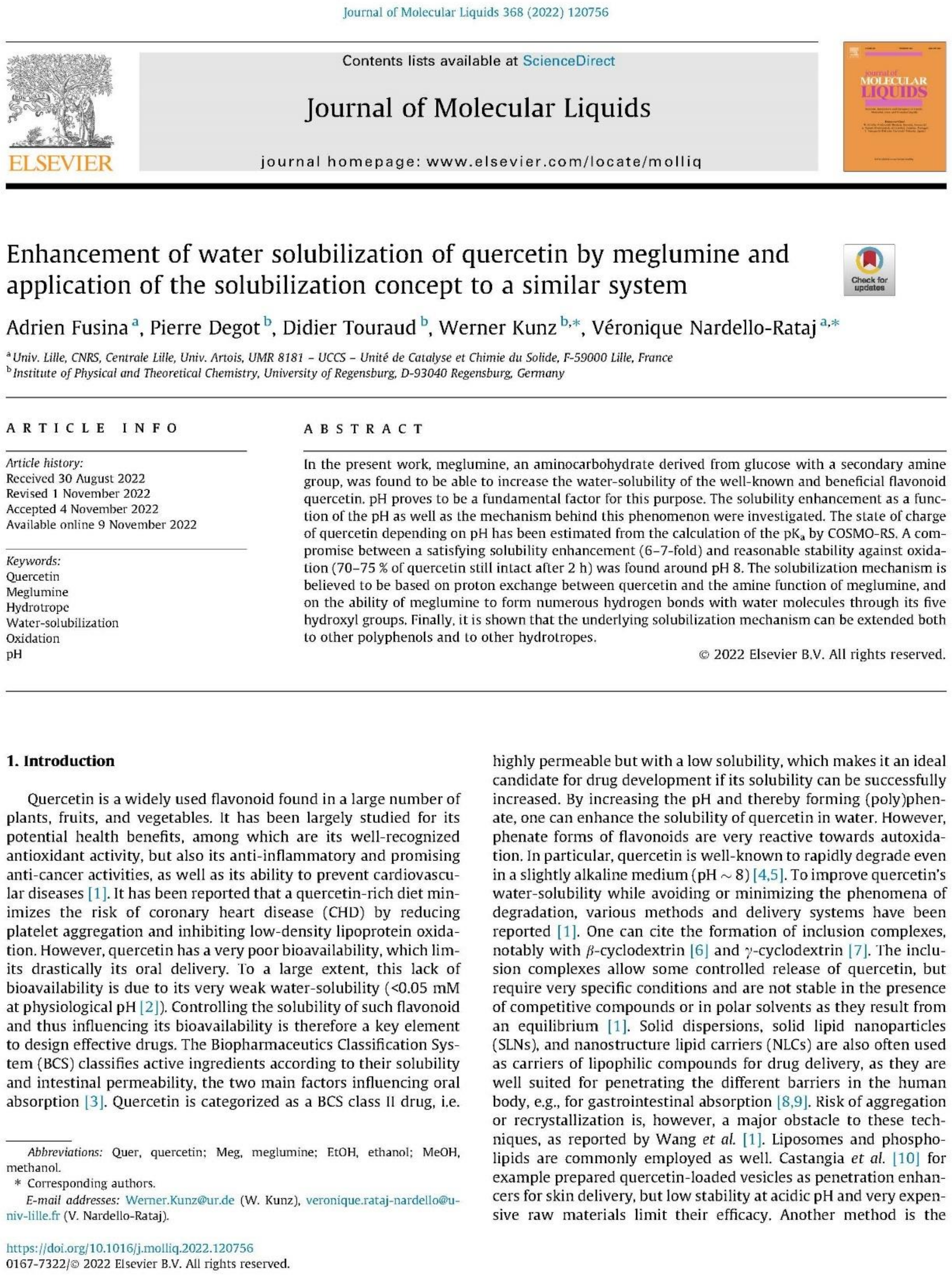

Journal of Molecular Liquids 368 (2022) 120756

Contents lists available at ScienceDirect

Journal of Molecular Liquids

journal homepage: www.elsevier.com/locate/molliq

Enhancement of water solubilization of quercetin by meglumine and application of the solubilization concept to a similar system

Adrien Fusina [a], Pierre Degot [b], Didier Touraud [b], Werner Kunz [b,*], Véronique Nardello-Rataj [a,*]

[a] *Univ. Lille, CNRS, Centrale Lille, Univ. Artois, UMR 8181 – UCCS – Unité de Catalyse et Chimie du Solide, F-59000 Lille, France*
[b] *Institute of Physical and Theoretical Chemistry, University of Regensburg, D-93040 Regensburg, Germany*

ARTICLE INFO

Article history:
Received 30 August 2022
Revised 1 November 2022
Accepted 4 November 2022
Available online 9 November 2022

Keywords:
Quercetin
Meglumine
Hydrotrope
Water-solubilization
Oxidation
pH

ABSTRACT

In the present work, meglumine, an aminocarbohydrate derived from glucose with a secondary amine group, was found to be able to increase the water-solubility of the well-known and beneficial flavonoid quercetin. pH proves to be a fundamental factor for this purpose. The solubility enhancement as a function of the pH as well as the mechanism behind this phenomenon were investigated. The state of charge of quercetin depending on pH has been estimated from the calculation of the pK_a by COSMO-RS. A compromise between a satisfying solubility enhancement (6–7-fold) and reasonable stability against oxidation (70–75 % of quercetin still intact after 2 h) was found around pH 8. The solubilization mechanism is believed to be based on proton exchange between quercetin and the amine function of meglumine, and on the ability of meglumine to form numerous hydrogen bonds with water molecules through its five hydroxyl groups. Finally, it is shown that the underlying solubilization mechanism can be extended both to other polyphenols and to other hydrotropes.

© 2022 Elsevier B.V. All rights reserved.

1. Introduction

Quercetin is a widely used flavonoid found in a large number of plants, fruits, and vegetables. It has been largely studied for its potential health benefits, among which are its well-recognized antioxidant activity, but also its anti-inflammatory and promising anti-cancer activities, as well as its ability to prevent cardiovascular diseases [1]. It has been reported that a quercetin-rich diet minimizes the risk of coronary heart disease (CHD) by reducing platelet aggregation and inhibiting low-density lipoprotein oxidation. However, quercetin has a very poor bioavailability, which limits drastically its oral delivery. To a large extent, this lack of bioavailability is due to its very weak water-solubility (<0.05 mM at physiological pH [2]). Controlling the solubility of such flavonoid and thus influencing its bioavailability is therefore a key element to design effective drugs. The Biopharmaceutics Classification System (BCS) classifies active ingredients according to their solubility and intestinal permeability, the two main factors influencing oral absorption [3]. Quercetin is categorized as a BCS class II drug, i.e. highly permeable but with a low solubility, which makes it an ideal candidate for drug development if its solubility can be successfully increased. By increasing the pH and thereby forming (poly)phenate, one can enhance the solubility of quercetin in water. However, phenate forms of flavonoids are very reactive towards autoxidation. In particular, quercetin is well-known to rapidly degrade even in a slightly alkaline medium (pH ~ 8) [4,5]. To improve quercetin's water-solubility while avoiding or minimizing the phenomena of degradation, various methods and delivery systems have been reported [1]. One can cite the formation of inclusion complexes, notably with β-cyclodextrin [6] and γ-cyclodextrin [7]. The inclusion complexes allow some controlled release of quercetin, but require very specific conditions and are not stable in the presence of competitive compounds or in polar solvents as they result from an equilibrium [1]. Solid dispersions, solid lipid nanoparticles (SLNs), and nanostructure lipid carriers (NLCs) are also often used as carriers of lipophilic compounds for drug delivery, as they are well suited for penetrating the different barriers in the human body, e.g., for gastrointestinal absorption [8,9]. Risk of aggregation or recrystallization is, however, a major obstacle to these techniques, as reported by Wang *et al.* [1]. Liposomes and phospholipids are commonly employed as well. Castangia *et al.* [10] for example prepared quercetin-loaded vesicles as penetration enhancers for skin delivery, but low stability at acidic pH and very expensive raw materials limit their efficacy. Another method is the

---

Abbreviations: Quer, quercetin; Meg, meglumine; EtOH, ethanol; MeOH, methanol.

* Corresponding authors.

E-mail addresses: Werner.Kunz@ur.de (W. Kunz), veronique.rataj-nardello@univ-lille.fr (V. Nardello-Rataj).

https://doi.org/10.1016/j.molliq.2022.120756

0167-7322/© 2022 Elsevier B.V. All rights reserved.

incorporation of the target material in micelles [11–13], but it requires a high amount of surface-active agent. The functionalization of quercetin with hydrophilic groups has also been used to increase its water-solubilization. However, on the one hand, this involves treatment of the raw material that can be quite severe or more complex than other methods. On the other hand, the new groups of the molecule can modify its intrinsic properties, thus going against the problem. Rebaudioside and rubusoside treatments have been shown to be efficient to enhance quercetin solubilization in water [14]. Other delivery systems such as polysaccharides and hyper-branched polymers have also been employed to increase the solubility of quercetin [15,16]. However, even in a 1:1 ratio with quercetin, macromolecules still represent a significant mass ratio to quercetin due to their extremely high molecular weight. The use of hyper-branched polymers is also limited due to the demixing behavior of the aqueous polymer phase, which restricts the solubility enhancement to relatively low values (1.3×10^{-6} wt fraction of quercetin) [16].

All these methods enhance more or less the solubility of quercetin in water and its bioavailability accordingly, but all suffer from various drawbacks. In addition, without considering the release rate of the compound, the main characteristics of a good solubilizer for quercetin should be safety, an easy formulation process, and low cost. In this context, hydrotropic solubilization appears as a relevant strategy, provided that the hydrotrope meets such criteria. Hydrotropes are slightly amphiphilic solubilization enhancers that do not form micelles or liquid crystals on their own, in contrast to true surfactants.

Derivatives of glycerol such as isopropylidene glycerol (solketal) or glycerol formal have been proved to act as hydrotrope regarding a number of natural antioxidants, including quercetin, as reported by Kerkel *et al.* [17]. However, in the present case we focus on an edible hydrotrope. *N*-Methyl-D-glucamine, known as meglumine (Meg) – for its structure, see Fig. 1**b** – is an edible [18] methylamino derivative of sorbitol used in pharmacy and also in cosmetics, where it acts as an excipient in hair conditioners. It has mainly been used to enhance the solubility of otherwise poorly water-soluble drugs such as sulfamerazine, indomethacin, or celecoxib [19,20] as a salt of weakly acidic compounds through proton exchange with its amino group. It is an inexpensive material with a high water-solubility (2.56 M i.e. 500 g/L). Meglumine is mostly known as flunixin meglumine, a nonsteroidal anti-inflammatory drug (NSAID) mainly for cattle and horses. Meglumine has also been described as a hydrotrope by Li *et al.* [21] to solubilize glimepiride. Degot *et al.* identified it as a solubilizer of curcumin [22] by means of complexation through the electron-accepting –OH and –NH groups of meglumine allowing the formation of multiple hydrogen bonds. They found that the addition of meglumine to a triacetin/ ethanol/ water system had a positive impact on the extraction efficiency of curcumin, reaching up to ~ 18.2 mg of curcuminoids per g rhizome with 15 %wt meglumine in a system with 5 %wt water, against ~ 15.6 mg of curcuminoids per g rhizome at the same pH value (~11.2) with NaOH and ~ 14 without any additive.

Herein, we report on a detailed study of the solubilization of quercetin in water in the presence of meglumine. Interestingly, meglumine notably enhances the water-solubility of this polyphenol over a wide pH range. The solubility enhancement (6.6-fold at pH 8, 11.4 at pH 10, and 47.6 at pH 11) is easily observable with UV–visible spectroscopy. The stability of the system regarding oxidation by air oxygen is quantified with ^{1}H NMR and HPLC against NaOH as a standard base. We also extended our study to the solubility of curcumin, another polyphenol and to some other hydrotropes with a similar solubilization mechanism.

2. Experimental part

2.1. Materials

Meglumine (>99 %) was purchased from TCI Chemicals and quercetin (HPLC grade) from Merck. Curcumin (≥97 %), Naringenin (≥93 %), and *trans*-resveratrol (≥98 %) were also purchased from TCI Chemicals, gallic acid (≥95 %) from Acros, and phloretin (≥90 %) from Symrise. NaOH, HCl, MeOH, and acetone, were used for pH adjustments and UV–vis measurements. Deionized water with 18.20 MΩ resistivity from Milli-Q Millipore equipment was used to prepare all solutions.

2.2. Techniques and methods

UV–vis spectroscopy. UV–vis spectra were recorded on an Agilent Technologies Cary 60 UV–vis spectrometer in 1 cm path length quartz cells. For the solubilization tests, two stock solutions of aqueous meglumine were prepared at 50 and 250 mM (these concentrations roughly correspond to 1 and 5 wt% of meglumine, respectively). Samples of 3 mL were prepared at 20 °C and pH adjusted with HCl and NaOH. Quercetin was added in large excess (until visible precipitation). The samples were shaken manually for about 30 s. The solutions were then centrifuged (5000 rpm, 5 min, 20 °C) and the supernatant recovered. After dilution in methanol (1:100 or 1:500 for high pH), they were analyzed using UV spectroscopy at λ = 370 nm. A Beer-Lambert calibration curve of quercetin diluted in methanol at different concentrations was used to calculate the amount of solubilized quercetin. All the measures were carried out within 10 min after the addition of quercetin to minimize the oxidation process. The same protocol was applied with the other phenols tested, namely curcumin, gallic acid, naringenin, phloretin, and *trans*-resveratrol.

HPLC. Monitoring of the oxidation process was carried out by High Performance Liquid Chromatography on a Shimadzu instrument equipped with a Uptisphere RP C_{18} (250 × 4.6 mm, 2.5 μm) protected by a guard column (LC_{18}). The column temperature was maintained at 30 °C. The mobile phase consisted of methanol–water (50:50, v/v) at a flow rate of 1 mL/min. The elutions were monitored with a UV–vis detector simultaneously at

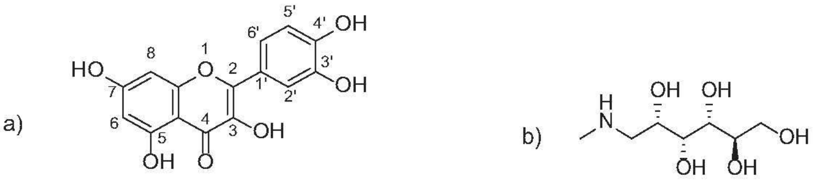

Fig. 1. Structure of (a) quercetin and (b) meglumine.

210 and 370 nm. A calibration curve of peak area versus concentration of non-oxidized quercetin was built in MeOH in order to determine the concentration of intact quercetin over time.

NMR. NMR spectra were recorded on an Avance III 3 (Bruker, US) at 300 MHz for ^{1}H. D_2O was used for meglumine and quercetin solubilized in aqueous phase and DMSO-d6 for pure quercetin analysis. For the temporal monitoring of quercetin oxidation, approximately 15 mg of quercetin was precisely weighed in a 5 mL volumetric flask with the appropriate mass of meglumine to obtain (1:1) and (5:1) meglumine to quercetin molar ratio. The samples were diluted in D_2O with TMSP-d4 for calibration. After 5 min of stirring in a water bath at 25 °C, the solutions were filtrated (PTFE, 0.2 μm) and analyzed with ^{1}H NMR.

COSMO-RS. COSMO-RS [23] (an acronym for Conductor-like Screening Model, Realistic Solvation) is a molecular modeling software based on quantum chemistry and statistical thermodynamics. It allows one to calculate the chemical potential μ of a solute in a pure liquid phase at infinite dilution, which is then converted into further physicochemical parameters. Quercetin was drawn in all possible states of charge and the COSMOconf script.19 was used for conformational analysis. COSMOtherm (C30_1301 version, COSMOlogic, Leverkusen, *Germany)* was then used to calculate the pK_a between two successive anions of quercetin.

3. Results and discussion

3.1. Determination of the pK_as of quercetin

There is no common agreement on the number of pK_a of quercetin as well as their values in the literature (see Table 1 in **Supporting Information**). Theoretically, as quercetin has five different hydroxyl groups (Fig. 1**a**), it could exist in six different states of charge, from completely protonated to five times negatively charged. In practice, quercetin becomes very unstable in alkaline media (pH > 8) and undergoes an oxidation process that results in the cleavage of the γ-pyrone fragment [24]. Thus, the dissociation constants that correspond to the fourth and fifth deprotonation can hardly be experimentally determined. It should also be reminded that pK_a may depend strongly on the ionic strength. Thus, pK_a values should be determined and compared with a constant ionic strength. The question of quercetin's state of charge is essential to gain insight on its solubilization mechanism and interactions with meglumine.

The preferential deprotonation order is expected to be: 4′-OH < 7-OH < 3′-OH < 3-OH < 5-OH [25]. 4′-OH and 7-OH deprotonations are facilitated by delocalization of the negative charge. Further, the more difficult ionization of 3-OH and 5-OH groups can be explained by the stabilization of the protonated forms by intramolecular hydrogen-bonds (H-bonds). This stabilization is thought to be greater for 5-OH than for 3-OH. There are discussions on whether the first group to be deprotonated is 4′-OH or 7-OH. Hence, by comparing the acidity of structurally similar compounds and through NMR data, it was concluded in [26] that the most acidic site should be the 7-OH.

To have a relative and reliable estimation of the different pK_a of quercetin, we used COSMO-RS software, which has already been proved to be well suited to determine the pK_a of acids as well as phenols [27,28]. Each pK_a is calculated using two successive ionization degrees, i.e. the first pK_a calculation is based on the neutral and the mono-ionic forms of quercetin, the second on the mono-ionic and di-ionic forms, etc. Every hydroxyl group was considered a possible deprotonation site. However, the use of COSMO-RS for pK_a prediction of molecules with multiple hydroxyl groups has limitations. The calculation is indeed partly based on a set of experimental data (94 acids and 75 bases) used for constants calculation [27]. Thus, these values should be taken with caution, especially for pK_a 5. Indeed, it is very unlikely that the totally deprotonated form exists in solution, or, if it does, then only with a very short lifetime. The purpose of these calculations is essential to find out, which ionic forms of quercetin are likely to be found in solution at a certain pH and to determine a logical sequence of increasing pK_a values that could provide an order of relative deprotonation ease. For each combination between two successive forms, the anionic one with the minimum pK_a value, thus requiring the lowest energy, was regarded as the most probable. In this regard, the most likely deprotonation order was found to be 4′-OH < 7-OH < 3-OH < 3′-OH < 5-OH (Fig. 2), in agreement with [29]. One can notice a slight variation with Lemańska *et al.* [25] between groups 3-OH and 3′-OH. Indeed, if we consider that group 4-OH is already deprotonated, then the deprotonation of group 3′-OH appears to be electronically disadvantaged compared to group 3-OH. Further, very close pK_a values could also indicate pH areas, where several different forms coexist at the same level of deprotonation. This is the case with the calculation of the first deprotonation, where the pKa values of groups 4′, 7, 3, and 3′ are all within a range of half a pK_a unit. Therefore, the mono-ionic forms of these four sites could all exist between pH 7 and 8, even if the forms whose 7-OH and 4′-OH groups are deprotonated should be the predominant species, as shown in Fig. 3.

3.2. Solubilization of quercetin in water

Quercetin in its neutral form is very poorly soluble in water (0.17–7.7 μg/mL [30] corresponding to 5.62 x10^{-4}-2.55 x10^{-2} mM). By raising the pH of the medium, quercetin becomes more and more negatively charged upon deprotonation, which increases its water-solubility. However, negative charges also favor the oxidation phenomena inducing the chemical modification of quercetin into smaller by-products [31]. This can be readily followed by monitoring changes in the UV spectrum of quercetin upon increasing the pH [31], but this is much more complex than a simple redshift expected with deprotonation. Consequently, the two phenomena overlap and following the increase in solubility of quercetin in water, while avoiding its oxidative degradation, is not straightforward. Thus, we measured the solubility of quercetin in water as a function of pH, alone and in the presence of meglumine. Maximum solubility was measured using UV–vis spectroscopy. The study was conducted over a wide enough pH range to discriminate between the solubility increase due to pH and the effect of meglumine. Samples were protected from light with aluminum foil and the solubilization experiments were carried out over a short period of time (about 20 min) to limit oxidation. Samples were saturated with quercetin, shaken for 30 s, and centrifuged for 5 min at 20 °C before being diluted in methanol and immediately measured by UV-spectroscopy. Samples were prepared at different meglumine concentrations before being saturated with quercetin.

The presence of quercetin in solution was confirmed by HPLC by comparing the retention times of quercetin with those of the oxidation products. Indeed, the retention time of quercetin obtained with the chosen parameters is about 13 min, while those of two of the main oxidation by-products, phloroglucinol, and phloroglucinic acid, are between 3 and 5 (see Fig. S2-4 in ESI). Fig. 4 shows the solubility values at different pH and for two concentrations of meglumine.

Fig. 4 clearly shows that the solubility of quercetin in water is strongly enhanced at pH 8 in the presence of meglumine. This phenomenon is more pronounced when the pH and the concentration of meglumine further increase. Below pH 8, no significant effect occurs. Therefore, the pH should be set around pH = 8 for a reasonable compromise between effective solubilization and low oxida-

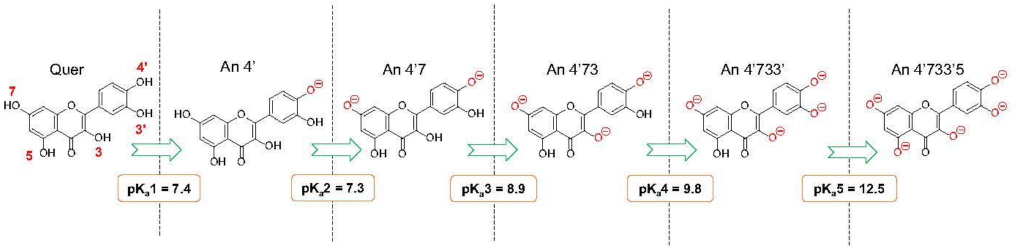

Fig. 2. Structures of anionic forms of quercetin in the most probable deprotonation order and pK_a values associated.

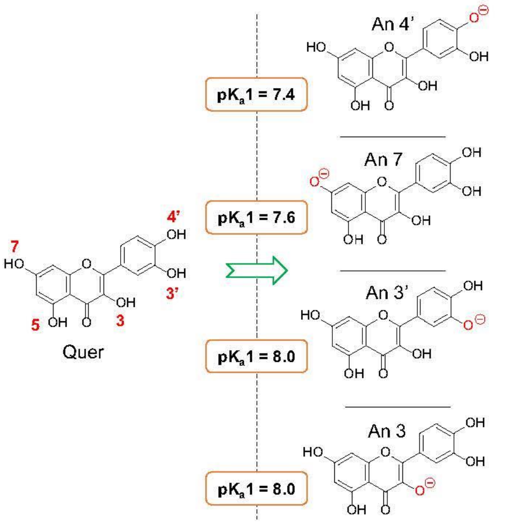

Fig. 3. Structures of most probable mono-anionic forms of quercetin and their associated pK_a values.

tion. At pH = 8, the solubilization of quercetin is increased by a factor of 5 with 250 mM meglumine.

3.3. Stability of quercetin in water

Upon oxidation, quercetin is quickly and almost completely transformed. Indeed, quercetin undergoes a complete degradation after 3 h at pH 8 at high temperature (aqueous solution at 100 °C) with air perfusion, as reported by Buchner *et al.* [5] and after 6 h at pH 10 at room temperature according to Moon *et al.* [32]. There are three main oxidation subproducts of quercetin, namely protocatechuic (3,4-dihydroxy-benzoic acid) and phloroglucinic (2,4,6-trihydroxybenzoic acid) acids and phloroglucinol (1,3,5-trihydroxybenzene) [24]. This rapid degradation makes quercetin a very effective but sacrificial antioxidant. However, to preserve its other health benefits, it is worth trying to maintain quercetin in its original form. Moreover, the negative charges induced by deprotonation speed up the oxidation [31] so the kinetics is particularly dependent on the pH. In order to analyze and quantify the influence of meglumine on this kinetics, the oxidation was monitored by an NMR and an HPLC follow-up.

NMR temporal monitoring focuses on the disappearance of characteristic signals of quercetin (peaks corresponding to protons 6 and 8, see Fig. 5) and the appearance of typical signals of the main oxidation products listed above. Fig. 5 shows the evolution of the ^{1}H NMR spectrum of quercetin with various equivalents of NaOH and meglumine.

The structure of protocatechuic acid makes its spectrum very similar to quercetin but both phloroglucinol and phloroglucinic acid should have only one signal, a singlet with a shift around 6 ppm. Thus, disappearance of the signal of proton 8 (around 6.2 ppm) should be a good indication of the chemical modification of the quercetin structure during the oxidation process (see reference spectrum in DMSO-d_6). It can be seen in Fig. 5 that with a 5 to 1 M ratio of NaOH to quercetin, the signals of protocatechuic acid are easily visible, which is not the case with the same ratio of meglumine to quercetin. However, with an equimolar ratio of NaOH or meglumine, the signal of proton 8 disappears after about one hour.

An HPLC study was performed at different pH to compare the degradation of quercetin in the presence of meglumine or NaOH. With NaOH, at pH 8, solubility of quercetin in water (**Figure S4**) is very low and the degradation is therefore difficult to quantify. However, for the meglumine system (**Figure S3**), it is possible to calculate the degradation of quercetin as its concentration is directly proportional to the surface area of the corresponding peak. After 2 h, there is still between 71 and 75 % of quercetin in the sample and after 4 h 35 % of quercetin remains intact. This result indicates that it is possible to benefit from this solubility enhancement by designing fast solubilization or extraction techniques that do not require long-term stability.

It is interesting to note that with HPLC data, one can calculate the concentrations of quercetin in the samples with a simple standard curve and thus confirm the UV–vis results. Indeed, at pH 8 and t_0, the calculation gives 0.454 mM with the HPLC method and 0.462 mM with UV spectroscopy.

3.3.1. Keto-enol tautomerization's role on stability and solubilization

The mechanism by which quercetin undergoes oxidation is still unclear and complex. Zenkevich *et al.* [24] have shown through direct head-space analysis that oxidative decarboxylation of quercetin is one of the preferable mechanisms and not decarbonylation as previously thought [33]. In any case, the keto-enolic equilibrium (Fig. 6) appears to play an important role in the solubilization and stability of quercetin. This could also explain why quercetin is stable in non-protic solvents such as DMSO, where the tautomerization is unfavored. Barvinchenko *et al.* [34] proved that the enol form of quercetin is more stable than the ketone one in water, and that the enol-to-ketone form transition is most probable, at least in surfactant solution. The planar or almost planar geometry of the enol form of quercetin in its preferential conformations [35,36] supports the idea of a more stable enol form through π-stacking.

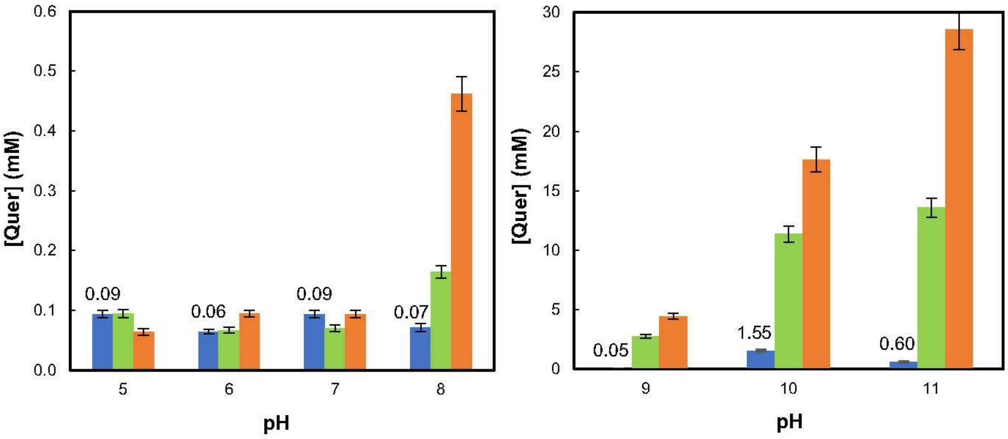

Fig. 4. Solubility of quercetin in water as a function of pH and meglumine concentration. **Blue**: Control experiment (without Meg). **Green**: [Meg] = 50 mM. **Orange**: [Meg] = 250 mM. Displayed data are the average values of two measurements. The pH of meglumine in water is naturally around 11. (For interpretation of the references to colour in this figure legend, the reader is referred to the web version of this article.)

In addition, Barvinchenko *et al.* [34] highlighted the fact that tautomerization preferentially occurred between the monoanionic forms of quercetin. This effect, triggered by a pH increase, certainly induces a solubility enhancement of quercetin alongside the formation of (poly)phenates, which are intrinsically more water-soluble than their neutral counterparts [37].

3.4. Mechanism of solubilization

3.4.1. Meglumine interactions with quercetin

Meglumine may exhibit different interactions regarding its association with solute. These interactions are highly dependent on the solvent. Cao *et al.* [38] have studied the structure of a flunixin-meglumine complex formed in an organic solvent. The cohesion of the resulting crystal is due to O — H O and N — H O hydrogen bonds, as the hydroxyl groups of meglumine act simultaneously as hydrogen bonds acceptors and donors.

On the other hand, Cassimiro *et al.* [39–41] proved that the association of meglumine with carboxylic acids in water can be explained by acid-base interactions that lead to ion-paired supramolecular adducts. In this case, the hydroxyl groups of meglumine form hydrogen bonds only with the solvent, thus enabling a significant increase in solubility.

In the case of quercetin, there are multiple sites for interactions with meglumine. The hydroxyl groups of quercetin may interact through proton exchange with the amine group of meglumine. The aromatic rings could also act as hydrogen bond acceptors toward hydrogen bonds donors such as the amine group of meglumine [42]. The interactions between quercetin and meglumine were investigated using ^{1}H NMR spectroscopy. Different solutions were prepared with increasing ratios of meglumine to quercetin. Since quercetin is not enough soluble in pure water, the reference spectrum for quercetin was performed in DMSO-d$_6$. Fig. 7 shows the evolution of the meglumine signals at different meglumine to quercetin ratios between 2.5 and 4.2 ppm.

Strong interactions of the protons located directly next to the amine function of the meglumine (signals 1 and 7 in Fig. 7 as well as proton 2 to a lesser extent), i.e. the de-shieldings of the protons with increasing amount of quercetin, suggest the formation of a salt between meglumine and quercetin. A salt formation would also be consistent with the almost immediate solubilization of quercetin in aqueous meglumine solutions. The highly hydrophilic nature of the sugar chain of meglumine also enables efficient hydration of quercetin, by carrying a large number of water molecules through hydrogen bonds.

Further, deprotonation of the hydroxyl functions enhances the ionic interaction with the positively charged meglumine at pH below 9.5. At higher pH values, quercetin is very negatively charged and thus able to bond strongly with meglumine. Finally, it is also hypothesized that the non-planar geometry of the ketone form allows an easier approach for meglumine molecules (Fig. 8). This could also be a reason for the better oxidation resistance of quercetin in the presence of an organic base like meglumine compared to NaOH, at the same pH.

3.4.2. Extension of the scope

Recently, Degot *et al.* have reported the possibility of using meglumine to extract curcumin, another well-known polyphenol primarily found in *Curcuma longa,* which exhibits antioxidant, anti-inflammatory, antimicrobial, and anticancer properties, but suffers from low bioavailability due to poor water-solubility [22]. The authors noticed that by adding meglumine to the triacetin/ ethanol/ water extraction system they used, the efficiency of extraction was improved, and subsequently observed the same phenomenon with meglumine in pure aqueous phase. The authors thus showed that 15 %wt of meglumine in water was efficient to extract 7.70 ± 0.42 mg/g of curcumin within an hour at room temperature, which is quite remarkable when compared to classical extraction methods such as pure ethanol (4.34 ± 0.08 mg/g) or Soxhlet extraction (11.64 ± 0.70 mg/g) [43].

In analogy with the results obtained with quercetin, we can make the hypothesis of an identical mechanism. Indeed, NMR study tends toward the same conclusions [41]. It was observed that the ^{1}H NMR signal of the hydroxy groups of meglumine in DMSO-d$_6$, which was broad due to the interaction with residual water in the solvent, became sharp and increasingly de-shielded with the addition of curcumin, indicating their interaction. Moreover, 2D NMR Overhauser Enhancement SpectroscopY (ROESY) results proved the existence of interactions between the aromatic rings of curcumin and the amine group of meglumine, as well as

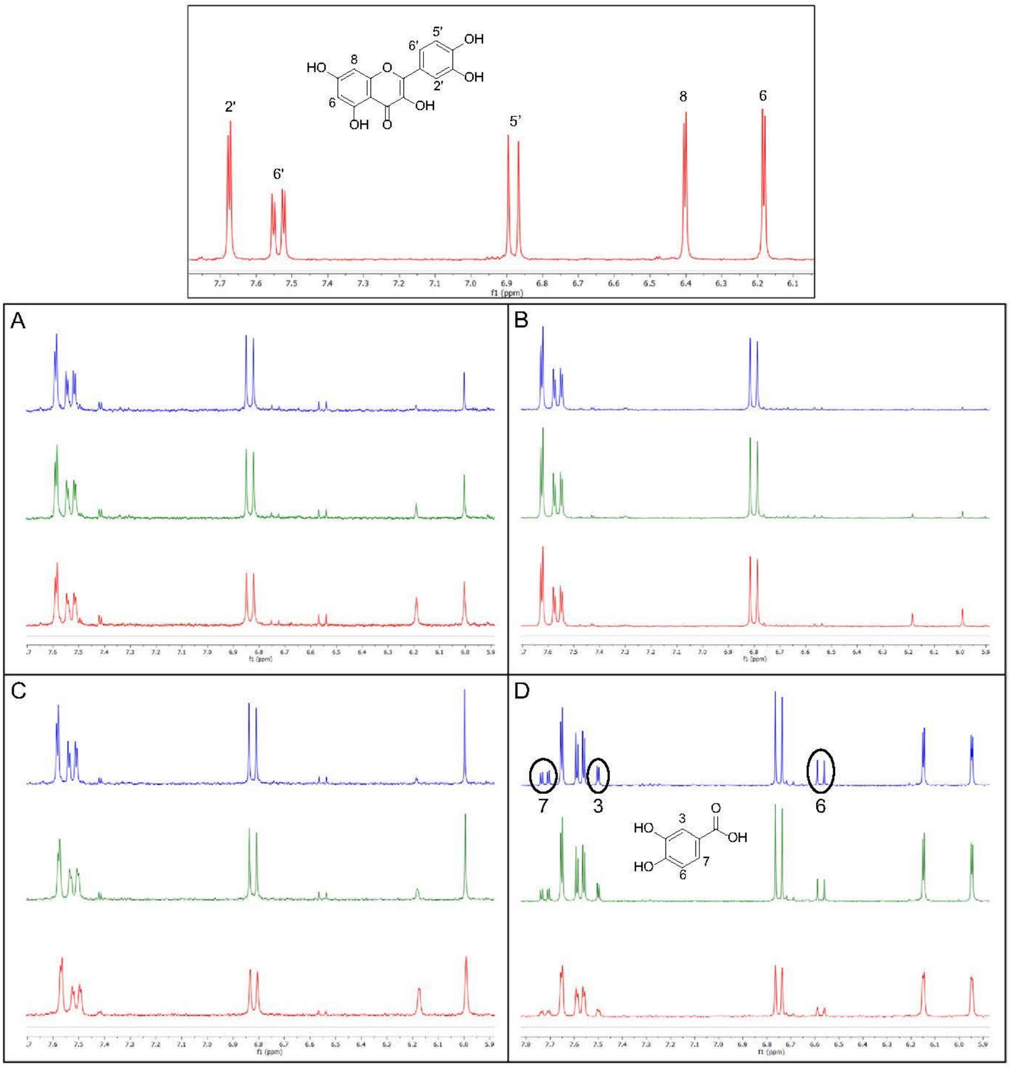

Fig. 5. ^{1}H NMR spectra of quercetin in DMSO-d_6 (**1**) and meglumine and quercetin in D_2O over time (**A-D**). **A**. Meglumine to quercetin molar ratio of (1:1) (pH = 9.0). **B**. Meglumine to quercetin molar ratio of (5:1) (pH = 10.0). **C**. NaOH to quercetin molar ratio of (1:1). **D**. NaOH to quercetin molar ratio of (5:1). **Red**: t_0. **Green**: t_0 + 30 min. **Blue**: t_0 + 1 h. The structure of protocatechuic acid is also given on the spectra **D**. (For interpretation of the references to colour in this figure legend, the reader is referred to the web version of this article.)

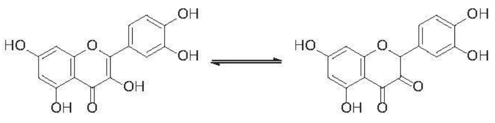

Fig. 6. Keto-enol tautomerization of quercetin.

its hydroxy groups [44]. This suggests that the aromatic rings of curcumin could act as hydrogen-bond acceptors towards the amine group of meglumine.

These findings tend to show that the phenomenon observed with quercetin can be extended to other polyphenols. Indeed, we have also tested under optimal conditions (regarding quercetin) a series of other polyphenols, namely curcumin, gallic acid, naringenin, phloretin, and resveratrol (see Table 1). These polyphenols were chosen as they are representative of different families of polyphenols, such as flavanones (naringenin), dihydrochalcones

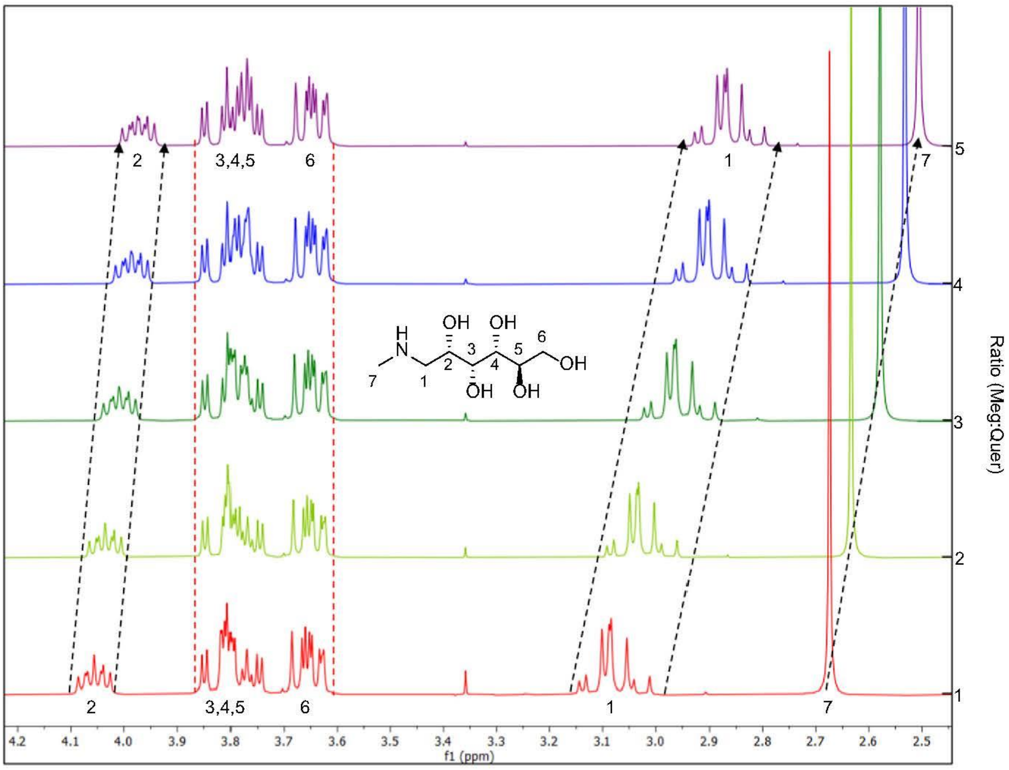

Fig. 7. ^{1}H NMR spectra of meglumine (Meg) and quercetin (Quer) in D_2O at increasing meglumine to quercetin molar ratios from bottom to top.

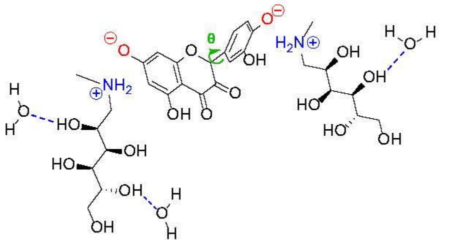

Fig. 8. Possible interactions between meglumine and quercetin. Quercetin is shown in its di-anionic form to represent the preferential state of charge of the molecule at pH 8 (based on the pK_a calculations in this work) and in its keto form. Dotted lines represent hydrogen bonds.

(phloretin), stilbenoids (resveratrol), or simple phenolic acids (gallic acid). Furthermore, they all exhibit interesting properties as antioxidants or have potential health benefits. Resveratrol for example is thought to play a major role in the prevention of cardiovascular diseases, and may even exhibit anticancer activities [45]. Naringenin, in addition to displaying antioxidant and antiulcer properties [46], differs from quercetin in that it has two fewer hydroxyl groups, including the one in position 3 suspected of being responsible for the very easy degradation of quercetin and its structure is not entirely conjugated (see Fig. 1). However, it shares the same two hydroxyl groups that deprotonate first in quercetin, which could lead to the same solubility enhancement. Finally, some of these polyphenols were chosen because they have at least one pK_a value below 8, while others (curcumin and resveratrol) have a first pK_a value around 8 or more.

As can be seen in Table 1, the water-solubility of gallic acid, naringenin, and phloretin increases with the meglumine concentration, at the same pH. This effect is far less pronounced for resveratrol and is not even visible for curcumin at this pH value. The strong interaction of gallic acid with the basic meglumine is not unexpected, but one can be surprised by the difference between phloretin and resveratrol which have rather similar structures, or by the results of curcumin. However, the first pK_a of resveratrol is around 9 [52,53], too high to interact effectively with meglumine (pK_a = 9.53) at pH 8, while the first pK_a of phloretin is about 7.4, low enough to be able to form a salt with meglumine. The same logic applies to curcumin, which could be efficiently extracted at pH 9 and above [22], but does not solubilize even with ca. 5 % meglumine at pH 8 as its first pK_a value is around 8–8.5.

One can thus expect that compounds having at least one aromatic ring and one or more hydroxyl functions with sufficient low pK_a values (<8) are suitable candidates to be solubilized by meglumine. Solubilization with meglumine, even if it requires particular conditions, can thus represent a concrete improvement compared to a method only based on a pH variation [37] by avoiding some stability problems of fragile compounds encountered in

Table 1
Water-solubility of tested polyphenols with different meglumine concentrations at pH 8.1 ± 0.1 (same protocol as for quercetin solubility tests).

Phenols tested	Structure	pK_a	Meglumine concentration (mmol/L)		
			0	48	201
Quercetin	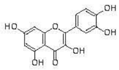	$pK_a1 = 7.4^a$ $pK_a2 = 7.3^a$ $pK_a3 = 8.9^a$ $pK_a4 = 9.8^a$ $pK_a5 = 12.5^a$	0.07	0.16	0.46
Curcumin	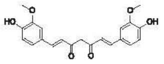	$pK_a1 = 8.4$[47], 7.7–8.5[48] $pK_a2 = 9.9$[47], 8.5–10.4[48] $pK_a3 = 10.5$[47], 9.5–10.7[48]	< 0.005	< 0.005	< 0.005
Gallic acid	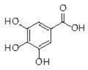	pK_a1 (acid) = 4.0[49] $pK_a2 = 8.7$[49] $pK_a3 = 11.4$[49] $pK_a4 > 13$[49]	207	283	319
Naringenin	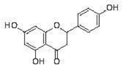	$pK_a1 = 7.5$[26], 7.1[46] $pK_a2 = 8.4$[26], 8.8[46] $pK_a3 = 9.8$[26]	1.5	1.7	2.0
Phloretin	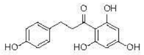	$pK_a1 = 7.3$[50], 7.6[51]	1.1	4.8	9.1
trans-resveratrol	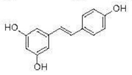	$pK_a1 = 8.8$[52], 9.1[53] $pK_a2 = 9.8$[52], 9.7[53] $pK_a3 = 11.4$[52], 10.5[53]	2.1	2.1	2.6

[a] This work. Calculated with COSMO-RS (see **Part 3.1.**).

highly alkaline medium by allowing to work at more reasonable pH values.

4. Conclusion

It has been shown that meglumine effectively increases the solubility of quercetin in an aqueous medium, even at a very slightly alkaline pH. The knowledge of the charge state of quercetin is decisive in understanding the mechanism of this solubilization. Therefore, the pK_a values of the five hydroxyl groups of quercetin were calculated with the COSMO-RS modeling software, and the deprotonation order was found to be 4′-OH < 7-OH < 3-OH < 3′-OH < 5-OH.

Solubilization is induced by the exchange of proton between the amine function of meglumine and the first hydroxyl groups of quercetin susceptible to being deprotonated. Meglumine molecules are thought to position themselves between the aromatic rings of quercetin, breaking the π-stacking and enabling better solvation. The very hydrophilic meglumine then enhances the solubilization of the complex through multiple hydrogen bonds with water molecules.

Oxidation can be troublesome to determine the solubility of quercetin in alkaline media. NMR and HPLC are two techniques well suited to quantify this degradation at high pH values (>9) in aqueous phase, yet remain limited around physiological pH. A reasonable compromise has been found between limited degradation (25–30 % degradation after 2 h) and sufficient solubility (around 0.45 mmol/L) around pH 8. The degradation at that pH should not be an issue for fast extraction processes. For other applications that require long-term stability, the addition of another antioxidant to the system could help preserve quercetin in an aqueous solution in its native state for a longer time.

All the results show the double role of meglumine compared to a base like sodium hydroxide which only allows to fix the pH at a given value. This study paves the way to find or design other solubilizing agents. Indeed, the hydrotrope-like (meaning solubilizing) behavior of meglumine is remarkable, when considering the absence of a hydrophobic part in its structure. That means that hydrotropy in its global sense of a water-solubility enhancement must be thought to be the consequence of various molecular mechanisms beyond “simple” amphiphilicity.

The next step could be the study of related structures, either meglumine derivatives with longer carbon chains or highly hydrophilic molecules having an easily accessible amine function. For example, **Figure S5** of the Supplementary Information shows the solubility of curcumin with different additives, among which several amines that exhibit interesting solubilization as well. Materials and methods used to produce these results are also found in the Supplementary Information. In any case, the generalization of the structure-properties relationship of meglumine as a solubilizer may help us to progress in the field of biocompatible actives’ solubilization and delivery.

CRediT authorship contribution statement

Adrien Fusina: Methodology, Investigation, Writing – original draft. **Pierre Degot:** . **Didier Touraud:** Methodology, Investigation, Validation. **Werner Kunz:** Conceptualization, Writing – review & editing, Validation. **Véronique Nardello-Rataj:** Conceptualization, Supervision, Funding acquisition, Writing – review & editing, Validation.

Data availability

Data will be made available on request.

Declaration of Competing Interest

The authors declare that they have no known competing financial interests or personal relationships that could have appeared to influence the work reported in this paper.

Appendix A. Supplementary material

Supplementary data to this article can be found online at https://doi.org/10.1016/j.molliq.2022.120756.

References

[1] W. Wang, C. Sun, L. Mao, P. Ma, F. Liu, J. Yang, Y. Gao, The Biological Activities, Chemical Stability, Metabolism and Delivery Systems of Quercetin: A Review, Trends Food Sci. Technol. 56 (2016) 21–38, https://doi.org/10.1016/j.tifs.2016.07.004.

[2] M.K. Kim, K. Park, W. Yeo, H. Choo, Y. Chong, In Vitro Solubility, Stability and Permeability of Novel Quercetin-Amino Acid Conjugates, Bioorg. Med. Chem. 17 (3) (2009) 1164–1171, https://doi.org/10.1016/j.bmc.2008.12.043.

[3] G.L. Amidon, H. Lennernäs, V.P. Shah, J.R. Crison, A Theoretical Basis for a Biopharmaceutic Drug Classification: The Correlation of *in Vitro* Drug Product Dissolution and *in Vivo* Bioavailability, Pharm. Res. 12 (3) (1995) 413–420, https://doi.org/10.1023/a:1016212804288.

[4] S.V. Jovanovic, S. Steenken, M. Tosic, B. Marjanovic, M.G. Simic, Flavonoids as Antioxidants, J. Am. Chem. Soc. 116 (1994) 4846–4851.

[5] N. Buchner, A. Krumbein, S. Rohn, L.W. Kroh, Effect of Thermal Processing on the Flavonols Rutin and Quercetin, Rapid Commun. Mass Spectrom. 20 (21) (2006) 3229–3235, https://doi.org/10.1002/rcm.2720.

[6] K. Manta, P. Papakyriakopoulou, M. Chountoulesi, D.A. Diamantis, D. Spaneas, V. Vakali, N. Naziris, M.V. Chatziathanasiadou, I. Andreadelis, K. Moschovou, I. Athanasiadou, P. Dallas, D.M. Rekkas, C. Demetzos, G. Colombo, S. Banella, U. Javornik, J. Plavec, T. Mavromoustakos, A.G. Tzakos, G. Valsami, Preparation and Biophysical Characterization of Quercetin Inclusion Complexes with β-Cyclodextrin Derivatives to Be Formulated as Possible Nose-to-Brain Quercetin Delivery Systems, Mol. Pharmaceutics 17 (11) (2020) 4241–4255, https://doi.org/10.1021/acs.molpharmaceut.0c00672.

[7] Z. Aytac, S. Ipek, E. Durgun, T. Uyar, Antioxidant Electrospun Zein Nanofibrous Web Encapsulating Quercetin/Cyclodextrin Inclusion Complex, J. Mater. Sci. 53 (2) (2018) 1527–1539, https://doi.org/10.1007/s10853-017-1580-x.

[8] H. Li, X. Zhao, Y. Ma, G. Zhai, L. Li, H. Lou, Enhancement of Gastrointestinal Absorption of Quercetin by Solid Lipid Nanoparticles, J. Controlled Release 133 (3) (2009) 238–244, https://doi.org/10.1016/j.jconrel.2008.10.002.

[9] N. Ahmad, V.T. Banala, P. Kushwaha, A. Karvande, S. Sharma, A.K. Tripathi, A. Verma, R. Trivedi, P.R. Mishra, Quercetin-Loaded Solid Lipid Nanoparticles Improve Osteoprotective Activity in an Ovariectomized Rat Model: A Preventive Strategy for Post-Menopausal Osteoporosis, RSC Adv. 6 (100) (2016) 97613–97628, https://doi.org/10.1039/C6RA17141A.

[10] I. Castangia, A. Nácher, C. Caddeo, D. Valenti, A.M. Fadda, O. Díez-Sales, A. Ruiz-Saurí, M. Manconi, Fabrication of Quercetin and Curcumin Bionanovesicles for the Prevention and Rapid Regeneration of Full-Thickness Skin Defects on Mice, Acta Biomater. 10 (3) (2014) 1292–1300, https://doi.org/10.1016/j.actbio.2013.11.005.

[11] A.B. Mirgorodskaya, R.A. Kushnazarova, S.S. Lukashenko, L.Y. Zakharova, Aggregation Behavior and Solubilization Properties of 3-Hydroxypiperidinium Surfactants, Russ. Chem. Bull. 68 (2) (2019) 328–333, https://doi.org/10.1007/s11172-019-2388-4.

[12] S. Tiwari, J. Ma, S. Rathod, P. Bahadur, Solubilization of Quercetin in P123 Micelles: Scattering and NMR Studies, Colloids Surf. A 621 (2021), https://doi.org/10.1016/j.colsurfa.2021.126555.

[13] L.A. Vasileva, D.A. Kuznetsova, F.G. Valeeva, E.A. Vasilieva, S.S. Lukashenko, G. A. Gaynanova, L.Y. Zakharova, Micellar Nanocontainers Based on Cationic Surfactants with a Pyrrolidinium Head Group for Increasing Drug Bioavailability, Russ. Chem. Bull. 70 (7) (2021) 1341–1348, https://doi.org/10.1007/s11172-021-3221-4.

[14] T.T.H. Nguyen, S.-H. Yu, J. Kim, E. An, K. Hwang, J.-S. Park, D. Kim, Enhancement of Quercetin Water Solubility with Steviol Glucosides and the Studies of Biological Properties, Funct. Foods Health Dis. 5 (12) (2015) 437, https://doi.org/10.31989/ffhd.v5i12.221.

[15] F. Liu, L. Sun, G. You, H. Liu, X. Ren, M. Wang, Effects of Astragalus Polysaccharide on the Solubility and Stability of 15 Flavonoids, Int. J. Biol. Macromol. 143 (2020) 873–880, https://doi.org/10.1016/j.ijbiomac.2019.09.148.

[16] D. Althans, P. Schrader, S. Enders, Solubilisation of Quercetin: Comparison of Hyperbranched Polymer and Hydrogel, J. Mol. Liq. 196 (2014) 86–93, https://doi.org/10.1016/j.molliq.2014.03.028.

[17] F. Kerkel, D. Brock, D. Touraud, W. Kunz, Stabilisation of Biofuels with Hydrophilic, Natural Antioxidants Solubilised by Glycerol Derivatives, Fuel 284 (2021) 119055, https://doi.org/10.1016/j.fuel.2020.119055.

[18] K. Manley, A. Bravo-Nuevo, A.R. Minton, S. Sedano, A. Marcy, M. Reichman, A. Tobia, C.M. Artlett, S.K. Gilmour, L.D. Laury-Kleintop, G.C. Prendergast, Preclinical Study of the Long-Range Safety and Anti-Inflammatory Effects of High-Dose Oral Meglumine, J. Cell. Biochem. 120 (7) (2019) 12051–12062, https://doi.org/10.1002/jcb.28492.

[19] C. Aloisio, G.A. de Oliveira, M. Longhi, Cyclodextrin and Meglumine-Based Microemulsions as a Poorly Water-Soluble Drug Delivery System, J. Pharm. Sci. 105 (9) (2016) 2703–2711, https://doi.org/10.1016/j.xphs.2015.11.045.

[20] P. Gupta, A.K. Bansal, Ternary Amorphous Composites of Celecoxib, Poly(Vinyl Pyrrolidone) and Meglumine with Enhanced Solubility, Pharmazie 8 (2005).

[21] H. Li, L. Ma, X. Li, X. Cui, W. Yang, S. Shen, M. Chen, A Simple and Effective Method to Improve Bioavailability of Glimepiride by Utilizing Hydrotropy Technique, Eur. J. Pharm. Sci. 77 (2015) 154–160, https://doi.org/10.1016/j.ejps.2015.06.016.

[22] P. Degot, D. Funkner, V. Huber, M. Köglmaier, D. Touraud, W. Kunz, Extraction of Curcumin from Curcuma Longa Using Meglumine and Pyroglutamic Acid, Respectively, as Solubilizer and Hydrotrope, J. Mol. Liq. 334 (2021) 116478, https://doi.org/10.1016/j.molliq.2021.116478.

[23] A. Klamt, Conductor-like Screening Model for Real Solvents: A New Approach to the Quantitative Calculation of Solvation Phenomena, J. Phys. Chem. 99 (7) (1995) 2224–2235, https://doi.org/10.1021/j100007a062.

[24] I. Zenkevich, A. Eshchenko, S. Makarova, A. Vitenberg, Y. Dobryakov, V. Utsal, Identification of the Products of Oxidation of Quercetin by Air Oxygenat Ambient Temperature, Molecules 12 (3) (2007) 654–672, https://doi.org/10.3390/12030654.

[25] K. Lemańska, H. Szymusiak, B. Tyrakowska, R. Zieliński, A.E.M.F. Soffers, I.M.C. M. Rietjens, The Influence of pH on Antioxidant Properties and the Mechanism of Antioxidant Action of Hydroxyflavones, Free Radical Biol. Med. 31 (7) (2001) 869–881, https://doi.org/10.1016/S0891-5849(01)00638-4.

[26] M. Musialik, R. Kuzmicz, T.S. Pawłowski, G. Litwinienko, Acidity of Hydroxyl Groups: An Overlooked Influence on Antiradical Properties of Flavonoids, J. Org. Chem. 74 (7) (2009) 2699–2709, https://doi.org/10.1021/jo802716v.

[27] A. Klamt, F. Eckert, M. Diedenhofen, M.E. Beck, First Principles Calculations of Aqueous pK_a Values for Organic and Inorganic Acids Using COSMO–RS Reveal an Inconsistency in the Slope of the pK_a Scale, J. Phys. Chem. A 107 (44) (2003) 9380–9386, https://doi.org/10.1021/jp034688o.

[28] F. Eckert, M. Diedenhofen, A. Klamt, Towards a First Principles Prediction of pK_a: COSMO-RS and the Cluster-Continuum Approach, Mol. Phys. 108 (3–4) (2010) 229–241, https://doi.org/10.1080/00268970903313667.

[29] R. Álvarez-Diduk, M.T. Ramírez-Silva, A. Galano, A. Merkoçi, Deprotonation Mechanism and Acidity Constants in Aqueous Solution of Flavonols: A Combined Experimental and Theoretical Study, J. Phys. Chem. B 117 (41) (2013) 12347–12359, https://doi.org/10.1021/jp4049617.

[30] Y. Gao, Y. Wang, Y. Ma, A. Yu, F. Cai, W. Shao, G. Zhai, Formulation Optimization and in Situ Absorption in Rat Intestinal Tract of Quercetin-Loaded Microemulsion, Colloids Surf. B: Biointerf. 71 (2) (2009) 306–314, https://doi.org/10.1016/j.colsurfb.2009.03.005.

[31] Z. Jurasekova, C. Domingo, J.V. Garcia-Ramos, S. Sanchez-Cortes, Effect of PH on the Chemical Modification of Quercetin and Structurally Related Flavonoids Characterized by Optical (UV-Visible and Raman) Spectroscopy, Phys. Chem. Chem. Phys. 16 (25) (2014) 12802–12811, https://doi.org/10.1039/C4CP00864B.

[32] Y.J. Moon, L. Wang, R. DiCenzo, M.E. Morris, Quercetin Pharmacokinetics in Humans, Biopharm. Drug Dispos. 29 (4) (2008) 205–217, https://doi.org/10.1002/bdd.605.

[33] S.B. Brown, V. Rajananda, J.A. Holroyd, E.G. Evans, A Study of the Mechanism of Quercetin Oxygenation by 18O Labelling, Biochem. J. 205 (1982) 6, https://doi.org/10.1042/bj2050239.

[34] V.N. Barvinchenko, N.A. Lipkovskaya, T.V. Fedyanina, Keto-Enol Tautomerization of Quercetin in Solutions of a Cationic Surfactant, Miramistin. *Colloid J.* 76 (1) (2014) 1–5, https://doi.org/10.1134/S1061933X13060021.

[35] O.O. Brovarets', D.M. Hovorun, Intramolecular Tautomerization of the Quercetin Molecule Due to the Proton Transfer: QM Computational Study, PLoS ONE 14 (11) (2019) e0224762, https://doi.org/10.1371/journal.pone.0224762.

[36] Protsenko, I. O.; Bulavin, L. A.; Hovorun, D. M. Investigation of Structural Properties of Quercetin by Quantum Chemistry Methods. *WDS'10 Proceedings of Contributed Papers* 4 **2010.**

[37] S. Peng, L. Zou, W. Zhou, W. Liu, C. Liu, D.J. McClements, Encapsulation of Lipophilic Polyphenols into Nanoliposomes Using PH-Driven Method: Advantages and Disadvantages, J. Agric. Food Chem. 67 (26) (2019) 7506–7511, https://doi.org/10.1021/acs.jafc.9b01602.

[38] X.-J. Cao, C.-R. Sun, Y.-J. Pan, The Complex of Flunixin and Meglumine, Acta Crystallogr. E Struct. Rep. Online 59 (10) (2003) 1471–1473, https://doi.org/10.1107/S1600536803019470.

[39] D.L. Cassimiro, M. Kobelnik, C.A. Ribeiro, M.S. Crespi, N. Boralle, Structural Aspects, Thermal Behavior, and Stability of a Self-Assembled Supramolecular Polymer Derived from Flunixin-Meglumine Supramolecular Adducts, Thermochim. Acta 529 (2012) 59–67, https://doi.org/10.1016/j.tca.2011.11.030.

[40] L.M.B. Ferreira, S.S.S. Kurokawa, J.D. Alonso, D.L. Cassimiro, A.L.R. Souza, M. de Fonseca, V.H.V. Sarmento, L.O. Regasini, C.A. Ribeiro, Structural and Thermal Behavior of Meglumine-Based Supra-Amphiphiles in Bulk and Assembled in Water, Langmuir 32 (45) (2016) 11878–11887, https://doi.org/10.1021/acs.langmuir.6b03176.

[41] D.L. Cassimiro, L.M.B. Ferreira, A.L.R. de Souza, M. Fonseca, S.S.S. Kurokawa, J.D. Alonso, V.H.V. Sarmento, C.A. Ribeiro, On the Influence of Fatty Acid Chain Unsaturation on Supramolecular Gelation of Aminocarbohydrate-Based Supra-Amphiphiles, J. Therm. Anal. Calorim. 134 (3) (2018) 1599–1609, https://doi.org/10.1007/s10973-018-7333-5.

[42] M. Levitt, M.F. Perutz, Aromatic Rings Act as Hydrogen Bond Acceptors, J. Mol. Biol. 201 (4) (1988) 751–754, https://doi.org/10.1016/0022-2836(88)90471-8.

[43] P. Degot, V. Huber, E. Hofmann, M. Hahn, D. Touraud, W. Kunz, Solubilization and Extraction of Curcumin from Curcuma Longa Using Green, Sustainable, and Food-Approved Surfactant-Free Microemulsions, Food Chem. 336 (2021) 127660, https://doi.org/10.1016/j.foodchem.2020.127660.

[44] Degot, P. Extraction and formulation of plant substances, PhD thesis, Universität Regensburg, **2022**.

[45] J. Gusman, A Reappraisal of the Potential Chemopreventive and Chemotherapeutic Properties of Resveratrol, Carcinogenesis 22 (8) (2001) 1111–1117, https://doi.org/10.1093/carcin/22.8.1111.

[46] L. Zhang, L. Song, P. Zhang, T. Liu, L. Zhou, G. Yang, R. Lin, J. Zhang, Solubilities of Naringin and Naringenin in Different Solvents and Dissociation Constants of

Naringenin, J. Chem. Eng. Data 60 (3) (2015) 932–940, https://doi.org/10.1021/je501004g.

[47] M. Bernabé-Pineda, M.T. Ramírez-Silva, M. Romero-Romo, E. González-Vergara, A. Rojas-Hernández, Determination of Acidity Constants of Curcumin in Aqueous Solution and Apparent Rate Constant of Its Decomposition, Spectrochim. Acta Part A 60 (5) (2004) 1091–1097, https://doi.org/10.1016/S1386-1425(03)00342-1.

[48] K. Priyadarsini, The Chemistry of Curcumin: From Extraction to Therapeutic Agent, Molecules 19 (12) (2014) 20091–20112, https://doi.org/10.3390/molecules191220091.

[49] A.C. Eslami, W. Pasanphan, B.A. Wagner, G.R. Buettner, Free Radicals Produced by the Oxidation of Gallic Acid: An Electron Paramagnetic Resonance Study, Chem. Cent. J. 4 (1) (2010) 15, https://doi.org/10.1186/1752-153X-4-15.

[50] M.L. Jennings, A.K. Solomon, Interaction between Phloretin and the Red Blood Cell Membrane, J. Gen. Physiol. 67 (4) (1976) 381–397, https://doi.org/10.1085/jgp.67.4.381.

[51] I. Kron, Z. Pudychová-Chovanová, B. Veliká, J. Guzy, P. Perjêsi, (E)-2-Benzylidenebenzocyclanones, Part VIII: Spectrophotometric Determination of PK a Values of Some Natural and Synthetic Chalcones and Their Cyclic Analogues, Monatsh. Chem. 143 (1) (2012) 13–17, https://doi.org/10.1007/s00706-011-0633-0.

[52] J.M. López-Nicolás, F. García-Carmona, Aggregation State and p K_a Values of (*E*)-Resveratrol As Determined by Fluorescence Spectroscopy and UV–Visible Absorption, J. Agric. Food Chem. 56 (17) (2008) 7600–7605, https://doi.org/10.1021/jf800843e.

[53] L. Zimányi, S. Thekkan, B. Eckert, A.R. Condren, O. Dmitrenko, L.R. Kuhn, I.V. Alabugin, J. Saltiel, Determination of the p K_a Values of *Trans* -Resveratrol, a Triphenolic Stilbene, by Singular Value Decomposition. Comparison with Theory, J. Phys. Chem. A 124 (31) (2020) 6294–6302, https://doi.org/10.1021/acs.jpca.0c04792.

Résumé

Les différentes problématiques soulevées dans ce travail portent sur la compréhension et l'utilisation de phénomènes de solubilisation en phase aqueuse, en particulier relevant de concepts d'hydrotropie, avec le double objectif de rationnaliser la recherche de nouveaux agents hydrotropiques et les comportements de solubilisation de composés polyphénoliques, notamment en vue d'applications en pharmaceutique, agroalimentaire ou en cosmétique. En effet, de nombreux composés naturels restent encore limités dans leur utilisation, ou bien leur exploitation de par leur faible solubilité aqueuse.

Dans le premier chapitre, l'utilisation de la méglumine pour solubiliser la quercétine en phase aqueuse en fonction du pH est étudiée par spectroscopie UV-visible. Le mécanisme de solubilisation investigué par RMN ^{1}H et l'oxydation de la quercétine est quantifiée par HPLC. Enfin, l'ordre de déprotonation de la quercétine est déterminé grâce au logiciel de modélisation COSMO-RS.

Le deuxième chapitre rapporte une application concrète cette solubilisation : l'encapsulation de la quercétine dans des liposomes depuis une solution aqueuse en milieu modérément basique.

L'étude de la solubilité des composés polyphénoliques est élargie dans le chapitre III pour mieux cerner les différentes causes de la faible solubilité aqueuse des polyphénols en relation avec leur structure chimique, et pour rationaliser l'effet solubilisant d'agents hydrotropiques sur des polyphénols précis en fonction de leur structure. Le π-stacking préférentiel entre le phloroglucinol et la quercétine est étudié en particulier.

Enfin, possibilité d'utiliser la méglumine ainsi que certains dérivés de la guanidine en association avec des acides gras linéaires est investiguée dans le chapitre IV. dans le but d'augmenter le caractère amphiphile des premiers et la solubilité aqueuse des seconds. Les amphiphiles obtenus sont caractérisés par des méthodes classiques du domaine des tensioactifs, notamment la température de Krafft, la solubilisation micellaire ou la stabilisation d'émulsions.

Mots-clés : Hydrotrope, Solubilisation, Polyphénols, Quercétine, Méglumine, Déprotonation

Abstract

The various issues raised in this work concern the understanding and use of solubilization phenomena in aqueous phase, in particular those related to hydrotropy concepts, with the dual aim of rationalizing the search for new hydrotropic agents and the solubilization behavior of polyphenolic compounds, with a view to applications in pharmaceuticals, agri-food and cosmetics. Indeed, many natural compounds are still limited in their use or their exploitation due to their low aqueous solubility.

In the first chapter, the use of meglumine to solubilize quercetin in aqueous phase as a function of pH is studied by UV-Visible spectroscopy. The solubilization mechanism is investigated by ^{1}H NMR and quercetin oxidation is quantified by HPLC. Finally, the order of quercetin deprotonation is determined using COSMO-RS modeling software.

The second chapter reports on a concrete application of this solubilization: the encapsulation of quercetin in liposomes from an aqueous solution in a mildly alkaline medium.

The study of the solubility of polyphenolic compounds is extended in chapter III, to better identify the various causes of their low aqueous solubility in relation to their chemical structure, and to rationalize the solubilizing effect of hydrotropic agents on specific polyphenols according to their structure. The preferential π-stacking between phloroglucinol and quercetin is studied specifically.

Finally, the possibility of using meglumine and certain guanidine derivatives in association with linear fatty acids is investigated in chapter IV, with the aim of increasing the amphiphilic character of the former and the aqueous solubility of the latter. The resulting amphiphiles are characterized by classic surface-active methods, including Krafft temperature, micellar solubilization and emulsion stabilization.

Keywords : Hydrotrope, Solubilization, Polyphenols, Quercetin, Meglumine, Deprotonation

Centrale Lille
Cité Scientifique – CS20048 – 59651 Villeneuve d'Ascq Cedex – France
Tél. + 33 (0)3 20 33 53 53 – https://centralelille.fr